EGE UNIVERSITY

GRADUATE SCHOOL OF APPLIED AND NATURAL SCIENCES

(PhD THESIS)

CATALYTIC WET AIR OXIDATION AND SONOLYTIC DEGRADATION OF SOME CARBOXYLIC ACIDS DISSOLVED IN WATER

Meral DÜKKANCI

Supervised by: Prof. Dr. Gönül GÜNDÜZ

Chemical Engineering Department

Discipline Code: 603.02.00
Presentation Date: 07.07.2010

Bornova-İZMİR
2010

Meral Dükkancı tarafından Doktora tezi olarak sunulan “Catalytic Wet Air Oxidation and Sonolytic Degradation of Some Carboxylic Acids Dissolved in Water” başlıklı bu çalışma E.Ü. Lisansüstü Eğitim ve Öğretim Yönetmeliği ile E.Ü. Fen Bilimleri Enstitüsü Eğitim ve Öğretim Yönergesi’nin ilgili hükümleri uyarınca tarafımızdan değerlendirilerek savunmaya değer bulunmuş ve 07/07/2010 tarihinde yapılan tez savunma sınavında aday oybirliği/oyçokluğu ile başarılı bulunmuştur.

Jüri Üyeleri:		**İmza**
Jüri Başkanı	**:Prof. Dr. Gönül Gündüz**	**……**
Raportör Üye	**: Prof. Dr. Özden Olgun**	**……**
Üye	**: Prof. Dr. Süheyda Atalay**	**……**
Üye	**: Prof. Dr. Ayşe Filibeli**	**……**
Üye	**: Doç. Dr. Oğuz Bayraktar**	**……...**

ÖZET

SUDA ÇÖZÜNMÜŞ BAZI KARBOKSİLLİ ASİTLERİN KATALİTİK ISLAK HAVA OKSİDASYONU VE ULTRASES İLE BOZUNMASI

DÜKKANCI, Meral

Doktora Tezi, Kimya Mühendisliği Bölümü
Tez Yöneticisi: Prof. Dr. Gönül GÜNDÜZ
Temmuz 2010, 180 sayfa

Katalitik ıslak hava oksidasyonu ve ultrases ile bozunma endüstriyel atık sulardaki zararlı kirleticilerin giderilmesini sağlayan etkin oksidasyon yöntemlerindendir. Bu çalışmada, bazı karboksilli asitlerin (maleik asit ve bütirik asit) katalitik ıslak hava oksidasyonu ve ultrases teknikleri ile parçalanarak zararsız hale getirilmeleri ve iki yöntemi karşılaştırmalı olarak incelemek amaçlanmıştır.

Araştırmanın birinci bölümünde organik kirleticilerin (bütirik ve maleik asit) sentetik çözeltilerinin ıslak hava ile oksidasyonunda kullanılmak üzere Pt, Pd ve Ru içeren alumina, silikajel, TiO_2 ve aktif karbon taşıyıcılı katalizörler ıslak emdirme yöntemiyle hazırlanmış, hazırlanan ve ticari katalizörler XRD, SEM, IR ve azot adsorpsiyon ölçümleri ile karakterize edilmiştir. Katalizörlerin aktiviteleri söz konusu karboksilli asitlerin atmosfer basıncında katalitik ıslak hava oksidasyonunda ölçülmüştür. Platin içeren alumina taşıyıcılı ticari katalizör en seçimli katalizör olarak belirlenmiştir. Daha sonra bu katalizör üzerinde oksidasyona sıcaklık, başlangıç derişimi, katalizör miktarı ve basınç gibi parametrelerin etkileri incelenmiştir. Söz konusu katalizör üzerinde 6.9 bar oksijen basıncında, 393 K sıcaklıkta bütirik asiti % 15.8 ve maleik asiti % 86.5 parçalamak mümkün olmuştur. Deneysel verilerin Langmuir-Hishelwood mekanizmasına dayalı bir kinetik modele uyduğu görülmüştür. İkinci bölümde ise yine aynı karboksilli asitlerin ultrases ile bozunmasına ultrases frekansı, ultrases gücü, ultrases modu, karboksilli asit başlangıç derişimi, H_2O_2, TiO_2, ve klinoptilolit esaslı doğal zeolit ilavesi gibi parametrelerin etkileri farklı sonikasyon sistemlerinde incelenmiştir.

Anahtar Kelimeler: Katalitik ıslak hava oksidasyonu, ultrasonik parçalanma, sonikasyon, maleik asit, bütirik asit, katalizör.

ABSTRACT

CATALYTIC WET AIR OXIDATION AND SONOLYTIC DEGRADATION OF SOME CARBOXYLIC ACIDS DISSOLVED IN WATER

DÜKKANCI, Meral

PhD in Chemical Eng.
Supervisor: Prof. Dr. Gönül GÜNDÜZ
July 2010, 180 pages

Catalytic wet air oxidation and ultrasonic degradation are useful oxidation techniques for treatment of industrial waste water by which the toxic organic pollutants are removed. The aim of this study is to investigate the destruction of some carboxylic acids (maleic acid and butyric acid) by using catalytic wet air oxidation and sonication and to compare the obtained results.

In the first part of the study Pt, Ru and Pd based catalysts with different supports such as alumina, silicagel, TiO_2 and activated carbon were prepared by incipient wetness impregnation method. The prepared and commercial catalysts used in this study were characterized by nitrogen adsorption, SEM, XRD and IR measurements. After a selectivity screening test at atmospheric pressure, the most selective catalyst to oxidation was determined to be the commercial platinum containing alumina catalyst and over this most selective catalyst, the effects of the parameters such as temperature, initial concentration of pollutant, catalyst loading and pressure of oxygen on the catalytic wet air oxidation of aqueous solutions of butyric acid and maleic acid were studied. It could be possible to achieve a degradation degree of 15.8% for butyric acid and 86.5% for maleic acid over this catalyst at an oxygen pressure of 6.9 bar and at a temperature of 393 K. A kinetic model based on the Langmuir-Hinshelwood mechanism fitted the experimental data best. In the second part of the study, the effects of parameters such as ultrasound frequency, ultrasonic power, sonication mode, initial concentration of pollutant, addition of H_2O_2, TiO_2 or clinoptilolite based natural zeolite to the solution, on the degradation of those acids were investigated by using different sonication system.

Keywords: catalytic wet air oxidation, ultrasonic degradation, sonication, maleic acid, butyric acid, catalyst.

ACKNOWLEDGEMENT

In the first place, I am heartily thankful to my supervisor, Prof. Dr. Gönül Gündüz for her supervision, advice and guidance from the preliminary to the concluding level of my research. Also, I wish to thank Assoc. Prof. Dr. Selahattin Yılmaz for his support and helps on the catalyst characterization studies at the İzmir Institute of Technology.

Also I would like to thank the members of the dissertation committee Prof. Dr. Süheyda Atalay and Prof. Dr. Ayşe Filibeli for their guidance and supports.

I also thank to Prof. Dr. Erol Gündüz for opening his laboratory to me and helpful touch on my experiments.

Words fail me to express my appreciation to all members of my family and my friends. Especially, I would like to give my special thanks to Research Asisstant Dr.Emine Sert, Research Asisstant Dr.Tuğba Gürmen Özçelik, Research Asisstant Banu Yener and Research Asisstant Berrin İkizler whose support enabled me to complete this work.

The thesis is financially supported by TUBITAK with the Project number of 106M206 and by the Fund of Scientific Research Projects of Ege University (BAP) with the Project numbers of 09MÜH055 and 2006BİL028.

TABLE OF CONTENT

Page

TABLE OF CONTENT (continued)

Page

TABLE OF CONTENT (continued)

Page

TABLE OF CONTENT (continued)

Page

TABLE OF CONTENT (continued)

Page

LIST OF FIGURES

LIST OF FIGURES (continued)

LIST OF FIGURES (continued)

LIST OF FIGURES (continued)

LIST OF FIGURES (continued)

LIST OF FIGURES (continued)

LIST OF FIGURES (continued)

LIST OF FIGURES (continued)

LIST OF FIGURES (continued)

LIST OF FIGURES (continued)

LIST OF FIGURES (continued)

LIST OF FIGURES (continued)

LIST OF FIGURES (continued)

LIST OF FIGURES (continued)

LIST OF TABLES

LIST OF TABLES (continued)

LIST OF TABLES (continued)

LIST OF TABLES (continued)

1. INTRODUCTION

1.1 The Aim of the Study

The aim of this study is to investigate the oxidation of butyric acid and maleic acid into CO_2 and low molecular weight less hazardous organic compounds by catalytic wet air oxidation and sonication processes.

Wet air oxidation (WAO) is a technology for treatment of streams with organic loads of 0.01-0.1 g/dm^3, which are too toxic for biodegradation (e.g. too acidic or phenol-containing streams) or too diluted for incineration (Gomes et al. 2000). In WAO process, organic compounds ($C_xH_yN_z$) are oxidized using air or pure oxygen in liquid phase into CO_2, low molecular weight carboxylic acids, NH_3, NO_3^- and molecular nitrogen, but not to NO_x, SO_2, HCl, dioxins and fly ash. For example in the oxidation of phenol and phenolic compounds unsaturated carboxylic acids such as muconic, maleic, fumaric and acrylic acids are formed. In the oxidation of unsaturated carboxylic acids more refractory short chain mono and di carboxylic acids such as, butyric, acetic, propionic, and oxalic acids are formed. These acids are also important pollutants like phenol and must be removed from waste water (Harmsen et al., 1997; Luck, 1999; Renard et al., 2005; Yang et al., 2006). WAO has been used successfully to treat a wide range of industrial waste waters which have been reported for high concentrated chemical wastewaters obtained from a petrochemical company, printing and dyeing. But WAO is an expensive process because of the required severe conditions, because in order to keep the water in liquid phase, high pressures and high temperatures (393-393 K) are required. Since the water is kept in liquid, considerably less energy is needed as compared to incineration. An alternative to reduce the costs is the use of suitable heterogeneous catalysts. Catalysts able to promote the WAO under milder operating conditions and shorter residence times. Catalysts can also lead to higher oxidation rate of organic compounds. In addition to these it is easy to remove the catalyst ions from solution in heterogeneous catalytic systems. Consequently, in the last few years, catalytic wet air oxidation (CWAO) has gained attention for the treatment of biologically refractory organic compounds. The CWAO process is capable of converting all organic contaminants ultimately to CO_2 and H_2O and can also remove oxidizable inorganic components such as cyanides and ammonia.

The application of ultrasound irradiation for the degradation of organic pollutants in water has received also considerable attention from environmental scientists and engineers, due to their undesirable effects in the water environment. But in this system destruction of organic pollutans needs long reaction time and high energy. To overcome this, sonication can be used with other advanced oxidation processes (AOPs) such as photolysis, Fenton's reagent and UV. Addition of TiO_2 as a solid particle and addition of H_2O_2 as a source of OH^* radicals can accelerate the efficiency of sonication reaction, as well (Dükkancı and Gündüz 2006; Wang et al., 2006).

In principle of sonication, ultrasonic waves consist of rarefaction and compression cycles, which can lead to the generation of cavitation bubbles in aqueous solution. During the violent collapse of the cavitation bubbles, high temperatures (> 5000 K) and high pressures (> 1000 atm) occur within the bubbles. Under these extreme conditions, organic compounds at the bubble/water interface can be thermally decomposed or a large number of the reactive radicals, such as H* and HO^* are generated via the thermal dissocation of water, which can initiate a series of radical reactions to decompose pollutants dissolved in water (Drijvers et al., 1999; Ince et al., 2001; Wu et al., 2001; Nam et al., 2003).

1.2 Waste Water Treatment

The sustainable water management is one of the critical issues to be addressed in the coming decades. Up to date, more than half of the available freshwater is appropriated for human uses, indicating a high degree of exploitation of the existing water resources. In the close future, the water resources may even suffer drastic variations on a local and/or global level, because of the foreseen population growth and climate changes. This fact, in combination with the water pollution caused by mankind activity, makes water re-use of outmost importance. However, one should keep in mind that, from a global point of view, the recycling of water is not environmentally benign if high energy input technologies are used for this purpose. Thus, the development of efficient wastewater technologies with low energetic and operation costs is essential for all types of wastewater.

Wastewater can be divided into four broad categories, according to its origin, namely domestic, industrial, public service and system loss/leakage. Among these, industrial wastewaters occupy a 42.4% of the total volume and

domestic a 36.4%. The types of contaminants that can be present in the aquatic effluents have been summarised as:

- Suspended Solids, Dissolved inorganics
- Biodegradable Organics & Nutrients
- Priority Pollutants (carcinogeneous etc.), Pathogens, Refractory (non-biodegradable) Organics, Heavy Metals

In particular, increasing quantities of wastewater with a high organic load result from numerous industrial and domestic applications. The most common depolluting technology in this case is the conventional biological treatment. However, its application becomes impossible for streams that contain high organic load and/or bio-toxic compounds. For example, aqueous phenol solutions with concentrations exceeding 0.5 g/dm^3 should not be treated in biological plants, even though acclimatised cultives in laboratory tests have performed depollution of solutions with up to 2 g/dm^3 of phenol. Phenol and phenol like compounds are frequently encountered in the end of pipe streams of several chemical industries, such as petrochemical, pharmaceutical etc. (Eftaxias, 2002). Some limitations for phenol concentration in the waste water were tabulated in Table 1.1.

Table 1.1. Limitations Phenol Concentration in the Waste Water.

	Phenol Concentration $x10^3$ (g/dm^3)
Recreation Areas (Coasts)	0.001
Sea Water	0.001
Discharge of Refinery	2
Deep Discharge to Sea	10
Discharge Industry to Purification Systems	20

Waste water treatment can be achieved by physical, chemical oxidation, biological, advanced oxidation methods and incineration.

1.2.1 Physical processes

In physical water treatment method, physical processes are used to treat the wastewater. Use of gross chemicals or executing biological changes is strictly avoided. A prominent physical water treatment method is sedimentation, wherein coarse screening of waste water is done to remove contaminating objects after allowing them to settle at the base. Once the contaminants have settled, the cleared effluent or waste stream is removed. Sedimentation is one of the most common methods, quite often used at the beginning and the end of many water treating processes. Aeration is another physical water treatment method used, wherein air is added to the wastewater physically to provide oxygen to it. In yet another method known as filtration, sewage is passed through filters to separate the contaminating solids from the water. Sand filter is a common filter used in this process. In a number of wastewater treatment methods, semi-solid contaminants like grease and oil are allowed to float on the surface of the water, and then they are physically removed (Buzzle.com, 2010).

1.2.2 Biological processes

Biological treatment — the use of bacteria and other microorganisms to remove contaminants by assimilating them — has long been a mainstay of wastewater treatment in the chemical process industries (CPI). Because they are effective and widely used, many biological-treatment options are available today. They are, however, not all created equal, and the decision to install a biological-treatment system requires ample thought. When considering biological waste water treatment for a particular application, it is important to understand the sources of the wastewater generated, typical wastewater composition, discharge requirements, events and practices within a facility that can affect the quantity and quality of the wastewater, and pretreatment ramifications.

There are three basic categories of biological treatment: aerobic, anaerobic and anoxic. Aerobic biological treatment, which may follow some form of pretreatment such as oil removal, involves contacting wastewater with microbes and oxygen in a reactor to optimize the growth and efficiency of the biomass. The microorganisms act to catalyze the oxidation of biodegradable organics and other contaminants such as ammonia, generating innocuous by products such as carbon dioxide, water, and excess biomass (sludge). Anaerobic (without oxygen) and an oxic (oxygen deficient) treatments are similar to aerobic treatment, but use mic-

roorganisms that do not require the addition of oxygen. These microorganisms use the compounds other than oxygen to catalyze the oxidation of biodegradable organics and other contaminants, resulting in innocuous by-products. The three individual types of biological-treatment technologies; aerobic, anaerobic or anoxic can be run in combination or in sequence to offer greater levels of treatment. Regardless of the type of system selected, one of the keys to effective biological treatment is to develop and maintain an acclimated, healthy biomass, sufficient in quantity to handle maximum flows and the organic loads to be treated (Schultz, 2005).

1.2.3 Incineration

Incineration is the other well established technology for the treatment of concentrated and toxic organic waste streams. Organic pollutants are burnt at atmospheric pressure and high temperatures between 1273 K and 1973 K. Thus, incineration can offer almost complete pollutant destruction, although at very high energy costs, because an organic load above 25% is necessary to guarantee auto thermal oxidation. Furthermore, this technique has been accused for the emission of toxic by-products such as dioxins and furans. (Eftaxias, 2002)

1.2.4 Chemical oxidation processes

This technology is established and has been safely employed to oxidize many organic contaminants including phenols, pesticides, chlorinated solvents, aromatic hydrocarbons, benzene and toluene. The organic contaminants that are amenable to oxidative treatment include sulphides, ammonia, cyanide and heavy metals. The chemicals commonly used as oxidants include chlorine, chlorine oxide, H_2O_2, potassium permanganate, oxygen, ozone and hydroxyl radicals.

Physical and chemical treatment is normally used to prepare the wastewater for the next treatment technique, in many cases biological treatment.

1.2.4.1 Wet air oxidation (WAO)

Wet air oxidation (WAO) can be defined as the oxidation of organic and inorganic substances in an aqueous solution or suspension by means of oxygen or air at elevated temperatures and pressures. Typical conditions for wet oxidation range from 453 K and 20 bar to 588 K and 150 bar. Residence times may range

from 15 to 120 min, and the chemical oxygen demand (COD) removal may typically be about 75–90%. In contrast to supercritical water oxygen (SCWO), a complete mineralization of the waste stream is impossible by WAO, since some low molecular weight oxygenated compounds (especially acetic and propionic acids, methanol, ethanol, and acetaldehyde) are resistant to oxidation (Levec and Pintar, 2007). For instance, removal of acetic acid is usually negligible at temperatures lower than 573 K. Organic nitrogen compounds are easily transformed into ammonia, which is also very stable in WAO conditions. Therefore, WAO is a pre-treatment of liquid wastes which requires additional treatment of the process liquid and gas streams. The degree of oxidation is mainly a function of pollutant stability, reaction temperature, oxygen partial pressure and residence time.

Figure 1.1 shows a basic flow diagram of a WAO plant, which consists mainly of a high-pressure pump, an air or oxygen compressor, a heat-exchanger as well as a reactor with a relief valve and a downstream separator. The waste is retained in the reactor for a sufficient period of time to achieve the desired chemical oxidation (30–120 min). The simplest reactor design is usually a cocurrent vertical bubble column with a height-to-diameter ratio in the range of 5–20. Several plants are in operation today, mostly to treat waste streams from petrochemical, chemical and pharmaceutical industries as well as residual sludges from wastewater treatment. These plants aim either at a complete oxidative decomposition of pollutants or at a partial oxidation into low-molecular weight compounds which can then be treated further by conventional biological processes.

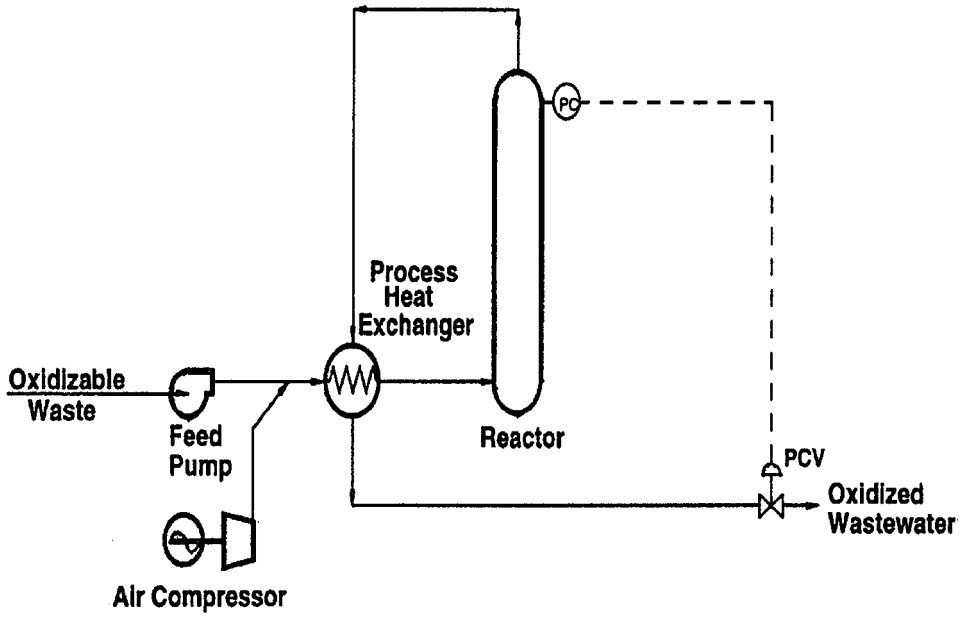

Figure 1.1. Flow diagram of a wet oxidation process.

The process selection should be tailored to the composition of the effluent, the desired conversion and the flow rate. In Figure 1.2, in which WAO appears to be the most suitable technology for wastewater containing between 20 and 200 g/dm^3 of COD (Chemical Oxygen Demand). The suitability of WAO would be further reinforced if a heterogeneous catalyst is successfully incorporated in the process.

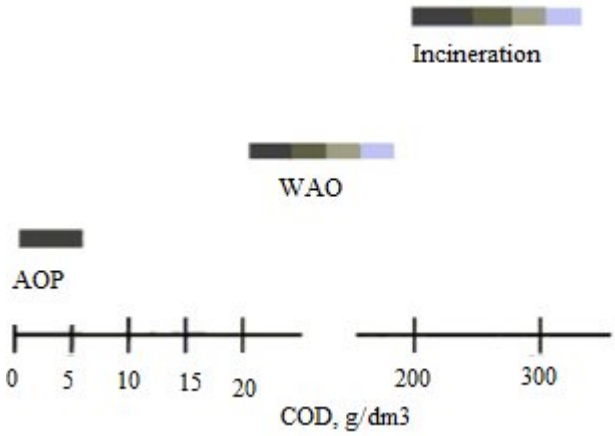

Figure 1.2. Suitability of water technologies according to COD contents.

The Wet Air Oxidation process was originally developed by F.J.Zimmermann and its first industrial applications appeared in the late 1950s. Currently, there are more than 200 plants operating around the world, the majority

being dedicated to the treatment of sewage sludge. Other main fields of application consist in the regeneration of activated carbon and the treatment of industrial wastewater.

According to this method, the dissolved or suspended organic matter is oxidised in the liquid phase by some gaseous source of oxygen, that may be either pure oxygen, or air. Typical operating conditions are in the range of 373-573 K and 5-200 bar. Some industrial applications are given in Table 1.2. The main differences between the distinct processes consist in the reactor type used and the incorporation, or not, of a catalyst.

The most widely spread variation is the non-catalytic Zimpro process, which uses a cocurrent bubble column reactor, operating at temperatures between 420 – 598 K and pressures of 20-210 bar. Alternative non-catalytic WAO processes are the Wetox process, that combines a series of agitated tank reactors, the Vertech process that uses the gravity to develop high pressures in a deep shaft reactor, the Kenox process which incorporates novel elements like static mixing and ultrasound energy and the oxyget process in which the liquid is fed in the reactor in form of droplets to eliminate oxygen transfer limitations.

WAO can achieve easily 90 to 95% conversion, which in general is not enough to meet effluent discharge regulations. Thus, most of WAO units are followed by biological treatment.

Despite its success in laboratory applications, catalytic WAO has yet not found the industrial recognition met with non-catalytic WAO. The main reasons, as pointed out earlier, are that the homogeneous catalysts have to be removed in a subsequent step, while the heterogeneous catalysts have to maintain their activity for sufficiently long periods. Homogeneous catalysts, such as Cu^{2+} or Fe^{2+} ions, are used in the Ciba-Geigy, LOPROX and WPO processes. The former uses Cu^{2+} ions at elevated temperatures (above 573 K) and is very successful in completely removing dioxins. In the reactor exit the catalyst is precipitated as copper sulphide and recycled to the reactor. The other two processes add $Fe^{2+,}$ in more moderate conditions (Luck, 1999; Eftaxias, 2002).

Table 1.2. Main industrial processes of Wet Air Oxidation.

Process	Waste type	NoPlant	Reactor Type	T (K)	P (Bar)	Catalyst
Zimpro	sewage sludge	200	Bubble Column	553-598	200	none
	spent AC	20				
	industrial	50				
Vertech	sewage sludge	1	deep shaft	<553	<110	none
Wetox	ns	ns	stirred tanks	473-523	40	none
Kenox	ns	ns	recirculation reactor	<513	45	none
Oxyget	ns	ns	tubular jet	<573	ns	none
Ciba-Geigy	industrial	3	-	573	ns	Cu^{2+}
LOPROX[1]	industrial	>1	Bubble column	<473	50-200	Fe^{2}+
NS-LC	ns	ns	Monolith	493	40	Pt — Pd/ $T\dot{I}O_2$ — ZrOi
Osaka gas	coal gasifier	ns	Slurry Bubble	523	70	ZrO_2 or TiO_2
	coke oven cyanide sewage sludge		Column			with noble or base metals
Kurita[2]	ammonia	ns	ns	>373	ns	supported Pt

ns: not specified
[1]This process uses organic quinone substances to generate hydrogen peroxide
[2]This process uses nitrite as oxidant

1.2.4.2 Catalytic wet air oxidation (CWAO)

The challenging operating conditions of WAO provided a strong driving force to investigate catalysts which would allow substantial gains on temperature, pressure and residence time. Another major benefit of using catalysts in WAO is the oxidation of the refractory compounds, namely acetic acid and ammonia, at much lower temperatures than in the absence of catalysts.

CWAO is particularly cost-effective for effluents that are highly concentrated (chemical oxygen demands of 10 to over 100 g/dm^3) or which contain components that are not readily biodegradable or are toxic to biological treatment systems. CWAO process plants also offer the advantage that they can be highly automated for unattended operation, have relatively small plant footprints, and are able to deal with variable effluent flow rates and compositions.

The process is not cost-effective compared with other advanced oxidation processes or biological processes for lightly contaminated effluents (COD less than about 5 g/dm^3).

The heterogeneous CWAO has scarcely found industrial applications. In Table 1.2, the NS-LC process uses a vertical monolith reactor with a Pt -Pd/TiO_2 - ZrO_2 catalyst. The operating conditions are 493 K and 40 bar. The Osaka gas process uses a mixture of precious and base metals on titania or zirconia-titania supports. Typical operating conditions are 523 K and 68.6 bar. The Kurita process uses nitrite instead of oxygen, and a similar catalyst (supported Pt), becoming more effective at lower temperatures, around 443 K (Eftaxias, 2002) .

Sometimes the wastewaters contain toxic, non-biodegradable and hazardous pollutants, which make them inefficient for biological treatment. In addition to this, biodegradation processes are inherently slow and this results in large installations for biochemical treatment of waste waters. They produce sludge that may pose environmental problems. Some wastewater streams are too concentrated to clean them efficiently by biological treatment.

Incineration at high temperature may be effective, but the energy efficiency is very low because large amounts of water have to be heated, addition to this extra fuel typically required. It is also necessary to treat the off-gas (Cybulski and Trawezynski, 2004). So, CWAO is suitable for treatment of streams which are too toxic for biodegradation or too diluted for incineration.

Catalytic wet air oxidation (CWAO) of organic waste in water seems to be a promising and environmental friendly method to improve water quality. The process uses air as the oxidant, which is contacted with the organic compound over a catalyst. Oxidation reaction takes place in the aqueous environment where the water is an integral part of the reaction. Water provides a medium for the dissolved oxygen to react with the organics. (Gündüz and Dükkancı, 2007)

Homogeneous catalysts, for example Cu, Fe, Mn salts have good activity in CWAO of organic compound. However, CWAO processes based on these catalysts induce a separation step such as precipitation to remove or recover the catalysts ions from the treated effluent. To overcome this drawback, attempts at developing stable active heterogeneous catalysts have been made. Several noble metals (Pt, Ru, Pd….) and transition metal oxides (Cu, Fe, Co, Mn …..) have been

tested. In the case of heterogeneous oxide transition metals, a partial leaching of metal ions has been observed during the reaction and a recovery step is necessary. Noble metals, stable in severe reaction conditions, were then investigated with a great attention (Renard et al., 2005)

Metal oxide catalysts (such as $CuO.ZnO/Al_2O_3$ and Co/Bi catalysts amongst others) were found effective for the complete removal of polyphenols, while noble metals (such as palladium, platinum and ruthenium on various supports) were found capable for effective removal of high molecular weight polymers, phenol and carboxylic acids. (Oliviero et al., 2001)

1.2.5 Advanced oxidation processes (AOPs)

The main mechanism of AOPs is the generation of highly reactive free radicals. Hydroxyl radicals (OH*) are effective in destroying organic chemicals because they are reactive electrophiles (electron preferring) that react rapidly and nonselectively with nearly all electron-rich organic compounds. They have an oxidation potential of 2.33 V and exhibit faster rates of oxidation reactions comparing to conventional oxidants such as H_2O_2 or KMnO4. Once generated, the hydroxyl radicals can attack organic chemicals by radical addition (Equation 1.1), hydrogen abstraction (Equation 1.2) and electron transfer (Equation 1.3). In the following reactions, R is used to describe the reacting organic compound.

$$R + HO^* \rightarrow ROH \quad (1.1)$$

$$R + HO^* \rightarrow R^* + H_2O \quad (1.2)$$

$$R^n + HO^* \rightarrow R^{n-1} + OH^- \quad (1.3)$$

A great number of methods are classified under the broad definition of AOPs. Most of them use a combination of strong oxidizing agents (e.g H_2O_2, O_3) with catalysts (e.g. transition metal ions) and irradiation (e.g. ultraviolet, visible). Among different available AOPs producing hydroxyl radicals, titanium dioxide/UV light process, hydrogen peroxide/UV light process, Fenton's reactions, sonolysis seem to be some of the most popular technologies for wastewater treatment as shown by the large amount of data available in the literature.

AOPs application is refering to the polluting load of wastes normally expressed as Chemical Oxygen demand (COD). Only wastes with relatively small COD contents (≤ 5 g/dm^3), Figure 1.2, can be suitably treated by AOPs since higher COD contents would require the consumption of too large amounts expensive reactants. Wastes with more massive pollutants contents can be more conventially treated by means of wet air oxidation or incineration (Andreozzi et al., 1999).

1.2.5.1 Titanium dioxide/UV light process

In TiO_2/UV light process, a titanium peroxide semiconductor absorbs UV light and generates hydroxyl radicals. Specifically, during UV illumination of TiO_2, conduction band electrons and valence band holes are initially yielded (Equation 1.4). Band electrons interact with surface adsorbed molecular oxygen to yield superoxide radical anions (Equation 1.5), while band holes interact with water to produce hydroxyl radical (Equation 1.6):

$$TiO_2 + h\nu \rightarrow e^- + h^+ \quad (1.4)$$

$$e^- + O_2 \rightarrow O_2^-* \quad (1.5)$$

$$h^+ + H_2O \rightarrow H^+ + HO* \quad (1.6)$$

Organic compounds can undergo oxidative degradation through their reactions with valence bond holes, hydroxyl and peroxide radicals as well as reductive cleavage through their reactions with electrons. So far, TiO_2/UV light process has been extensively used for wastewater treatment. The key advantages of this process are the operation at ambient conditions, the lack of mass transfer limitations when nanoparticles are used as photocatalysts and the possible use of solar irradiation. Moreover, TiO_2 is a cheap, readily available material and the photogenerated holes are highly oxidizing. In addition, TiO_2 is capable for oxidation of a wide range of organic compounds into harmless compounds such as CO_2 and H_2O. The major factors affecting TiO_2/UV light process are: initial organic load, amount of catalyst, reactor's design, UV irradiation time, temperature, solution's pH, light intensity and presence of ionic species.

1.2.5.2 Hydrogen peroxide/UV light process

This process includes H_2O_2 injection and mixing followed by a reactor that is equipped with UV light (200 to 280 nm). During this process, ultraviolet radiation is used to cleave the O-O bond in hydrogen peroxide and generate the hydroxyl radical. The reactions describing UV/H_2O_2 process are presented below:

$$H_2O_2 + h\nu \rightarrow 2\ HO^* \quad (1.7)$$

$$H_2O_2 + HO^* \rightarrow HO_2^* + H_2O \quad (1.8)$$

$$H_2O_2 + HO_2^* \rightarrow HO^* + H_2O + O_2 \quad (1.9)$$

$$2HO^* \rightarrow H_2O_2 \quad (1.10)$$

$$2\ HO_2^* \rightarrow H_2O_2 + O_2 \quad (1.11)$$

$$HO^* + HO_2^* \rightarrow H_2O + O_2 \quad (1.12)$$

In the aforementioned equations, Equation 1.7 is the rate limiting reaction because the rates of the other reactions are much higher than that of Equation 1.7. Theoretically in UV/H_2O_2 process, the higher initial hydrogen peroxide concentration produces higher hydroxyl radical concentration (Equation 1.7), which decomposes more target compound. However, an optimal hydrogen peroxide concentration exists because overdosing of hydrogen peroxide would lead to reaction with hydroxyl radical and formation of HO_2^* (Equation 1.8).

UV/H_2O_2 process is efficient in mineralizing organic pollutants. A disadvantage of this process is that it can not utilize solar light as the source of UV light due to the fact that the required UV energy for the photolysis of the oxidizer is not available in the solar spectrum. Moreover, H_2O_2 has poor UV absorption characteristics and if the water matrix absorbs a lot of UV light energy, then most of the light input to the reactor will be wasted. Finally, special reactors designed for UV illumination are required, while residual H_2O_2 should be addressed.

The major factors affecting this process are the initial concentration of the target compound, the amount of H_2O_2 used, wastewater pH, presence of bicarbonate and reaction time (Stasinakis, 2008).

1.2.5.3 Fenton's reagent technique

H.J.H. Fenton in 1894 reported that ferrous ions strongly promote the oxidation of malic acid by hydrogen peroxide. Subsequent work has shown that the combination of H_2O_2 and a ferrous salt "Fenton's reagent" is an effective oxidant of a wide variety of organic substrates. About 40 years later, Haber andWeiss proposed that the hydroxyl radical is the actual oxidant in such systems. In 1940s, Merz and Waters proposed the mechanistic scheme. Since then, oxidations with hydroxyl radicals have been studied with increasing vigour.

The oxidation with Fenton's reagent based on ferrous ion and hydrogen peroxide is proven and hydroxyl radicals (OH^*) are produced by interaction of hydrogen peroxide with ferrous salts (equation (1.13)).

$$Fe^{2+} + H_2O_2 \longrightarrow Fe^{3+} + OH^* + {}^-OH \qquad (1.13)$$

Iron (III) can then react with hydrogen peroxide in the so-called Fenton-like reaction (equation (1.14) and (1.15))

$$Fe^{3+} + H_2O_2 \rightleftharpoons FeOOH^{2+} + H^+ \qquad (1.14)$$

$$FeOOH^{2+} \longrightarrow HO_2^* + Fe(II) \qquad (1.15)$$

$$Fe(III) + HO_2^* \longrightarrow Fe(II) + O_2 + H^+ \qquad (1.16)$$

in order to regenerate iron (II) and, thus, supporting the Fenton process. The $^*OH$ species formed through will then attack the organic substrates present in the wastewater. Nevertheless, numerous competitive reactions can also occur, namely the following ones, which negatively affect the oxidation process.

$$H_2O_2 + HO^* \longrightarrow HO_2^* + H_2O \qquad (1.17)$$

$$Fe^{2+} + HO^* \longrightarrow Fe^{3+} + HO^- \qquad (1.18)$$

The OH^* radical is the main reactant in process capable of detoxifying a number of organic substrates via oxidation. It is twice as reactive as chlorine and its position is second in the oxidation potential series next to fluorine. The kinetic

activity of this radical is also tremendous. It reacts almost in a diffusion-controlled manner with second-order rate constant in the range 10^9-10^{10} $dm^3mol^{-1}s^{-1}$.

Nevertheless, the method of Fenton's oxidation may not be applicable to alkaline solutions or sludges with the strong buffering capacities. Another disadvantage of Fenton's treatment is the production of iron sludge, which must be disposed. Costs of application of Fenton's reagent are expected to be quite low as compared to other oxidation processes. The main chemical cost of Fenton's reagent is the cost of H_2O_2. So, it is important to optimize the amount of H_2O_2 in the Fenton oxidation technology. Because of the relatively higher H_2O_2 concentrations, the competition of OH* radicals clutching between the substrate and H_2O_2 has began and H_2O_2 reacts with OH* radicals to constitute less reactive perhidroxly radicals, HO_2^*, (Dutta et al., 2001; Guedes et al., 2003; Torrades et al., 2004).

1.2.5.4 Sonication (Ultrasonic Degradation)

Sound is nothing more than waves of compression and expansion passing through gases, liquids or solids. We can sense these waves directly through our ears if they have frequencies from about Hertz to 16 kHz (the Hertz unit is cycles of compression or expansion per second; kiloHertz, abbreviated kHz, is thousands of cycles per second). These frequencies are similar to low frequency radio waves, but sound is intrinsically different from radio or other electromagnetic radiation. For example, electromagnetic radiation (radio waves, infrared, visible light, ultraviolet, x-rays, gamma rays) can pass through a vacuum without difficulty; on the other hand, sound cannot because the compression and expansion waves of sound must be contained in some form of matter. High intensity sound and ultrasound are generally produced in a similar fashion: electric energy is used to cause the motion of a solid surface, such as a speaker coil or a piezoelectric ceramic. Piezoelectric materials expand and contract when an electric field is applied. For ultrasound a high frequency alternating electric current is applied to a piezoelectric attached to the wall of a metal container (as in an ultrasonic cleaning bath of the kind used, for example, by jewelers).

Ultrasound has found many uses in many areas. At home, we use ultrasound for dog whistles, burglar alarms, and jewelery cleaners. In hospitals, doctors use ultrasound to remove kidney stones without surgery, to treat cartilage injuries (such as "tennis elbow"), and to image fetal

development during pregnancy. In industry, ultrasound is important for emulsifying cosmetics and foods, welding plastics, cutting alloys and large-scale cleaning (Suslick, 1994).

Ultrasound is the part of the sonic spectrum which ranges from 20 kHz to 10 MHz and can be roughly subdivided in three main regions:

- ✓ Low frequency, high power ultrasound (20-100 kHz)
- ✓ High frequency, medium power ultrasound (100 kHz-1 MHz)
- ✓ High frequency, low power ultrasound (1-10 MHz)

The range from 20 kHz to around 1 MHz is used in sonochemistry whereas frequencies far above 1 MHz are used as medical and diagnostic ultrasound (Fındık, 2005).

In principle ultrasonic waves consist of rarefaction and compression cycles, which can lead to the generation of cavitation bubbles in aqueous solution. Figure 1.3 shows the cavitation bubble in a liquid irradiated with ultrasound. Cavitation can be defined as the phenomena of formation, growth and subsequent violent collapse of microbubbles or cavities occurring in extremely small intervals of time releasing large magnitudes of energy over a very small location but at millions of places in the reactor simultaneously (Guo et al., 2005; Lim et al., 2007; Berberidou et al., 2007).

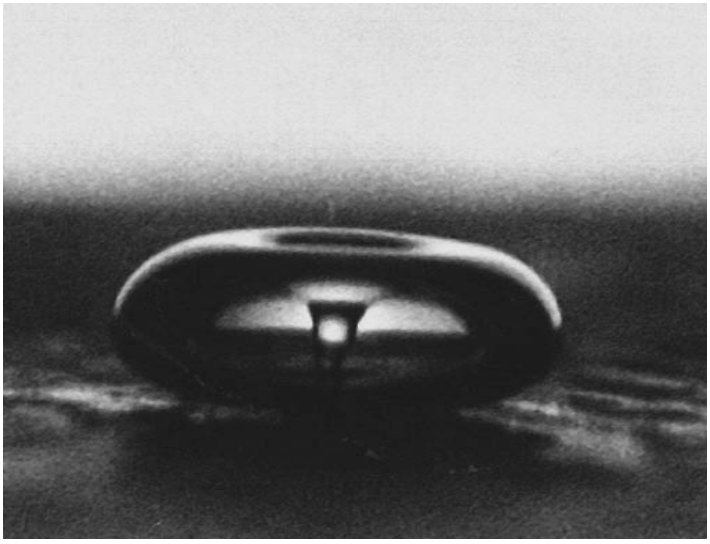

Figure 1.3. Bubble in a liquid irradiated with ultrasound.

During the formation of bubbles, resulting from expansion of cavities present in solution under ultrasound field, vapour from liquid medium or dissolved organic compound penetrate into these bubbles. These bubbles pulsate in the oscillating pressure field till they reach a critical resonant size. At this stage the bubble can no longer efficiently absorb energy from the sound field to sustain itself. The bubbles then implode (Pandit et al., 2001; Kidak and İnce, 2006). Figure 1.4 shows this acoustic cavitation process.

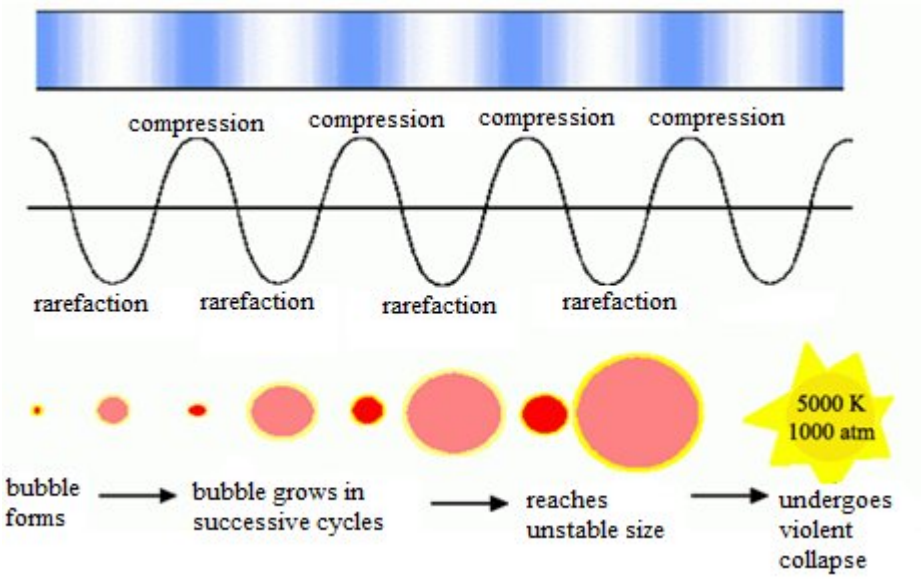

Figure 1.4. Acoustic cavitation process.

The heat from the cavity implosion decomposes water into extremely reactive hydrogen atoms and hydroxyl radicals and hydrogen atoms recombine to form hydrogen peroxide (H_2O_2) and molecular hydrogen (H_2), respectively. Thus, in such a molecular environment, organic compounds and inorganic compounds are oxidized or reduced depending on their reactivity (Sivakumar et al., 2002). Theoretically it has been shown that the temperature inside the cavity could reach about 5000 K in the collapsing bubbles and 1900 K in the interfacial region between the solution and the collapsing bubbles. Also, the effective pressure is around of 1000 atm at the hot spot and the life time of hot spot is under 1 μs (Goel et al., 2004; Lim et al., 2007).

The chain of reactions occurring during sonication of pure water is the following:

$$H_2O))) \rightarrow OH^* + H^* \text{ (Thermolysis)} \quad (1.19)$$

$$OH^* + H^* \rightarrow H_2O \quad (1.20)$$

$$OH^* + OH^* \rightarrow H_2O_2 \quad (1.21)$$

$$2H^{*} \rightarrow H_2 \qquad (1.22)$$

where))) refers to the application of ultrasound.

Three different reaction zones, included by ultrasound in aqueous solution, have been defined during the cavitation process. The first is a gas phase cavity where extremely high temperatures of the order of 5000 K and pressures of the order of 1000 atm are attained. Under such extreme conditions, water molecules dissociate into OH^{*} and H^{*}. The radical species can either recombine or react other gaseous substrates within the cavity. A volatile substrate would be readily taken into cavity and its main decomposition reaction pathway may be one of the thermal decomposition due to direct pyrolysis inside the cavitatation bubbles.

The second region is the interfacial zone between the gas phase and the bulk solution, where large temperature (≈2000 K) and pressure gradient exist. Therefore, at this site substrate can be degraded by two reaction pathways, either by oxidation with hydroxyl radical or by thermal reaction.

The third possible reaction zone involves the bulk solution, where the decomposition of pollutants might occur by the reaction of ultrasonically produced bubbles of hydroxyl radicals diffusing into the bulk solution. Thus, the reaction zone, or degradation pathways, of a particular substrate depends on its chemical nature, for example its volatility, solubility and chemical structure (Okuno et al., 2000; Nam et al., 2003; Kidak and İnce, 2006). Apolar, hydrophobic pollutants with high vapour pressure (volatile organic compounds), such as carbon tetrachloride, tetrachloromethane, tetrachloroethane and chlorobenzene are decomposed according to the direct pyrolysis in the cavitation bubbles, while polar, hydrophilic pollutants with low vapor pressure (non-volatile or semi-volatile) such as phenol, chlorophenol, p-nitrophenol degrade ultrasonically mainly by reaction with hydroxyl radicals in the bulk solution or in the interface between the collapsing cavitation bubble and bulk solution. Sonolysis alone does not achieve the target of total degradation particularly in the case of hydrophilic compounds since it is difficult for them to transfer the hydrophobic regions of the cavitation bubbles, where most of the degradation occurs (Drijvers et al., 1999; Gonze et al., 1999; Wu et al., 2001; Jiang et al., 2002; Entezari et al., 2006; Liang et al., 2007). The mentioned possible reaction zones are shown in Figure 1.5.

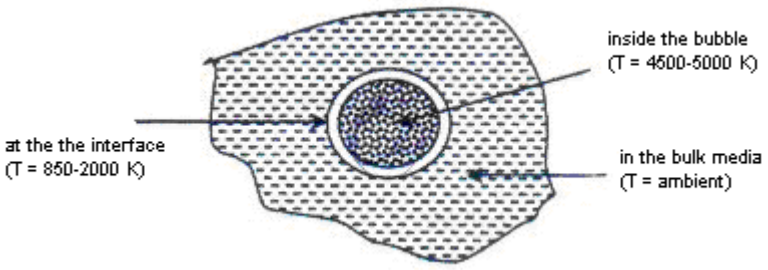

Figure 1.5. Possible reaction zones (Ince et al., 2001).

Ultrasonication can be applied in analytical chemistry in two ways: directly to the sample or indirectly through the walls of the sample container. Direct application is achieved through ultrasonic probes, which are immersed into sample, performing ultrasonication directly over the solution without any barrier to be crossed by the ultrasonication wave other than the solution itself. This approach has several drawbacks. For instance, sample contamination with metals detaching from the probe can be expected. Although modern ultrasonic probes are made from high purity titanium, contamination by metals such as Cr or Al has been reported (Wibetoe et al., 1999). Modern ultrasonic probes made from glass greatly reduce this problem (Santos and Capelo, 2007). Another disadvantage arises from the fact that most ultrasonic probes are used in open approaches, that is, the sample container is not sealed during sample treatment. Consequently, some volatile compounds can be lost. As an example, when the content of the 16 polycyclic aromatic hydrocarbons in the Environmental Protection Agency (USEPA) priority list was studied in sediments, a significant fraction of the most volatile compounds was lost due to the heating produced by the sonication probe used for the solid–liquid extraction process (Capelo et al., 2005).

Indirect application is performed, generally, using an ultrasonication bath, although modern approaches take advantage of the powerful sonoreactor (Santos and Capelo, 2007). In both cases the ultrasonic wave needs first to cross the liquid inside the ultrasonic device and then to cross the wall of the sample container. Therefore, ultrasonication intensity inside the sample container is lower than expected. As ultrasonic baths are not powerful devices, their applications are greatly limited by the lack of ultrasonic intensity. In fact, many ultrasonic applications related to baths can be linked to the heating produced in the liquid that the bath contains – heat that is transmitted to the sample – rather than to actual ultrasonic effects, that is, cavitation (Patricio et al., 2006). However, as

mentioned above, nowadays, a sonoreactor can be used instead of an ultrasonic bath in some regular applications (Santos and Capelo, 2007). A sonoreactor works like a powerful, small ultrasonic bath; it has been shown to be a reliable approach for speeding up chemical reactions in modern areas of analytical chemistry, such as protein identification and metal speciation (Rial-Otero et al., 2007).

1.3 Literature Survey on CWAO of some Carboxylic Acids

Oxidation of lower molecular weight monobasic and dibasic acids such as formic acid, acetic acid, glyoxalic acid, and oxalic acid is often the rate-controlling step during wet air oxidation (WAO) of an aqueous waste stream exhibiting very high chemical oxygen demand (COD). WAO of formic acid, acetic acid, glyoxalic acid and oxalic acid were studied by Shende and Mahajani (1994). The kinetics of WAO of glyoxalic acid and oxalic acid was studied in absence and presence of a cupric sulfate catalyst in the temperature range of 393-518 K and oxygen partial pressure of 3.45- 13.80 bar. The wet oxidation of oxalic acid was found to require more severe conditions as compared to glyoxalic acid. The reaction mechanism and kinetic model have been discussed.

CWAO of aqueous solutions (5 g /dm^3) of formic, oxalic, acetic and maleic acids was carried out with air at 293–463 K on carbon-supported platinum catalysts by Gallezot et al. (1996). CWAO reactions were performed at 1 or 15 bar air pressure in stirred, batch reactors. Total conversion of formic and oxalic acids into carbon dioxide was obtained under very mild conditions (air at atmospheric pressure, 326 K). The Pt/C catalyst was almost inactive for the oxidation of acetic acid but maleic acid was oxidized under moderate conditions (15 bar of air pressure, 405 K).

Gallezot et al. (1997) studied the CWAO of aqueous solution of acetic acid with ruthenium catalysts prepared by ion-exchange of active carbons and high surface area grafites. A total conversion into CO_2 could be achieved between 448 and 473 K using air as oxidizing agent. From measurements of the reaction rates on the Ru/grafite catalyst at different temperatures, pressures and acetic acid concentrations, it was established that the reaction orders were zero and 0.65 with respect to the concentration of acetic acid and oxygen pressure, respectively.

The kinetics of WO of formic acid was studied in the absence and presence of a cupric sulphate as catalyst in the temperature range 423-513 K and oxygen

partial pressure range 3.45-13.80 bar by Shende and Mahajani (1997). And also, wet oxidation of acetic acid was carried out in the presence of cupric sulphate in the temperature range 488-508 K. So, they found that homogeneous copper sulphate as catalyst was very good for oxidation of formic acid and acetic acid.

The study of the intrinsic kinetics of the oxidation of formic acid in a continous-flow stirred slurry reactor over a 1 % Pt/C catalyst was studied by Harmsen et al. (1997) in a temperature range of 282-293 K and a total pressure of 6 bar. The prepared model was based on Langmuir-Hinshelwood kinetics which could predict the steady state disappearance rate of formic acid as a function of the oxygen concentration, the formic acid concentration, the temperature and the pH.

Barbier et al. (1998) studied the total oxidation of acetic acid at 20 bar of O_2 pressure, at a temperature of 473 K over ruthenium catalysts (1-5 %) which were prepared by exchange or impregnation of different supports : CeO_2, TiO_2 or ZrO_2. They found that Ru catalysts supported on a high-surface area ceria had an excellent activity for the oxidation of acetic acid. The following order of activity was obtained: Ru >Ir > Pd≈Fe≈Cu>Ag≈Ni≈Co≈Cr≈unpromoted CeO_2. A kinetic study was performed on a catalyst with Ru particles about 20-30 nm, kinetic order was negative in acetic acid (-0.5) and positive in oxygen (0.5).

The aqueous phase oxidation of acetic acid, used as a model compound for the treatment of controlled ecological life support system (CELSS) waste, was carried out in the monolith froth reactor which utilizes two-phase flow in the monolith channels in the study done by Klinghoffer et al. (1998). The catalytic oxidation of acetic acid was carried out over a Pt/Al_2O_3 catalyst at temperatures and pressures below the critical point of water. Multivariable non-linear regression of temperature-dependent data revealed a reaction order of 1.22 ± 0.54 and an activation energy of 89.8±13.4 kJ/mol. Since the reaction order bracketed first-order kinetics, a pseudo- first-order rate constant of $k_1=10^{5.713\pm2.0}$ exp [81.04±19.0 kJ/mol)/RT] was obtained.

Over a temperature range of 415 -478 K, the catalytic and non-catalytic degradation of an aqueous solution of MA was studied both in the presence of oxygen and under inert atmosphere (nitrogen) by Rivas et al. (1999). In the nitrogen atmosphere, the presence of 0.5 wt% platinum on γ-alumina catalyst pellets significantly enhanced the rate of maleic acid removal. After a reaction

period of 1 h at 443 K, the presence of the catalyst increased MA conversion from 50% to over 90%. In an oxidizing environment, oxygen did not play direct role in heterogeneous catalytic maleic acid degradation. The observed increase in maleic acid removal when oxygen was present was due to the contribution from homogeneous non-catalytic oxidation reactions.

In the oxidation of MA under control of the platinized platinum catalyst potential at 1-5 bar of oxygen pressurized electrochemical reactor at temperatures higher than 343 K, similar catalytic activities and similar evolution of activities versus potential values with and without the control of the catalyst potential were obtained implying the same mechanism involving the occurrence of gaseous oxygen as oxygen source (Epron et al., 1999). It was concluded that the maleic acid needed more severe experimental conditions to be oxidized (T = 383 K, P_{O2} = 1-5 bars) than those for oxalic acid (T = 333 K, $P_{O2} \leq 1$ bar) under the potential control of platinum catalysts (Chollier et al., 1999).

In the study of Beziat and coworkers [1999], the total oxidation of aqueous solutions of carboxylic acids, such as succinic, acetic, glycine, chloroacetic and glycolic acid was investigated using air in a slurry reactor over the temperature range 453-473 K and oxygen partial pressure of 3-18 bar in the presence of a 2.8 % Ru/TiO_2 catalyst. In the study, the influence of various parameters was presented; CWAO of succinic acid was zero order with respect to succinic acid, the order with respect to oxygen pressure was 0.4.

In another study of Shende and Levec, (1999a), wet oxidation kinetics of aqueous solutions of formic, acetic, oxalic, and glyoxalic acids was investigated in a titanium autoclave at a temperature range of 423-593 K and oxygen partial pressures between 8 and 60 bar. They found that oxidation reactions obeyed a first-order kinetics with respect to concentration of all substrates and the activation energies on the basis of acid concentration for acetic, oxalic, and glyoxalic acid oxidation were determined to be 178, 137, and 97 kJ/mol, respectively.

Oxidation of aqueous solutions of 3-hydroxypropionic (3-HPA) and propionic acids (PA) was studied in a titanium high-pressure reactor at 553-583 K using oxygen partial pressures between 10 and 45 bar in the study done by Shende and Levec, (1999b). Oxidation of both acids was found to obey first-order kinetic with respect to their concentrations as well as to their lumped TOC

concentrations. Oxidation rate revealed a half order dependence with respect to oxygen for oxidation of both acids. In the case of 3-HPA oxidation, the activation energy was found to be 135 kJ/mol, and it was 140 kJ/mol when lumped concentration TOC was used. The activation energy for PA oxidation is 150 kJ/mol, and it is slightly higher, 158 kJ/mol, for TOC reduction. Almost complete conversion of 3-HPA was achieved at 573 K after 1 h, whereas 95% conversion of PA acid was obtained at 583 K after 3 h. During oxidation of 3-HPA, 3-oxopropionic and acetic acids were identified as intermediate products. Oxidation of PA yielded acetic and formic acids as intermediates; at oxygen partial pressures above 25 bar and 583 K, the formation of acetic acid was appreciably reduced. In both cases, however, direct oxidation to carbon dioxide and water was found to be the main reaction route.

Oxidation of various acids (acrylic, succinic and acetic acids) was investigated by Oliviero et al. (1999). Depending on the support morphology and the metal/support contact, Ru/CeO_2 catalysts showed very different behavior in catalytic wet air oxidation of acrylic, succinic and acetic acids. TEM and electron diffraction studies favored the hypothesis of a specific role of ceria in oxygen transfer from gas phase to metal sites. About 45 % , 41 % and 97 % conversions were obtained over Ru/CeO_2 catalyst in the oxidation of acrylic, acetic and succinic acids at temperatures of 433 K and 473 K, respectively.

Catalytic wet air oxidation (CWAO) of phenol and of acrylic acid (433 K and 20 bar of O_2) was investigated over Ru/C catalyst and their performance (activity, selectivity to intermediate compounds) compared with that of a reference Ru/CeO_2 catalyst in the study done by Oliviero et al. (2000). Carbon-supported catalysts were very active for the CWAO of phenol but not for acrylic acid. Although high conversions were obtained, phenol was not totally mineralized after 3 h. It was shown that acrylic acid was more strongly adsorbed than phenol. Moreover, the number of contact points between Ru particles and CeO_2 crystallites constituted a key parameter in these reactions. A high surface area of ceria was required to insure O_2 activation when the organic molecule was strongly adsorbed.

In the study of Gomes et al. (2000), aqueous solutions of low molecular weight carboxylic acids, such as acetic, propionic and butyric acids were treated by catalytic wet air oxidation using a carbon supported platinum catalyst. Oxidation in the presence of the catalyst, in a stirred reactor was carried out at 473

K and 6.9 bar of oxygen partial pressure. The conversions obtained after 2 h were 60.2, 75 and 59.4 % for the acetic, propionic and butyric acid.

Centi et al. (2000), compared the CWAO with H_2O_2 of carboxylic acids (formic acid, acetic acid, propionic acid solutions) on homogeneous, Fe_3C catalysts, and heterogeneous Fe_3C-containing zeolite, Fenton type catalysts. Heterogeneous catalyst had a higher reactivity and a reduced dependence on the pH of the solution, but it also had a higher rate of the side reaction of hydrogen peroxide decomposition to water and oxygen.

In another study, catalytic wet air oxidation of maleic acid, oxalic acid and formic acid was carried out in a batch reactor operated at 11 bar or atmospheric pressure. Pt/Al_2O_3 and sulfonated polyresin were used as catalyst. Maleic acid could not be oxidized on the Pt/Al_2O_3 catalyst at all atmospheric pressure and needed high temperature and high pressure operation for its oxidation. On the contrary, oxalic acid and formic acid were readily oxidized into carbondioxide and water at 353 K and atmospheric pressure. When the sulfonated resin catalyst was present together with the Pt/Al_2O_3 catalyst, maleic acid could be oxidized at 353 K and atmospheric pressure (Lee and Kim, 2000).

Oliviero et al. (2001) studied the catalytic wet air oxidation of maleic acid over 5 % Ru/CeO_2 catalysts at temperatures of 433 and 473 K and an oxygen partial pressure of 20 bar. They followed the concentration profiles of liquid phase reaction intermediates of maleic acid; acetic acid was the major compound formed and was relatively refractory at the studied conditions. They found that, at the conditions under consideration, maleic acid is highly reactive and susceptible to both thermal and oxidative degradation.

The catalytic wet air oxidation (WAO) of *p*-coumaric acid (PCA) has been investigated over Fe- and Zn-promoted ceria catalysts in the study done by Neri et al. (2002). The catalysts have been prepared by the coprecipitation method and have been characterized by X-ray diffraction (XRD), BET surface area, SEM–EDX and temperature programmed reduction (TPR). The oxidation reaction was carried out in a batch reactor under an air pressure of 20 bar and in the temperature range 353–403 K. Fe-CeO_2 catalysts, with 20–50 mol% of iron, were found more effective than the unpromoted and Zn-promoted ceria catalysts.

Gomes et al. (2002a), investigated the aqueous solutions of butyric acid by catalytic wet air oxidation using carbon-supported iridium catalyst. Oxidation was carried out under the operating conditions of 6.9 bar of oxygen partial pressure and 473 K of temperature in a stirred reactor. They found that the performance of the iridium catalyst was depent on the method (two and one step incipient wetness impregnation method) of catalyst preparation and pretreatment used (reduction temperature). They also identified the oxidation intermediates such as propionic and acetic acid. A rate equation was modeled considering a heterogeneously catalysed free radical mechanism.

In another study of Gomes et al. (2002b), CWAO of butyric and iso-butyric acid aqueous solutions was investigated in a stirred reactor at 473 K and 6.9 bar of oxygen partial pressure over carbon supported iridium catalysts which were prepared by different incipient wetness impregnation methods and by organometallic chemical vapor deposition. The conversions obtained after 2 h were 43 and 52 % with respect to each caraboxylic acid, when the most active catalyst was used.

The relationship between the state of Ru on CeO_2 and catalytic activity in the wet oxidation of acetic acid was investigated for Ru/CeO_2 catalysts prepared by different methods in the study done by Hosokawa et al. (2003). The temperature programmed reduction (TPR) experiments of Ru/CeO_2 showed that the oxygen species of RuO_2 was reduced at different temperatures depending upon the methods of preparation. Ru species reduced at low temperatures could not be observed by TEM and XRD. It was concluded that Ru–O–Ce bonds in the well-dispersed Ru species are highly fragile and its mobile oxygen was the active species in the wet oxidation.

In the study done by Besson et al. (2003), catalytic wet air oxidation of a representative organic compound (aqueous solution of 5 g/ dm^3 succinic acid at 473 K and 50 bar total air pressure) was investigated over gold on titania prepared from the deposition–precipitation method (with urea or NaOH). The results were compared with the experiments performed over a Ru/TiO_2 catalyst. These preliminary results demonstrated that gold catalysts were efficient for the degradation of succinic acid. The catalytic activity was strongly dependent on the gold particle size characterized by transmission electron microscopy (TEM) with smaller particles producing higher turnover frequencies. Modification of metal dispersion occured during reaction, leading to minor activity.

The wet air oxidation of long-chain carboxylic acids was investigated in the study done by Sanhez-Oneto et al. (2004). Caprylic and oleic acids were selected for the degradation studies. The oxidation process was studied in the temperature range of 473-573 K with a total pressure of 150 bar of synthetic air which means an oxygen excess. The effectiveness of the process was followed in terms of the dissapearance of carboxylic acids and in tems of COD removal. The oxidation was found to be pseoudo first order with respect to the carboxylic acid concentration and the activation energies were 55.5 kJ/mol for caprylic acid and 53.8 kJ/mol for oleic acid. Acetic acid was found to be the main intermediate in the oxidation process and therefore a generalized kinetic model based on the formation and elimination of acetic acid was also applied to the experimental data.

In the study done by Gomes et al. (2004) carbon supported platinum and iridium catalysts were tested in butyric acid oxidation in the temperature range of 453-473 K at an oxygen partial pressure of 6.9 bar. A significant conversion above 70 % was obtained depending on the catalyst used. The long term deactivation resistance of the Pt/C catalyst was higher than that of the Ir/C catalyst. The deactivation observed with the Ir/C catalyst was attributed to the over oxidation of the surface of iridium by molecular oxygen. A kinetic model describing the observed deactivation phenomena in the Ir/C catalyst was proposed and tested using the experimental data obtained in the CWAO of the systems studied.

In another study done by Gomes et al. (2005) carbon supported Pt catalyst was prepared by incipient wetness impregnation and by organometallic chemical vapor deposition methods to test their activity in the oxidation of butyric acid at temperatures reange of 453-473 K at an oxygen partial pressure of 6.9 bar. Significant conversions and 100 % selectivity towards water and non-carboxylic acid products were observed for both systems. The initial rate was used to compare the performance of the two catalytic materials and direct correspondence to the metal dispersion was found. No metal leaching was observed during the reactions and no significant deactivation occurred in the runs. A kinetic model based on the Langmuir-Hinshelwood formulation was applied and the results were analyzed in terms of a heterogeneously catalyzed free radical mechanism.

In another study, CWAO of acetic, succinic and p-coumaric acids were investigated over Pt and Ru catalysts on TiO_2 and ZrO_2 supports in an autoclave reactor at 413 and 463 K and 50 bar total air pressure (Perkas et al. 2005). Pt and

Ru catalysts on mesoporous (MSP) TiO_2 and ZrO_2 were developed using sonochemical irradiation. The catalysts were characterized by XRD, TEM, HR TEM, EDX, and BET methods. The high homogeneity of the active metal phase was confirmed by electron microscopy. The high activity and stability of Pt supported on a TiO_2 (MSP) catalyst in the removal of succinic and p-coumaric acids, and intermediates of their oxidation were demonstrated. The catalytic performances of Ru/TiO_2 (MSP) were similar to those of the catalysts prepared by incipient-wetness impregnation of commercial TiO_2 supports.

Catalytic wet air oxidation of stearic acid was carried out in a batch reactor over ceria supported Ru, Pd, Pt and Ir catalyts at a tempertaure of 473 K and 20 bar of oxygen partial pressure in the study done by Renard et al. (2005). The influence of reaction conditions such as temperature, oxygen partial pressure and stearic acid concentration were investigated. They observed that reaction occured via a complex mechanism. The molecule of the stearic acid could be oxidized by succesive carboxydecarboxylation yielding essentially CO_2. The catalyst characterization indicated that both noble metal and CeO_2 particles remained stable during the reaction.

Vospernik et al. (2006) applied a catalytic membrane reactor to CWAO of formic acid. A series of Pt doped, tubular ceramic membranes were prepared by the evaporation-crystallization technique. The activity of these membranes was measured in the process of liquid-phase oxidation of aqueous formic acid solutions (0.2-10 g/dm^3), carried out in a semi-batch three phase reactor system by using air or oxygen. The influence of trans-membrane pressure difference, reaction temperature, catalyst loading and re-circulation rate on the extent of formic acid removal was measured in a wide range of operating conditions. A mathematical model that captured essential physics of the process was developed to predict concentration profiles of reactants within the membrane wall and the thickness of reaction zone. The calculations showed that the productivity of membrane contactor was influenced by the concentration of dissolved oxygen in the reaction zone as well as by the molar ratio of reactants, the latter being dependent on formic acid conversion.

No-noble metal CeO_2–TiO_2 catalysts prepared by sol–gel method were developed and examined for catalytic wet air oxidation (CWAO) of acetic acid in the study done by Yang et al. (2006) . The structure of the catalysts was measured by BET, SEM, XRD, XPS and DTA-TG. They investigated the effect of the

interactions of Ce and Ti on the structure of CeO_2–TiO_2 catalysts. The mechanisms of the relationships between the different content of Ti and the activity of CeO_2– TiO_2 catalysts were discussed. The results showed that the average crystal size of CeO_2 decreased and the surface areas increased; the low valence of Ce^{3+} increased, and the chemisorbed oxygen slightly decreased with the increase of Ti content on the surface of CeO_2–TiO_2 catalysts. The order of the activity in CWAO of acetic acid followed: Ce/Ti 1/1 > Ce/Ti 3/1 > Ce/Ti 1/3 > Ce/Ti 5/1 > CeO_2 > TiO_2 > no catalyst. In CWAO of acetic acid, the optimal atomic ratio of Ce and Ti was 1, and the highest COD removal was over 64% at 503 K, 50 bar and 180 min reaction time over Ce/ Ti 1/1 catalyst. The excellent activity and stability of CeO_2–TiO_2 catalysts were observed in this study.

The WAO kinetics of aqueous solutions of butyric acid was studied in a stainless steel autoclave over a temperature range of 473-593 K with a total pressure of 150 bar of synthetic air, which provided an excess of oxygen in the study done by Sanchez-Oneto et al. (2006). Kinetic models were developed with respect to various concentrations of butyric acid and chemical oxygen demand (COD). Oxidation reactions always obeyed a pseudo-first-order kinetic, but two different activation energies were needed to represent the temperature dependence in two ranges, namely 473-543 K and 543-593 K.

In the study done by Milone et al. (2006) catalytic wet air oxidation of p-coumaric acid was investigated at 353 K at P = 20 bar, using CeO_2, Pt and Au supported on CeO_2 catalysts. The influence of the metal and of the preparation method of the catalysts on the catalytic activity was investigated. Upon addition of Pt to CeO_2, the rate of oxidation of p-coumaric acid increased whereas addition of gold did not lead to a significant difference of the activity of CeO_2. On all the catalysts investigated, the abatement of total organic carbon (TOC) was ≥ 80% after 300 min of reaction. Catalysts containing metallic platinum were the most effective towards the mineralization of the organic carbon to CO_2 and the degree of mineralization (DM%) was higher than 50%. On CeO_2 and Au–CeO_2 catalysts a great contribute to the abatement of TOC was given from a significant adsorption of the organic substrates on the solid.

In the study of Gündüz and Dükkancı (2007), CWAO of oxalic acid was investigated in a stirred reactor over a Pt (0.7 % in wt) /Al_2O_3 catalyst at atmospheric pressure in a concentration range of oxalic acid 0.5-3 g/dm^3 and at a temperature range of 313-353 K. The conversions obtained after 5 h were 29.0 %,

45.9 % and 30.7 % for initial concentrations of 0.5, 1.5 and 3 g/dm^3, respectively. A rate equation of oxalic acid was determined from measurements of initial rates at different temperatures, catalyst mass loads and at different initial concentrations of oxalic acid.

Catalytic wet air oxidation (CWAO) of aqueous solution of acetic acid was carried out with pure oxygen (20 bar) at 473 K in a stirred batch reactor on platinum supported oxide catalysts (Pt/oxide, oxide = CeO_2, $Zr_{0.1}Ce_{0.9}O_2$, $Zr_{0.1}(Ce_{0.75}Pr_{0.25})_{0.9}O_2$ and ZrO_2) prepared by sol-gel method by Mikulova et al. (2007a). The highest conversion was obtained for Pt catalyst supported over pure ceria. Platinum was loaded on oxides by impregnation (5 wt%), and then the catalysts were reduced under H_2. Homogenous dispersions of 2–3 nm metal crystallites were obtained. The catalytic activity depended on the ability of the support to resist to the formation of carbonates.

In the study done by Mikulova et al. (2007b), platinum catalysts were prepared by impragnation on pure commercial ceria and $Zr_{0.1}(Ce_{0.75}Pr_{0.25})_{0.9}$ O_2 sol-gel mixed oxides were synthesized for CWAO of acetic acid. The influence of the platinum sintering (reducing treatment) was studied for both supports. They observed poisining effect occured during the catalytic testing. PtZrCePr samples were less active than ceria support catalysts.

Catalytic wet-air oxidation of aqueous solutions of formic acid, acetic acid and phenol was carried out in a trickle-bed reactor at T = 328–523 K and total pressures up to 50 bar over various Ru/TiO_2 catalysts in the study done by Pintar et al. (2008). Complete oxidation of formic acid was obtained at mild operating conditions, and no catalyst deactivation occurred that could be attributed to the dissolution of active ingredient material. It was observed that besides oxidation route thermal decomposition contributed significantly to the removal of formic acid; Ru/TiO_2 catalysts could be thus efficiently used for transformation of HCOOH to H_2 and CO_2 in an inert atmosphere. Liquid-phase oxidation of acetic acid was found to be structure sensitive; the highest catalyst activity was obtained, when Ru phase on the catalyst surface prevailed in zero-valent state. Due to simultaneous oxidation of metallic Ru to RuO_2 during the reaction course, correspondingly lower conversion of acetic acid was measured in the reactor outlet. The employed Ru/TiO_2 catalysts enabled complete removal of phenol and TOC at temperatures above 483 K; at these conditions, no carbonaceous deposits were accumulated on the catalyst surface. Apparent catalyst deactivation observed

at temperatures below 463 K was attributed to strong adsorption of partially oxidized intermediates on the catalyst surface, which could be avoided by conducting the CWAO process at sufficiently high temperatures.

In the study done by Wang et al. (2008) ruthenium catalysts were prepared by impregnation of different supports: ZrO_2, CeO_2, TiO_2, ZrO_2–CeO_2 and TiO_2–CeO_2. Their activities for acetic acid oxidation in aqueous solution were investigated in a stirred reactor at a reaction temperature of 473 K and total pressure of 40 bar. The order of the catalyst activity obtained was RuO_2/ZrO_2–CeO_2 > RuO_2/CeO_2 > RuO_2/TiO_2–CeO_2 > RuO_2/ZrO_2 > RuO_2/TiO_2, which corresponded to surface concentration of non-lattice oxygen (defect-oxide or hydroxyl-like group) of these catalysts. The non-lattice oxygen on the catalyst surface played an important role in the catalytic activity.

In another study CWAO of acetic acid was investigated over CeO_2 supported Ru catalysts and results were compared with the oxidation of acetic acid over Pt catalysts by Gaalova et al. (2010). Commercial CeO_2 and CeO_2 which was prepared by sol-gel method was used in the experiments. The comparison of the results showed that initial intrinsic activity of ruthenium was not significantly influenced by the type of the support, which was contrast to platinum. Furthermore, the particle size of Ru had an important effect on CWAO activity: the higher the particle size, the better the activity. This was different with Pt-catalysts, where the optimal particle size was smaller, having about 15% of metal dispersion.

As seen from the literature survey, up to now, CWAO of BA was studied only on carbon supported Pt, Ir, Cu, Co or Ni catalysts. On the other hand, in literature, CWAO of butyric acid was studied in a temperature range of 453 K – 493 K (Gomes et al., 2000, Gomes et al., 2002a, Gomes et al., 2002b, Gomes et al., 2004, Gomes et al., 2005) and in non-catalytic oxidation of BA a temperature range of 473-593 K (Sanchez-Oneto et al., 2006). No study on CWAO of butyric acid was declared at temperatures lower than 453 K. In this PhD Thesis, CWAO of butyric acid aqueous solution was investigated at atmospheric pressure over TiO_2, SiO_2, Al_2O_3 or AC supported Pt, Pd and Ru catalysts and on two commercial catalysts. In addition to this, oxidation of BA was investigated on the commercial catalyst, in an oxygen pressure range of 2.8 – 9.7 bar and in a temperature range of 393- 453 K which was lower than that in literature.

On the other hand, it was seen that CWAO of MA was studied in literature on Pt/Al_2O_3 , platinized platinum, potential controlled platinum catalyst and Ru/CeO_2 catalysts (Epron et al., 1999, Chollier et al., 1999, Rivas et al., 1999, Lee and Kim, 2000, Oliviero et al., 2001). The temperature range of 415-478 K used for CWAO of MA on Pt/Al_2O_3 was rather high with respect to the temperatures used in this study (393-423 K). The effect of support on oxidation degree of butyric and maleic acids was not also presented up to now. Therefore, we will concentrate our attention on the effect of support type for noble metal catalysts such as Pt, Pd and Ru, impregnated on the support in CWAO of butyric and maleic acids dissolved in water. A search of the literature reveals that no study has been reported on the CWAO of above mentioned acids at atmospheric pressure over noble metal catalysts prepared on several supports such as SiO_2, TiO_2 and Al_2O_3, excepts the one done by Lee et al. 2000. And also there is not any study on CWAO of BA and MA over Ru-Pd/AC catalyst.

For this purpose, in the first part of this study CWAO of maleic and butyric acid over prepared catalysts was carried out at atmospheric pressure. The prepared catalysts were characterized by nitrogen adsorption, SEM, XRD and IR studies. After the selectivity studies at atmospheric pressure, the effect of initial concentration, catalyst loading, temperature and oxygen pressure on CWAO of butyric and maleic acid were discussed over the most selective catalyst in a high pressure reactor. The proper kinetic model was also developed for CWAO of butyric and maleic acid.

The literature survey is summarized in Table 1.3.

Table 1.3. Summary of the literature survey on CWAO of some carboxylic acids.

Authors	Year	Compounds	Reaction conditions	Analysis Technique	Catalyst	Results
Shende and Mahajani	1994	Glyoxalic and oxalic acids	393-518 K 3.45-13.80 bar of oxygen partial pressure	COD	Cupric sulfate	100% and 30 % conversions for glyoxalic and oxalic acid after 5h
Gallezot et al.	1996	Formic, oxalic, acetic and maleic acids	293-463 K 1-15 bar air	HPLC	Pt/C	At atmsopheric pressure for FA and OA %100 conversion, catalyst was inactive on the oxidation of acetic acid but maleic acid was oxidized under moderate conditions (15 bar of air pressure, 405 K).
Gallezot et al.	1997	Acetic acid	448-473 K 100 bar	HPLC, TOC	Ru/C and Ru/HSAG* graphite catalyst	100 % conversion over 3.4 % Ru/HSAG after 80 min.
Shende and Mahajani	1997	Formic and Acetic acids	3.45-.13.80 bar O_2 partial pressure. 423-513 K for Formic acid, 488-508 K for Acetic acid.	GC and IR Spectroscopy	Cupric Sulphate	Catalyst was active for both acids, noncatalytic wet oxidation of both formic and acetic acids were found to be 1st order.
Harmsen et al.	1997	Formic acid	282-293 K 6 bar total pressure	HPLC and GC	Pt/C	Rate increases as both the formic acid conc. and oxygen partial pressure increases, at 300 mol/m^3 conc. of formic acid rate is 50 mmol/kg_{cat}.s
Barbier et al.	1998	Acetic acid	473 K 20 bar of oxygen partial pressure	HPLC and GC	Ru/CeO_2, Ru/TiO_2 and Ru/ZrO_2	82 %, 14 %, 12 % conversions for Ru/CeO_2, Ru/TiO_2 and Ru/ZrO_2 catalyst after 60 min.
Klinghoffer et al.	1998	Acetic acid	473-513 K 138 bar of O_2 pressure	GC	Pt/Al_2O_3	50 % conversion at 513 K after 200 min
Rivas et al.	1999	Maleic acid	415-478 K 4-14 bar of O_2 partial pressure	HPLC and COD	Pt/Al_2O_3	100 % COD reduction after 20 min at 463 K
Epron et al.	1999	Maleic acid	398 K 1-5 bar of O_2 pressure	HPLC	Platinized-platinum catalyst	90 % after 1000 min at 398 K
Chollier et al.	1999	Maleic and oxalic acids	333-383 K 1-5 bar of O_2 pressure	HPLC	Platinized-platinum catalyst	100 % conversion for oxalic acid at 333 K, 1 bar 90 % after at 398 K, 5 bar
Beziat et al.	1999	Succinic, acetic, chloroacetic and glycolic acids	453-473 K 3-18 bar oxygen partial pressure	HPLC	Ru/TiO_2	100 % and 80 % conversions of succinic, glycolic, chloroacetic acids and acetic acid after 180, 30 and 420 min.

Shende and Levec	1999a	Formic, acetic, oxalic and glyoxalic acids	423-593 K 8-60 bar of O_2 partial pressure	HPLC and TOC	$CuSO_4$	90 %, 20 %, 67.7 % and 100 % TOC conversions for formic, acetic, oxalic and glyoxalic acids
Shende and Levec	1999b	Propionic and 3-hydroxypro-pionic acids	553-583 K 10-45 bar	HPLC and TOC	-	100 % and 95% for 3-HPA and propionic acids at 573 and 583 K after 60 min and 180 min
Oliviero et al.	1999	Acrylic, succinic and acetic acids	433-473 K 20 bar of O_2 partial pressure	HPLC and COD	Ru/CeO_2	45 % , 41 % and 97 % conversions for acrylic, acetic and succinic acids
Oliviero et al.	2000	Phenol and acrylic acid	433 K 20 bar of O_2 partial pressure	HPLC	$Ru\text{-}CeO_2/C$ Ru/CeO_2 Ru/C	40 %, 100% and 38 % conversions for acrylic acid over $Ru\text{-}CeO_2/C$, Ru/CeO_2 and Ru/C catalysts
Gomes et al.	2000	Acetic, propionic and butyric acids	473 K 6.9 bar of O_2 partial pressure	GC	Pt/C	For acetic, propionic and butyric acids after 120 min 60.2%, 75.0% and 59.4 % conversions
Centi et al.	2000	Formic, acetic and propionic acids	343 K H_2O_2 as O_2 source	IC	Homoge-neous Fe_3C, heterogene ous Fe_3C-zeolit	80%, 60% and 20% conversions for propionic, formic and acetic acids after 250 min
Lee and Kim	2000	Maleic, oxalic and formic acid	453 K-11 bar for maleic acid 353 K at atm pressure for oxalic and formic acid	HPLC	Pt/Al_2O_3	100 % conversion of maleic acid after 40 min and 90 % and 100 % conversions for oxalic and formic acid, respectively after 30 and 20 min.
Oliviero et al.	2001	Maleic acid	433-473 K 20 bar of oxygen partial pressure	HPLC	Ru/CeO_2	100 % conversion after 60 min
Neri et al.	2002	p-coumaric acid	353-403 K 20 bar	HPLC and TOC	Fe/CeO_2	100 % conversion at 373 K after 50 min
Gomes et al.	2002a	Butyric acid	453-473 K 6.9 bar of O_2 partial pressure	GC	Ir/C, Pt/C, Cu/C, Co/C, Ni/C, C	80 %, 65 %, 15 %, for Pt/C, Ir/C, Cu/C and about 2 % for Co/C, Ni/C, C catalysts after 500 min.
Gomes et al.	2002 b	Butyric acid iso-butyric acid	453-473 K 6.9 bar of O_2 partial pressure	GC	Ir/C	43 % and 52 % for butyric and i-butyric acid after 120 min

Hosokawa et al.	2003	Acetic acid	443-463 K 15 bar of O_2 pressure	TOC	Ru/CeO_2	100 % TOC conversion after 60 min
Besson et al.	2003	Succinic acid	473 K 50 bar of total air pressure	HPLC	Au/TiO_2	100 % conversion after 120 min
Sanchez-Oneto et al.	2004	Caprylic and oleic acids	453-473 K 150 bar of synthetic air pressure	GC and COD	-	90 % COD removal after 10 min at 573 K for both acids
Gomes et al.	2004	Butyric acid	453-473 K 6.9 bar of O_2 partial pressure	GC	Pt/C Ir/C	75% and 60% conversion over Pt/C and Ir/C catalysts after 500 min
Gomes et al.	2005	Butyric acid	453-473 K 6.9 bar of O_2 partial pressure	GC	Pt/C	59.4% and 46.6% conversion according to catalyst preparation tech. After 500 min
Perkas et al.	2005	Acetic, succinic and p-coumaric acids	413-463 K 50 bar of total air pressure	HPLC and TOC	Pt and Ru on TiO_2 and ZrO_2	100 % conversion after 70 and 180 min.
Renard et al.	2005	Stearic acid	473 K 20 bar of O_2 partial pressure	HPLC and GC	Ru, Pd, Pt ve Ir supported on CeO_2	Over Pt/CeO_2, Pd/CeO_2, Ir/CeO_2, Ru/CeO_2, CeO_2 catalysts 95 %, 80%, 75%, 70% and 65% conversions after 180 min
Vospernik et al.	2006	Formic acid	298-318 K 1 bar	TOC	Pt doped, tubular ceramic membranes	90% conversion at 308 K after 160 min
Yang et al.	2006	Acetic acid	503 K 50 bar of total pressure	COD	CeO_2–TiO_2 With diffrent interrac-tions	64% COD removal at 503 K over Ce/ Ti 1/1 catalyst after 180 min
Sanchez-Oneto et al.	2006	Butyric acid	473-593 K 150 bar of synthetic air	GC and COD	-	100 % conversion at 593 K after 80 min

Milone et al.	2006	p-coumaric acid	353 K 20 bar	HPLC and TOC	Pt/CeO_2 and Au/CeO_2	Up to 80 % TOC conversion over different Pt/CeO_2 and Au/CeO_2 catalysts
Gündüz and Dükkancı	2007	Oxalic acid	313-353 K At atmospheric pressure	Titration with NaOH	Pt/Al_2O_3	45.9 % conversion after 300 min
Mikulova et al.	2007a	Acetic Acid	473 K 20 bar	HPLC and TOC	Pt on CeO_2, $ZrCeO_2$, $ZrPrCeO_2$ and $ZrCeO_2$	Conversion in the range of 20 - 80 % according to support type
Mikulova et al.	2007b	Acetic Acid	473 K 20 bar	HPLC and TOC	Pt on CeO_2, $ZrPrCeO_2$	Conversion in the range of 5 - 30 % according to supoort type
Pintar et al.	2008	Formic, acetic acid and phenol	328-523 K 50 bar of total pressure	HPLC and TOC	Ru/TiO_2	90 % and 95% TOC removal at 433and 523 K for formic acid and acetic acid and phenol
Wang et al.	2008	Acetic acid	473 K 40 bar of total pressure	HPLC	Ru on ZrO_2, CeO_2, TiO_2, ZrO_2–CeO_2 and TiO_2–CeO_2 supports	Order of catalytic activity RuO_2/ZrO_2–CeO_2 > RuO_2/CeO_2 > RuO_2/TiO_2–CeO_2 > RuO_2/ZrO_2 > RuO_2/TiO_2
Gaalova et al.	2010	Acetic acid	473 K 20 bar of O_2 pressure	HPLC and TOC	Ru and Pt on CeO_2	Conversion in the range of 30 - 40 % according to support type

1.4 Literature Survey on Ultrasonic Degradation of Some Carboxylic Acids

Ultrasonic degradation of volatile fatty acids (propionic, butyric and valeric acids) were investigated by Yoo et al. (1997), with concentrations of about 0.9 mM at 200 kHz ultrasound with a power of 6 W/m^2 per unit volume in a sonochemical reactor under ambient temperature and pressure conditions. They observed that, the concentration of acid decreased with irradiation time, indicating pseudo-first order kinetics. Obtained degradation degrees were about 40 %, 72 % and 78 % for propionic, butyric and valeric acids after 120 min.

Gogate et al. (2003) studied the sonolytic degradation of formic acid using dual frequency flow cell, triple frequency flow cell, ultrasonic horn and ultrasonic bath. Larger frequencies of irradiation were found to be more beneficial in degradation of formic acid. They investigated the effect of several operating parameters such as time of destruction, initial concentration of the pollutant, intensity and frequency of irradiation, introduction of air and liquid level in the case of ultrasonic bath on the extent of degradation.

Efficiency of a novel configuration for large-scale wastewater treatment applications was investigated in the study done by Bhirud et al. (2004) using formic acid degradation as a model reaction. The reactor was first characterized using energy efficiency measurements and the optimum operating volume for maximum transfer of supplied energy and hence maximum cavitational effects was established. Effect of initial concentration of the pollutant on the rates of degradation was investigated. Comparison was also made with the conventional ultrasonic horn in terms of energy efficiency and cavitational yield for the model reaction.

In another study, ultrasonic degradation of aqueous solution of oxalic acid was investigated by Dükkancı and Gündüz (2006). The effect of parameters such as ultrasonic power, H_2O_2, NaCl, external gases on the degradation of oxalic acid was discussed by using ultrasonic bath. In the study, the obtained degradation of oxalic acid was about 10 % and it was found that degradation of oxalic acid could be described by first order kinetics.

Direct and indirect sonication of acetic acid was studied by Fındık et al. (2006) and Fındık and Gündüz (2007). In the direct sonication, ultrasonic degradation of acetic acid was investigated at low powers (0.1-0.4 W) and in a

frequency range of 30-100 kHz by using an ultrasonic transducer. In the first study, the results showed that there was an optimum frequency at 60 kHz and degradation rate increased up to a power of 0.2 W and then it decreased. In the other study on indirect degradation of acetic acid, the effect of parameters such as, power, initial concentration, addition of NaCl or several oxides was investigated by using ultrasonic bath at a frequency of 40 kHz with the power range of 70-98 W.

In the study on direct sonication of aqueous solution of oxalic acid, different frequencies (30-100 kHz) and low powers (0.1-0.4 W) were tested by using ultrasonic transducer. The obtained conversion was about 4 % for direct sonication of oxalic acid. Degradation of oxalic acid could be described by first order kinetics (Dükkancı et al., 2007).

In the study done by Okitsu et al. (2009) the sonochemical decomposition of butyric acid was performed in an aqueous solution by use of 200 kHz ultrasound to discuss the reaction kinetics and molecular behavior during cavitation., They proposed a heterogeneous reaction kinetics model, taking into account a Langmuir-type adsorption model, which was based on the local reaction zone at the interface region of the cavitation bubbles, where the adsorption and desorption of butyric acid molecules from the bulk solution occured during bubble oscillation and then the existing molecules inside the local reaction zone were finally decomposed. Also the rates of decomposition were investigated as a function of the initial concentration of butyric acid in the different pH solutions. It was found that the rate of the butyric acid decomposition was faster in the acidic solution.

The literature survey is summarized in Table 1.4.

Table 1.4. The summary of literature survey on the ultrasonic degradation of some carboxylic acids.

Authors	Year	The studied compounds	Analysis Technique	Experimental conditions	Results
Yoo et al.	1997	Propionic, butyric and valeric acid	Ion chromatog-raphy	Multiwave ultrasonic generator and barium titanate oscillator, at 200 kHz and 6 W/m^2	40 %, 72 % and 78 % for propionic, butyric and valeric acids after 120 min.
Gogate et al.	2003	Formic acid	Volumetric titration with NaOH	22.7 kHz-240 W Ultrasonic horn, 22 kHz-120 W ultrasonic bath, 25 and 40 kHz-120 W dual frequency flow cell, 20, 30 and 50 kHz-900 W triple frequency flow cell was used as cavitation equipment. The effects of the parameters; time of destruction, initial conc., intensity, frequency, introduction of air and liquid level were investigated.	15 % conversion at 0.1g/dm^3 after 120 min for ultrasonic horn; 5 %, 4.5 % and 4 % conversion at 25+40, 40 and 25 kHz; 6.5 %, 5 %, 4 %, 3.5 %, 3 % and 2.5 % at 20+30+50 kHz, 50 kHz, 20+50 kHz, 20+30 kHz, 30 kHz and 20 kHz after 90 min.
Bhirud et al.	2004	Formic acid	HPLC	Sonochemical reactor 36 kHz, 150 W (supplied power 127.5 W)	About 25 %, 13 %, 9% and 5 % degradations for 0.1, 0.5, 0.75 and 1 g/dm^3 initial conc.
Fındık et al.	2006	Acetic acid	Volumetric titration with NaOH	Ultrasonic transducer was used for sonication, the effects of the parameters; frequency (30-100 kHz) and power (0.1-04.W) were studied	7 % conversion at 60 kHz-0.2 W after 60 min.

Dükkancı and Gündüz	2006	Oxalic acid	Volumetric titration with NaOH	Ultrasonic bath (40 kHz and 70-112 W) was used for sonication, the effects of the parameters; ultrasonic power, H_2O_2, NaCl, external gases were investigated.	15 % conversion at 112 W, 0.3 g/dm^3 after 60 min.
Fındık and Gündüz	2007	Acetic acid	Volumetric titration with NaOH	Ultrasonic bath (40 kHz and 70-112 W) was used for sonication, the effects of the parameters; ultrasonic power, initial conc., addition of NaCl or several metal oxides were investigated.	12 % conversion at 84 W, 0.15 g/dm^3 after 60 min.
Dükkancı et al.	2007	Oxalic acid	Volumetric titration with NaOH	Ultrasonic transducer was used for sonication, the effects of the parameters; frequency (30-100 kHz) and power (0.1-04.W) were studied	4 % conversion at 60 kHz-0.2 W after 60 min.
Okitsu et al.	2009	Butyric and benzoic cid	Ion chromatog-raphy	200 kHz and 200 W ultrasonic generator, Effects of pH and initial conc. were investigated	Butyric acid decomposition was faster in the acidic solution heterogeneous reaction kinetics model

As seen from the litureture survey, only few studies were devoted to ultrasonic degradation of carboxylic acids and most of them were done by our group.

In the second part of this study ultrasonic degradation of butyric and maleic acid was investigated, the effects of parameters such as ultrasonic frequency, ultrasonic power, sonication mode, initial concentration of pollutant, addition of H_2O_2, TiO_2 or natural zeolite to the solution were studied by using three different ultrasound equipment like ultrasonic bath, ultrasonic probe system and ultrasonic reactor.

2. GENERAL INFORMATION ABOUT MATERIALS

Butyric acid and maleic acid and other low molecular weight acids such as, oxalic, formic and acetic acid are formed during the destruction of chemicals including longer chain aliphatic acids or compounds like phenol. As known well, phenol is very toxic to humans and it has been listed as the priority pollutant in the list of the EPA, USA. The acids which mentioned above are also pollutants and are difficult to oxidize by conventional methods because of the extreme conditions required. For this reason maleic and butyric acid were selected as model compounds for CWAO and sonolytic degradation.

Butyric acid is a saturated four-carbon carboxylic acid. It occurs naturally in rancid butter, in much animal fat and in plant oil. Butyric acid is a strong acid and reacts with bases, strong oxidants and metals. It is used to eliminate calcium in leather industry. Butyric acid family products, such as their esters, are used for production of plastics, plasticizer, surfactants and textile auxiliaries. Also they are used as disinfectants (Xu et al., 2005). Table 2.1 presents the chemical and physical properties of butyric acid.

Table 2.1. Physical and chemical properties of butyric acid.

Properties	
Molecular weight	88.1051 g/mol
Appearance	Colorless liquid
Density	0.96 kg/dm^3 (liquid)
Melting point	265 K
Boiling point	437 K
Solubility in water	miscible
Acidity (pK_a)	At 298 K 4.82

Maleic acid is an unsaturated carboxylic acid which is trans form isomer of fumaric acid. Both are used in making polyesters, alkyd resins, plasticizers and lubricating oils. Maleic acid is also used in the preparation of fumaric acid by catalytic isomerization and other chemical products as a carboxylating agent. It is used as an oil and fat preservative and food acidulant, used in dyeing and finishing wool, cotton and silk; and preparing the maleate salts of antihistamines and similar drugs. These acids are present in the waste water of above mentioned industries. Table 2.2 presents the chemical and physical properties of maleic acid.

Table 2.2. Physical and chemical properties of maleic acid.

Properties	
Molecular weight	116.1 g/mol
Appearance	White solid
Density	1.59 kg/dm^3 (solid)
Melting point	404 – 412 K decomposes
Boiling point	408 K decomposes
Solubility in water	78 g/100 ml (298 K)
Acidity (pK_a)	pk_{a1} = 1.92 pk_{a2} = 6.27

These acids and their solutions are corrosive, they are harmful if inhaled or absorbed through the skin, they may burn skin. Contact with the eyes cause irradiation (Oxford University, 2009; Wikipedia, 2010).

3. EXPERIMENTAL STUDIES

3.1 Catalyst Preparation

In this study, Pt, Ru, Pd catalysts in 1 weight percent over different supports such as Al_2O_3 (Riedel), TiO_2 (Sigma), SiO_2 (Camag) and AC (Merck) were prepared in the light of the literature especially using the studies done by Gomes et al., (2000) and by Lee and Kim, (2000). In the catalyst preparation incipient wetness impregnation method was applied.

Support material, except AC, was saturated with n-Hexane (Lab-Scan) or toluene (Merck) (molecular diameter of n-hexane and toluene are 0.45 and 0.57 nm, respectively and both of them are reported in literature for saturation) in order to locate the active metal particles at the exterior surface of support (to eliminate internal mass transfer resistance). Pt (II) acethyl acetonate ($C_{10}H_{14}O_4Pt$) (Acros) or hexachloroplatinic acid (H_2PtCl_6; 5 % aqueous solution) (Riedel) were used as platinum sources. Ruthenium III chloride ($RuCl_3\ 4H_2O$) (Sigma) and Palladium II Nitrate hydrate ($Pd(NO_3)_2\ 12.85\ H_2O$) (Aldrich) were used as Ru and Pd sources, respectively.

3.1.1 Preparation of Pt catalysts from platin (II) acetylacetonate

For the preparation of Pt catalysts on TiO_2, SiO_2 or Al_2O_3 supports in the case that metal source was platin (II) acetylacetonate, firstly, precursor aqueous solution was prepared and added to the support, prior saturated with n-hexane or toluene, drop by drop under good mixing. After processing the catalyst in the ultrasonic bath for good impregnation, it was dried in the vacuum oven at 323 K. Then, catalyst was calcined at 673 K in the programmable furnace with a heating rate of 348 K/min for 4h. Figure 3.1 describes the catalyst preparation schematically.

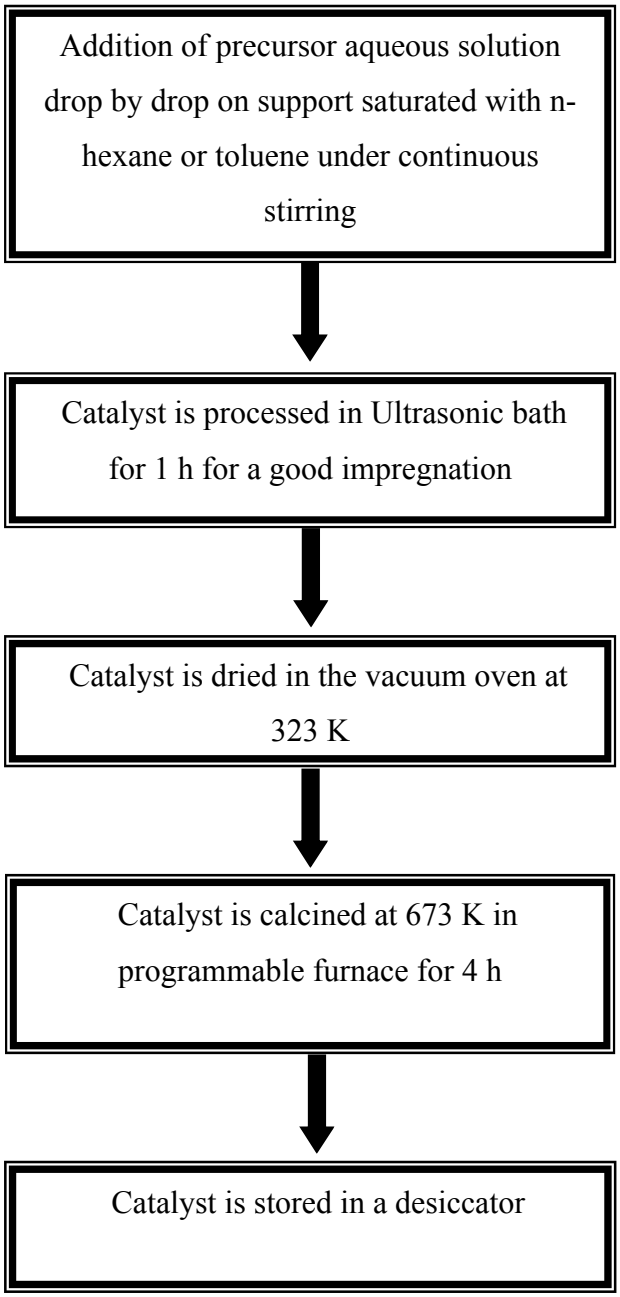

Figure 3.1. Preparation of TiO_2, SiO_2 or Al_2O_3 supported Pt catalysts using platin (II) acetylacetonate as precursor.

3.1.2 Preparation of Pt, Ru and Pd catalysts from hexachloroplatinic acid, Ruthenium III chloride and Palladium II Nitrate hydrate

For the preparation of Pt, Ru and Pd catalysts, in the case that metal source were hexachloroplatinic acid for platinum, Ruthenium III chloride for Ru and Palladium II Nitrate hydrate for Pd, the metal salt aqueous solution was prepared and solution was poured onto the support. Then, the catalyst was processed in the

ultrasonic bath for good impregnation. After drying in oven, they were calcined in a glass reactor under nitrogen flow at 673 K for 2h. After that, reduction was carried out under hydrogen flow at 623 K for 3h. Then finally the catalyst was flushed with nitrogen at 623 K for 30 min. Figure 3.2 describes this second method.

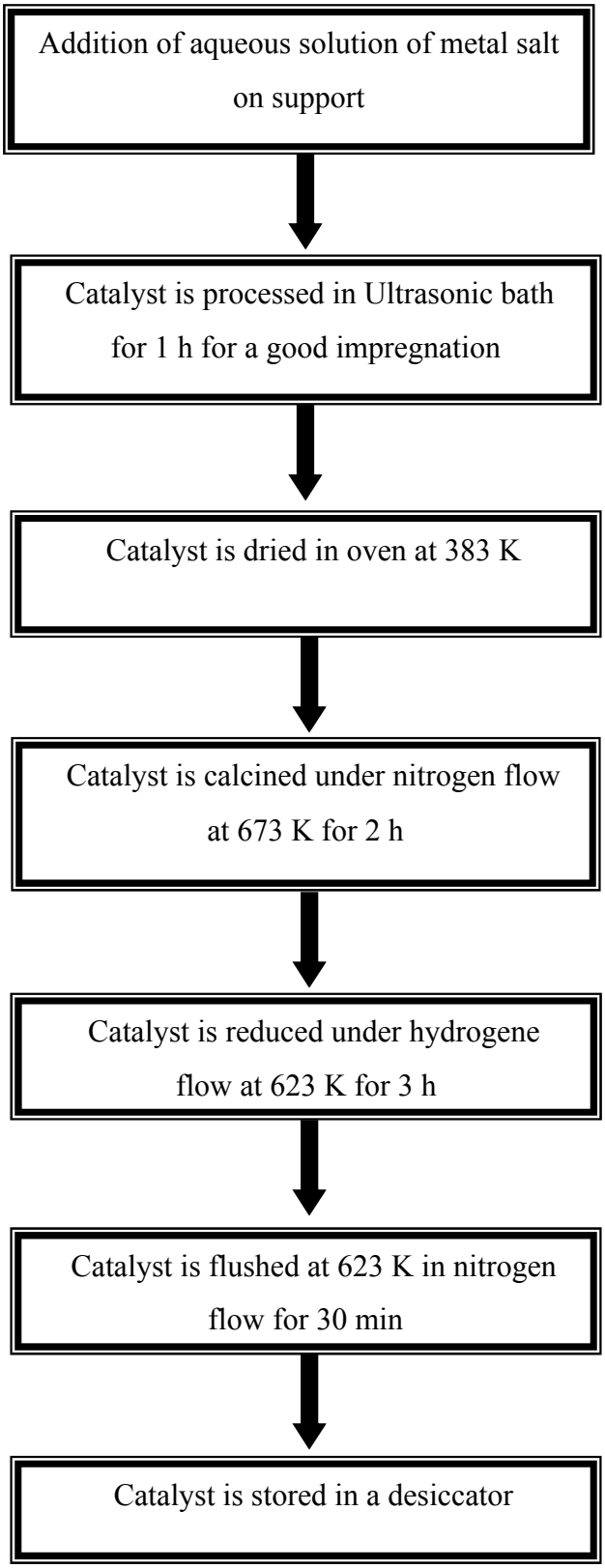

Figure 3.2. Preparation of Pt, Pd or Ru catalysts over TiO_2, SiO_2 or Al_2O_3 supports.

3.1.3 Preparation of Ru-Pd/AC catalyst

Pd-Ru catalyst (1 wt % Pd and 1 wt % Ru) supported on activated carbon (AC) was prepared by coimpregnation method. For the preparation of AC supported Pd-Ru catalyst, firstly carbon (Merck) was washed with deionised water until the effluent was clear in color. The washed carbon was soaked in deionised water for 41 h. After removing the water by filtration, the carbon particles were soaked in a HCl solutions (5 wt %) with stirring to remove impurities on the carbon surface. The acid solution was then removed by filtration and washing with deionised water, then followed by oven drying at 378 K under ambient pressure and then vacuum drying at room temperature for 24 h. After that aqueous solutions of Ruthenium III chloride and Palladium II Nitrate hydrate were poured onto the support. Then, the catalyst for good impregnation was processed in the ultrasonic bath. After drying in oven, it was calcined in a glass reactor under nitrogen flow at 673 K for 2h. After that, reduction was carried out under hydrogen flow at 623 K for 3h. Then, catalyst was flushed in nitrogen at 623 K for 30 min. Figure 3.3 shows the preparation procedure of Ru-Pd/AC catalyst.

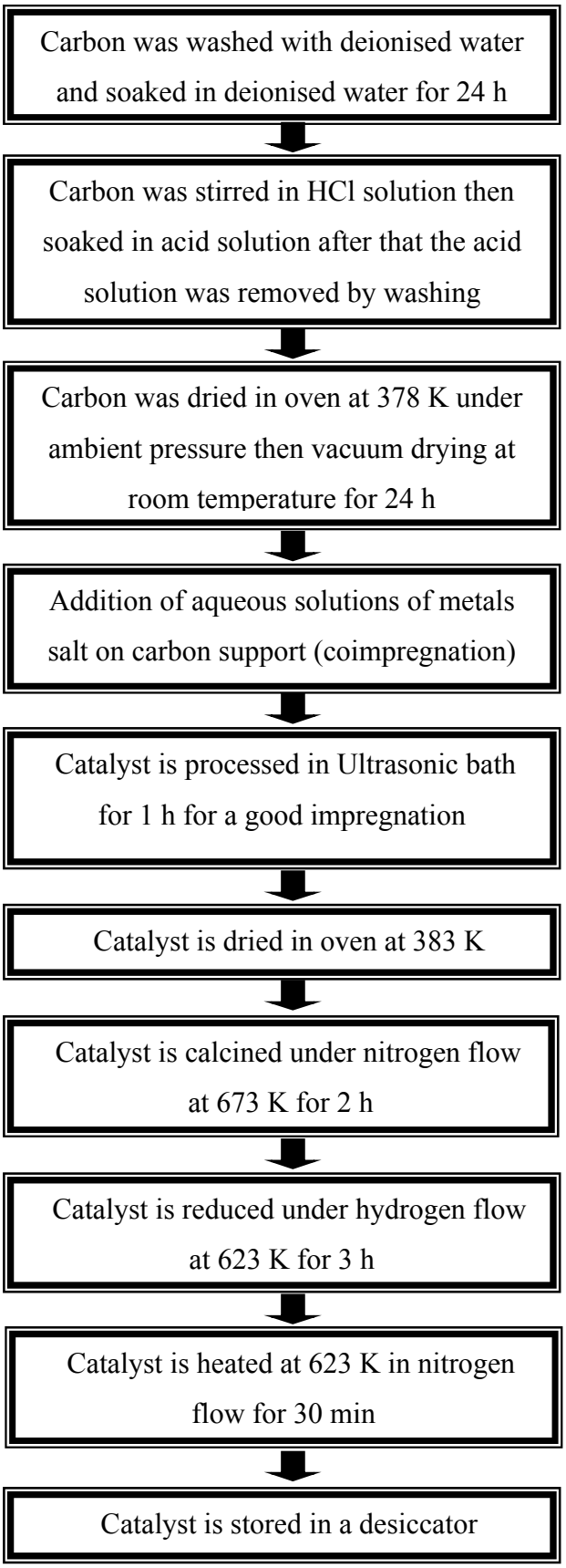

Figure 3.3. Preparation of Ru-Pd/AC catalyst.

Table 3.1 shows all the prepared catalysts with catalyst code, metal source, support material and preparation method used. Table 3.1 includes two commercial catalysts tested in CWAO studies, as well.

Table 3.1. Prepared catalysts.

Catalyst Name	Catalyst Code	Metal Source	Information
Pt-Re/Al_2O_3 (% 0.25 Pt+%0.4 Re /Al_2O_3)	CAT1	-	Commercial
Pt/Al_2O_3 (% 0.29 Pt /Al_2O_3)	CAT2	-	Commercial
Pt/Al_2O_3	Pt/Al_2O_3-1	Pt(II)Acetylacetonate	Saturated with n-hexane Calcined at 673 K
	Pt/Al_2O_3-2	Pt(II)Acetylacetonate	Saturated with toluene Calcined at 673 K
	Pt/Al_2O_3-3	Hexachloroplatinic Acid	Calcined in N_2 flow at 673K Reduced with H_2 at 623 K
Pt/TiO_2	Pt/TiO_2-1	Pt(II)Acetylacetonate	Saturated with n-hexane Calcined at 673 K
	Pt/TiO_2-2	Pt(II)Acetylacetonate	Saturated with toluene Calcined at 673 K
	Pt/TiO_2-3	Hexachloroplatinic Acid	Calcined in N_2 flow at 673K Reduced with H_2 at 623 K
Pt/Silicagel	Pt/SiO_2-1	Pt(II)Acetylacetonate	Saturated with n-hexane Calcined at 673 K
	Pt/SiO_2-2	Pt(II)Acetylacetonate	Saturated with toluene Calcined at 673 K
	Pt/SiO_2-3	Hexachloroplatinic Acid	Calcined in N_2 flow at 673K Reduced with H_2 at 623 K
Ru/ Al_2O_3	Ru/ Al_2O_3-3	Ruthenium III Chloridehydrate	Calcined in N_2 flow at 673K Reduced with H_2 at 623 K
Ru/ TiO_2	Ru/ TiO_2-3	Ruthenium III Chloridehydrate	Calcined in N_2 flow at 673K Reduced with H_2 at 623 K
Ru/ Silicagel	Ru/ SiO_2-3	Ruthenium III Chloridehydrate	Calcined in N_2 flow at 673K Reduced with H_2 at 623 K
Pd/ Al_2O_3	Pd/ Al_2O_3-3	Palladium II Nitratehydrate	Calcined in N_2 flow at 673K Reduced with H_2 at 623 K
Pd/ TiO_2	Pd/ TiO_2-3	Palladium II Nitratehydrate	Calcined in N_2 flow at 673K Reduced with H_2 at 623 K
Pd/ Silicagel	Pd/ SiO_2-3	Palladium II Nitratehydrate	Calcined in N_2 flow at 673K Reduced with H_2 at 623 K
Ru-Pd/Activated carbon	Ru-Pd/AC	Palladium II Nitratehydrate and Ruthenium III Chloridehydrate	Calcined in N_2 flow at 673K Reduced with H_2 at 623 K

3.2 Characterization of Prepared Catalysts

The catalysts prepared were characterized by nitrogen adsorption, SEM, XRD and IR studies. Nitrogen adsorption data of the Al_2O_3 supported catalysts were measured by Demo Tristar 3000 V6.07 A in Italy. Nitrogen adsorption data of AC supported catalyt and Pd/SiO_2-3 were measured using Micromeritics Gemini V2.00. Catalysts were degassed at 573 K for 24 h. Nitrogen adsorption data of the other catalysts were measured at 77 K (normal boiling temperature of liquid nitrogen) in a static volumetric apparatus, Micromeritics ASAP 2010. Catalysts were degassed at 573 K for 3 hours under 5 μm Hg vacuum.

The SEM microphototographs were taken on Philips XL SFEG 30S scanning electron microscopy (SEM).

XRD studies were done on a Philips X-Pert Pro diffractometer (XRD) with CuKα radiation in the region of 2θ between 0-80 °.

The IR measurements of the prepared catalysts were performed at room temperature and atmospheric pressure by Shimatsu 470 IR Spectrophotometer.

3.3 Experimental Set-ups

3.3.1 Experimental set-up for CWAO of butyric acid and maleic acid at atmospheric pressure

A schematic diagram of the experimental set-up used in CWAO of butyric acid (BA) and maleic acid (MA) at atmopsheric pressure was illustrated in Figure 3.4.

The experiments were carried out at atmospheric pressure in a glass reactor. The reactor had four necks. The necks housed a contact thermometer connected to the control unit, a reflux condenser open to atmosphere and a sampling injector. Remained neck was used for adding catalyst. The reactor was heated with a heating mantle (Electrothermal) and the reaction mixture was stirred continuously with a magnetic bar. Air used for oxidation was metered by a U manometer after passing through a serious of columns (containing silica gel and KOH for removal of moisture and CO_2, respectively) and was bubbled into the reaction mixture by a

"L" shaped pipe, inserted through the condenser to the solution. The end of the pipe in the solution had very fine holes (0.5 mm in diameter) for bubbling of air.

For a typical run, 0.15 dm^3 of carboxylic acid aqueous solution with a concentration of 3 g/dm^3 was placed in the reactor and temperature was adjusted to 333 K. After reaching the desired temperature, a sample was taken to determine thermal decomposition of acid during the heating period (about 10 min). The corresponding time was recorded as the starting time of the reaction. Then 1 g of catalyst and air at a flow rate of 0.003dm^3/s were introduced immediately into the reactor while a magnetic bar continuously stirred (500 rpm) the solution.
The samples taken periodically, after centrifugation for 0.5 h, were analyzed with HPLC (HP Agilent 1200). CO_2 was determined by titration of a NaOH solution into which gas outlet stream was bubbled continuously.

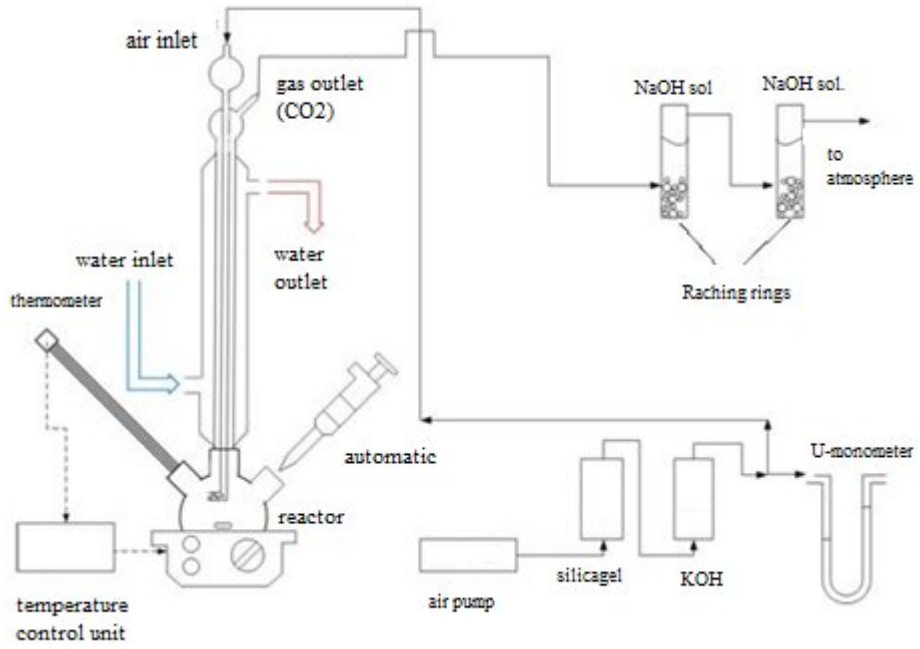

Figure 3.4. Experimental Set-up used in the CWAO of BA and MA at atmospheric pressure.

3.3.2 Experimental set-up for CWAO of butyric acid and maleic acid at pressures higher than atmospheric

A schematic diagram of the experimental set-up used in CWAO of butyric acid (BA) and maleic acid (MA) at pressures higher than atmospheric was illustrated in Figure 3.5.

Oxidation studies of butyric acid (BA) and maleic acid (MA) were performed in a 0.25 dm^3 stainless steel high pressure reactor (Parr 4576) with stirrer, gas supply system and temperature controller. High pressure reactor can be operated at pressures up to 350 bar and at temperatures up to 773 K with a stirrer speed up to 630 rpm. A glass liner (0.25 dm^3) was immersed into the reactor to prevent severe corrosion problems. In a typical run, the reactor was loaded with 0.1 dm^3 of butyric acid (BA) or maleic acid (MA) aqueous solution with known concentration and with known amount of catalyst. Before pressurization with oxygen, the reactor was flushed with nitrogen and then heated to the reaction temperature under continuous stirring (500 rpm). After reaching the desired temperature, the reactor was pressurized with oxygen and this was recorded as the starting time of the reaction. The samples taken periodically, after centrifugation for 0.5 h, were analyzed with HPLC (Agilent 1200).

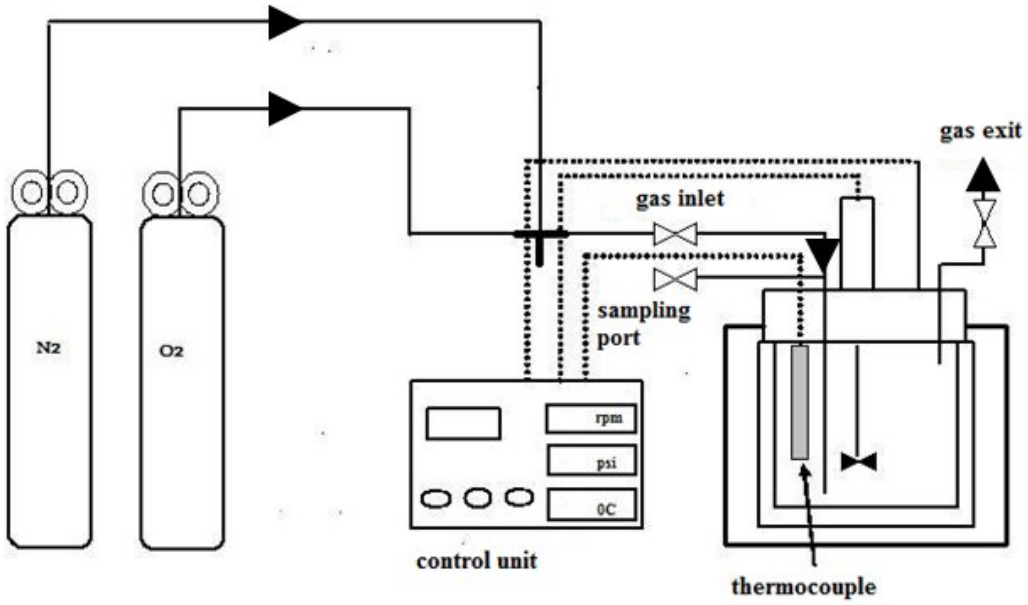

Figure 3.5. Experimental Set-up for CWAO of butyric acid and maleic acid at pressures higher than atmospheric.

3.3.3 Experimental set-ups for ultrasonic degradation of butyric and maleic acids

Three different experimental set-ups, Ultrasonic Reactor, Ultrasonic Bath and Ultrasonic Probe System, were used for the degradation of aqueous solutions of butyric acid and maleic acid.

3.3.3.1 Ultrasonic reactor

The ultrasonic reactor system consisted of an ultrasonic signal generator (Meinhardt, K8) operating between 25-100 W to convert electrical power input into mechanical energy, a piezoelectric transducer with titanium diaphragm (Meinhardt, E/805/T) emiting ultrasound waves at 850 kHz, about 0.75 dm^3 of glass reactor (Meinhardt, 5/1575) to house the butyric or maleic acid solutions, a water cooling jacket to keep the reactor content at constant temperature (293±5 K).

Generator can be used in continuous mode or in pulse mode. Continuous mode produces permanent ultrasound and pulse mode produces square wave pulse ultrasound. Pulse duty factor and pulse duration ratios can be also adjusted. A schematic diagram of the set-up is presented in Figure 3.6.

In this system, during the runs, 0.35 dm^3 of butyric acid or maleic acid solution with a known concentration was sonicated in the desired mode for 1 hour. The temperature of the reaction mixture was kept constant at the 293±5 K by adjusting the flow rate of cooling water. The samples taken periodically from the reaction mixture were analyzed by HPLC. All the experiments repeated at least 3 times mostly 5 times.

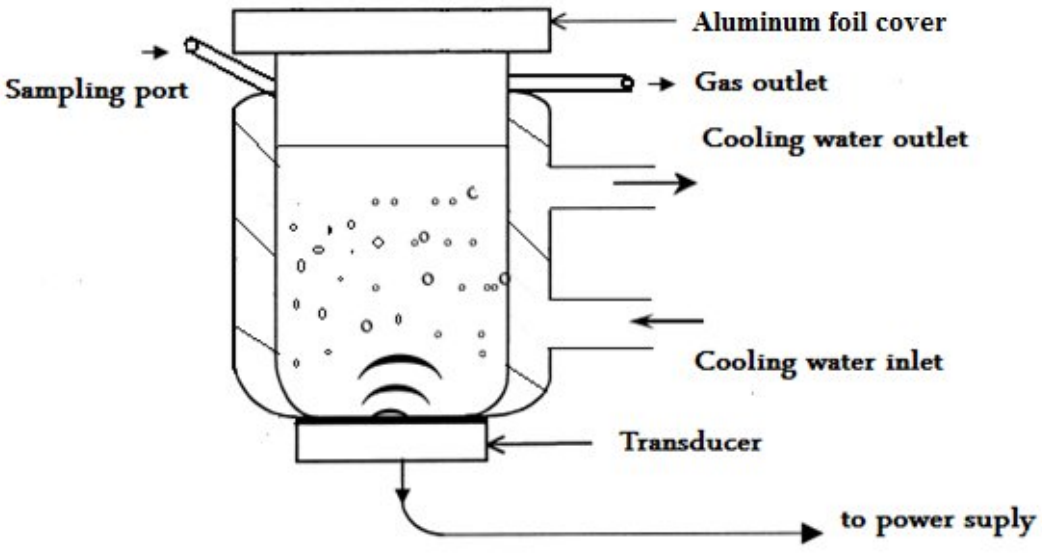

Figure 3.6. Ultrasonic reactor used in the sonication of butyric and maleic acid.

3.3.3.2 Ultrasonic bath

Figure 3.7 shows the ultrasonic bath used in the experiments.

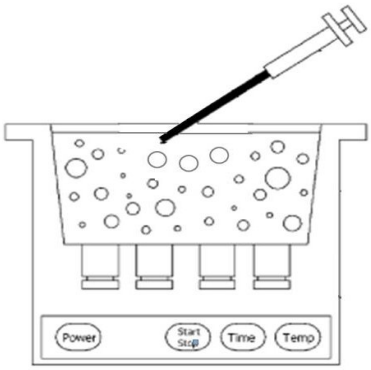

Figure 3.7. Ultrasonic bath used in the experiments.

The bath (C.E.I.A model CP 102 digit, Italy) had a fixed frequency of 40 kHz and ultrasound power could be changed from 70 W to 140 W. Operation temperature of bath could be regulated between 293 K and 353 K. Sonication time could be adjusted to a desired time in the range of 1-60 min. The volume of the reaction mixture in the bath was 1.5 dm^3 for all runs.

For a typical run, ultrasonic bath was filled with 1.5 dm^3 of butyric or maleic acid solution with specified concentration. Temperature, time and power were adjusted to the desired values. After reaching the desired experimental conditions, 2 ml sample was taken and corresponding time value was recorded as starting time of the reaction. At appropriate time intervals, samples of 2 ml were taken for HPLC analysis.

3.3.3.3 Ultrasonic probe system

Ultrasonic probe system used in ultrasonic degradation of butyric or maleic acid was shown in Figure 3.8.

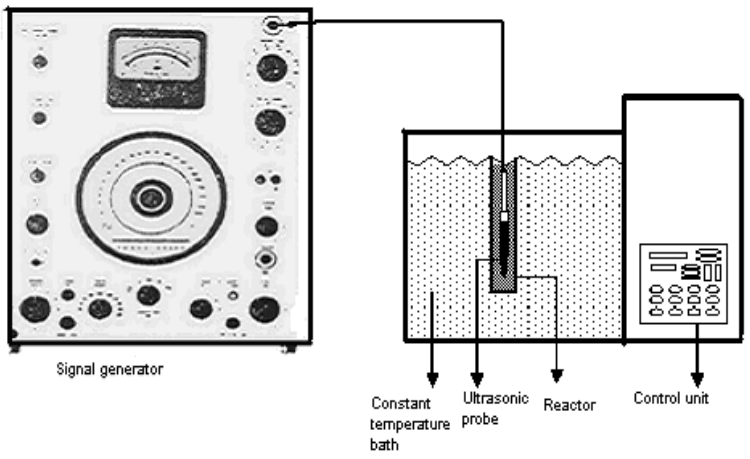

Figure 3.8. Sonication system with ultrasonic probe used in ultrasonic degradation of butyric and maleic acid.

This experimental system included a rectangular prism reactor (6 cm in width, 10 cm in height and 9 cm in length), a water bath (Nüve) to obtain constant temperature for the reaction, a signal generator (Beat Frequency Oscillator, Bruel Kjaer type 1013) and an ultrasonic transducer (Bruel Kjaer type 8100) which operated at frequency range of 0.1 Hz – 125 kHz.

In this system, ultrasonic power was calculated from the equation 3.1:

$$P = 2 \pi c f V^2 \qquad (3.1)$$

where P: power in W, c: capacitance in F (c= 7500×10^{-12} F), f: frequency in Hz, V: voltage in volt

For a typical run, rectangular prism reactor was filled with 0.35 dm^3 solution of butyric or maleic acid solution at a known concentration and then, the reactor was inserted into the water bath. After temperature, power and frequency were adjusted to desired values, the ultrasonic probe was inserted into the reactor. The probe was about 1 cm above the bottom of the reactor for all runs. To avoid the scattering of ultrasonic waves in the reaction medium, inside of the reactor walls was covered with a plastic packaging material.

3.4 Material and Methods

In this study, CWAO and sonication of butyric and maleic acid were investigated and compared with each other. In the experiments butyric acid (purity

of +99%, Aldrich) and maleic acid (purity of 99%, Merck) were used without further purification. The samples taken periodically from the reaction mixture was analyzed by HPLC (Agilent 1200) at conditions given below:

The column used in HPLC analysis was Zorbax Eclipse XDB-C18, 4.6x150 mm, 5μm.

Analysis conditions of maleic acid in HPLC

Mobile phase: 0.45 mM NaH_2PO_4 $2H_2O$ (pH:2.85) : MeOH = 95:5
Wave length: 210 nm
Temperature: 25 °C
Flow rate: 1 ml/min
Volume of Sample: 20 μl

Analysis conditions of butyric acid in HPLC

Mobile phase: H_2O:MeOH:H_3PO_4 = 9:6:0.005 (in volume) pH:2.75
Wave length: 210 nm
Temperature: 10 °C
Flow rate: 1 ml/min
Volume of Sample: 20 μl

Figures 3.9 and 3.10 show the calibration curves for maleic and butyric acid in HPLC analysis. Figures 3.11 and 3.12 present the example chromatograms of maleic and butyric acid with their possible intermediates which will be formed during the oxidation.

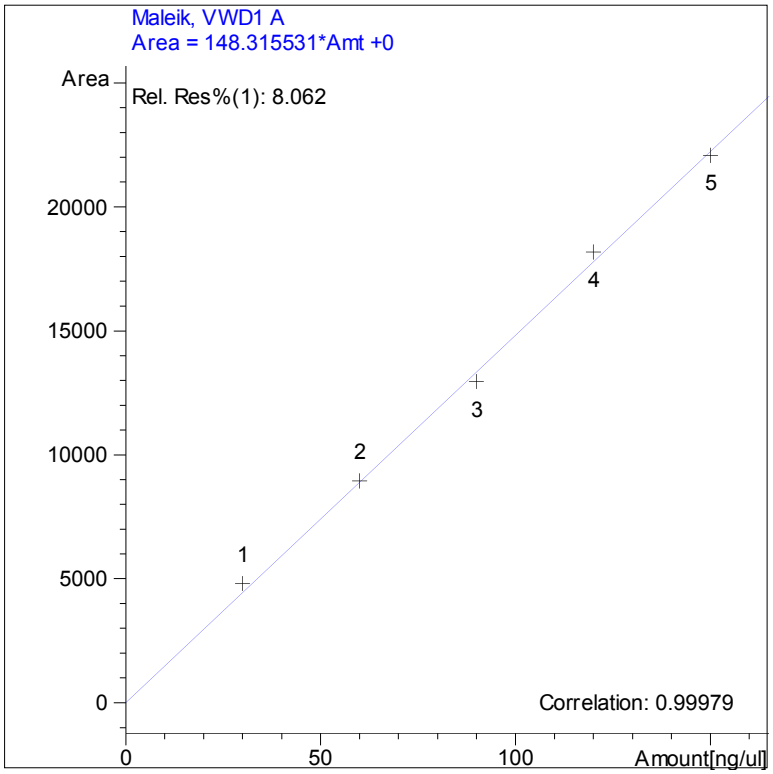

Figure 3.9. Calibration curve for maleic acid in HPLC analysis.

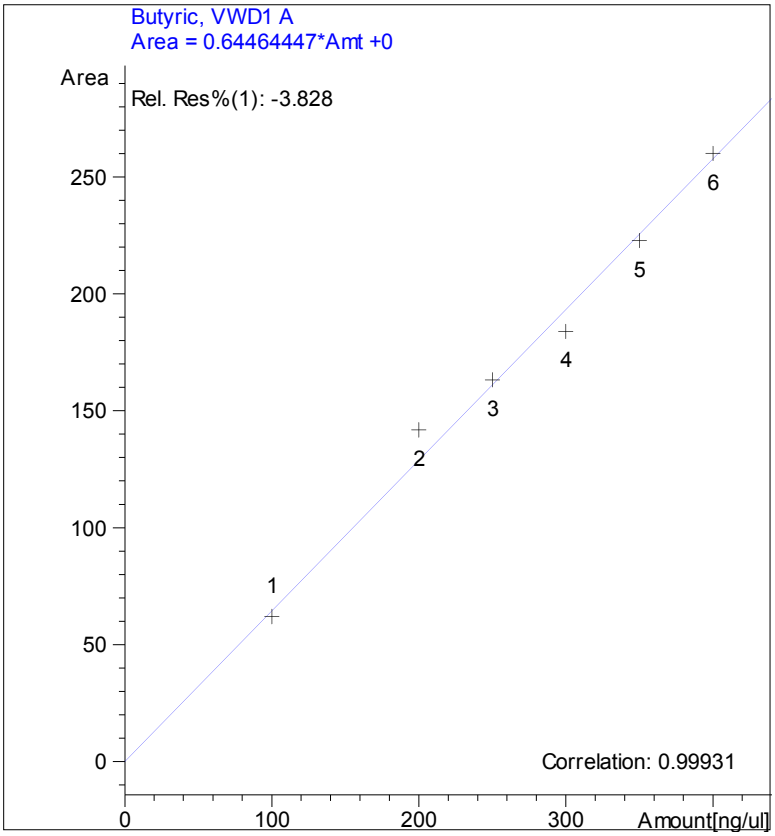

Figure 3.10. Calibration curve for butyric acid in HPLC analysis.

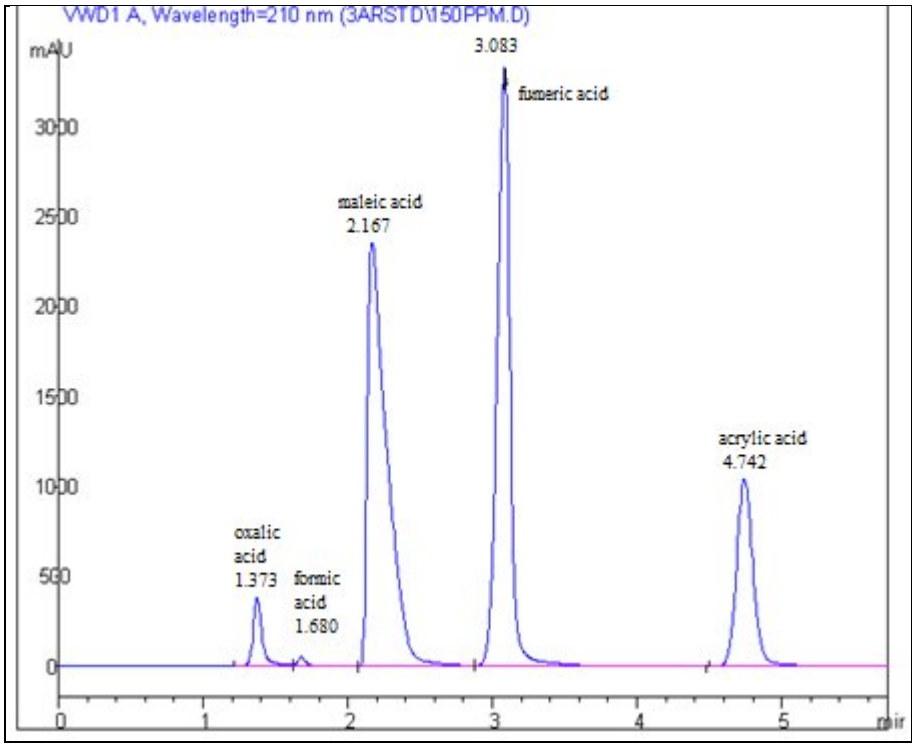

Figure 3.11. Example chromatogram of maleic acid in HPLC analysis

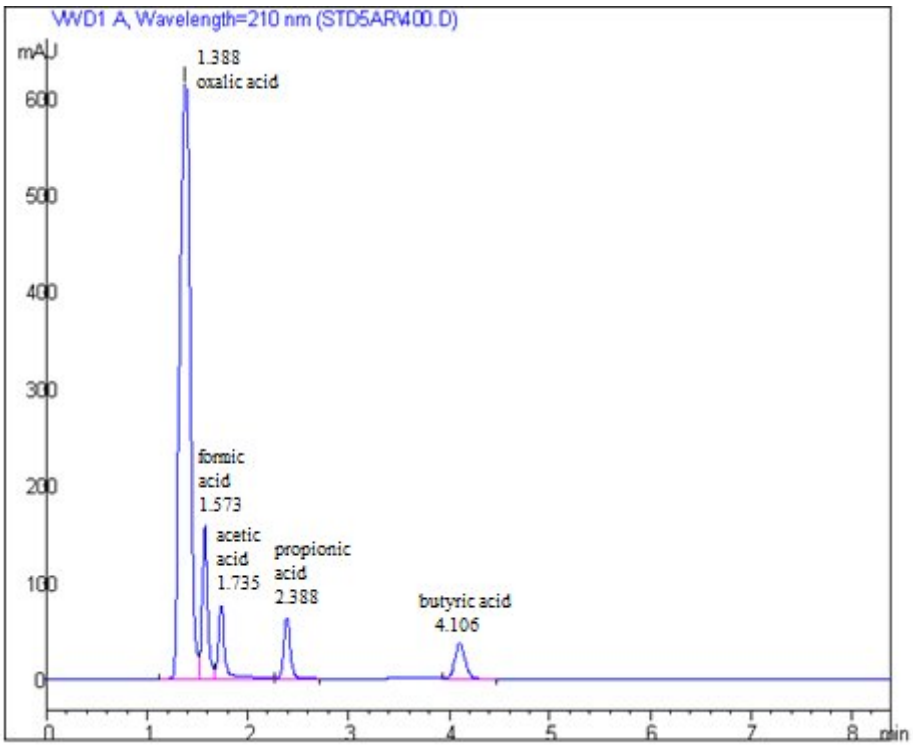

Figure 3.12. Example chromatogram of butyric acid in HPLC analysis

The amount of CO_2 generated during the CWAO of butyric and maleic acid at atmospheric pressure was detemined by absorption in a NaOH solution at known concentration. The reactor gas outlet stream was continuously bubbled into the NaOH solution in a gas washing bottle. At every half an hour, the NaOH bottle containing absorbed CO_2 was titrated with HCl solution with known concentration, that is, 10 ml of 0.01 N NaOH solution taken at every half an hour was titrated with 0.01 N HCl solution. Indicators were phenol phtalein which turned the colour of the solution to red and methyl orange that turned the color to orange. The amount of produced CO_2 was calculated by the equations of 3.2 – 3.4.

In the equations p is the volume of consumed titrant to change its colour from red to colorness (ml), b is the total consumed volume of titrant to change its colour to light orange (ml) (Dükkancı, 2004).

If 2p>b; there are NaOH and Na_2CO_3 in the solution

$$m_{CO2} = (b-p) \times M_{HCl} \times M_{CO2} \text{ (mg)} \quad (3.2)$$

If b=p; there is only NaOH in the solution.

If b=2p; there is only Na_2CO_3 in the solution.

If b>2p; there are Na_2CO_3 and $NaHCO_3$ in the solution

$$(b-2p) \times 0.84 = \text{(mg) } NaHCO_3 \text{ in the 10 ml solution} \quad (3.3)$$

$$p \times 1.106 = \text{(mg) } Na_2CO_3 \text{ in the 10 ml solution} \quad (3.4)$$

These equations were derived by using the reaction equations given below:

$\underline{HCO_3^-}$ and $\underline{CO_3^=}$ formation:

$$CO_2 + OH^- \rightarrow HCO_3^- \quad (3.5)$$

$$CO_2 + 2OH^- \rightarrow CO_3^= + H_2O \quad (3.6)$$

Titration of excess NaOH with HCl:

$$OH^- + HCl \rightarrow H_2O + Cl^- \quad (3.7)$$

To determine the leaching of metal, atomic absorption spectraphotometer measurements were performed after centrifugation of samples for about 1 h.

pH measurements were done during the experiments by a pH meter (WTW, inoLab pH Level1, Germany).

The percentage of degradation of butyric and maleic acid by CWAO and sonication was calculated as below:

$$\text{Degradation, } \% = \frac{C_{A0} - C_A}{C_{A0}} x100 \qquad (3.8)$$

where C_{A0}= initial concentration, C_A= concentration measured at corresponding time.

4. RESULTS AND DISCUSSION

4.1 Catalyst Characterization

4.1.1 Nitrogen adsorption studies

Table 4.1 gives nitrogen adsorption results of prepared catalysts and commercial ones (CAT1 and CAT2) used in the study.

As seen from Table 4.1, platinum catalysts supported on silicagel had the highest BET surface area, it was followed by AC supported catalyst and CAT1 and CAT2. Al_2O_3 supported catalysts had lower surface areas than the others.

BET and micropore surface area of Pt catalyst on silicagel which was prepared by saturation with toluene, Pt/SiO_2-2, were higher than those for Pt/SiO_2-1 prepared by saturation with n-hexane. Molecular diameter of toluene (0.57 nm) is greater than that of n-hexane (0.45 nm). Toluene can not access into the pores smaller than 0.57 nm, but n-hexane can. The pores of support unfilled with liquid might be plugged by platinum particles causing a decrease in BET surface area, in pore area and in total pore volume when silicagel was saturated with n-hexane. With the use of hexachloroplatinic acid as platinum source instead of platinum II acetylacetonate, an increase in BET surface area of silicagel supported Pt catalyst was observed, while there was not a significant change in BET area of alumina supported platinum catalyst (comparison of the pair of Pt/SiO_2-1 and Pt/SiO_2-3 and the pair of Pt/Al_2O_3-1 and Pt/Al_2O_3-3). On the other hand, calcination step during the preparation affected the pore size distribution.

No micropore area was measured for Al_2O_3 and AC supported catalysts. As seen, BET and macro + meso pore surface area of Ru-Pd/AC catalyst are higher than AC support. This indicated that, active components, Ru and Pd, were deposited at the outer surface of the support, AC. Average pore diameter showed the following ordering: Al_2O_3 supported samples > CAT1 and CAT2 > SiO_2 supported samples > TiO_2 supported samples > AC and Ru-Pd/AC.

Table 4.1. Nitrogen adsorption data of the catalysts prepared.

	BET Surface area, m^2/g	Micropore area [1], m^2/g	Macro+Meso pore Surface area, m^2/g	Total pore volume, cm^3/g	Micropore Volume, cm^3/g	Macro+Meso Pore Volume, cm^3/g	Max. Volume Adsorbed, cm^3/g	Average pore diameter, (4V/A by BET),nm	Average pore diameter, (4V/A by BJH),nm
CAT1[a]	248.48	48.71	199.77	0.545	0.025	0.520	352.243	8.771	8.020
CAT2[a]	166.80	18.46	148.35	0.338	0.009	0.329	218.605	8.109	8.380
TiO_2[a]	16.11	0.38	15.73	0.019	0.0002	0.0188	12.542	4.816	4.680
Pt/TiO_2-1[a]	15.98	3.93	12.06	0.018	0.002	0.016	12.052	4.664	4.960
Pt/TiO_2-2[a]	16.22	3.03	13.18	0.0207	0.0016	0.019	13.422	5.121	5.346
Pt/TiO2-3[a]	15.31	1.72	13.59	0.019	0.0009	0.0185	12.589	5.088	5.107
Pd/TiO_2-3[a]	16.57	4.66	11.91	0.019	0.002	0.017	12.478	4.659	4.820
Ru/TiO_2-3[a]	14.99	2.77	12.21	0.017	0.001	0.016	11.098	4.582	4.720
SiO_2[a]	325.49	28.79	296.70	0.703	0.015	0.688	454.374	8.637	6.650
Pt/SiO_2-1[a]	297.72	23.84	273.88	0.746	0.013	0.733	482.299	10.023	7.980
Pt/SiO_2-2[a]	340.68	37.36	303.32	0.797	0.020	0.777	514.950	9.352	7.170
Pt/SiO_2-3[a]	355.04	-	418.31	0.507	-	0.546	327.677	5.710	4.430
Pd/SiO_2-3[b]	201.45	-	217.69	0.436	0.004	0.382	255.460	1.122	5.732
Pt/Al_2O_3-1[c]	1.12	-	1.28	0.0037	-	0.0037	2.372	7.816	11.594
Pt/Al_2O_3-3[c]	1.16	-	1.26	0.0062	-	0.0062	4.015	9.589	19.738
Ru/Al_2O_3-3[c]	1.67	-	1.81	0.0073	-	0.0073	4.687	10.567	16.145
Pd/Al_2O_3-3[c]	1.06	-	1.11	0.0057	-	0.0057	3.677	10.792	20.626
AC[b]	155.30	-	161.89	0.294	0.109	0.152	164.102	3.667	3.559
Ru-Pd/AC[b]	294.51	-	331.15	0.561	0.194	0.299	310.996	3.562	3.473

[a]ASAP 2010; [b]Micromeritics Gemini V2.00; [c]DEMO Tristar 3000 V6.07A (Italy) [1]-Micropore area=BET area- t-plot area (macro and mesoporous area)

Figures 4.1 – 4.5 show nitrogen adsorption isotherm of prepared catalysts.

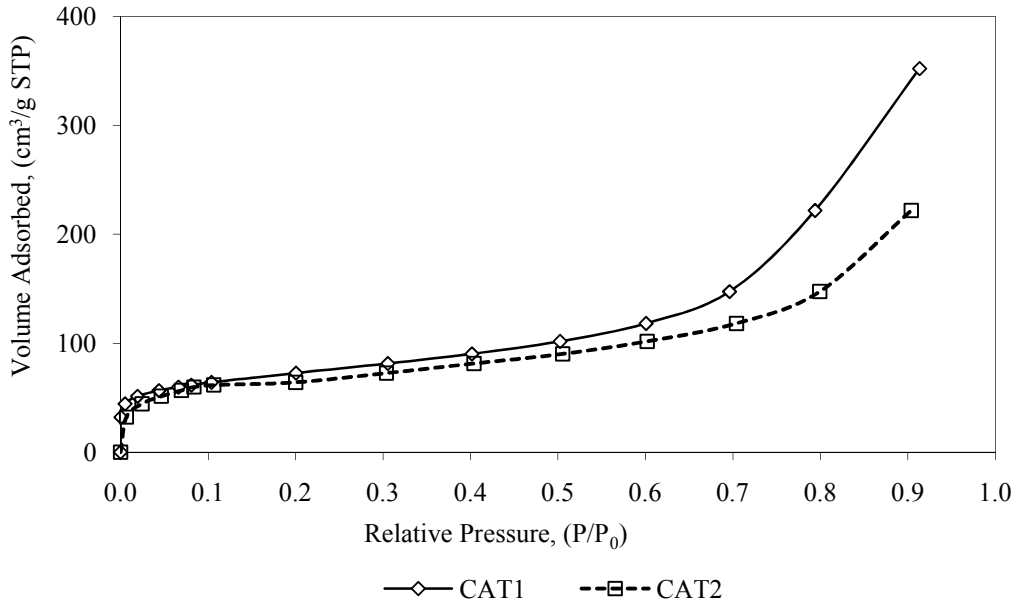

Figure 4.1. Nitrogen adsorption isotherm of CAT1 and CAT2.

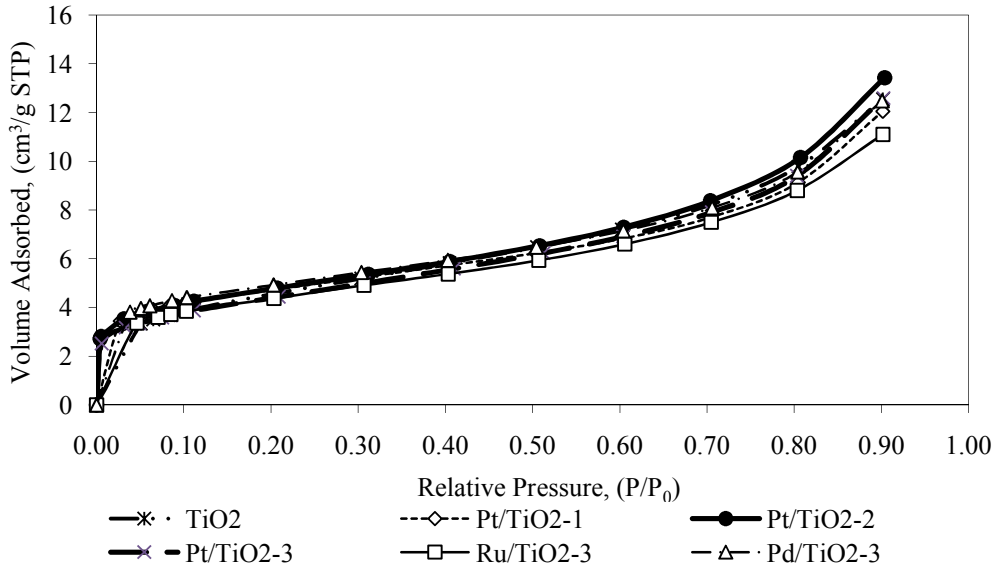

Figure 4.2. Nitrogen adsorption isotherm of TiO_2 supported catalysts.

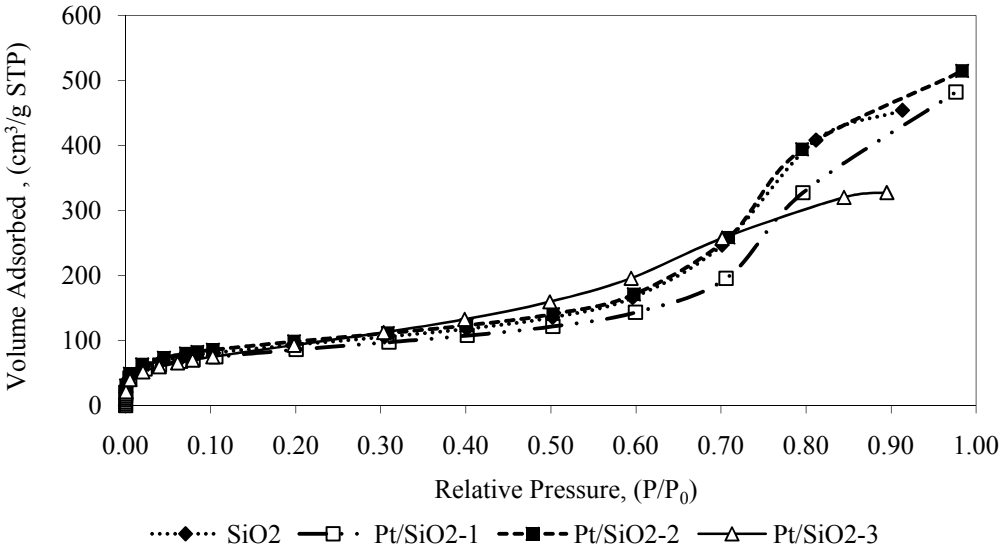

Figure 4.3. Nitrogen adsorption isotherm of SiO_2 supported catalysts.

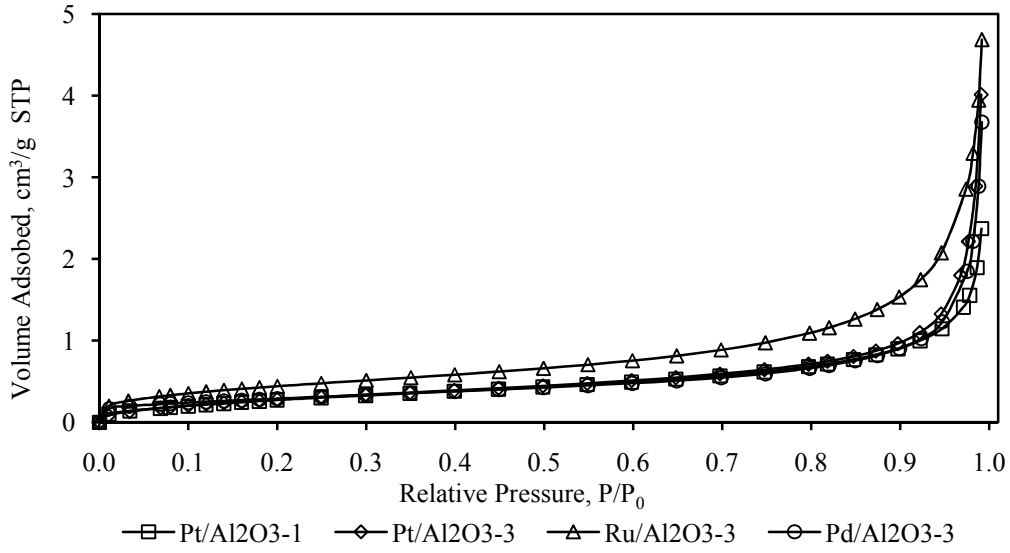

Figure 4.4. Nitrogen adsorption isotherm of Al_2O_3 supported catalysts.

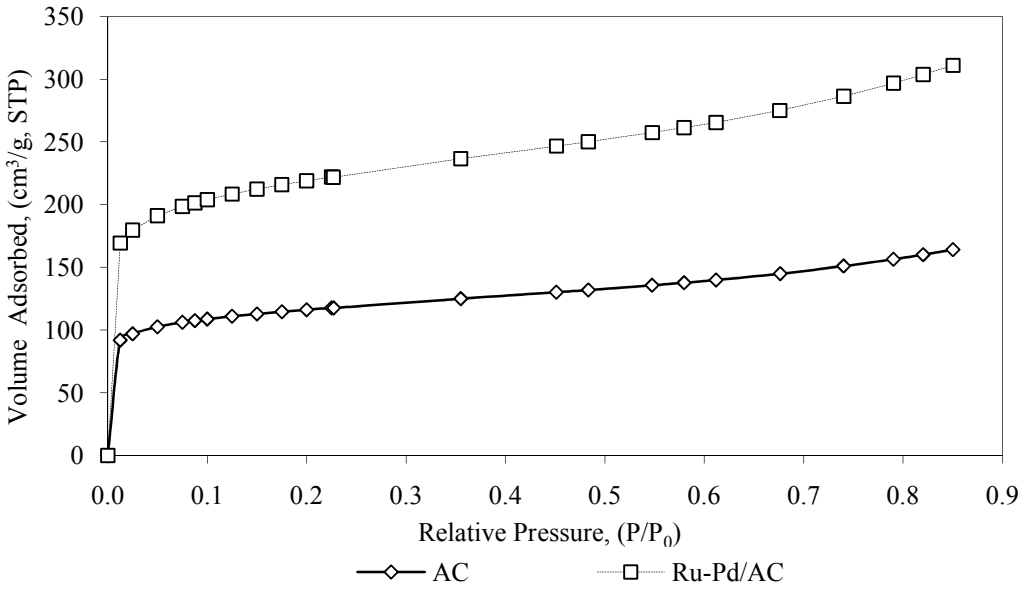

Figure 4.5. Nitrogen adsorption isotherm of AC support and Ru-Pd/AC catalyst.

As seen from the Figures 4.1 – 4.5, the isotherms were of type II except SiO_2 supported samples (type IV) according to IUPAC classification. It is well known that the isotherm of type II corresponds to multilayer formation and is commonly obtained in the case of physical adsorption and type IV represent the existence of capillary condensation (Sangwichien et al., 2002; Becer, 2003).

4.1.2 Scanning electron microscopy (SEM) images of the prepared catalysts

Figure 4.6 shows SEM microphotographs of alumina and alumina supported catalysts. Platinum, ruthenium and palladium particles were distributed as small agglomerates. The distribution of metal agglomerated on the support was not uniform.

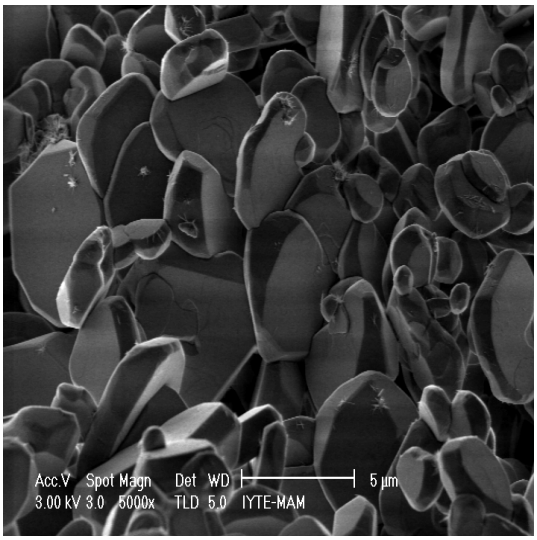
Acc.V Spot Magn Det WD 5 µm
3.00 kV 3.0 5000x TLD 5.0 IYTE-MAM

a.

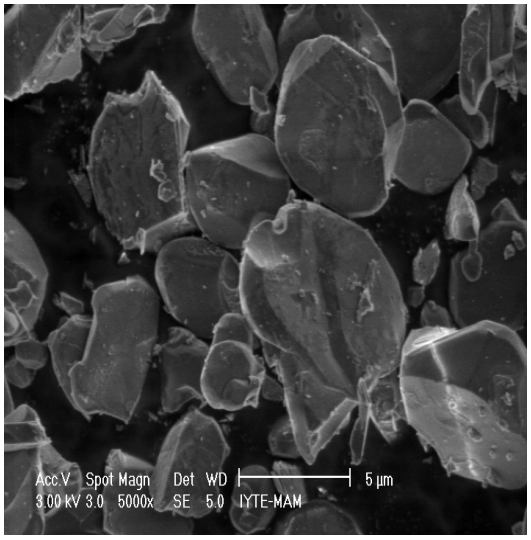
Acc.V Spot Magn Det WD 5 µm
3.00 kV 3.0 5000x SE 5.0 IYTE-MAM

b.

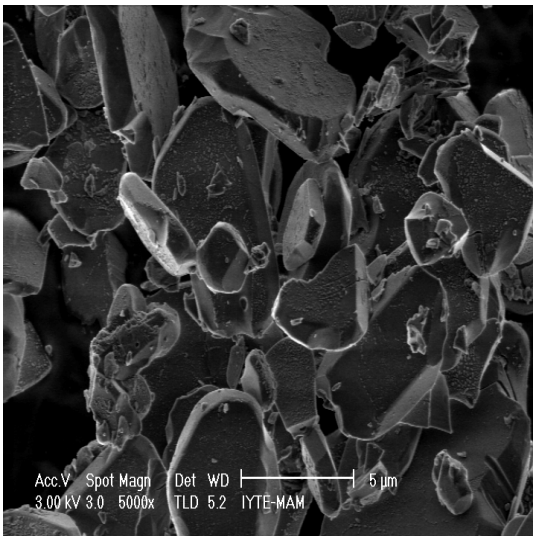
Acc.V Spot Magn Det WD 5 µm
3.00 kV 3.0 5000x TLD 5.2 IYTE-MAM

c.

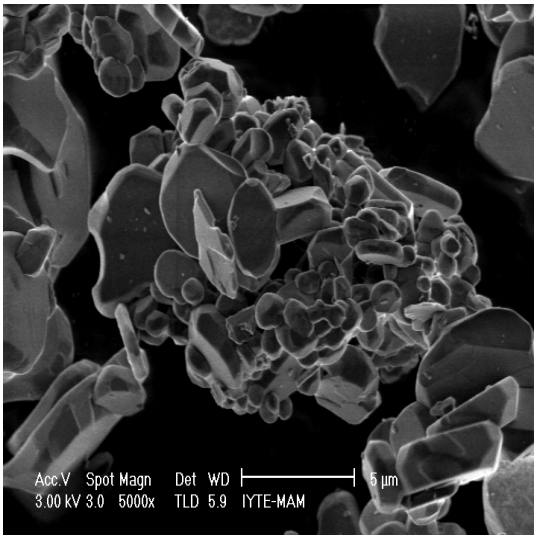
Acc.V Spot Magn Det WD 5 µm
3.00 kV 3.0 5000x TLD 5.9 IYTE-MAM

d.

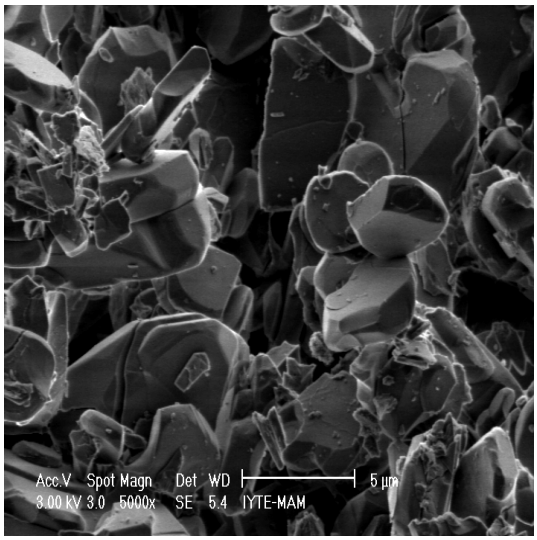

e.

Figure 4.6. SEM images of Al_2O_3 and Al_2O_3 supported samples.
a. Al_2O_3 **b.** Ru/Al_2O_3-3 **c.** Pd/Al_2O_3-3 **d.** Pt/Al_2O_3-1 **e.** Pt/Al_2O_3-3

The SEM images of titania and titania supported noble metal samples were given in Figure 4.7. It was observed that loading of support with noble metal caused agglomeration resulting in a decrease in meso + macro pore area (Table 4.1).

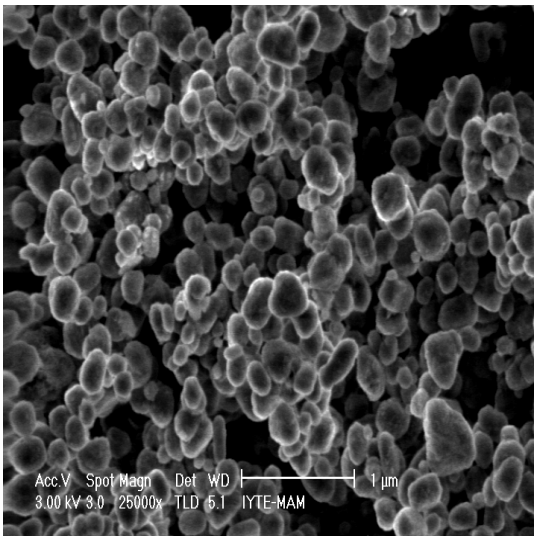

a.

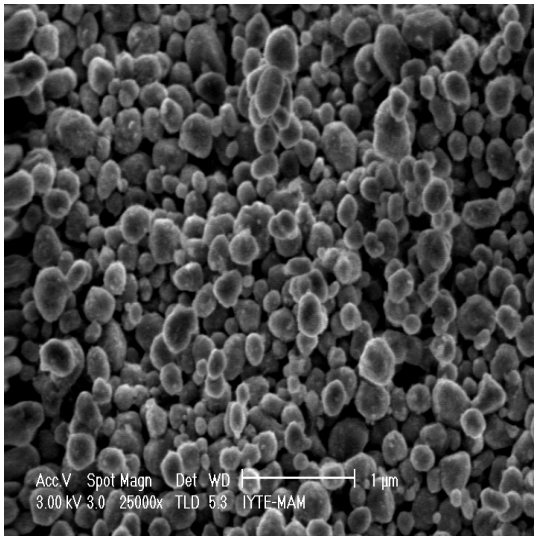

b.

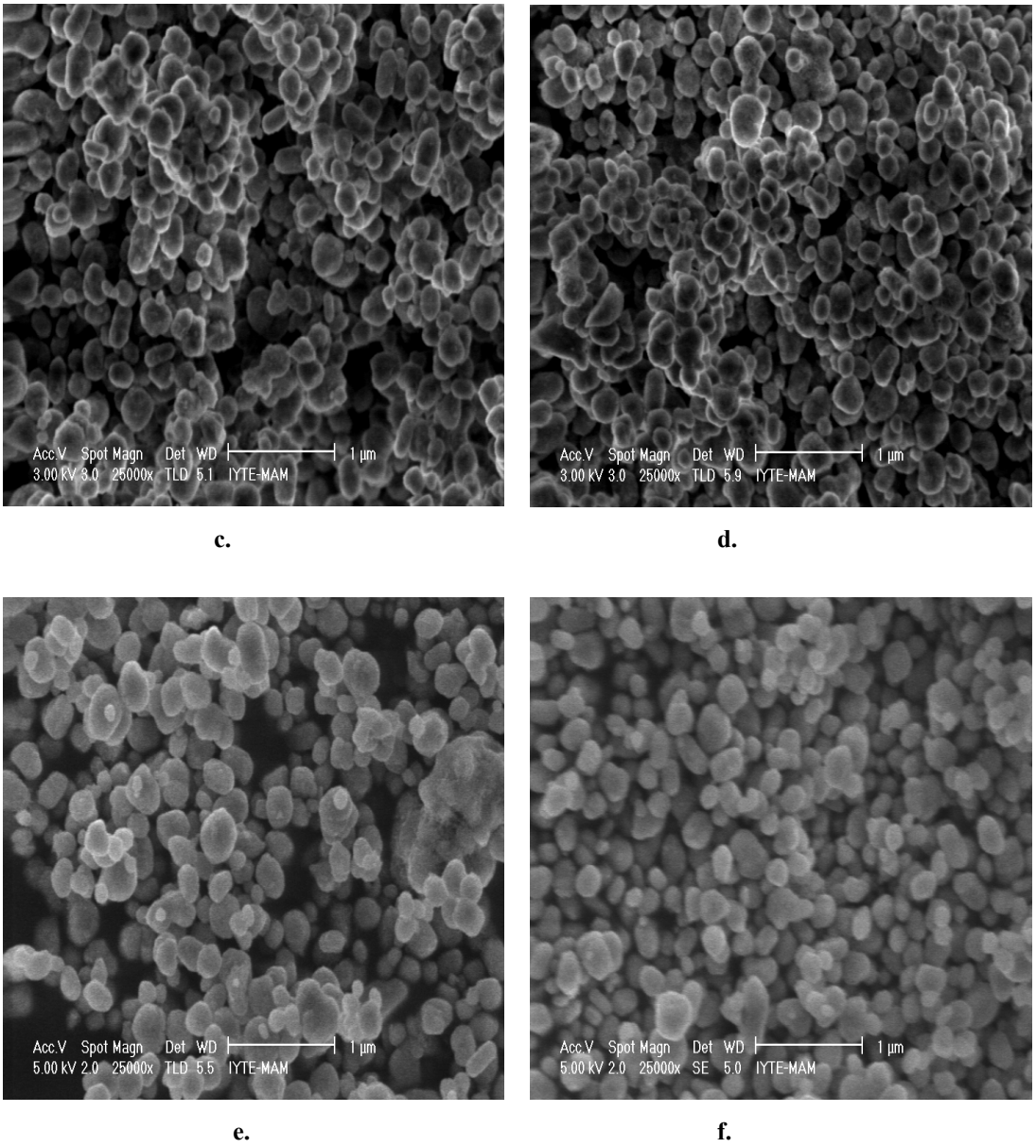

c. **d.**

e. **f.**

Figure 4.7. SEM images of TiO_2 and TiO_2 supported samples.
a. TiO_2 **b.**Pd/TiO_2-3 **c.** Ru/TiO_2-3 **d.** Pt/TiO_2-1 **e.** Pt/TiO_2-2 **f.** Pt/TiO_2-3

The SEM images of silicagel and silicagel supported samples were given in Figure 4.8. It was observed that in Pt/SiO_2-3 and Pd/SiO_2-3 catalysts, particles tended to agglomerate. In all samples, particles were not homogeneously distributed.

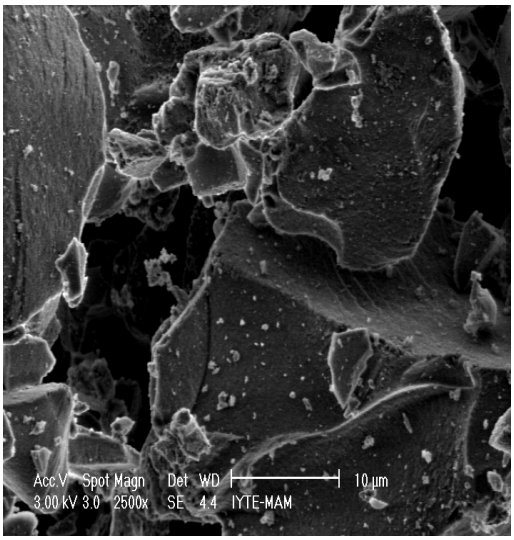
Acc.V Spot Magn Det WD 10 µm
3.00 kV 3.0 2500x SE 4.4 IYTE-MAM

a.

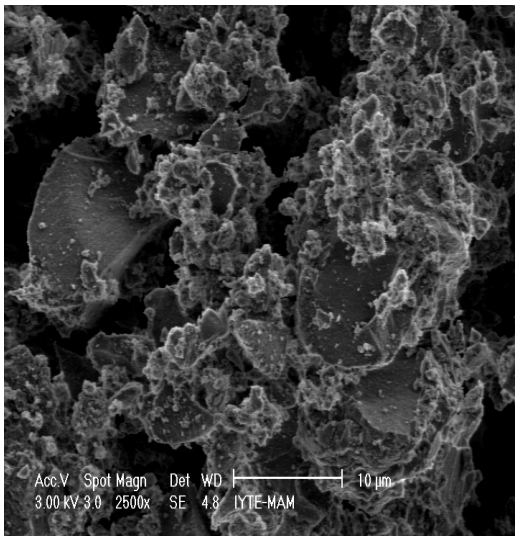
Acc.V Spot Magn Det WD 10 µm
3.00 kV 3.0 2500x SE 4.8 IYTE-MAM

b.

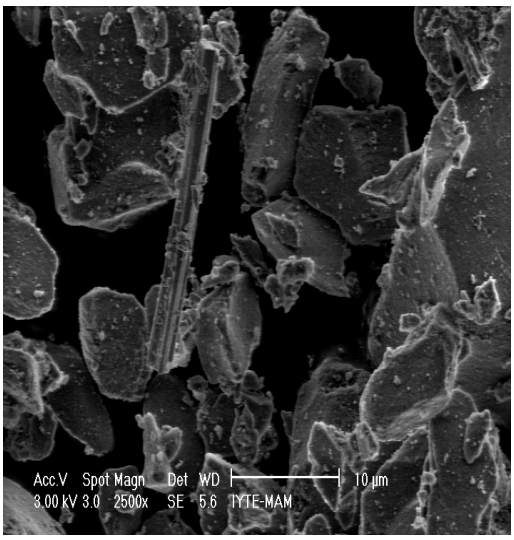
Acc.V Spot Magn Det WD 10 µm
3.00 kV 3.0 2500x SE 5.6 IYTE-MAM

c.

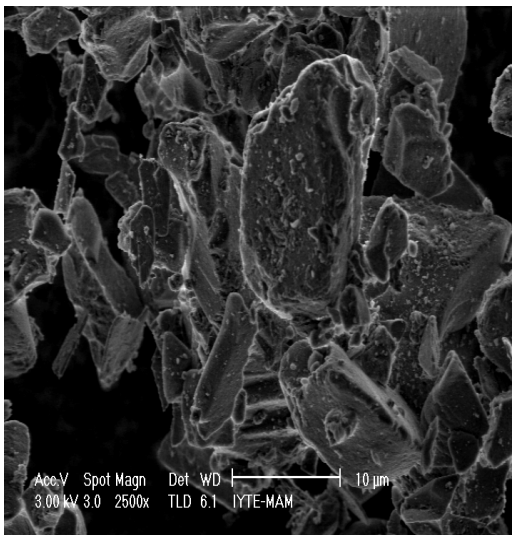
Acc.V Spot Magn Det WD 10 µm
3.00 kV 3.0 2500x TLD 6.1 IYTE-MAM

d.

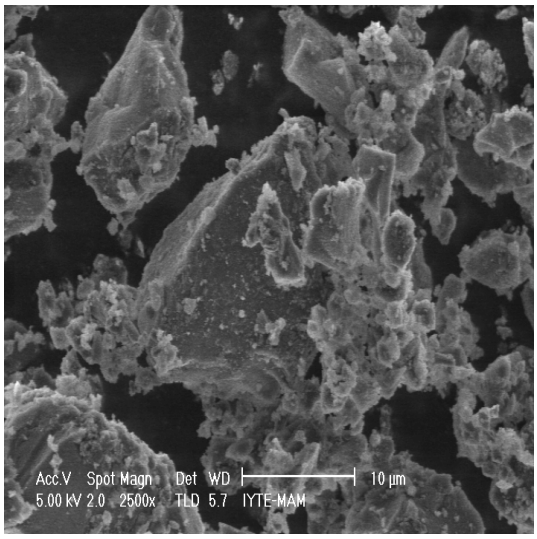

e.

Figure 4.8. SEM images of SiO_2 and SiO_2 supported samples.
a. SiO_2 **b.** Pt/SiO_2-3 **c.** Pt/SiO_2-2 **d.** Pt/SiO_2-1 **e.** Pd/SiO_2-3

Figure 4.9 shows SEM images of AC support and Ru-Pd/AC sample. Loading of support with noble metals Ru and Pd could be clearly seen.

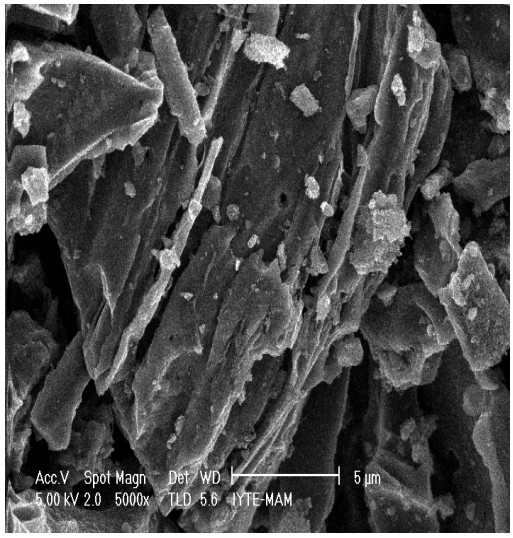

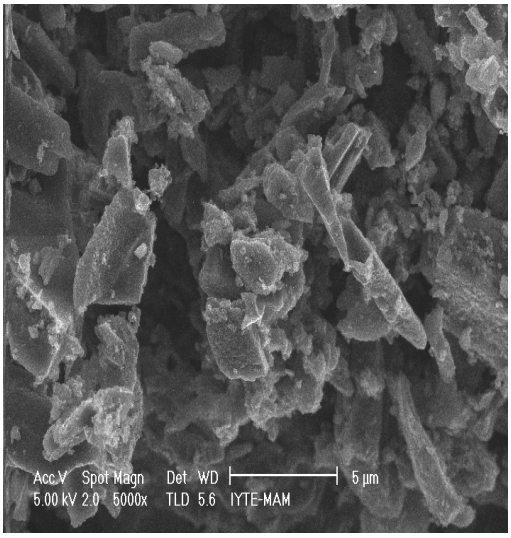

a. **b.**

Figure 4.9. SEM images of AC and AC supported sample.
a. AC **b.** Ru-Pd/AC

Figure 4.10 gives SEM images of commercial catalysts (CAT1 and CAT2). As seen, active components were rather uniformly distributed.

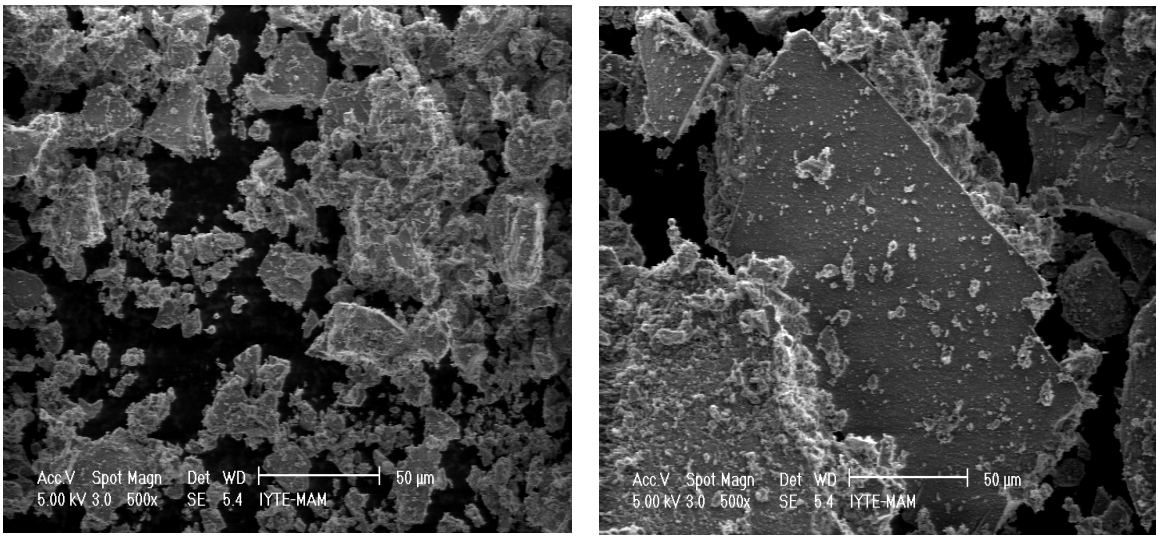

a. **b.**

Figure 4.10. SEM images of CAT1 and CAT2.
a. CAT1 **b.** CAT2

4.1.3 XRD studies

Figures 4.11 – 4.16 present the XRD patterns of some catalysts. In XRD Analysis of CAT1 and CAT2 samples, Figure 4.11, peaks at 2 Theta = 37.5°, 46° and 67° characterized the Al_2O_3 crystals and the peaks at 2 Theta = 39.8°, 46° and 66.8° platinum crystals. Figure 4.12 showed the XRD patterns of Pd and Ru supported on TiO_2. The peaks observed at 2 Theta = 27.5°, 36.1° and 54.2° were attributed to TiO_2. The peaks at 2 Theta = 40.1°, 46.7° and 68.1° characterized Pd crystals and peaks at 2 Theta = 38.7°, 42.4° and 58.3° correspond to Ru. Addition of Ru or Pd to titania support reduced the peak intensities of TiO_2 support which might be due to coverage of the crystal surface by metal loading. Figure 4.13 showed XRD patterns of TiO_2 supported Pt catalysts. Figure 4.14 showed XRD patterns of SiO_2 supported Pt and Pd catalysts. Silicagel exhibited a halo around 2 Theta =22°, the amorph structure of silicagel, besides the peaks around 2 Theta = 25.4°, 31.4° and 38.8° were attributed to gypsium ($CaSO_4$) which was an impurity (5%) in silicagel. Figure 4.15 gave XRD pattern of alumina supported Pt, Ru and Pd catalysts. The peaks observed at 2 Theta = 34.0°, 54.9° and 60.3° corresponded to PdO showing that PdO were not reduced to Pd completely during the reduction step in the catalyst preparation.

Figure 4.16 presented the XRD patterns of AC support and Ru-Pd/AC catalyst. The peaks at 2 Theta = 40.1°, 46.7° and 68.1° characterized Pd crystals. Peaks at 2 Theta = 38.7°, 42.4° and 58.3° corresponded to Ru which were not observed clearly. Because it was likely very finely dispersed as small crystallites on the surface of AC. The halo for AC at 2 Theta=24° was observed. The peaks observed at 2 Theta = 34°, 54.9° and 60.3° corresponded to PdO.

On the other hand, in all the XRD diagrams of the catalysts prepared, the characteristic peaks of the support used were preserved. It showed that the structure of the support was not destroyed by addition of Pt, Pd or Ru metals in 1 wt %.

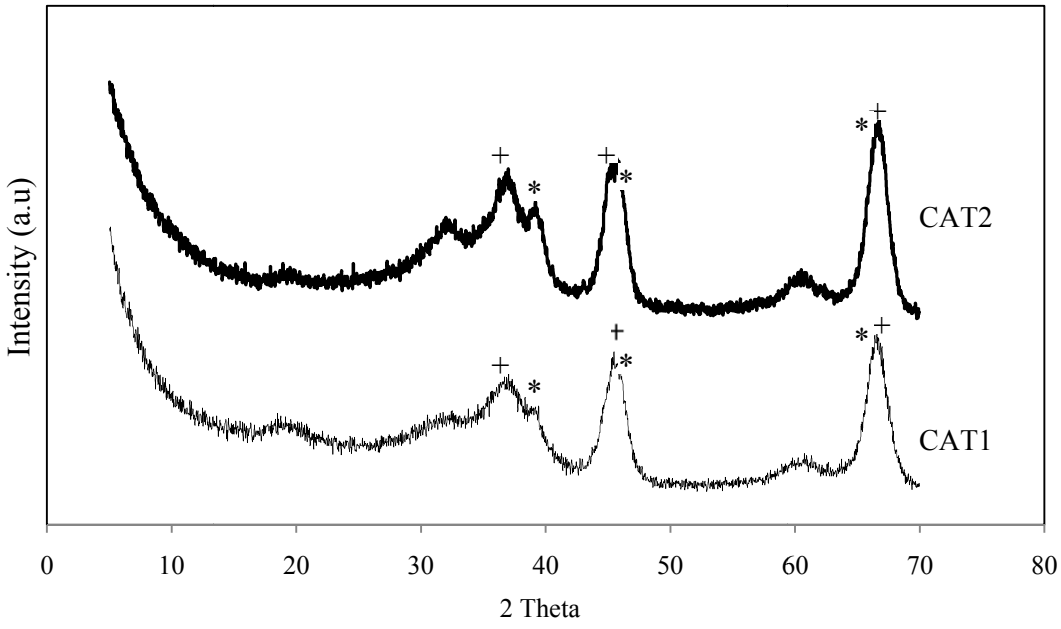

Figure 4.11. XRD patterns of CAT1 and CAT2.
(* :Pt; + **:**Al_2O_3 **)**

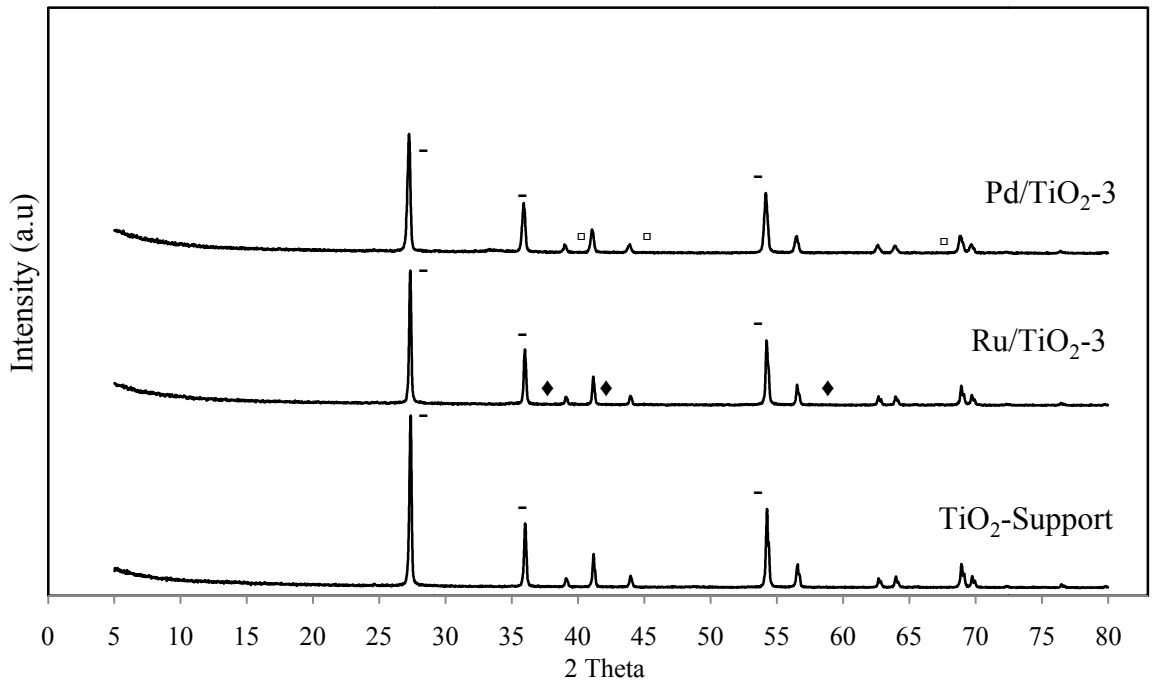

Figure 4.12. XRD patterns of TiO_2 , TiO_2 supported Ru and Pd catalysts.
(▫ :Pd; ♦ :Ru; - :TiO_2)

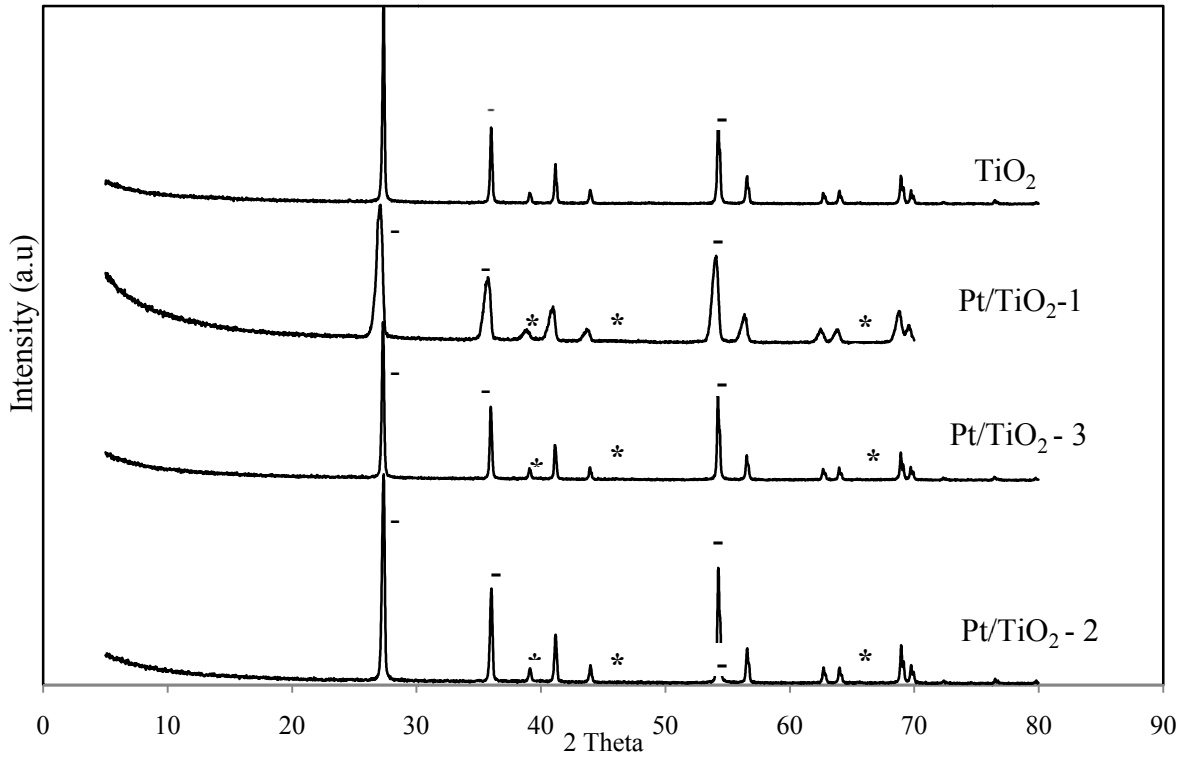

Figure 4.13. XRD patterns of TiO_2 , TiO_2 supported Pt catalysts.
(* :Pt; - :TiO_2)

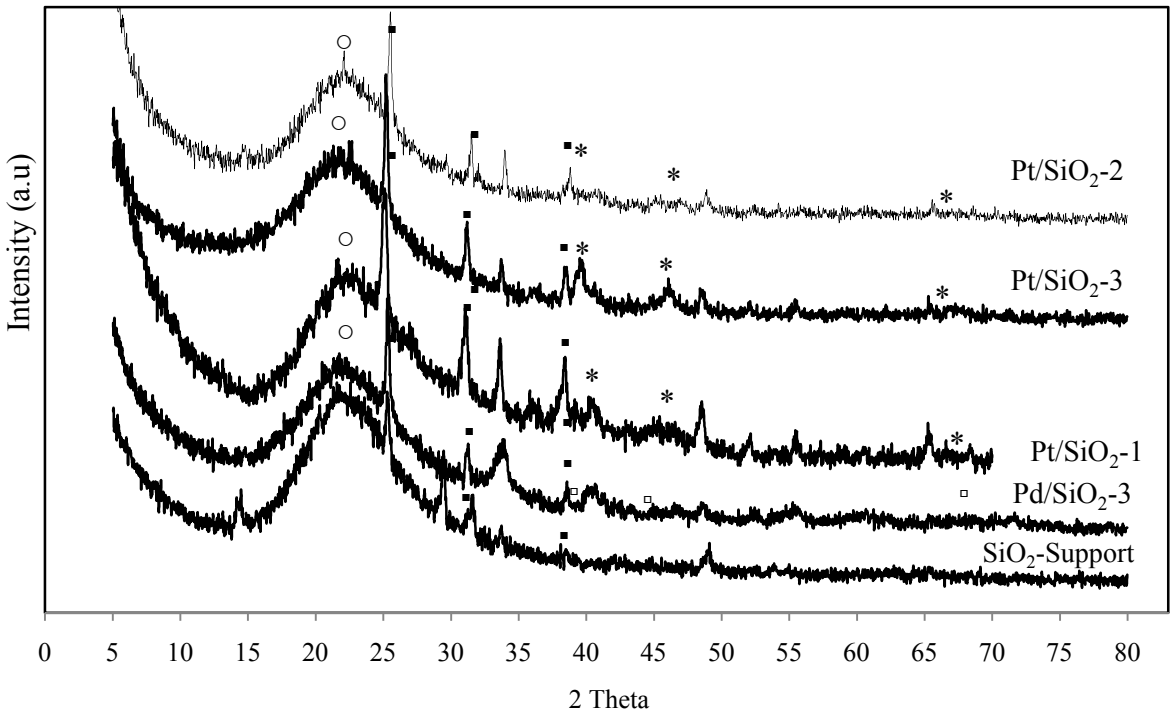

Figure 4.14. XRD patterns of SiO_2 , SiO_2 supported Pt and Pd catalysts.
(▫ :Pd; * :Pt; ○ :SiO_2; ▪ :$CaSO_4$)

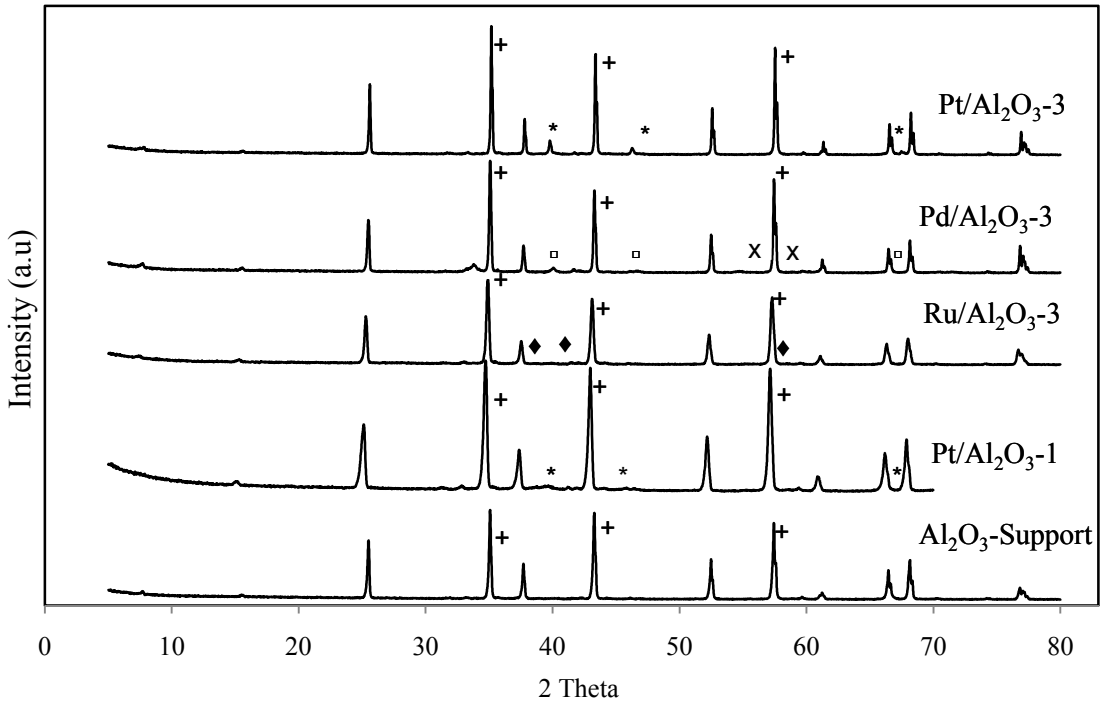

Figure 4.15. XRD patterns of Al_2O_3 and Al_2O_3 supported catalysts.
(▫ :Pd; ♦ :Ru; * :Pt; + :Al_2O_3; × : PdO)

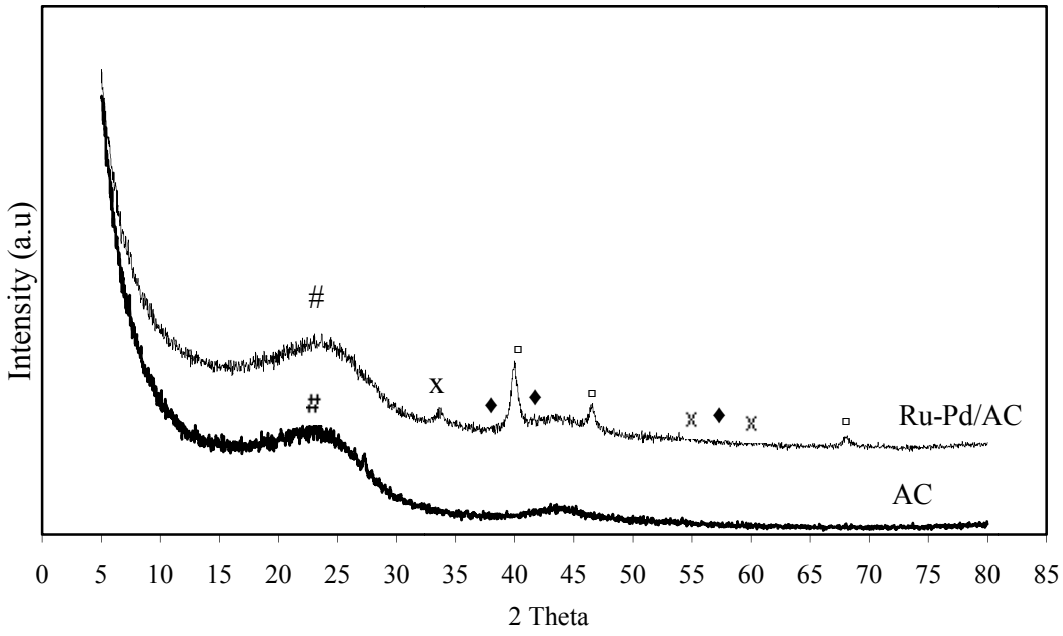

Figure 4.16. XRD patterns of AC and AC supported catalyst.
(▫ **:**Pd**;** ♦ **:**Ru**;** × **:** PdO; #: AC)

4.1.4 IR studies

IR spectra of commercial (CAT1 and CAT2) and prepared catalysts were shown in Figures 4.17 – 4.20. The measurements were performed at room temperature and atmospheric pressure by Shimatsu 470 IR Spectrophotometer.

In Figure 4.17, IR bands of silicagel are; asymmetric band of Si-O of stretching vibration at 1085 -1200 cm^{-1}, bending band of Si-OH at 970 cm^{-1}, stretching band of Si-O at 795 cm^{-1}. In addition, at 465 cm^{-1} bending band of Si-OH and at 3490 cm^{-1} stretching band of hydrogen bonded OH were observed. Band intensity was affected a bit by metal loading.

Although metal loading on alumina did not change the band intensity at 765 cm^{-1}, band intensities at 640, 560, 455 and 420 cm^{-1} were little affected by metal loading, Figure 4.18.

Peaks belonging to TiO_2 and TiO_3 were observed at 640, 520-620 cm^{-1} (Figure 4.19). The peak intensities were not significantly affected by metal loading on TiO_2.

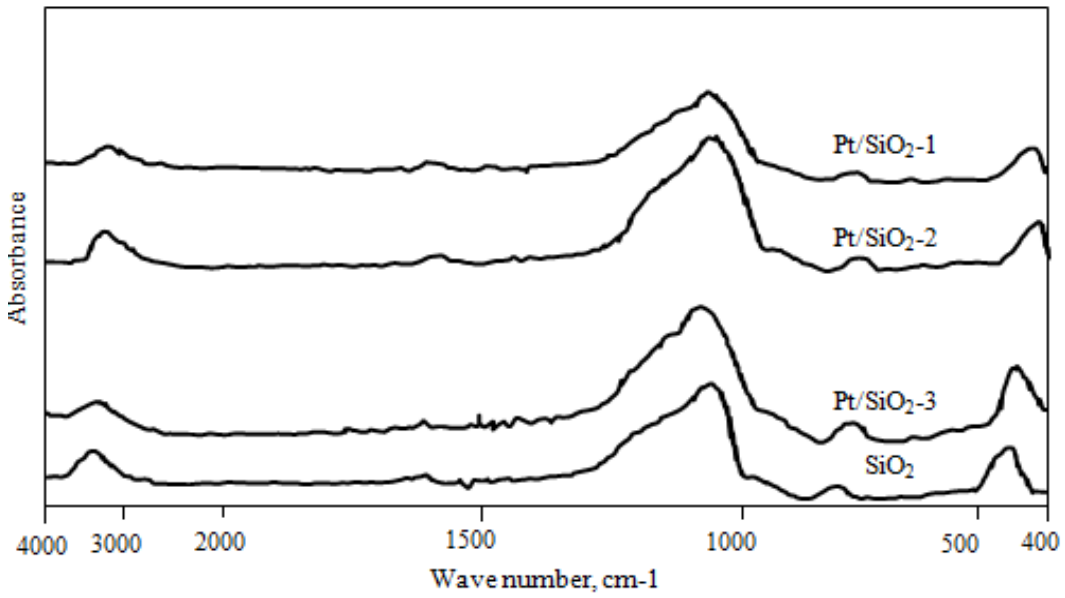

Figure 4.17. IR spectra of catalysts supported on silicagel.

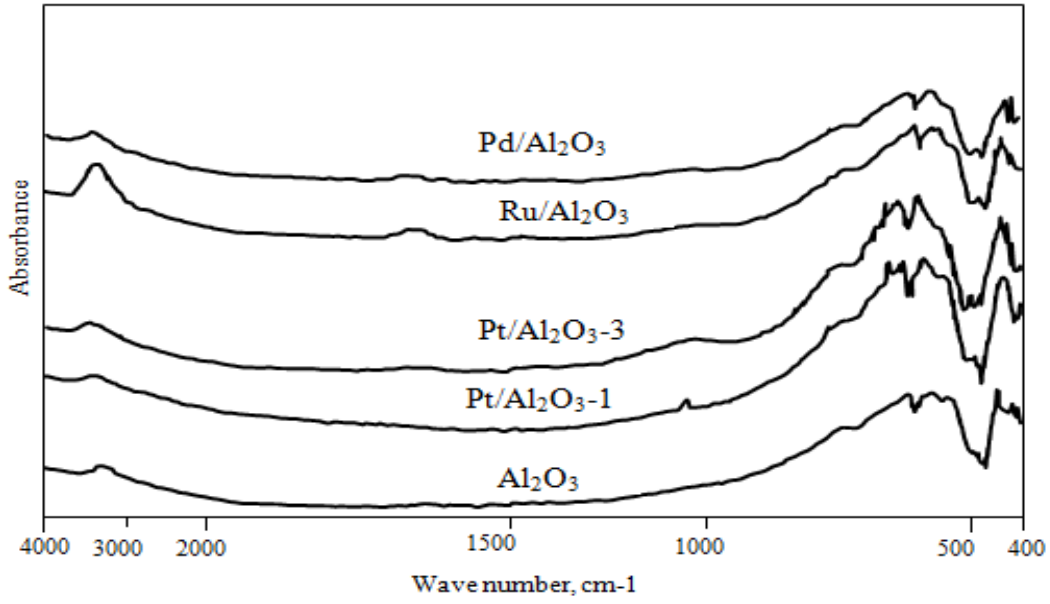

Figure 4.18. IR spectra of catalysts supported on alumina.

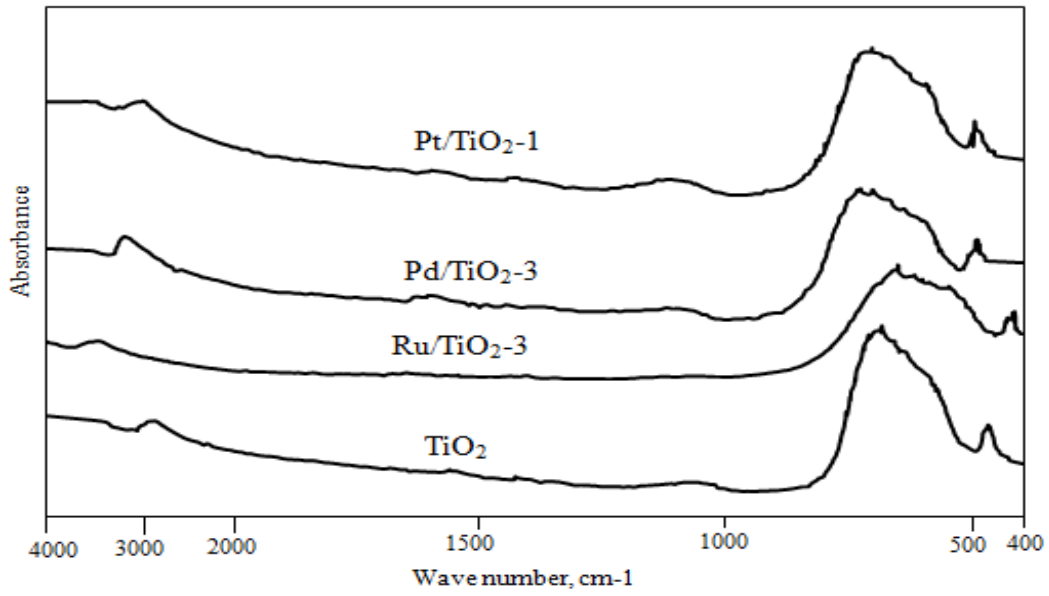

Figure 4.19. IR spectra of catalysts supported on TiO_2.

Figure 4.20 shows IR studies of commercial catalysts.

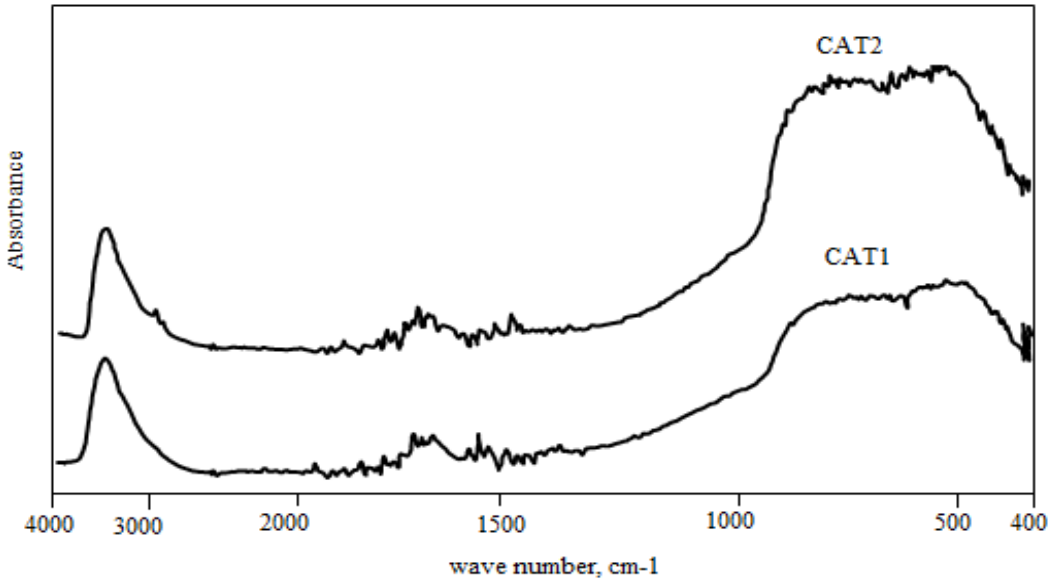

Figure 4.20. IR spectra of commercial CAT1 and CAT2 catalysts.

It could be said that, in general, no significant change occurred in the IR spectra of support material, TiO_2, SiO_2 or Al_2O_3, by addition of noble metal (Pt, Ru or Pd) at a low weight precent of 1 wt %. That is, IR spectra of the supports were preserved during preparation of the catalysts.

4.2 Catalytic Wet Air Oxidation of Butyric and Maleic Acid at Atmospheric Pressure

Table 4.2 shows the degradation results of butyric and maleic acid in CWAO runs at atmospheric pressure over the prepared and commercial catalysts. Experiments were carried out at a reaction temperature of 333 K with an air flow rate of 0.003 dm^3/s at a stirring speed of 500 rpm in the presence of 1 g of catalyst in 3 g/dm^3, 0.15 dm^3 aqueous solution of BA or MA. The reaction duration was 3 hours.

Most of the prepared catalysts were inactive in the CWAO of BA and MA at atmospheric pressure. However, the catalysts of Pt/TiO_2-1, AC and Ru-Pd/AC showed some activity for MA oxidation and the catalysts of Pt/TiO_2-2, Pt/TiO_2-3, Pd/TiO_2-3, AC and Ru-Pd/AC for BA oxidation. The commercial catalyst, CAT1, which had high BET surface area was the most active one (7.9 % and 11 % degradation in BA and MA oxidation, respectively) in the CWAO of aqueous solutions of both acids. CAT1 was suggested to hydrolyze butyric and maleic acid into readily oxidizable compounds. During the preparation of the Pt/TiO_2-1 catalyst, platinum particles were located mainly at the exterior surface of the support by saturating the pores of the support with n-hexane. Such a process was not applied to the catalysts of Pt/TiO_2-3 and Pd/TiO_2-3. So, maleic acid which was a larger molecule than butyric acid could not enter the pores of the latter catalysts in order to reach the active sites for oxidation, resulting in no conversion of maleic acid on those samples.

To assess the extent of the uncatalyzed thermal oxidation of butyric and maleic acids and to understand the catalytic effect of support, WAO runs were performed without catalyst and with metal-free support, respectively. The uncatalysed thermal oxidation occurred as 0.75 % for BA while no thermal oxidation for MA was observed after an oxidation of 180 min. Except oxidation over silicagel and activated carbon (3.9 % for BA over silicagel, 24.4 % for BA and 21.2 % for MA over activated carbon, AC) no significant support effect on the oxidation was observed with the use of metal-free support in the CWAO runs of BA and MA. The high degradation degree for BA and MA measured over AC could be due to the adsorption on carbon surface. Activated carbon is a well known adsorbent. For this reason, adsorption experiments of BA and MA on all the supports used in this study (Al_2O_3, TiO_2, SiO_2, AC), were carried out at 333 K without air flow under continuous stirring at 500 rpm. No adsorption of MA was

observed on Al_2O_3, TiO_2 and SiO_2 but 11% of MA was adsorbed on AC. For BA, 22.5% and 1.6% adsorption were observed on AC and SiO_2 supports, respectively whereas no adsorption was observed on Al_2O_3 and TiO_2 supports. Adsorption results of BA and MA on activated carbon showed that BA and MA could be removed from their aqueous solutions by adsorption with removal degrees of 22.5 % and 11%, respectively. It must be into account that degradation of BA and MA, Figure 4.21, not only due to the oxidation. Adsorption runs of BA on AC were carried out at temperatures of 333 K, 353 K and 383 K at atmospheric pressure and found to be 22.5 %, 23.6 % and 18.5 %, respectively. As seen, adsorption of BA on AC support surface was very important at atmospheric pressure and decreased with the increase in temperature from 333 K to 383 K, being still high.

Conversions of BA and MA given as a function of time in Figure 4.21 and as degradation degrees obtained after 3h oxidation in Table 4.2 over Ru-Pd/AC catalyst included adsorption and oxidation together.

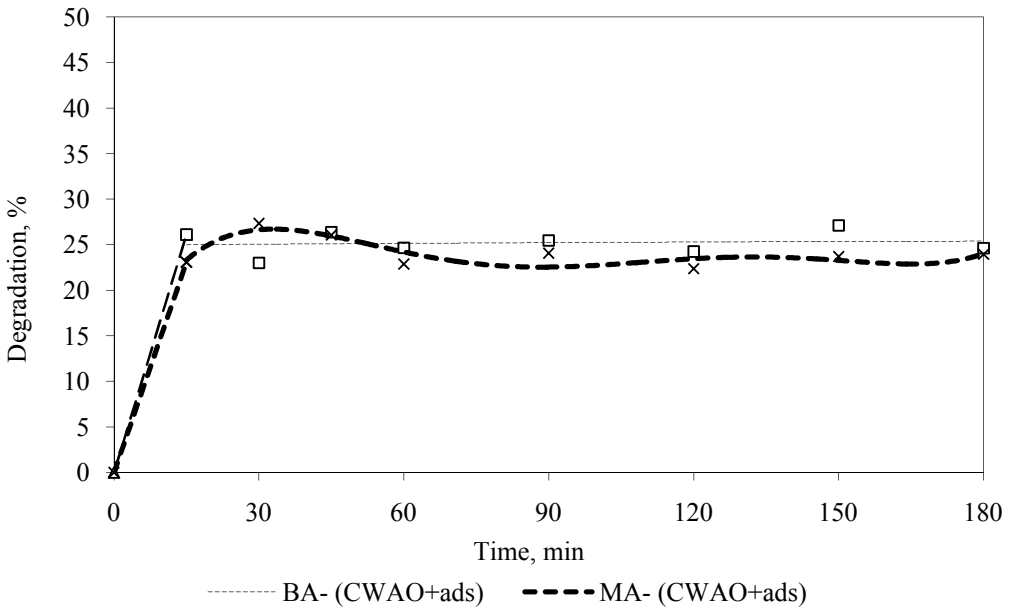

Figure 4.21. Conversion of butyric and maleic acid solutions over Ru-Pd/AC catalyst in CWAO and adsorption together.
(Initial concentration= 3 g/dm^3, Catalyst amount = 1g/0.15 dm^3 solution, Temperature = 333 K, Air flow rate = 0.003 dm^3/s)

Table 4.2. Oxidation results of butyric and maleic acids over the prepared and commercial catalysts.
(Reaction duration = 3 h, Initial concentration = 3 g/dm^3, Catalyst amount = 1gram/0.15 dm^{3}of aqueous solution, Temperature = 333 K, Air flow rate = 0.003 dm^3/s)

Catalyst Code	Degradation, %	
	Butyric acid	Maleic acid
CAT1	7.9	11.0
CAT2	3.6	3.0
Al_2O_3	0.9	0.0
Pt/Al_2O_3-1	0.0	0.0
Pt/Al_2O_3-2	0.0	0.0
Pt/Al_2O_3-3	1.1	0.0
TiO_2	0.0	0.0
Pt/TiO_2-1	0.0	2.1
Pt/TiO_2-2	2.6	0.0
Pt/TiO_2-3	1.8	0.0
SiO_2	3.9	0.0
Pt/SiO_2-1	0.0	0.0
Pt/SiO_2-2	0.0	0.0
Pt/SiO_2-3	0.5	0.0
Ru/ Al_2O_3-3	0.0	0.0
Ru/ TiO_2-3	0.4	0.0
Ru/SiO_2-3	0.0	0.0
Pd/ Al_2O_3-3	0.6	0.0
Pd/ TiO_2-3	2.3	0.0
Pd/ SiO_2-3	0.1	0.0
AC	24.4	21.2
Ru-Pd/AC	24.6	23.9

In Figure 4.22, the conversions of BA and MA were given as a function of time over CAT1, CAT2 and some prepared catalysts which were active in the oxidation reaction. The initial rates measured from the slope at the origin of the conversion versus time curves were found to be as a function of the active component in the catalyst as $4.4x10^{-3}$ and $1.36x10^{-3}$ mol min^{-1} g_{Pt+Re}^{-1} on CAT1 and $2.35x10^{-3}$ and $1.38x10^{-3}$ mol min^{-1} g_{Pt}^{-1} on CAT2, for the CWAO of BA and MA, respectively. The initial rates of BA oxidation were higher than those of MA oxidation on CAT1 and CAT2. On the other hand, CAT1 gave an initial rate greater than that on CAT2 in butyric acid oxidation. Initial rates calculated for MA oxidation were almost similar on CAT1 and CAT2. Figure 4.22, indicated a deactivation of the CAT1 and CAT2 around 10% and 5% in the conversions of BA, respectively, though an increase was expected as long as the reactant concentration is sufficiently high. This might be caused by the formation of deposits on the catalyst or by leaching of the catalyst. However, IR spectra of fresh and used catalysts were the same which indicated that no deposit was formed on the catalysts. On the other hand, no noble metal leaching occurred with the reaction. Some results from the literature revealed the existence of strongly adsorbed reaction products that partically blocked the surface, producing deactivation. In the CWAO runs of butyric acid, in this study, acetic acid was observed as an intermediate compound which was strongly adsorbed on platinum group metals (Gallezot et al., 1997). It partically blocked the surface, producing a genuine deactivation. Acetic acid had a retardation effect on the oxidation rate of BA. The presence of acetic acid in the reaction products also supported the idea that the oxidation of butyric acid was proceeded via the formation of acetic acid (Gomes et al., 2004). Acetic acid was also dedected by Gomes et al. **(**2002a**)** as an intermediate in the butyric acid oxidation on carbon supported iridium catalysts. It was reported by Lee and Kim (2000) oxalic acid and formic acid were produced as intermediates in the CWAO of maleic acid on a Pt/Al_2O_3 catalyst. Formation of acrylic, oxalic, pyruvic, fumaric, succinic, formic and acetic acids were successfully identified by Oliviero et al. (2001) on Ru/CeO_2 catalyst at temperatures of 433-473 K with an oxygen partial pressure of 20 bar in the CWAO of maleic acid. However, no study was reported on the observation of formic and oxalic acids in the CWAO of butyric acid on supported platinum group metal catalysts. They were highly reactive and at temperatures of 473 K and at an oxygen partial pressures of 6.9 bar their reactivity increased in the presence of noble metal catalysts and they were oxidized into CO_2 at a very high rate. In the present study, the temperature and pressure are too low (333 K and atmospheric pressure) for oxidation of formic acid and oxalic acid into CO_2 on the

studied catalysts and these acids were detected as intermediates in the CWAO of butyric and maleic acids.

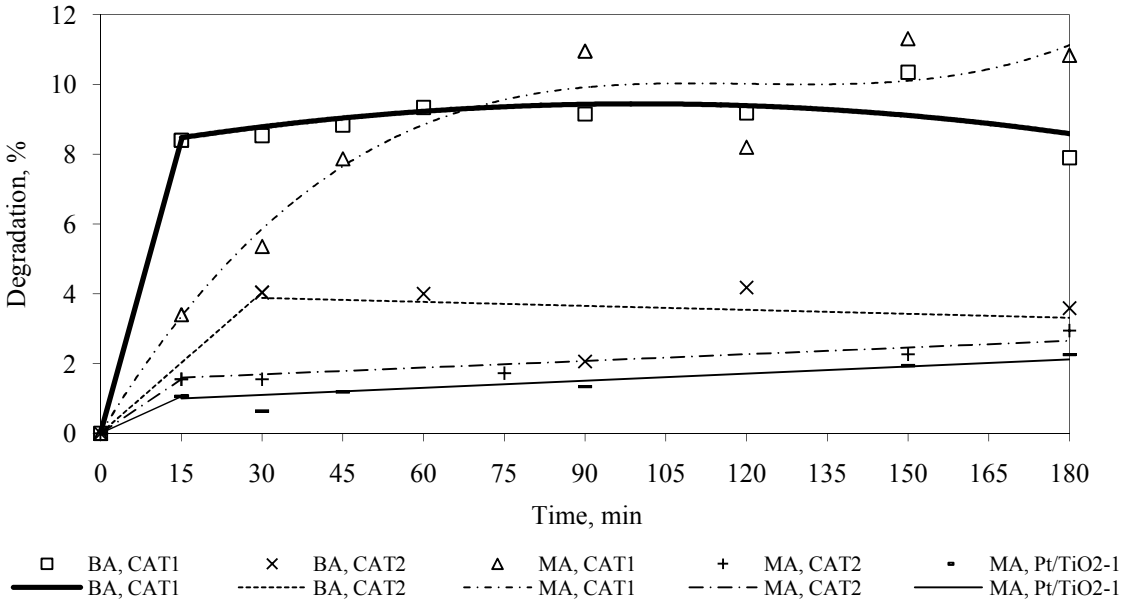

Figure 4.22. Degradation of butyric and maleic acids at atmospheric pressure.

Figure 4.23 showed the total carbon balance for BA and MA oxidation on CAT1. The sum of the organic carbon contributions calculated from all the individually detected liquid phase organic intermediates and the CO_2 measured (C_t=t) was expressed as a percentage of the initial carbon content (C_t=0) and plotted against the reaction time. As can be seen, after a reaction duration of 180 min, the MA oxidation is around 14 % and the BA oxidation is around 10% of the initial carbon content that was detected. In the reaction conditions used in this study, partial oxidation reactions were important and a substantial fraction of the initial carbon was present in various intermediates. Oxalic acid (OA) and formic acid (FA) were formed in the oxidation of both acids. However, in BA oxidation, acetic acid (AA) was also detected. At such low conversion conditions, the limitations of the HPLC-UV analysis became important and accurate quantification became difficult at relatively low intermediate concentrations due to the weak UV response factors, as well as in the determination of CO_2 concentration by titration. Total oxidation into CO_2 was very small and ranged from 0.0 to 0.6 % for BA and from 0.04 to 1.7 % for MA. Selectivity to CO_2, which is defined as the ratio of number of the moles carboxylic acid converted into CO_2, to total number of moles of carboxylic acid consumed, was 4.4 % and 5.3 % in the oxidation of BA and MA over CAT1, respectively. However, selectivity to CO_2 was rather high (55 %) for CAT2 in the oxidation of MA

(Dükkancı and Gündüz, 2009). The catalyst Pt/TiO_2-1 showed some activity (2.1 %) for MA oxidation and Pd/TiO_2-3 for BA oxidation (2.3 %) with CO_2 selectivities of 21 % and 15.2 %, respectively.

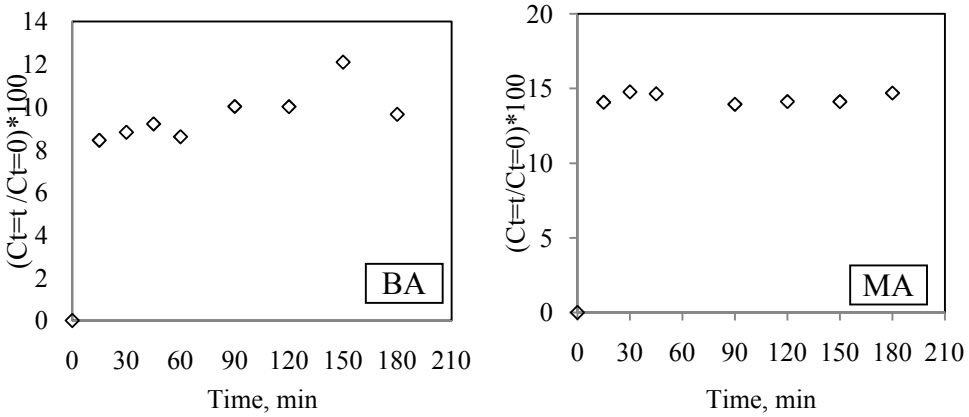

Figure 4.23. Total carbon balance for BA and MA oxidation on CAT1.

Figure 4.24 and 4.25 showed the change in composition of the reaction medium as a function of time in the CWAO of BA and MA, respectively on CAT1 which was the most active one among the catalysts tested.

It was observed that formic acid had a higher initial formation rate than those of oxalic acid and acetic acid in the CWAO of butyric acid on CAT1 (Figure 4.24). The concentrations of acetic acid, formic acid and oxalic acid in the reaction mixture presented the following ordering: FA > AA> OA. In the CWAO of maleic acid, oxalic acid and formic acid were dedected as intermediates and the formic acid concentration was greater than that of oxalic acid in the reaction medium (Figure 4.25). It supports the idea that maleic acid was converted into oxalic acid and then into formic acid and the rate determining step was the conversion of maleic acid to oxalic acid (Lee and Kim, 2000).

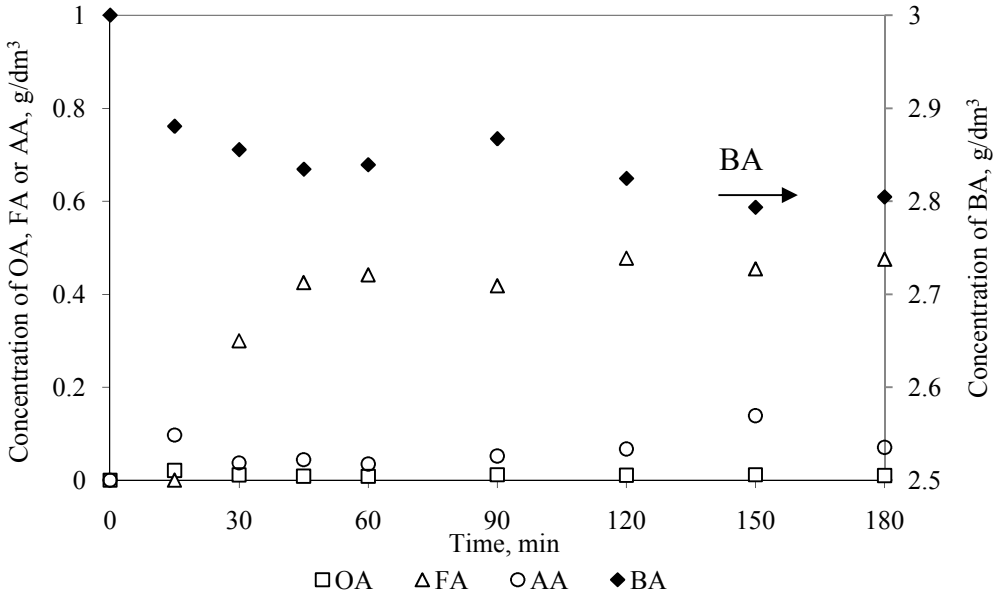

Figure 4.24. Change in the composition of the reaction medium as a function of time in CWAO of BA on CAT1.
(Initial conc. of BA = 3 g/dm^3, Catalyst amount = 1g/0.15 dm^{3}solution, Temperature = 333 K, Air flow rate = 0.003 dm^3/s)

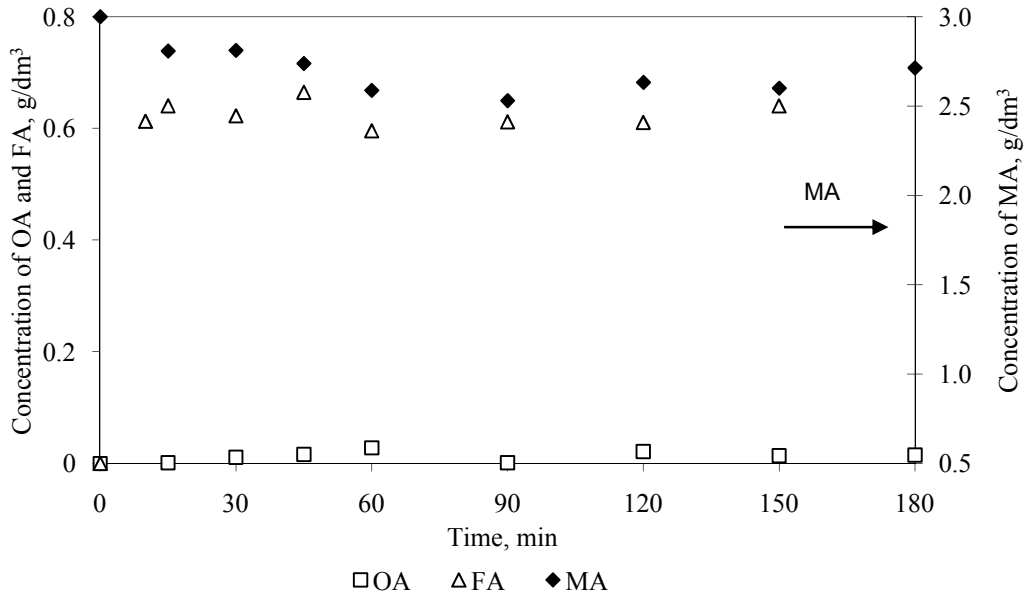

Figure 4.25. Change in the composition of the reaction medium as a function of time in CWAO of MA on CAT1.
(Initial conc. of MA = 3 g/dm^3, Catalyst amount = 1g/0.15dm^3 solution, Temperature = 333 K, Air flow rate = 0.003 dm^3/s)

Leaching of the metals has been assayed during the experiments. No measurable Pt leaching was observed with CAT1 and CAT2 in CWAO of BA and

MA. On Al_2O_3 supported catalysts, the leaching of Pt was less than 1 % for oxidation of BA and MA. On silicagel and TiO_2 supported Pt catalysts, Pt leaching ranged from zero to 1 %. No leaching of Pd was observed in CWAO experiments of BA over Ru-Pd/AC catalyst. However, Pd leaching was around 45.5% in MA oxidation runs. In order to decrease Pd leaching, pH of MA aqueous solution was increased from 2 to 3.13. The CWAO run of MA with pH 3.13 resulted in a degradation degree of 11.40% and a Pd leaching of 4.78 %. The decrease in MA degradation showed that the maleate anion formed at high pH was much more difficult to oxidize than the maleic acid (Barbier et al., 1998).

Figures 4.26 and 4.27 give the change in the composition of the reaction medium as a function of time in CWAO of BA and MA over Ru/Pd/AC catalyst. The formed intermediates were OA and FA in oxidation of BA and MA over this catalyst under the experimental conditions used. Similar to the oxidation BA and MA over CAT1 catalyst the formation rate of FA is higher than the formation rate of OA, expecially in MA oxidation over Ru-Pd/AC catalyst.

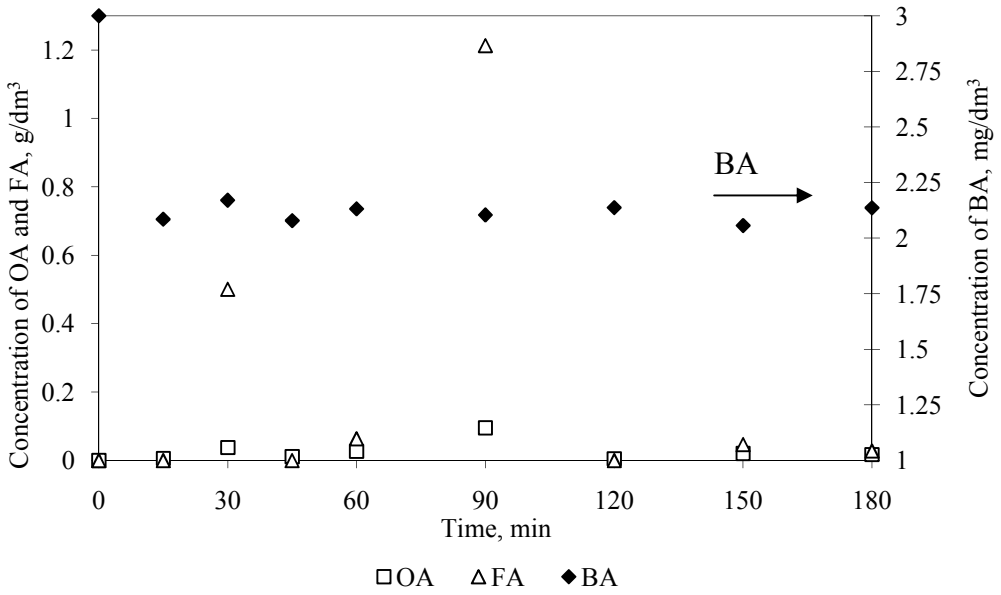

Figure 4.26. Change in the composition of the reaction medium as a function of time in CWAO of BA over Ru-Pd/AC catalyst.
(Initial conc. of BA = 3 g/dm^3, Catalyst amount = 1g/0.15 dm^{3}solution, Temperature = 333 K, Air flow rate = 0.003 dm^3/s)

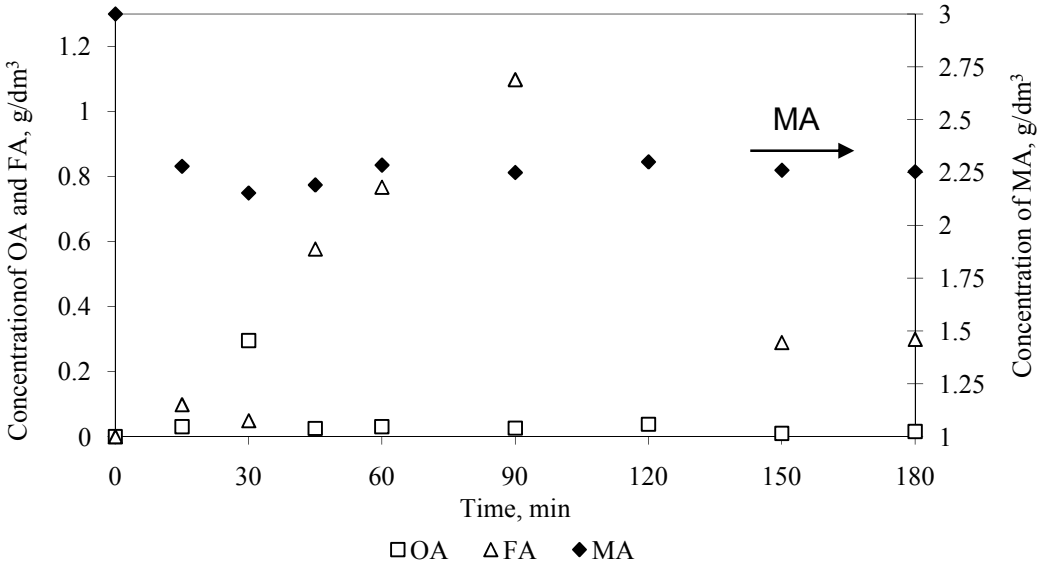

Figure 4.27. Change in the composition of the reaction medium as a function of time in CWAO of MA over Ru-Pd/AC catalyst.
(Initial conc. of MA = 3 g/dm^3, Catalyst amount = 1g/0.15 dm^{3}solution, Temperature = 333 K, Air flow rate = 0.003 dm^3/s)

4.3 Catalytic Wet Air Oxidation of Butyric and Maleic Acid at Pressures Higher than Atmospheric

The degradation degrees of butyric and maleic acids over different catalysts at atmospheric pressure had been given in Part 4.2 (Table 4.2) and CAT1 had been found to be the most active catalyst in CWAO of BA or MA dissolved in water with degradation degrees of 7.9 % and 11%, respectively. So in this part of the study, catalytic wet air oxidation of butyric acid and maleic acid were studied on commercial CAT1 catalyst at pressures higher than atmospheric. Oxidation studies of butyric acid (BA) and maleic acid (MA) were performed in a 0.25 dm^3 stainless steel high pressure reactor (Parr 4576) explained in detail in Part 3.3.2.

4.3.1 Oxidation of butyric acid

4.3.1.1 Effect of oxygen pressure on degradation of butyric acid

The effect of oxygen pressure on the degradation degree of 3 g/dm^3 aqueous BA solution was investigated by the runs with an oxygen pressure range of 2.8-9.7 bar, keeping the temperature at 393 K and the catalyst amount at 10 g/dm^3

constant under continuous stirring (500 rpm). The highest degradation degree (17.3%) was obtained at 9.7 bar of oxygen pressure after 3 hours, Figure 4.28.

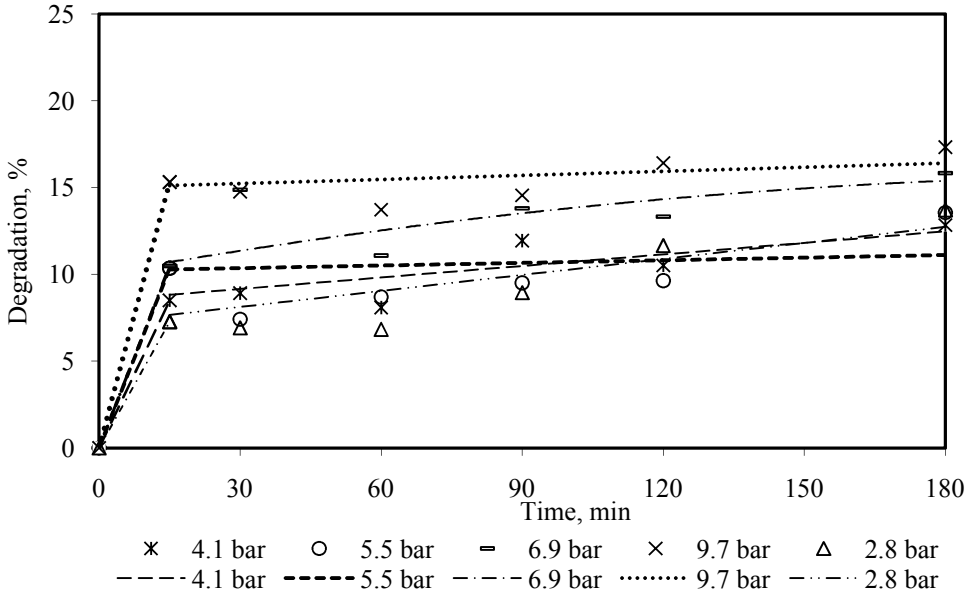

Figure 4.28. Influence of oxygen pressure on the degradation degree of BA.
(Initial concentration of BA=3 g/dm^3, Temperature=393 K, Catalyst=10 g/dm^3, Volume=0.1 dm^3, Stirring speed=500 rpm)

Initial rates ($r_{BA,0}$) were increased with increasing oxygen pressure (P_{O2}) in the range of 2.8 to 9.7 bar. Figure 4.29 showed the $\ln(r_{BA,0})$ vs. $\ln(P_{O2})$ curve in CWAO of butyric acid under the conditions studied. For a given concentration of BA, equal to 3 g/dm^3 (3.4×10^{-2} M), the plot of $\ln(r_{BA,0})$ versus $\ln(P_{O2})$ gives a straight line from which a reaction order of 0.56 with respect to oxygen pressure could be calculated keeping the temperature and initial concentration of BA constant. This result was in a good accordance with literature on CWAO of BA over carbon supported iridium catalyst. Gomes and coworkers 2002a and 2002b expressed the initial specific rate in the CWAO of butyric acid with an order of 0.61 over a commercial 5 wt % Ir/C-α catalyst and with an order of 0.68 over a 5 wt % Ir/C catalyst (prepared by two step impregnation method over non oxidized support) in oxygen partial pressure.

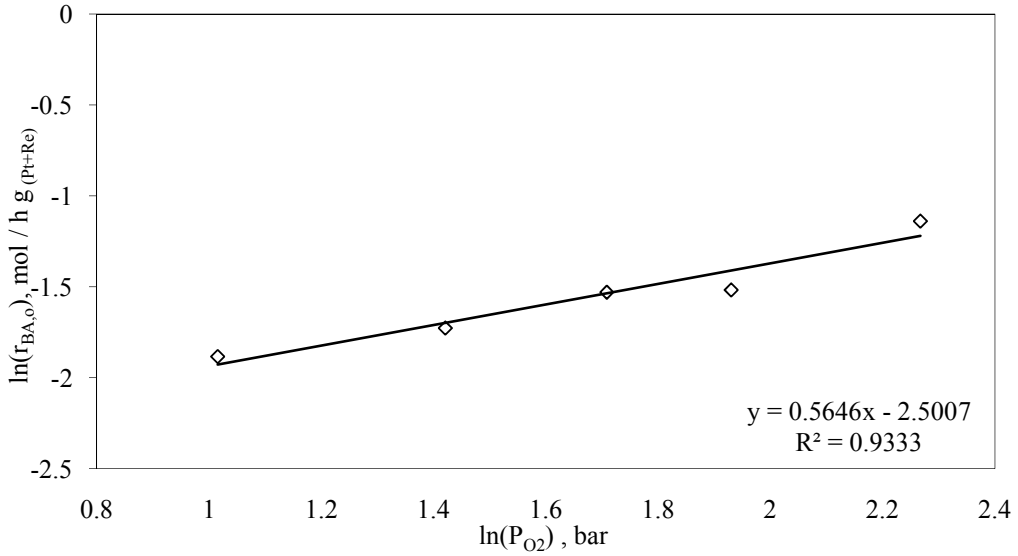

Figure 4.29. Dependency of oxygen pressure on the initial rate of BA.

4.3.1.2 Effect of temperature on degradation of BA

The effect of temperature on CWAO of 3 g/dm^{3}butyric acid was tested at 6.9 bar of oxygen pressure on CAT1 catalyst for a catalyst loading of 10 g/dm^3 at four different temperatures namely; 393, 408, 423 and 453 K. The temperature effect on the degradation degree of BA was presented in Figure 4.30. The highest degradation degree (25.9 %) was observed after an oxidation time of 3 h, at the highest temperature of 453 K, as expected, due to the increase in reaction rate constant, k, with temperature.

From the Arrhenius – type plot of $\ln(r_{BA,0})$ as a function of 1/T (Figure 4.31), from the slope of the straight line, an activation energy of 24.6 kJ mol^{-1} was measured. In the oxidation experiments of butyric acid done by Gomes et al. (2002a - 2002b) and Gomes et al. (2000) , the measured activation energies were 59 and 58 kJ/mol on Ir/C and 57 kJ/mol on Pt/C catalysts at 6.9 bar of partial oxygen pressure and at a temperature range of 453 – 493 K for an empirical initial rate equation in the oxidation of butyric acid. The obtained activation energy in this study, 24.6 kJ/ mol, on CAT1 catalyst, was lower than those of CWAO of BA on carbon supported Ir or Pt catalysts under the experimental conditions used. It indicated that the presence of CAT1 catalyst caused a significant drop in activation energy of the CWAO reaction of BA dissolved in water.

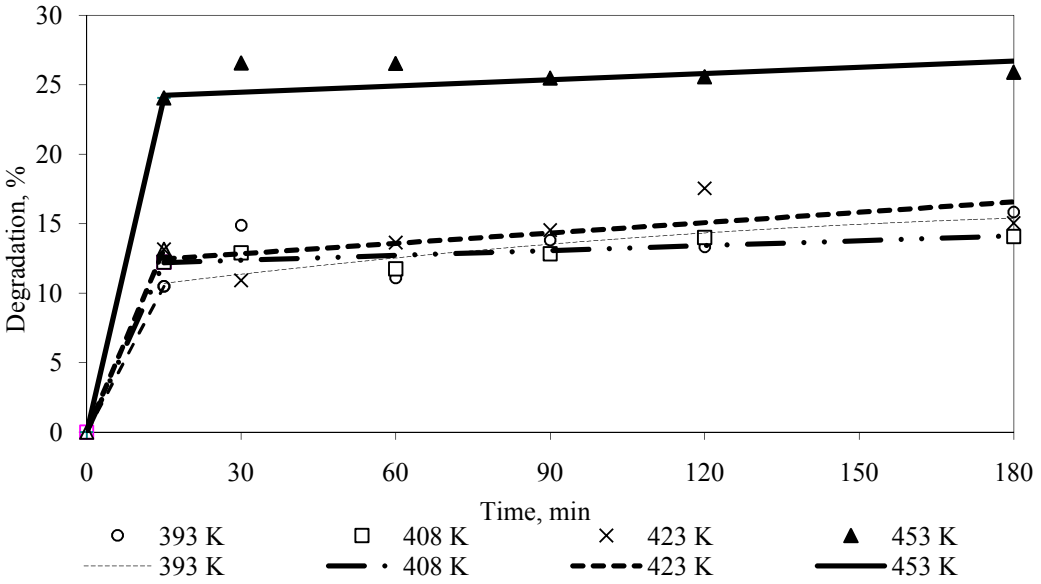

Figure 4.30. Influence of temperature on the degradation degree of BA.
(Initial concentration of BA=3 g/dm^3, Pressure=6.9 bar, Catalyst=10 g/dm^3, Volume=0.1 dm^3, Stirring speed=500 rpm)

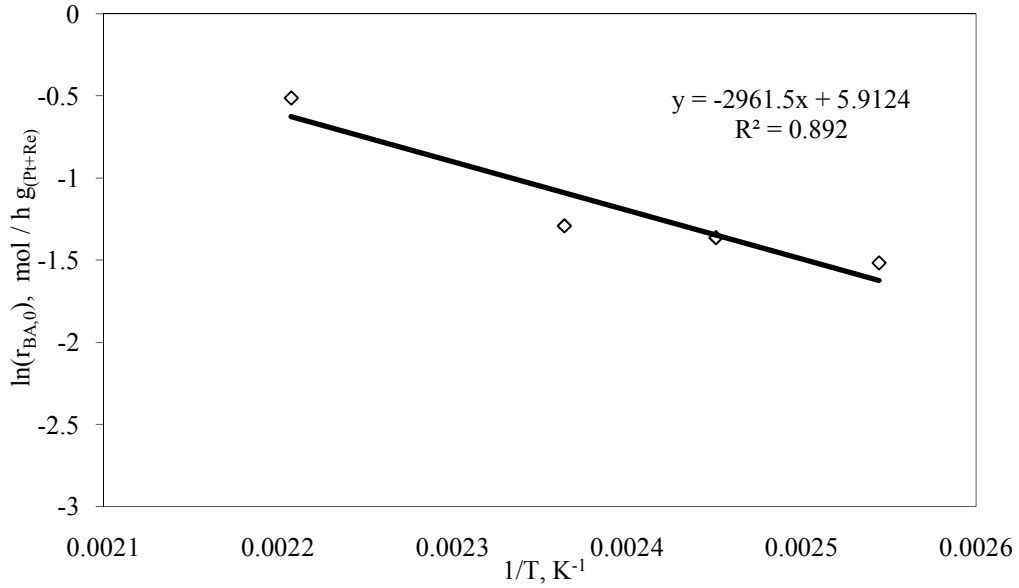

Figure 4.31. ln(-$r_{BA,0}$) vs. 1/T graph.

As given in Part 4.2, catalytic wet air oxidation of butyric acid had been carried out in a batch reactor operated at 333 K and at atmospheric pressure. In CWAO of BA under those experimental conditions, the obtained degradation degree was about 7.9 % which was lower than conversions obtained in butyric acid oxidation at pressures higher than atmospheric. In the CWAO of butyric acid on CAT1 catalyst at atmospheric pressure, acetic, formic and oxalic acids were

observed as intermediate compounds (Figure 4.24) (Dükkancı and Gündüz, 2009). However, at high pressure, only formic (FA) and oxalic acids (OA) were detected as intermediates, as seen from Figure 4.32. Acetic acid and propionic acid were reported by Gomes et al. (2002a and 2002b) as intermediates in the CWAO of butyric acid on carbon supported iridium catalyst and carbon supported Pt catalyst (Gomes et al., 2005). The formation of formic and oxalic acids in this study indicated that, those acids could not be completely oxidized into CO_2 and water on the CAT1 catalyst under the operating conditions used. Table 4.3 presents the CWAO results of BA at different oxygen pressures. Selectivity to CO_2 increased with increasing oxygen pressure. In addition to this, when oxygen pressure was increased from 2.8 to 9.7 bar at 393 K, selectivity to OA and FA were decreased from 4.5 % to 2.2 % and from 85.7 % to 56.7 %, respectively while selectivity to CO_2 was increased from 9.8 % to 41.1 %. These results indicated that butyric acid was converted into oxalic acid which subsequently degraded into formic acid. Finally formic acid was oxidized into CO_2 and water.

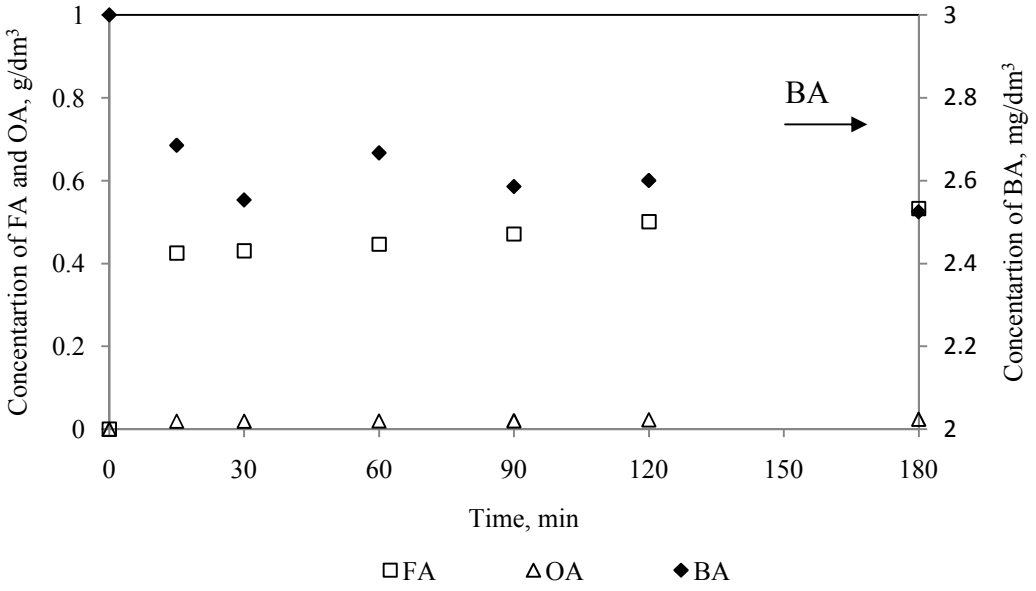

Figure 4.32. Change in the composition of the reaction medium as a function of time in CWAO of BA over CAT1 catalyst.
(Initial concentration of BA=3 g/dm^3, Temperature=393 K, Pressure=6.9 bar, Catalyst=10 g/dm^3, Volume=0.1 dm^3, Stirring speed=500 rpm)

Table 4.3. CWAO results of BA at different oxygen pressures and temperatures.

BA concentration (g/dm^3)	P_{O2} (bar)	Temperature (K)	Degradation of BA (%)	Selectivity (%) to		
				Oxalic acid	Formic acid	CO_2
3	2.8	393	13.7	4.5	85.7	9.8
3	4.1	393	12.8	4.5	82.0	13.5
3	5.5	393	13.6	4.5	81.9	13.6
3	6.9	393	15.8	5.0	69.2	25.8
3	9.7	393	17.3	2.2	56.7	41.1
3	6.9	408	14.1	5.0	60.4	34.6
3	6.9	423	15.0	8.1	64.7	27.2
3	6.9	453	25.9	6.9	55.6	37.5

4.3.1.3 Effect of initial concentration of BA on degradation

The effect of initial concentration of BA on the degradation degree of butyric acid was determined at 6.9 bar of oxygen pressure by the runs with different initial concentrations of butyric acid ($C_{BA,0}$) such as 0.5, 1, 2 and 3 g/dm^3 keeping the temperature at 393 K, stirring rate at 500 rpm and the catalyst amount at 10 g/dm^3 constant, Figure 4.33. The highest degradation degree (18.3 %) was obtained for an initial concentration of 0.5 g/dm^3 BA. It was followed by 17.7 % for 1 g/dm^3 initial concentration of BA. Lower degradation degrees were obtained for initial concentrations of 2 and 3 g/dm^3 (14.7 % and 15.8 %) after 3 h oxidation. The decrease in degradation degree with increasing initial concentration could be explained by the presence of less oxygen than required for higher concentrations of BA.

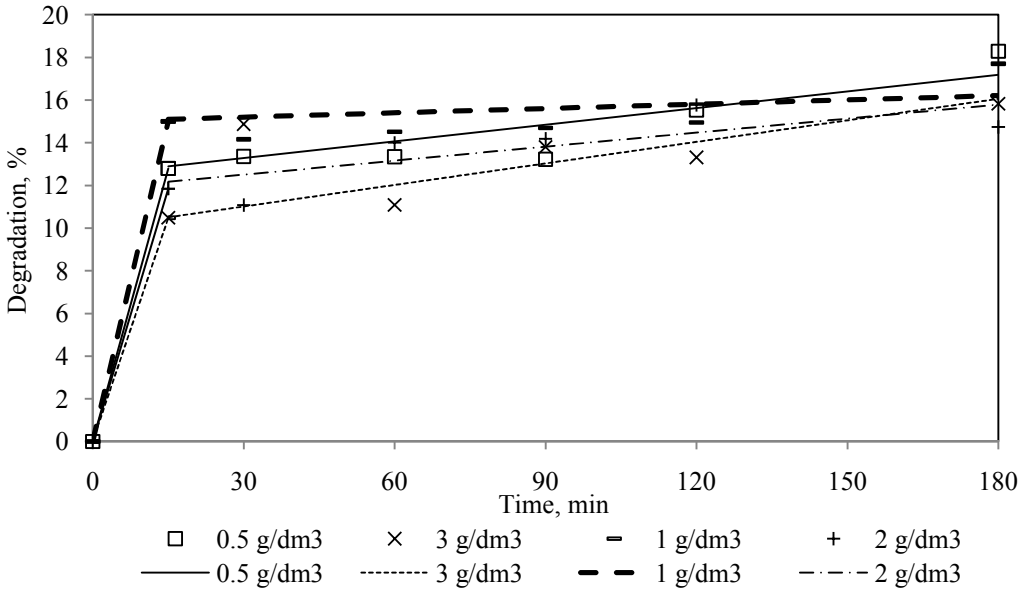

Figure 4.33. Influence of initial concentration of BA on the degradation degree. (Temperature=393 K, Pressure=6.9 bar, Catalyst=10 g/dm^3, Volume=0.1 dm^3, Stirring speed=500 rpm)

By ploting $\ln(-r_{BA,0})$ vs. $\ln C_{BA,0}$, Figure 4.34, the reaction order with respect to BA can be found from the slope of the straight line obtained, which was equal to 0.87 ~ 1.0. The degradation of BA followed first order or pseudo first order kinetics in literature (Gomes et al., 2002a, 200b), as well.

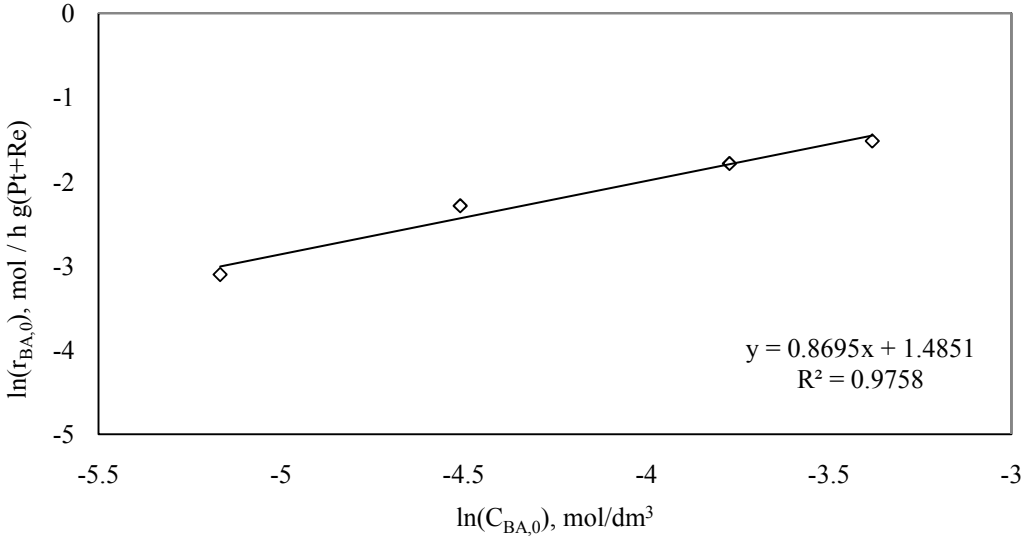

Figure 4.34. $\ln(-r_{BA,0})$ vs. $\ln(C_{BA,0})$ graph in CWAO of BA.

By combining all the data obtained from Figures 4.29, 4.31 and 4.34 , the initial rate of BA oxidation, $-r_{BA,0}$, (in mol h^{-1} $g^{-1}_{(Pt+Re)}$) was described by the following empirical rate law equation (4.1):

$$r_{BA,0} = 2.25x10^3 \times e^{-24.6/RT} C_{BA,0}^{0.87} P_{O2}^{0.56} \quad (4.1)$$

with $C_{BA,0}$ in moL/dm^3, P_{O2} in bar. The validity of this equation has to be limited to the used ranges of operating conditions, which are $2.8 < P_{O2} < 9.7$ bar, $0.5 < C_{BA,0} < 3$ g/dm^3, catalyst loading=10 g/dm^3 and $393 < T < 453$ K.

4.3.1.4 Effect of catalyst loading on degradation of BA

The effect of catalyst loading on CWAO of butyric acid was studied at 393 K and at 6.9 bar of oxygen pressure for an initial concentration of 3 g/dm^3 with different catalyst loadings such as 5, 10 and 15 g/dm^3. Figure 4.35 showed degradation % vs time curves. The degradation degrees obtained after 3 h were 9.6 %, 15.8 % and 16.3 % for catalyst loadings of 5, 10 and 15 g/dm^3, respectively. The initial rates were calculated as 0.136, 0.219 and 0.243 mol h^{-1} $g^{-1}_{(Pt+Re)}$ for 5, 10 and 15 g/dm^3 of catalyst loadings, respectively. The initial rates were almost similar for catalyst loadings of 10 and 15 g/dm^3. It showed that external mass transfer resistance is negligible for catalyst loadings equal or greater than 10 g/dm^3.

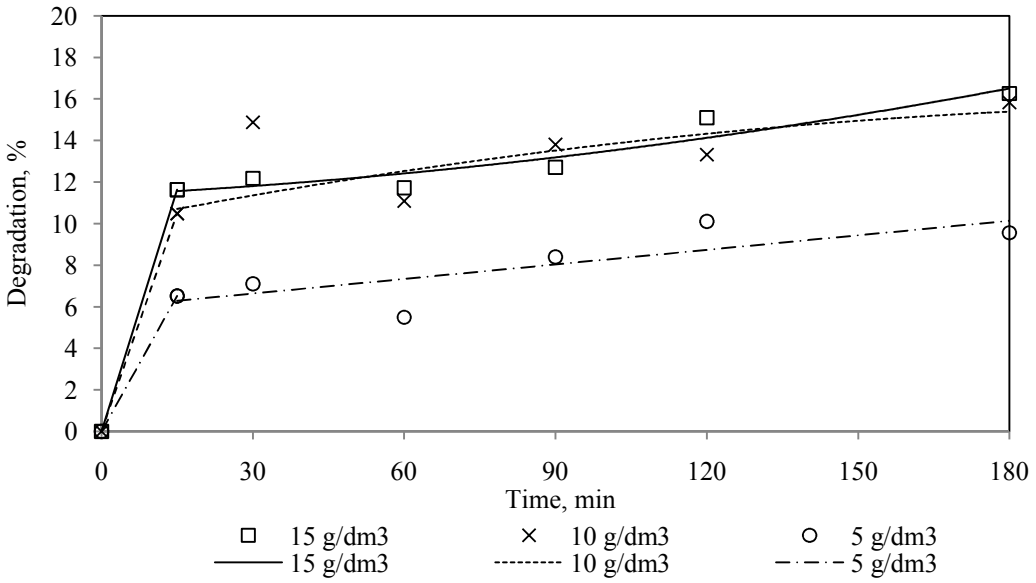

Figure 4.35. Influence of catalyst loading on the degradation degree of BA.
(Initial concentration of BA=3 g/dm^3, Temperature=393 K, Pressure=6.9 bar, Volume=0.1 dm^3, Stirring speed=500 rpm)

It can be concluded that the reaction rates were not limited by the external mass transfer resistance under the standard reaction conditions involving 10 g/dm^3 of catalyst loading. On the other hand, under the standard conditions, the reaction mixture was stirred vigorously at 500 rpm. Stirrer speeds higher than 500 rpm (for instance 630 rpm) did not affect the oxidation rate of BA. Internal diffusion resistance was also negligible due to the powder form of the catalyst used in the runs (Beziat et al., 1999). So measured rates were intrinsic rates which did not involve the effects of the physical processes.

Leaching of Pt, measured by atomic absorption spectrometer (Varian 10 plus), was about 2.5 mg/dm^3 in CWAO of BA after a reaction time of 3 hours. These values corresponded to a leaching of 3.33 % of the total amount of platinum per hour in CWAO of BA. The obtained Pt leaching value was rather close to European Union directives (<2 mg/dm^3) (Ramirez et al., 2007).

In the oxidation studies of BA on Pt/C catalyst done by Gomes and coworkers (2004 and 2005), it was concluded that almost no Pt leaching occurred under the experimental conditions used in those studies. Carbon based materials are much more resistant to leaching in acidic solutions under WAO conditions than typical oxide supports (Cybulski and Trawezynski, 2004).

CWAO of BA was also investigated on Pt/TiO_2-2 and Ru-Pd/AC catalysts which had rather good activity in CWAO of BA at atmospheric pressure, Table 4.2. Degradation degrees versus time curves were presented in Figure 4.36 over the catalysts mentioned above on CWAO of BA at an oxygen pressure of 6.9 bar, at a temperature of 393 K with 10 g/dm^3 catalyst for initial concentration of BA of 3 g/dm^3 under the continuous stirring at 500 rpm.

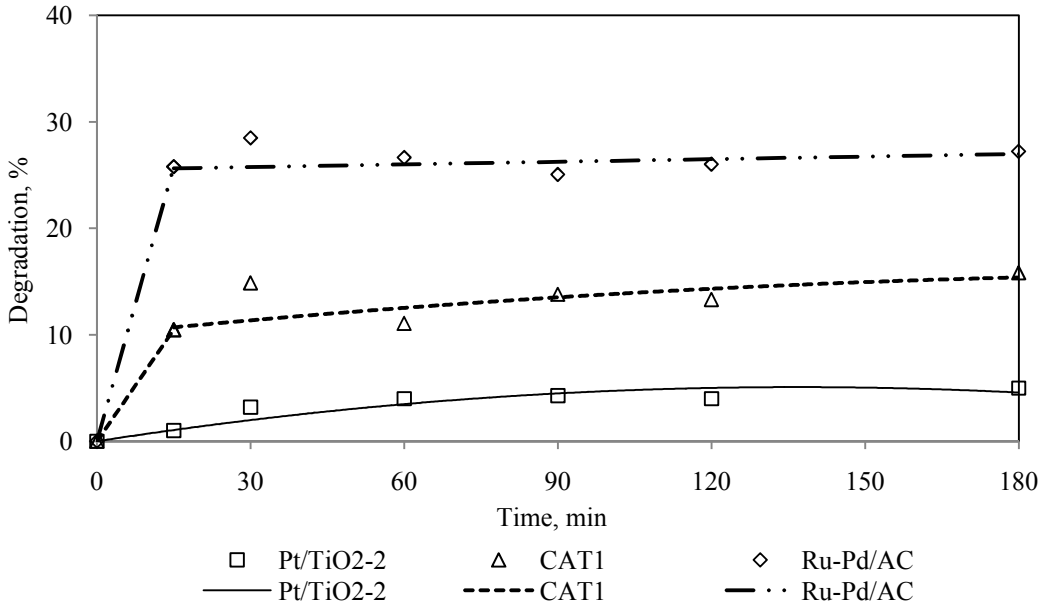

Figure 4.36. CWAO of BA on different catalysts at 6.9 bar oxygen pressure. (Initial concentration of BA=3 g/dm^3, Temperature=393 K, Pressure=6.9 bar, Volume=0.1 dm^3, Catalyst=10 g/dm^3, Stirring speed=500 rpm)

The degradation degree of BA on different catalysts at atmospheric pressure and at pressures higher than atmospheric pressure was given in Table 4.4. As seen from Table 4.4, the obtained degradation degree of BA at 6.9 bar of oxygen pressure was higher than that obtained at atmospheric pressure on each catalyst after 3 h of oxidation.

Table 4.4. Degradation degree of BA on different catalysts at atmospheric pressure and at pressures higher than atmospheric pressure.

Catalyst Name	Degradation degree at atmospheric pressure after 3h oxidation, %	Degradation degree at 6.9 bar of oxygen pressure after 3h oxidation, %
Ru-Pd/AC	24.6	27.2
CAT1	7.9	15.8
Pt/TiO_2-2	2.6	5.0

Catalytic wet air oxidation of butyric acid was studied on Ru-Pd/AC catalyst at 6.9 bar of oxygen pressure for an initial concentration of 3 g/dm^3 with a catalyst loading of 10 g/dm^3 at different temperatures. Results were given in Figure 4.37.

As seen from Figure 4.37, degradation degree and initial degradation rate increased with increasing temperature. The degradation degrees obtained after 3h

were 27.2 %, 33.5 % and 34.2 % for temperatures of 393 K, 408 K and 423 K, respectively. The initial rates at 393, 408 and 423 K were calculated as 0.18, 0.21 and 0.25 mol h^{-1} $g^{-1}_{(Ru+Pd)}$, respectively.

In literature, in the catalytic wet air oxidation of butyric acid at an oxygen pressure of 6.9 bar and at a temperature of 473 K over carbon supported Ir catalysts which were prepared by two different incipient wetness impregnation method with different reduction temperatures, the conversions of BA were in the range of 24. 1 % - 52.9 % (Gomes et al., 2002a) and 9.5 % - 42.6 % (Gomes et al., 2002b) after an oxidation time of 2 h.

In the catalytic wet air oxidation of BA on carbon supported Pt catalysts prepared by incipient wetness impregnation method and by organometallic chemical vapor deposition, the conversions of BA were obtained to be 59.4 % and 46.6 %, respectively, at a an oxygen pressure of 6.9 bar and at a temperature of 473 K (Gomes et al., 2005).

In another study (Gomes et al., 2004) in the catalytic wet air oxidation of BA over Pt/C and Ir/C catalysts at a temperature of 473 K and an oxygen pressure of 6.9 bar, degradation degree of BA was found to be 75 and 60 %, respectively.

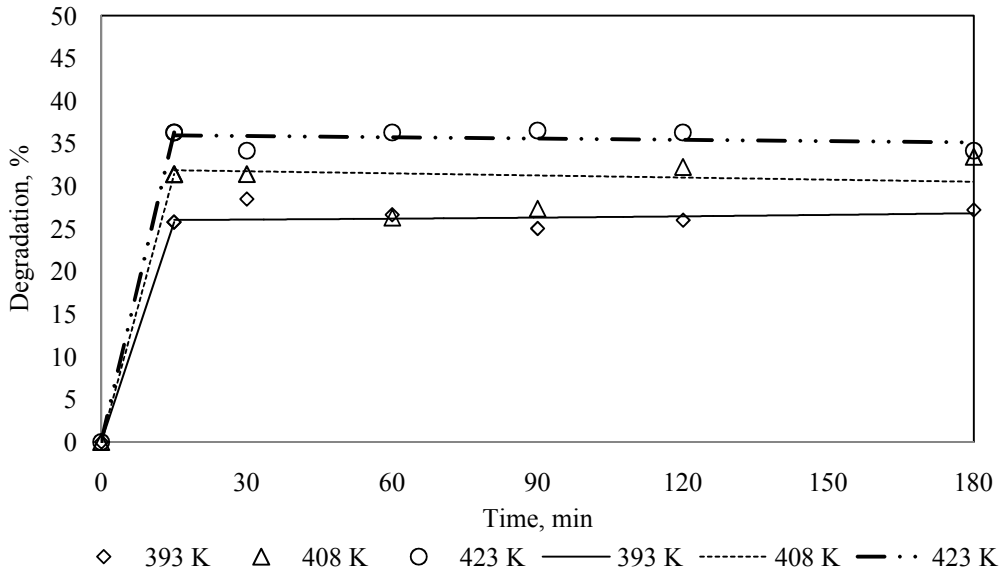

Figure 4.37. Effect of temperature on degradation degree of BA over Ru-Pd/AC catalyst. (Initial concentration of BA=3 g/dm^3, Volume=0.1 dm^3, Catalyst amount= 10 g/dm^3, Pressure=6.9 bar, Stirring speed=500 rpm)

On the other hand, in the presence of activated carbon as support, which is known as a good adsorbent, adsorption of BA on surface may be more important than oxidation of BA on surface. To distinguish this, adsorption runs of BA on Ru-Pd/AC were carried out at temperatures of 393 K, 408 K and 423 K at an inert (nitrogen) pressure of 6.9 bar. Adsorption of 17.62 %, 16,42 % and 17 % were observed at temperatures of 393 K, 408 K and 423 K , respectively. These results showed that, under the conditions used, adsorption was an important contribution to the removal of BA with CWAO over Ru-Pd/AC catalyst. In literature, in the oxidation of BA over carbon supported Pt or Ir catalysts, there was no information about the adsorption of BA on AC support or on those catalysts (Gomes et al., 2000; Gomes et al., 2002a, 2002b; Gomes et al., 2004; Gomes et al., 2005).

4.3.1.5 Kinetic modeling of CWAO of butyric acid over CAT1 catalyst in high temperature-pressure reactor

The experimental data obtained for the CWAO of butyric acid over CAT1 catalyst at four different temperatures, namely 393, 408, 423 and 453 K at an oxygen pressure of 6.9 bar were modeled considering the reaction scheme presented in Figure 4.38. As mentioned Part in 4.3.1.2 , during the oxidation BA, oxalic acid and formic acid were formed as intermediates.

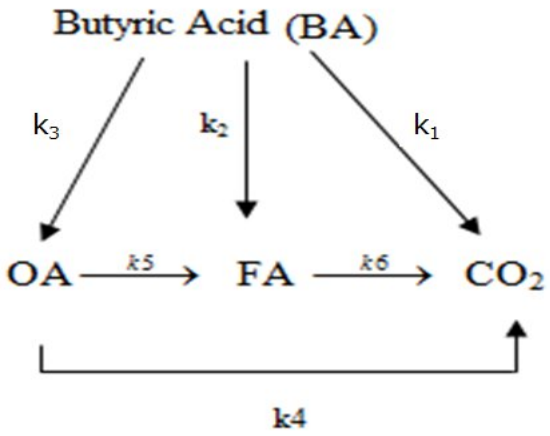

Figure 4.38. Proposed scheme for butyric acid degradation.

In literature, in the CWAO of BA on Ir/AC catalyst at 473 K and at a pressure of 6.9 bar, the employed model was based on a Langmuir-Hinshelwood mechanism. It was assumed that the reaction occurs in the adsorbed state between an organic molecule and oxygen adsorbed dissociatively characterized by

adsorption equilibrium constants K_i and independent rate constants k_i (Gomes et al., 2002b).

In another study, same model was used in the CWAO of BA on Ir/AC catalyst at 6.9 bar of oxygen pressure and at a temperature of 473 K by taking catalyst deactivation into account (Gomes et al., 2004).

In the study on the CWAO of BA over Pt/AC catalyst, it was assumed that reaction occurred in the adsorbed state between BA and oxygen adsorbed dissociatively with no appreciable adsorption of any intermediates. In that study deactivation of catalyst was taken into account, too (Gomes et al., 2005).

In this study, the concentrations of butyric acid (C_{BA}), oxalic acid (C_{OA}) and formic acid (C_{FA}) in model equations were obtained by HPLC analysis of the reaction mixture at the corresponding time. It was thought that, the concentration of oxygen decreased with time in the complete oxidation reaction of BA, OA or FA to H_2O and CO_2 according to Equations 4.2 – 4.4.

Oxidation of BA to CO_2 and H_2O;

$$C_4H_8O_2 + 5O_2 \rightarrow 4\ CO_2 + 4\ H_2O \qquad (4.2)$$

Oxidation of OA to CO_2 and H_2O;

$$C_2H_2O_4 + 0.5\ O_2 \rightarrow 2CO_2 + H_2O \qquad (4.3)$$

Oxidation of FA to CO_2 and H_2O;

$$CH_2O_2 + 0.5\ O_2 \rightarrow CO_2 + H_2O \qquad (4.4)$$

Concentration of oxygen in gas phase, $(C_{O2})_g$, was calculated by equation 4.5 (Gomes et al., 2004) and it was used to determine oxygen pressure (P_{O2}) by equations 4.6.

$$\left(C_{O2}\right)_g V_g = \left(C_{O2}\right)_{g0} V_g - 5\left(\left(C_{BA}\right)_0 - \left(C_{BA}\right)\right)V_L + 0.5\left(C_{OA}\right)V_L + 0.5\left(C_{FA}\right)V_L \qquad (4.5)$$

where, $(C_{O2})_g$= concentration of oxygen in gas phase (mmol/dm^3), Vg= Volume of gas (0.150 dm^3), $(C_{O2})_{g0}$= initial oxygen concentration in gas phase (mmol/ dm^3), V_L=Volume of liquid (0.1 dm^3), $(C_{BA})_0$=initial concentration of butyric acid (mmol/dm^3) and (C_{BA}), (C_{OA}), (C_{FA}) are the liquid phase concentrations of butyric, oxalic and formic acids at the corresponding time (mmol/dm^3), respectively.

$$P_{O2} = \left(C_{O2}\right)_g R\,T \tag{4.6}$$

where $\left(C_{O2}\right)_g$ is in mol/dm^3, R=0.082 is in atmdm^{3}mol^{-1}K^{-1} , T (temperature) is in K and P_{O2} is in atmosphere units.

Oxygen concentration in the liquid phase was estimated by Equation (4.7) (Tromans, 1998).

$$\left(C_{O2}\right) = P_{O2} \exp\left\{\frac{0.046T^2 + 203.35T\ln\left(T/298\right) - \left(299.378 + 0.092T\right)\left(T - 298\right) - 20.591x10^3}{\left(8.3144\right)T}\right\} \tag{4.7}$$

In the oxidation of butyric acid nine different model equations were tested. Tested models are described below.

MODEL I

In this model, the reaction rate expression is derived on the assumption that reaction occurs at the catalyst surface between the adsorbed butyric acid and dissociatively adsorbed oxygen (Langmuir-Hinshelwood Mechanism). It is given in Equation (4.8).

$$-\frac{dC_{BA}}{dt}\frac{1}{W} = \frac{\left(k_1 + k_2 + k_3\right)K_{BA}C_{BA}K_{O2}{}^{1/2}C_{O2}{}^{1/2}}{\left(1 + K_{BA}C_{BA} + K_{OA}C_{OA} + K_{FA}C_{FA} + K_{O2}{}^{1/2}C_{O2}{}^{1/2}\right)^2} \tag{4.8}$$

MODEL II

In this model, the reaction rate expression is derived on the assumption that reaction occurs at the catalyst surface between the adsorbed butyric acid and

molecular adsorbed oxygen (Langmuir-Hinshelwood Mechanism). It is given in Equation (4.9).

$$-\frac{dC_{BA}}{dt}\frac{1}{W}=\frac{(k_1+k_2+k_3)K_{BA}C_{BA}K_{O2}C_{O2}}{(1+K_{BA}C_{BA}+K_{OA}C_{OA}+K_{FA}C_{FA}+K_{O2}C_{O2})^2} \tag{4.9}$$

MODEL III

In this model, reaction is like MODEL II but adsorption of OA and FA which are the intermediates formed during the reaction are ignored. Oxidation rate of BA can be written as in Equation (4.10).

$$-\frac{dC_{BA}}{dt}\frac{1}{W}=\frac{k_{sr}K_{BA}C_{BA}K_{O2}C_{O2}}{(1+K_{BA}C_{BA}+K_{O2}C_{O2})^2} \tag{4.10}$$

MODEL IV

In this model, reaction is occurred as given in MODEL I but the adsorption of OA and FA are ignored. In this case oxidation rate of BA can be written as in Equation (4.11).

$$-\frac{dC_{BA}}{dt}\frac{1}{W}=\frac{k_{sr}K_{BA}C_{BA}K_{O2}^{1/2}C_{O2}^{1/2}}{\left(1+K_{BA}C_{BA}+K_{O2}^{1/2}C_{O2}^{1/2}\right)^2} \tag{4.11}$$

MODEL V

In this model, reaction is occurred as given in MODEL I but the adsorption of FA is ignored. In this case oxidation rate of BA can be written as in Equation (4.12).

$$-\frac{dC_{BA}}{dt}\frac{1}{W}=\frac{(k_1+k_2+k_3)K_{BA}C_{BA}K_{O2}^{1/2}C_{O2}^{1/2}}{\left(1+K_{BA}C_{BA}+K_{OA}C_{OA}+K_{O2}^{1/2}C_{O2}^{1/2}\right)^2} \tag{4.12}$$

MODEL VI

In this model, it is assumed that molecular adsorbed oxygen is reacting with BA in the bulk fluid (Eley Rideal Mechanism). The oxidation rate of butyric acid can be written as in Equation (4.13).

$$-\frac{dC_{BA}}{dt}\frac{1}{W}=\frac{k_{sr}C_{BA}K_{O2}C_{O2}}{\left(1+K_{O2}C_{O2}\right)} \tag{4.13}$$

MODEL VII

In this model, it is assumed that dissociatively adsorbed oxygen is reacting with BA in the bulk fluid (Eley Rideal Mechanism). The oxidation rate of butyric acid can be written as in Equation (4.14).

$$-\frac{dC_{BA}}{dt}\frac{1}{W}=\frac{k_{sr}C_{BA}K_{O2}^{1/2}C_{O2}^{1/2}}{\left(1+K_{O2}^{1/2}C_{O2}^{1/2}\right)} \tag{4.14}$$

MODEL VIII

In this model, MODEL VII is taken as a base model but it is assumed that also OA and FA are adsorbed on the catalyst surface. The oxidation rate of butyric acid can be written as in Equation (4.15).

$$-\frac{dC_{BA}}{dt}\frac{1}{W}=\frac{k_{sr}C_{BA}K_{O2}^{1/2}C_{O2}^{1/2}}{\left(1+K_{OA}C_{OA}+K_{FA}C_{FA}+K_{O2}^{1/2}C_{O2}^{1/2}\right)} \tag{4.15}$$

MODEL IX

In this model, MODEL VI is taken as a base model but it is assumed that also OA and FA are adsorbed on the catalyst surface. The oxidation rate of butyric acid can be written as in Equation (4.16).

$$-\frac{dC_{BA}}{dt}\frac{1}{W}=\frac{k_{sr}C_{BA}K_{O2}C_{O2}}{\left(1+K_{OA}C_{OA}+K_{FA}C_{FA}+K_{O2}C_{O2}\right)} \tag{4.16}$$

In these equations, k_1-k_3 are independent reaction rate constants (mmol min^{-1} $g^{-1}_{(Pt+Re)}$), k_{sr} is surface reaction rate constant (mmol min^{-1} $g^{-1}_{(Pt+Re)}$ for Models III and IV and dm^3 min^{-1} $g^{-1}_{(Pt+Re)}$ for Models VI-IX), K_{BA}, K_{OA}, K_{FA} and K_{O2} are adsorption equilibrium constants of butyric acid, oxalic acid, formic acid and oxygen (dm^3 $mmol^{-1}$), (C_{BA}), (C_{FA}), (C_{OA}) and (C_{O2}) are the concentrations of butyric, formic, oxalic acids and oxygen in liquid phase (mmol/ dm^3) and W is the concentration of active component (Pt+Re) in catalyst (0.065 $g_{(Pt+Re)}/dm^3$) (Smith, 1981).

Methods Used in Analysis of Kinetic Models

In the analysis of kinetic models, firstly the rate ($-\frac{dC_{BA}}{dt}\frac{1}{W}$) was calculated by using the experimental data. For this purpose, concentration of butyric acid, $C_{BA,}$ vs. time data were fitted to an n^{th}-order polynomial, Equation 4.17. After that, $\frac{dC_{BA}}{dt}$, Equation 4.18, was obtained by differentiating the resulting polynomial (Equation 4.17) with respect to time. Finally, experimental rate for each time, $-\frac{dC_{BA}}{dt}\frac{1}{W}$, was obtained by multiplying the derivative for the appropriate time with ($-\frac{1}{W}$).

The plot of concentration of BA as a function of time and third degree polynomial fit were given in Figure 4.39.

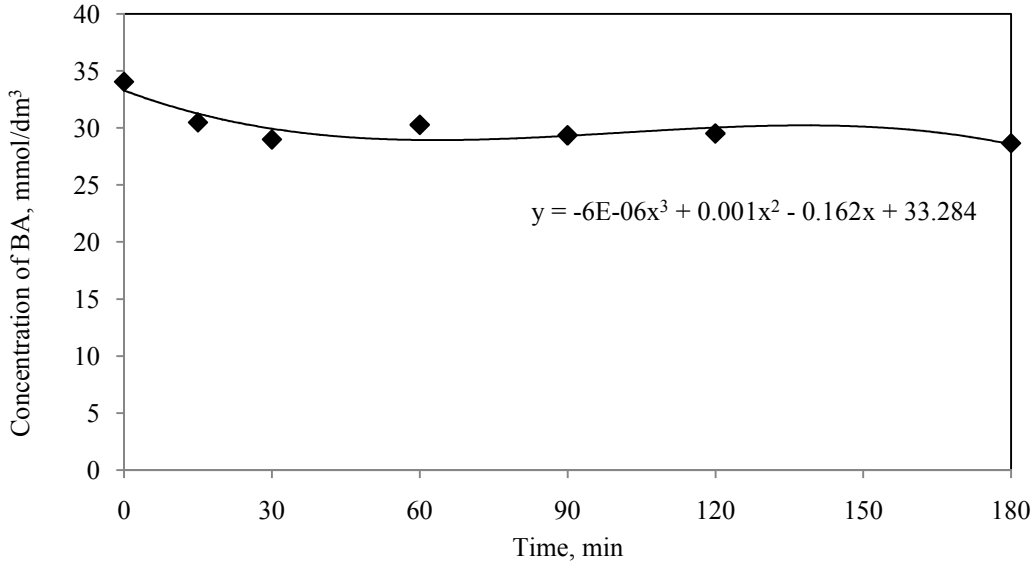

Figure 4.39. C_{BA} vs. time plot and polynomial fit.
(Initial concentration of BA=3 g/dm^3, Volume=0.1 dm^3, Catalyst amount= 10 g/dm^3, Pressure=6.9 bar, Temperature =393 K, Stirring speed=500 rpm)

$$C_{BA}(t) = -6x10^{-6}t^3 + 0.001t^2 - 0.162t + 33.284 \quad (4.17)$$

$$\frac{dC_{BA}}{dt} = -18x10^{-6}t^2 + 0.002t - 0.162 \quad (4.18)$$

In the analysis of model equations, nonlinear least-squares analysis was applied to reaction rate data to determine the rate law parameters. It was searched for the values of the constants present in the model equations that would minimize the sum of the squared differences of the measured rates, r_{exp}, and the calculated rates, r_{cal}. That is, the sum of $\sum_{all\ data\ samples}\left(r_{\exp} - r_{cal}\right)^2$ was requested to be minimum. Mean relative error percentage between the experimental and calculated rate obtained from models were wanted to be also minimum.

Mean relative error percantage was calculated according to equation 4.19:

$$\text{Mean relative error, \%} = \frac{\sum_{all\ data\ samples}\left(\frac{r_{\exp} - r_{cal}}{r_{\exp}}\right) * 100}{n_{sample}} \quad (4.19)$$

In each model, 6 criteria were used for model elimination (Tufan and Akgerman, 1982);

a. The rate constants can not be negative.

b. All rate constants must obey Arrhenius Law, that is (lnk) must be a linear function of inverse temperature.

c. The adsorption equilibrium constants must be decreased with increasing temperature.

d. The adsorption equilibrium constants can not be negative.

e. The sum of the squared differences of the experimental reaction rates and the calculated reaction rates $\sum_{all\ data\ samples}\left(r_{\exp}-r_{cal}\right)^2$ will be minimum

f. Model should fit the data with minimum error. That is, mean relative error percantage will be minimum.

Tested models were evaluated according to the first four criteria and the results were given in Table 4.5.

Table 4.5. Model elimination in CWAO of BA.

MODEL Number	Criterion Number			
	a	b	c	d
I	+	+	-	+
II	+	+	+	+
III	+	+	+	+
IV	+	+	-	+
V	+	+	-	+
VI	+	-	-	+
VII	+	-	-	-
VIII	+	-	-	-
IX	+	+	-	-

As seen from Table 4.5, MODEL II and MODEL III verify the first four criteria. For this reason, last two criteria (e) and (f) were checked for these models and results were given in Table 4.6.

Table 4.6 gives the $\sum_{all\ data\ samples}\left(r_{\exp}-r_{cal}\right)^2$ values and mean relative error percentages between the experimental and calculated rates for MODEL II and III at four different temperatures namely, 393 K, 408 K, 423 K and 453 K.

Table 4.6. Calculated $\sum_{all\ data\ samples}\left(r_{\exp}-r_{cal}\right)^2$ values and mean relative error at different temperatures for MODEL II and III.

MODEL Number	$\sum_{all\ data\ samples}\left(r_{\exp}-r_{cal}\right)^2$				Mean Relative Error , %			
	393 K	408 K	423 K	453 K	393 K	408 K	423 K	453 K
II	**1.79×10^{-5}**	**0.33**	**1.87**	**11.84**	**0.07**	**22.67**	**30.95**	**35.86**
III	0.80	0.34	1.89	24.19	12.22	35.18	31.12	40.90

As seen from Table 4.6, the sum up of the squared differences of the measured reaction rates and the calculated reaction rates and the mean relative error are minimum for MODEL II at all the reaction temperatures. It means, in the CWAO of BA on CAT1 catalyst under the experimental conditions studied, the best fitted model is MODEL II. Although the the mean relative error are minimum for MODEL II, these values are a bit high. Because in the oxidation of BA over CAT1 catalyst under the experimental conditions used, conversion of BA and the concentration of intermediates were not so high and this may cause some error to evaluate concentration of these acids by HPLC analysis. This error may affect the mean relative error percentage between the experimental and calculated rate obtained from model II.

Figure 4.40 presents the plot of calculated rates obtained from MODEL II vs. experimental rates. As seen the regression coefficient is equal to 0.9991 ~ 1.

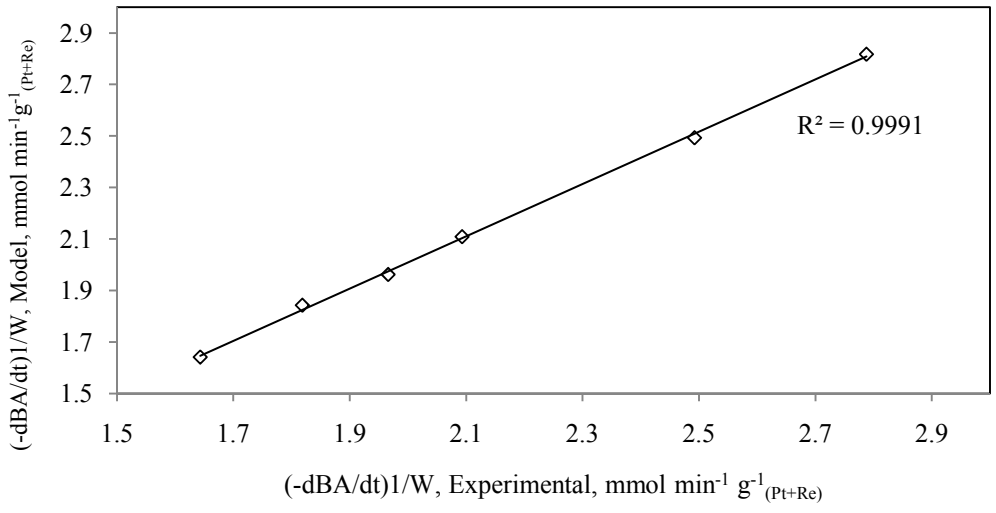

Figure 4.40. Experimental rate vs. calculated rate graph for MODEL II at 393 K.

The independent reaction rate constants (k_1, k_2 and k_3 (mmol min^{-1} $g^{-1}_{(Pt+Re)}$) and adsorption equilibrium constants (K_{BA}, K_{OA}, K_{FA} and K_{O2} (dm^3 $mmol^{-1}$)) at different temperatures for MODEL II are given in Tables 4.7 and 4.8.

Table 4.7. Calculated reaction rate constants at different temperatures for MODEL II.

Temperature, K	k_1, mmol min^{-1} $g^{-1}_{(Pt+Re)}$	k_2, mmol min^{-1} $g^{-1}_{(Pt+Re)}$	k_3, mmol min^{-1} $g^{-1}_{(Pt+Re)}$
393	$4.9x10^3$	$8.91x10^5$	$8.9x10^2$
408	$1x10^4$	$1.9x10^6$	$1x10^3$
423	$3.9x10^4$	$5.97x10^6$	$4.3x10^3$
453	$1.1x10^5$	$7.97x10^7$	$1.2x10^4$

Table 4.8. Calculated adsorption equilibrium constants at different temperatures for MODEL II.

Temperature, K	K_{BA}, dm^3 $mmol^{-1}$	K_{OA}, dm^3 $mmol^{-1}$	K_{FA}, dm^3 $mmol^{-1}$	K_{O2}, dm^3 $mmol^{-1}$
393	$5.1x10^{-6}$	$7.48x10^{-5}$	0.0012	0.0029
408	$5.97x10^{-7}$	$5.48x10^{-5}$	0.0010	0.0026
423	$4.35x10^{-7}$	$3.28x10^{-5}$	0.0002	0.0021
453	$7.87x10^{-8}$	$2.20x10^{-5}$	0.00018	0.0020

The reaction rate constant, $k=k_1+k_2+k_3$, obtained from MODEL II was plotted against the inverse of temperature (1/T) according to Equation 4.21. Figure 4.41 shows this plot.

$$k = A \exp\left(\frac{-E}{RT}\right) \tag{4.20}$$

$$\ln k = \ln A - \frac{E}{R}\frac{1}{T} \tag{4.21}$$

From the slope of Arrhenius plot, -E/R, where R was universal gas constant ($8.314x10^{-3}$ kJ/mol K), activation energy (E) was calculated to be 112.8 kJ/mol. The regression coefficient of Arrhenius line was very close to 1 (0,979) which showed that MODEL II was acceptable in CWAO of butyric acid.

In literature, in the study of CWAO of BA over Ir/AC catalyst the obtained activation energy was 266±7 kJ/mol for total oxidation of BA into CO_2 and water (Gomes et al., 2004).

In another study done by Gomes et al. (2005), the calculated activation energy was 182±35 kJ/mol in the oxidation of BA over Pt/AC catalyst at an oxygen partial pressure of 6.9 bar at the temperature range of 463 K to 493 K.

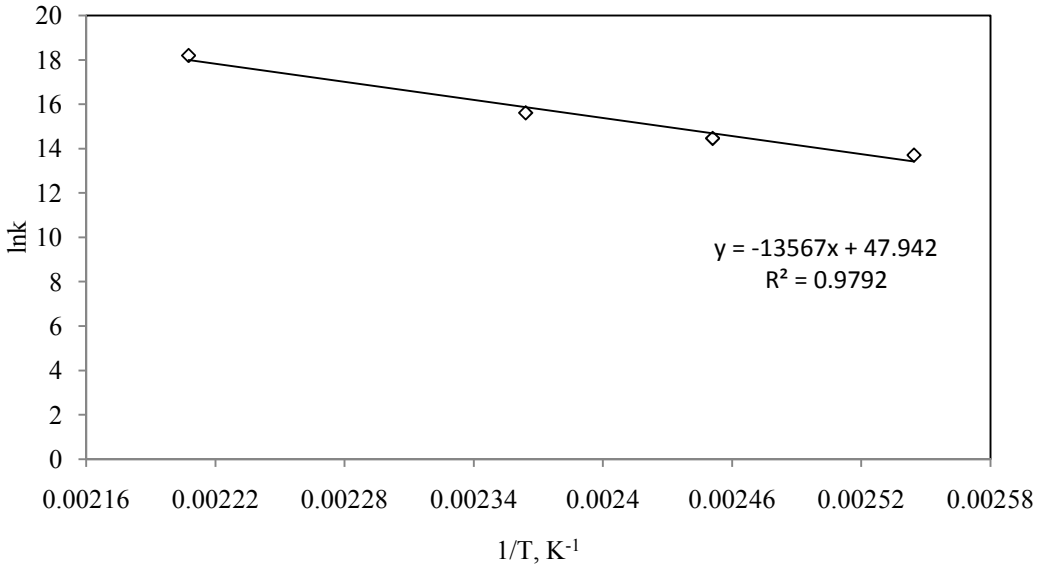

Figure 4.41. lnk vs. 1/T plot for CWAO of BA.

In Figure 4.42, independent reaction rate constants, k_1 (reaction from BA to CO_2), k_2 (reaction from BA to FA), k_3 (reaction from BA to OA), Figure 4.38, obtained from MODEL II were plotted against the inverse of temperature (1/T) according to Equation 4.21. From the slope of Arrhenius plot, activation energies of E_1= 79.5 kJ/mol, E_2=112.8 kJ/mol and E_3 = 69.7 kJ/mol were calculated.

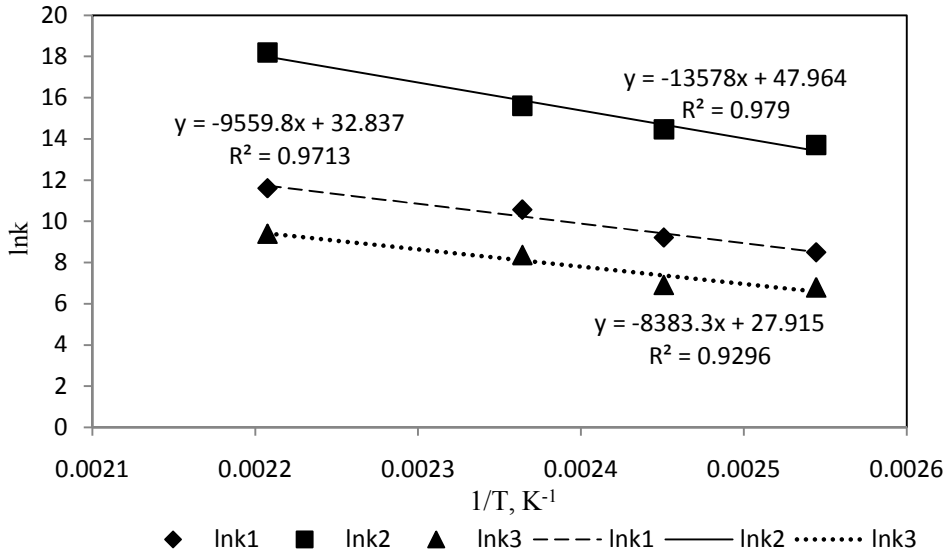

Figure 4.42. lnk_1, lnk_2 and lnk_3 vs. 1/T plot for CWAO of BA.

Consequently, the reaction rate expression can be written according to MODEL II as follows;

$$-r_{BA} = -\frac{dC_{BA}}{dt}\frac{1}{W} = \frac{6.61x10^{20}\exp\left(-\frac{112.8}{RT}\right)K_{BA}C_{BA}K_{O2}C_{O2}}{\left(1+K_{BA}C_{BA}+K_{OA}C_{OA}+K_{FA}C_{FA}+K_{O2}C_{O2}\right)^2} \quad (4.22)$$

where rate ($-r_{BA}$) is in units of mmol min^{-1} g^{-1} $_{(Pt+Re)}$.

The temperature dependency of adsorption equilibrium constants of BA, OA, FA and O_2 are given below

$$K_{BA} = 5.99x10^{-19}\exp\left(\frac{11530}{T}\right) \quad (4.23)$$

$$K_{OA} = 5.47x10^{-9}\exp\left(\frac{3734.7}{T}\right) \quad (4.24)$$

$$K_{FA} = 1.27x10^{-10}\exp\left(\frac{6309.3}{T}\right) \quad (4.25)$$

$$K_{O2} = 1.5x10^{-4}\exp\left(\frac{1152.4}{T}\right) \quad (4.26)$$

4.3.2 Oxidation of maleic acid

4.3.2.1 Effect of oxygen pressure on degradation of MA

To investigate the effect of oxygen pressure (P_{O2}) on the oxidation of MA, studies were carried out at four oxygen pressures namely, 2.8, 4.1, 5.5 and 6.9 bar, keeping the initial concentration of MA, temperature and catalyst amount constant at 3 g/dm^3, 393 K and 10 g/dm^3, respectively. Figure 4.43 gives the results.

As seen from Figure 4.43, the highest degradation degree (86.5 %) was obtained for the oxygen pressure of 6.9 bar. A drastic increase in initial rate of MA ($r_{MA,0}$) was observed for this pressure, as well. It is known that an increase in oxygen pressure has a beneficial effect on oxygen solubility.

Initial rates ($-r_{MA,0}$) were calculated from Figure 4.43 and $\ln(-r_{MA,0})$ was plotted against ln (P_{O2}). Figure 4.44 shows this plot where the slope is equal to reaction order with respect to oxygen pressure. The slope was found to be 0.96 which was very close to 1.

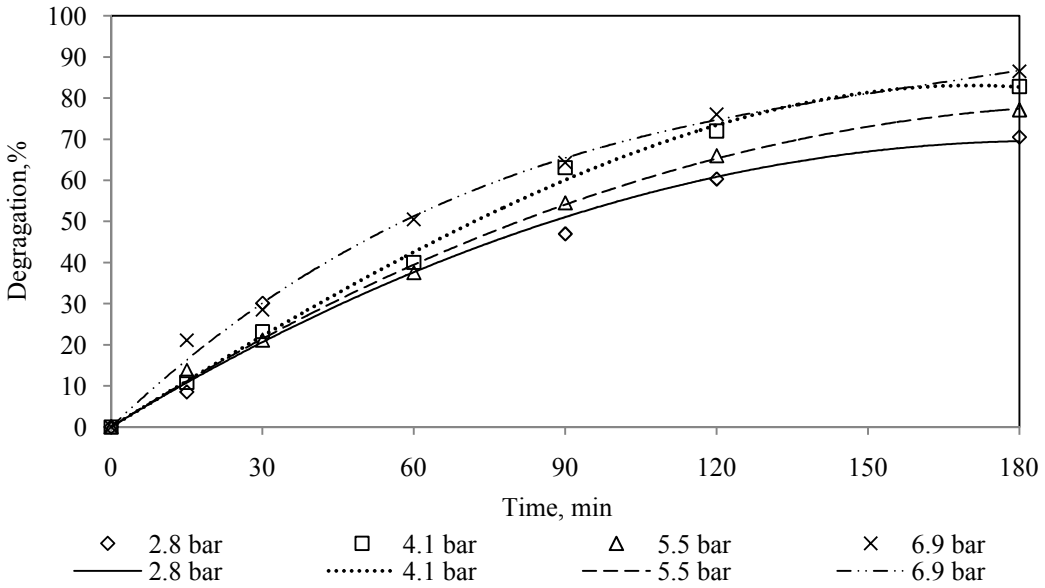

Figure 4.43. Influence of oxygen pressure on the degradation of MA.
(Initial concentration of MA=3 g/dm^3, Temperature=393 K, Catalyst amount=10 g/dm^3, Volume 0.1 dm^3, Stirring speed=500 rpm)

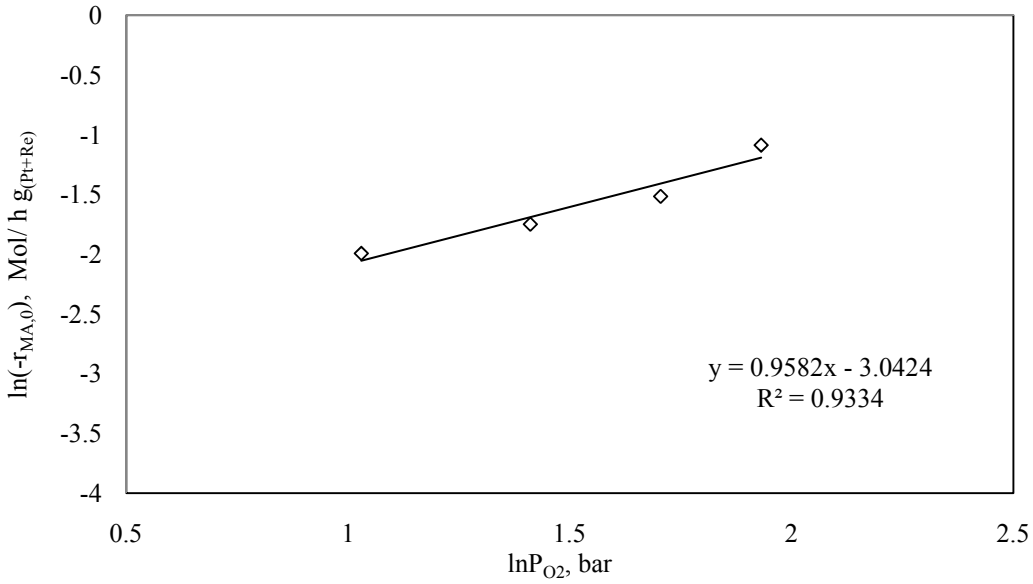

Figure 4.44. ln($-r_{MA,0}$) versus ln (P_{O2}) graph.

Rivas et al. (1999) found that reaction was zero order in oxygen over a partial pressure range of 4-14 bar in the non-catalytic oxidation of MA. The temperatures used in that study (415-478 K) are higher than that (393 K) in this study. The effect of the increase in O_2 pressure seems to be masked by the exponential increase of rate constant with temperature in the non-catalytic oxidation of MA.

4.3.2.2 Effect of temperature on degradation of MA

CWAO of MA was studied at 6.9 bar of oxygen pressure, in the presence of 10 g/dm^3 catalyst for an initial concentration of 3 g/dm^3 for different temperatures such as 393, 408 and 423 K. The results were presented in Figure 4.45. Initial rate and degradation degree of MA (after 3h oxidation) increased with increasing temperature. The highest degradation degree was observed at the highest temperature, 423 K, as 96.8 %.

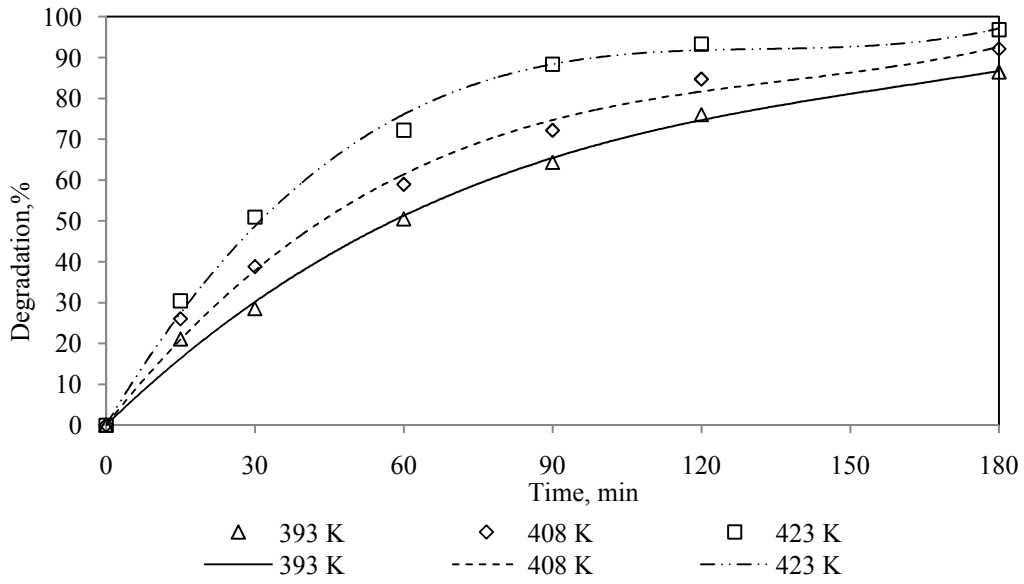

Figure 4.45. Influence of temperature on the degradation degree of MA.
(Initial concentration of MA=3 g/dm^3, Oxygen pressure=6.9 bar, Catalyst amount=10 g/dm^3, Volume=0.1 dm^3, Stirring speed=500 rpm)

By Lee and Kim (2000), CWAO of MA was studied in the temperature range of 393-453 K at an oxygen partial pressure of 11 bar on a Pt/Al_2O_3 catalyst. In that study, total degradation of MA was achieved at a temperature of 453 K. Degradation degrees of 60, 25 and 5% were observed for MA oxidation at temperatures of 433, 413 and 393 K, respectively. However, in our study almost total oxidation was achieved at 423 K and at an oxygen pressure of 6.9 bar, showing that CAT1 catalyst used was very active for CWAO of MA.

From the plot of $\ln(r_{MA,0})$ as a function of inverse of temperature (1/T) (Figure 4.46), the slope of the straight line gave the activation energy of 16.9 kJ/mol.

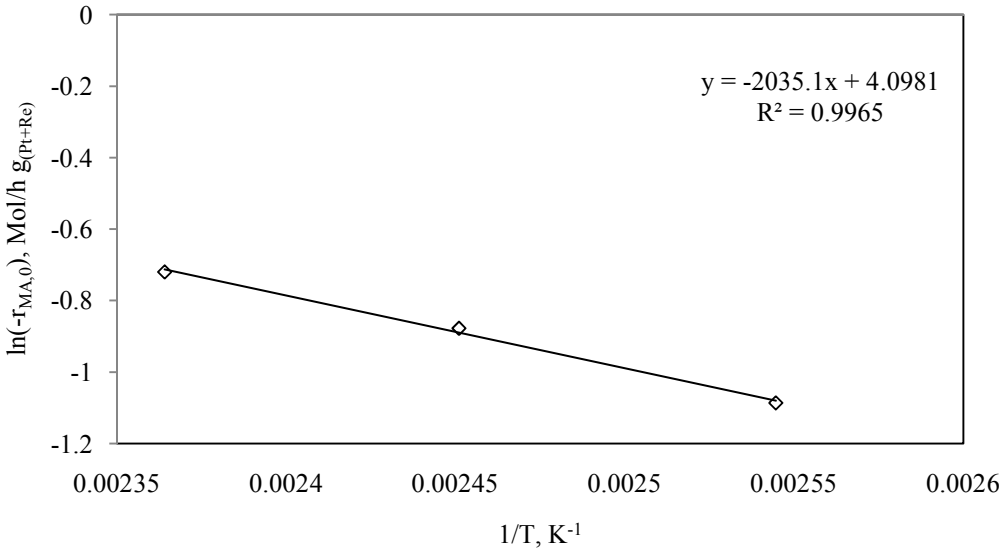

Figure 4.46. $\ln(-r_{MA,0})$ vs. 1/T graph.

In the study done by Rivas and coworkers (1999), for the non-catalytic removal of maleic acid, the apparent activation energies were calculated to be 66.7 and 131.5 kJ/mol under a nitrogen and air environment, respectively. When these results were compared with the activation energy calculated in this study, it could be concluded that CAT1 catalyst used in this study caused a significant drop in activation energy of the reaction.

In the CWAO of MA, oxalic acid (OA), formic acid (FA) and fumaric acid (Fum) were detected as intermediates. Oliviero et al. (2001) detected fumaric, pyruvic, oxalic, acetic and acrylic acids as intermediates in the CWAO of MA on 5% in wt Ru/CeO_2 catalyst at an oxygen partial pressure of 20 bar and in the temperature range of 433-473 K.

Chollier et al. (1999) observed that during the oxidation reaction of MA, a partial isomerization of MA in fumaric acid occurred (~ 10 %) over platinized wire catalyst at a temperature of 383 K and in the oxygen pressures range of 1-5 bar. They found no other compounds, produced by partial oxidation of MA. Oxidation of maleic acid was complete and led to the formation of CO_2 .

In the study done by Rivas et al. (1999) on the non-catalytic oxidation of maleic acid under nitrogen atmosphere, only fumaric and malic acids were found as organic species in the reaction media.

Table 4.9 gives the selectivity study and degradation results of MA after an oxidation time of 3h in the temperature and pressure ranges of 393-423 K and 2.8-6.9 bar, respectively. As seen from Table 4.9, selectivity to OA and CO_2 were decreased from 1.2 % to zero and from 71.4 to 63.7 % with increasing oxygen pressure from 2.8 bar to 6.9 bar. Besides these, selectivity to FA was enhenced from 27.4 to 36.3 % in the same oxygen pressure range mentioned above. Selectivity to fumaric acid was ascended from zero to 1.5 % in the temperature range of 393-423 K at an oxygen pressure of 6.9 bar. Fumaric acid is cis-trans isomerization product of MA. From the sequence of the formation of OA, FA as intermediates in this study under the experimental conditions used, it may be said that maleic acid and fumaric acid were converted into OA which subsequently degraded into FA. Finally FA was oxidized into CO_2 and water. Similar results were reported for MA oxidation over a Pt/Al_2O_3 catalyst (Lee and Kim, 2000).

Table 4.9. CWAO results of MA at different oxygen pressures and temperatures.

MA concentration (g/dm^3)	PO_2 (bar)	Temperature (K)	Degradation of MA (%)	Selectivity (%) to			
				Oxalic acid	Formic acid	CO_2	Fumaric acid
3	2.8	393	79.6	1.2	27.4	71.4	0.0
3	4.1	393	82.8	0.4	26.8	72.8	0.0
3	5.5	393	77.2	1.1	36.8	62.1	0.0
3	6.9	393	86.5	0.0	36.3	63.7	0.0
3	6.9	408	92.1	1.9	33.6	62.8	1.7
3	6.9	423	96.8	0.0	34.8	63.7	1.5

Figure 4.47 shows the proposed reaction pathways of maleic acid.

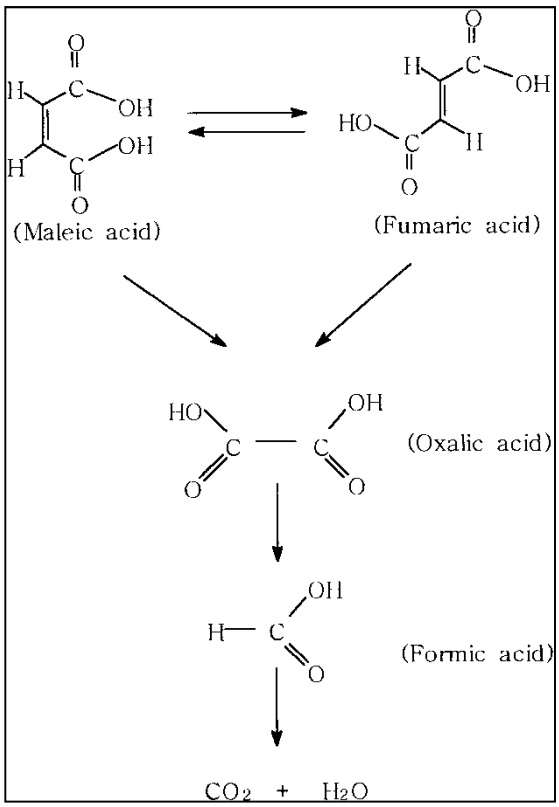

Figure 4.47. Proposed reaction pathways of CWAO of maleic acid.

Figure 4.48 shows the change in the composition of the reaction medium as a function of time in CWAO of MA over CAT1 catalyst at an oxygen pressure of 6.9 bar at a temperature of 393 K for an initial concentration of 3 g/dm^3. As seen from Figure 4.48, fumaric acid and OA were formed in the earliest stage of the reaction. Fumaric acid and oxalic acid concentrations reached a maximum at a time of 120 min, after that time they decreased to zero. The formation of FA was increased with time.

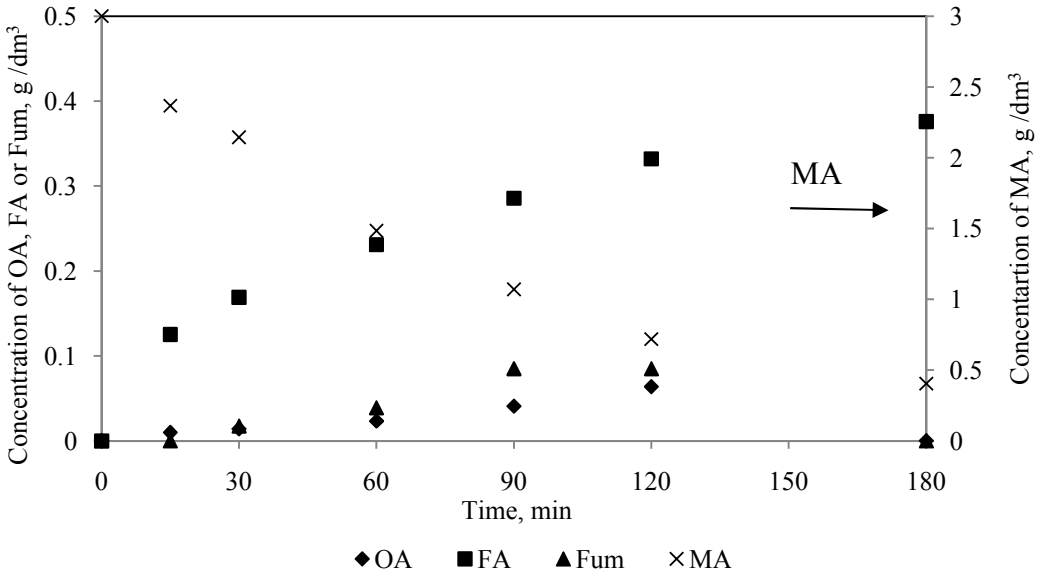

Figure 4.48. Change in the composition of the reaction medium as a function of time in CWAO of MA over CAT1 catalyst.
(Initial concentration of MA=3 g/dm^3, Temperature=393 K, Oxygen pressure=6.9 bar, Catalyst amount=10 g/dm^3, Volume= 0.1 dm^3, Stirring speed=500 rpm)

4.3.2.3 Effect of initial concentration of MA on degradation

In order to determine the effect of initial concentration of MA, experiments were carried out at 6.9 bar of oxygen pressure and at four different initial concentrations of maleic acid such as 0.5, 1, 2 and 3 g/dm^3, keeping the temperature at 393 K, stirring rate at 500 rpm and the catalyst amount at 10 g/dm^3 constant during the runs, Figure 4.49. The highest degradation degree (97.5 %) was observed at an initial concentration of 0.5 g/dm^3 MA after 3h oxidation.

By ploting $\ln(-r_{MA,0})$ vs. $\ln C_{MA,0}$, Figure 4.50, the reaction order with respect to MA was found to be 0.34 from the slope of the straight line obtained.

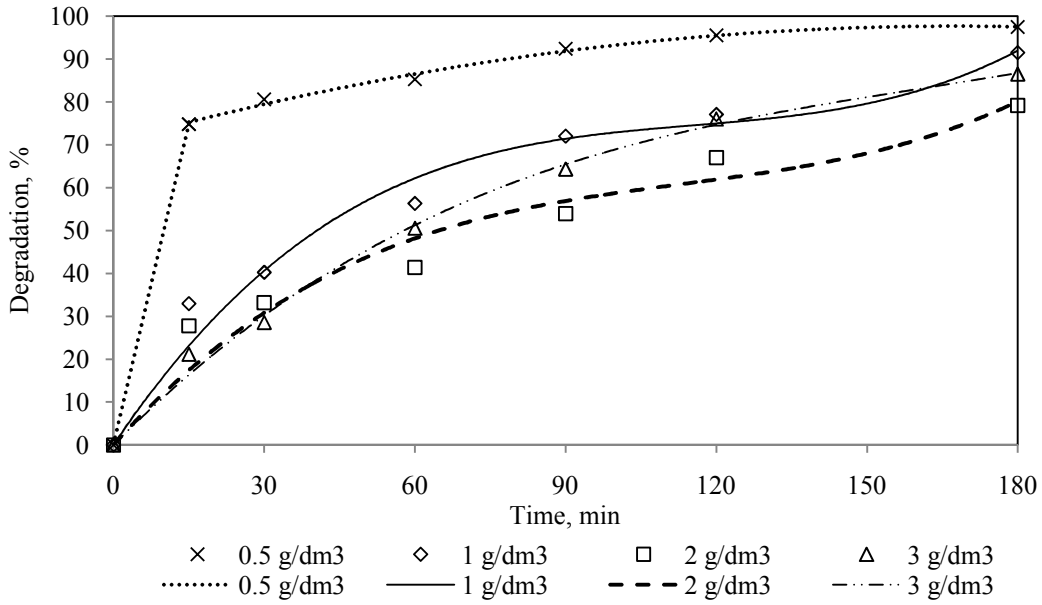

Figure 4.49. Influence of initial concentration of MA on the degradation degree. (Temperature=393 K, Oxygen pressure=6.9 bar, Catalyst amount=10 g/dm^3, Volume= 0.1 dm^3, Stirring speed=500 rpm)

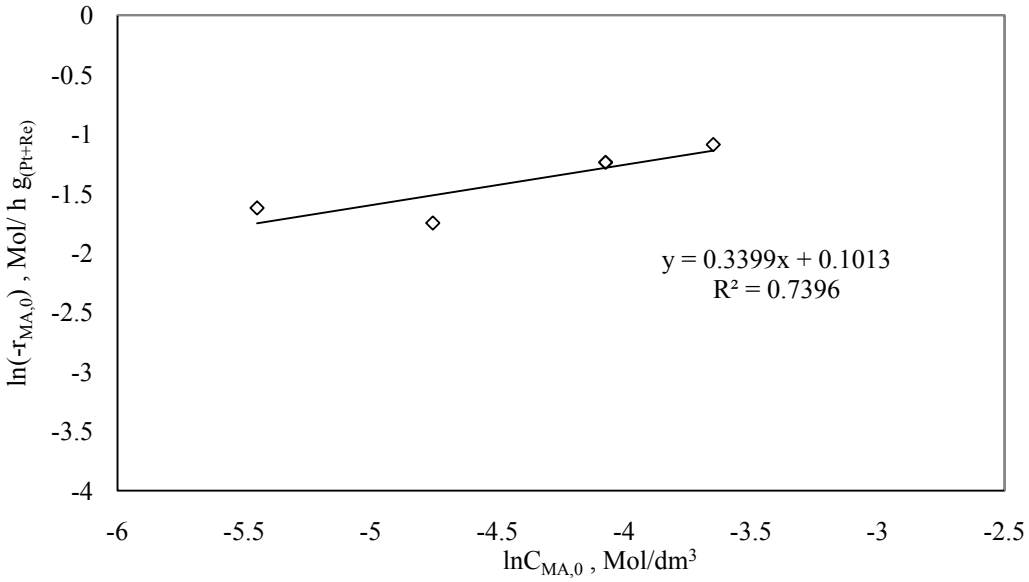

Figure 4.50. ln(-$r_{MA,0}$) vs. ln($C_{MA,0}$) graph in CWAO of MA.

Rivas et al. (1999) found that the catalytic and non-catalytic degradation of an aqueous solution of maleic acid was a first order reaction in maleic acid concentration over a temperature range of 415-478 K both in the presence of oxygen and under inert atmosphere.

By combining all the data obtained from Figures 4.44, 4.46 and 4.50, the initial rate of MA oxidation, $-r_{MA,0}$, (in mol h^{-1} $g^{-1}_{(Pt+Re)}$) was expressed by the following rate equation:

$$r_{MA,0} = 29.5\ e^{-16.9/RT}\ C_{MA,0}^{0.34}\ P_{O2}^{0.96} \qquad (4.27)$$

with $C_{MA,0}$ in moL/dm^3, P_{O2} in bar. The validity of this equation has to be limited to the used ranges of operating conditions, which are $2.8 < P_{O2} < 6.9$ bar, $0.5 < C_{MA,0} < 3$ g/dm^3, catalyst loading=10 g/dm^3 and $393 < T < 423$ K.

4.3.2.4 Effect of catalyst loading on degradation of MA

For the investigation of the effect of catalyst loading on the degradation degree of MA, experiments were carried out at 393 K, at an oxygen pressure of 6.9 bar for an initial concentration of MA of 3 g/dm^3 with different catalyst loadings; 5-15 g/dm^3. The results are presented in Figure 4.51. The lowest degradation degree (68.7 %) was observed with a catalyst amount of 5 g/dm^3 after an oxidation time of 3h. The obtained degradation degrees were almost the same at a catalyst amount of 10 and 15 g/dm^3 as 86.5 % and 84.9 %, respectively. The initial rates were also very close to each other for the latter catalyst loadings (0.29 and 0.33 mol h^{-1} $g^{-1}_{(Pt+Re)}$, respectively). It showed that external mass transfer resistance could be neglected for catalyst loadings equal or greater than 10 g/dm^3. In all the oxidation runs, catalyst was used in powder form so it could be said that internal diffusion resistance was also negligible (Beziat et al., 1999).

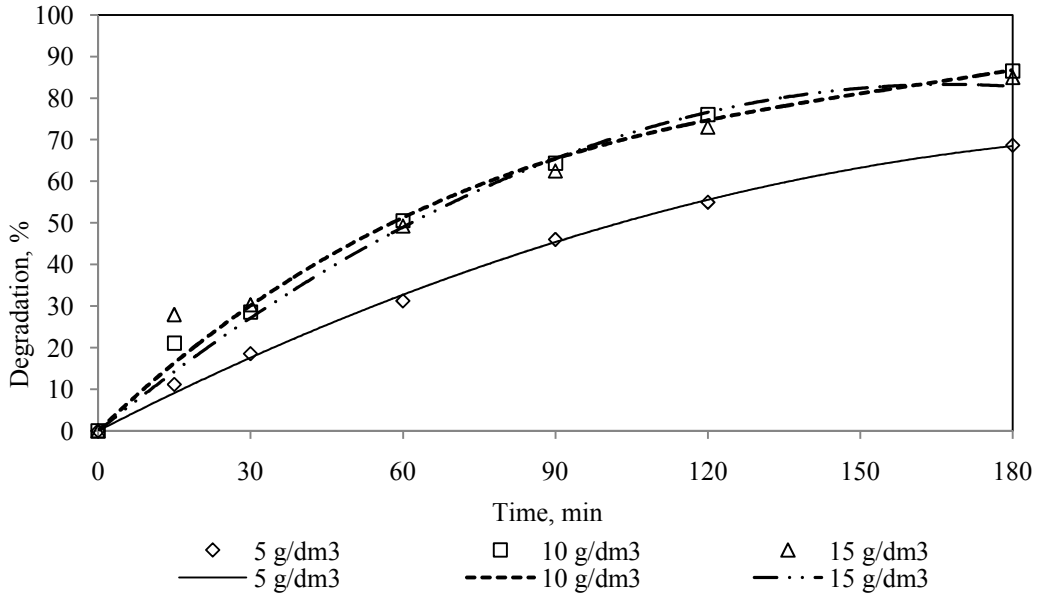

Figure 4.51. Effect of catalyst loading on the degradation of MA.
(Initial concentration of BA=3 g/dm^3, Temperature=393 K, Oxygen pressure=6.9 bar, Volume= 0.1 dm^3, Stirring speed=500 rpm)

Leaching of Pt, measured by atomic absorption spectrometer (Varian 10 plus), was about 3 mg/dm^3 in CWAO of MA after a reaction time of 3 hours. This value corresponds to a leaching of 4 % of the total amount of platinum per hour in CWAO of MA. The obtained Pt leaching value is rather close to European Union directives (<2 mg/dm^3) (Ramirez et al., 2007). No information was given in literature about the Pt leaching in CWAO of MA.

4.3.2.5 Kinetic modeling of CWAO of maleic acid over CAT1 catalyst in high temperature-pressure reactor

The experimental data obtained for the CWAO of maleic acid over CAT1 catalyst at three different temperatures, namely 393, 408 and 423 at an oxygen pressure of 6.9 bar were modeled by considering Langmuir-Hinshelwood mechanism. Four different models given below were tried. As mentioned in Part 4.3.2.2, during the oxidation of MA, oxalic acid (OA), formic acid (FA) and fumaric acid (Fum) were detected as intermediates. Fumaric acid was believed to be formed through the cis-trans isomerization of MA by a reversible reaction. From the sequence of the formation of OA and FA as intermediates in this study under the experimental conditions used, it may be said that maleic acid and fumaric acid were converted into OA which subsequently degraded into FA. Finally FA was oxidized into CO_2 and water. However, in kinetic analysis,

isomerization reaction from maleic acid to fumaric acid was neglected due to small thermodynamic equilibrium constant (K) (at 408 K (K= 0.2) and at 423 K (K= 0.5)) and it was thought that the formation of OA and FA were due to the oxidation of maleic acid only because the conversion of fumaric acid from maleic acid was very low which was less than 3 %.

Maleic acid concentration (C_{MA}) and concentrations of reaction intermediates, oxalic acid (C_{OA}) and formic acid (C_{FA}), were obtained by HPLC analysis of the reaction mixture at the corresponding time. The calculation procedure used in butyric acid oxidation was followed. Similar to BA oxidation, it was thought that, the concentration of oxygen decreased with time in the complete oxidation reaction of MA, OA or FA to H_2O and CO_2 according to Equations 4.28 – 4.30.

Oxidation of maleic acid to CO_2 and H_2O;

$$C_4H_4O_4 + 3O_2 \rightarrow 4\ CO_2 + 2\ H_2O \qquad (4.28)$$

Oxidation of oxalic acid to CO_2 and H_2O;

$$C_2H_2O_4 + 0.5\ O_2 \rightarrow 2CO_2 + H_2O \qquad (4.29)$$

Oxidation of formic acid to CO_2 and H_2O;

$$CH_2O_2 + 0.5\ O_2 \rightarrow CO_2 + H_2O \qquad (4.30)$$

Concentration of oxygen in gas phase was calculated by using Equation 4.31:

$$(C_{O2})_g V_g = (C_{O2})_{g0} V_g - 3((C_{MA})_0 - (C_{MA}))V_L + 0.5(C_{OA})V_L + 0.5(C_{FA})V_L \qquad (4.31)$$

where, $(C_{O2})_g$= concentration of oxygen in gas phase (mmol/dm^3), Vg= Volume of gas (0.150 dm^3), $(C_{O2})_{g0}$= initial oxygen concentration in gas phase (mmol/dm^3), V_L=Volume of liquid (0.1 dm^3), $(C_{MA})_0$=initial concentration of maleic acid (mmol/dm^3) and (C_{MA}), (C_{OA}), (C_{FA}) are the liquid phase concentrations of maleic, oxalic and formic acids at the corresponding time (mmol/dm^3), respectively.

After the calculation of concentration of oxygen in gas phase, the concentration of oxygen in liquid phase (C_{O2}) was calculated according to Equation 4.6 and 4.7.

In maleic acid oxidation, MODEL III, IV, VI and VII were tested.

MODEL III

In this model, the reaction rate expression is derived on the assumption that reaction occurs at the catalyst surface between adsorbed maleic acid and molecular adsorbed oxygen (Langmuir-Hinshelwood Mechanism) with negligible adsorption of OA and FA. It is given in Equation (4.32).

$$-\frac{dC_{MA}}{dt}\frac{1}{W}=\frac{k_{sr}K_{MA}C_{MA}K_{O2}C_{O2}}{\left(1+K_{MA}C_{MA}+K_{O2}C_{O2}\right)^2} \tag{4.32}$$

MODEL IV

In this model, the reaction rate expression is derived on the assumption that reaction occurs at the catalyst surface between adsorbed maleic acid and dissociative adsorbed oxygen (Langmuir-Hinshelwood Mechanism) with negligible adsorption of OA and FA. In this case oxidation rate of MA can be written as in Equation (4.33).

$$-\frac{dC_{MA}}{dt}\frac{1}{W}=\frac{k_{sr}K_{MA}C_{MA}K_{O2}^{1/2}C_{O2}^{1/2}}{\left(1+K_{MA}C_{MA}+K_{O2}^{1/2}C_{O2}^{1/2}\right)^2} \tag{4.33}$$

MODEL VI

In this model, it is assumed that molecular adsorbed oxygen on catalyst surface is reacting with maleic acid in the bulk fluid (Eley Rideal Mechanism). The oxidation rate of maleic acid can be written as in Equation (4.34).

$$-\frac{dC_{MA}}{dt}\frac{1}{W}=\frac{k_{sr}C_{MA}K_{O2}C_{O2}}{\left(1+K_{O2}C_{O2}\right)} \tag{4.34}$$

MODEL VII

In this model, it is assumed that dissociative adsorbed oxygen is reacting with MA in the bulk fluid (Eley Rideal Mechanism). The oxidation rate of maleic acid can be written as in Equation (4.35).

$$-\frac{dC_{MA}}{dt}\frac{1}{W}=\frac{k_{sr}C_{MA}K_{O2}{}^{1/2}C_{O2}{}^{1/2}}{\left(1+K_{O2}{}^{1/2}C_{O2}{}^{1/2}\right)} \tag{4.35}$$

In these equations, k_{sr} is surface reaction rate constant (mmol min^{-1} $g^{-1}_{(Pt+Re)}$ for Models III and IV and dm^3 min^{-1} $g^{-1}_{(Pt+Re)}$ for Models VI and VII), K_{MA} and K_{O2} are adsorption equilibrium constants of maleic acid and oxygen (dm^3 $mmol^{-1}$), (C_{MA}) and (C_{O2}) are the concentrations of maleic acid and oxygen in liquid phase ($mmol/dm^3$) and W is the concentration of active component (Pt+Re) in catalyst ($0.065\ g_{(Pt+Re)}$ / dm^3)

Methods used in analysis of Kinetic Models

In the analysis of kinetic models, the procedure given in kinetic analysis of experimental data for BA was used. Figure 4.52 presents the plot of concentration of MA as a function of time and third degree polynomial fit. Equation 4.36 and Equation 4.37 give polynomial fit and the derivative of MA concentration with respect to time, respectively.

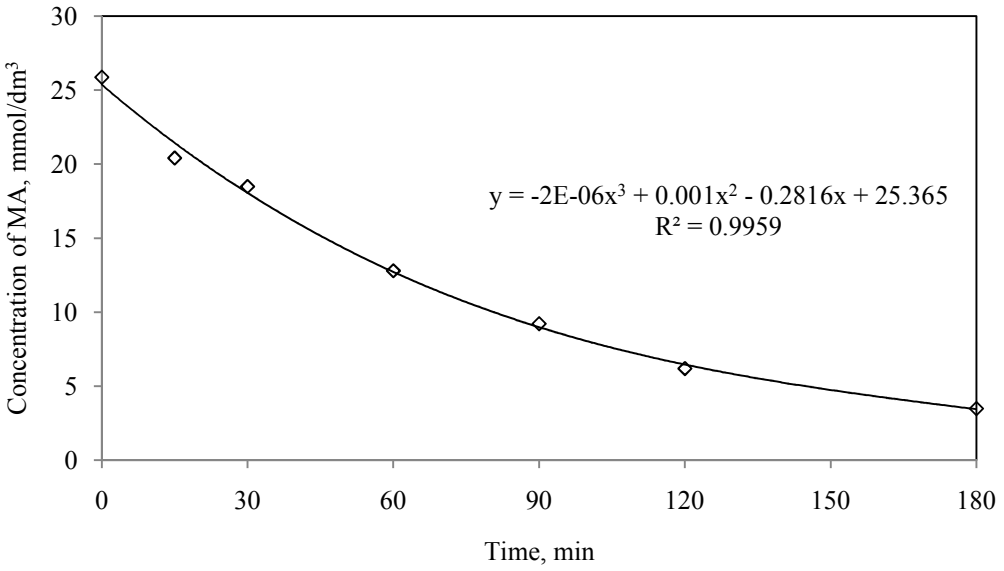

Figure 4.52. C_{MA} vs. time plot and polynomial fit.
(Initial concentration of MA=3 g/dm^3, Volume=0.1 dm^3, Catalyst amount= 10 g/dm^3, Pressure=6.9 bar, Temperature=393 K, Stirring speed=500 rpm)

$$C_{MA}(t) = -2x10^{-6}t^3 + 0.001t^2 - 0.2816t+25.365 \tag{4.36}$$

$$\frac{dC_{MA}}{dt} = -6x10^{-6}t^2 + 0.002t - 0.2816 \tag{4.37}$$

Model equations were solved as given in Part in 4.3.1.5 for model analysis of butyric acid oxidation. In each model first four criteria were checked for model elimination, Table 4.10.

Table 4.10. Model elimination in CWAO of MA.

MODEL Number	Criteria Number			
	a	b	c	d
III	+	+	+	+
IV	+	-	-	+
VI	+	+	+	+
VII	+	+	+	+

As seen from Table 4.10 except MODEL IV other three models verify the first four criteria. For this reason, last two criteria (e) and (f) were checked for these models and results were given in Table 4.11.

Table 4.11 gives the $\sum_{all\ data\ samples}\left(r_{\exp}-r_{cal}\right)^2$ values and mean relative error percentages between the experimental and calculated rates for MODEL III, MODEL VI and MODEL VII at three different temperatures namely, 393 K, 408 K and 423 K.

Table 4.11. Calculated $\sum_{all\ data\ samples}\left(r_{\exp}-r_{cal}\right)^2$ values and mean relative error at different temperatures for MODEL III, VI and VII.

MODEL Number	$\sum_{all\ data\ samples}\left(r_{\exp}-r_{cal}\right)^2$			Mean Relative Error , %		
	393 K	408 K	423 K	393 K	408 K	423 K
III	**0.49**	**1.93**	**1.16**	**8.98**	**8.19**	**3.53**
VI	3.87	4.52	2.31	26.91	19.80	31.96
VII	3.22	3.80	1.68	24.35	16.26	27.36

Table 4.11 shows that, $\sum_{all\ data\ samples}\left(r_{\exp}-r_{cal}\right)^2$ and mean relative error are minimum at all the reaction temperatures for MODEL III. That is, MODEL III which was based on Langmuir Hinshelwood mechanism with the assumption that

reaction occured at the catalyst surface between the adsorbed maleic acid and molecular adsorbed oxygen fitted the experimental data best.

Figure 4.53 presents the plot of calculated rates obtained from MODEL III vs. experimental rates. As seen from Figure 4.53, the regression coefficient is 0.9817 which is very close to 1.

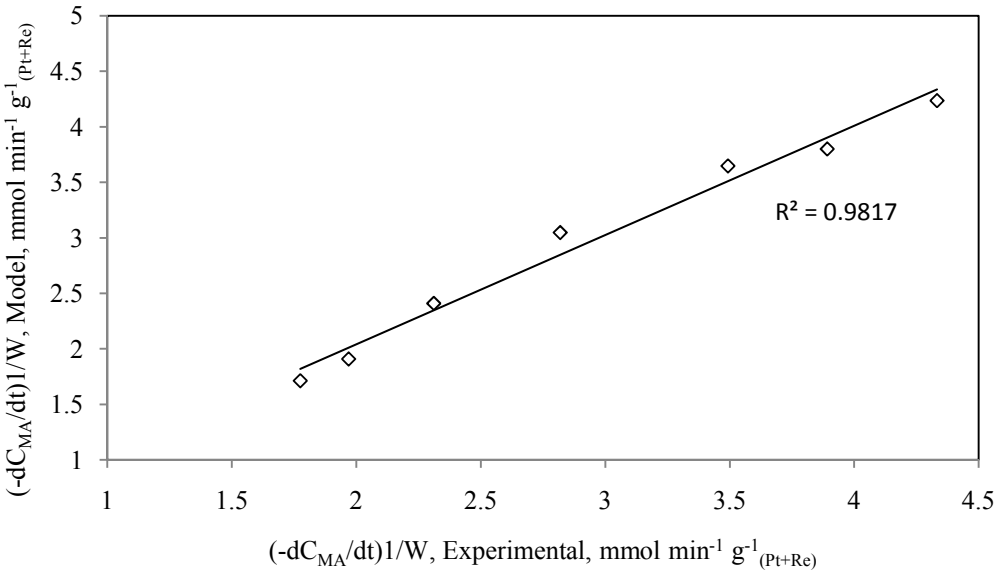

Figure 4.53. Experimental rate vs. calculated rate graph for MODEL III.
(Initial concentration of MA=3 g/dm^3, Volume=0.1 dm^3, Catalyst amount= 10 g/dm^3, Pressure=6.9 bar, Temperature=393 K, Stirring speed=500 rpm)

For MODEL III the reaction rate constant (k_{sr} (mmol min^{-1} g^{-1} $_{(Pt+Re)}$)) and adsorption equilibrium constants (K_{MA} and K_{O2} (dm^3 mmol^{-1})) at different temperatures were given in Table 4.12.

Table 4.12. Calculated reaction rate constant and adsorption equilibrium constants at different temperatures for MODEL III.

Temperature, K	$k_{sr,}$ mmol min^{-1} g^{-1} $_{(Pt+Re)}$	$K_{MA,}$ dm^3 mmol^{-1}	$K_{O2,}$ dm^3 mmol^{-1}
393	32.62	0.051	0.21
408	102.12	0.023	0.056
423	467.86	0.019	0.0085

The reaction rate constant, k_{sr}, obtained from MODEL III was plotted against the inverse of temperature (1/T), from the slope of Arrhenius plot, -E/R, where R was universal gas constant ($8.314x10^{-3}$ kJ/mol K), activation energy (E) was found to be 122.3 kJ/mol, Figure 4.54. The regression coefficient of Arrhenius plot was very close to 1 (0,989) which showed that MODEL III was acceptable in CWAO of maleic acid under the experimental conditions used in this study.

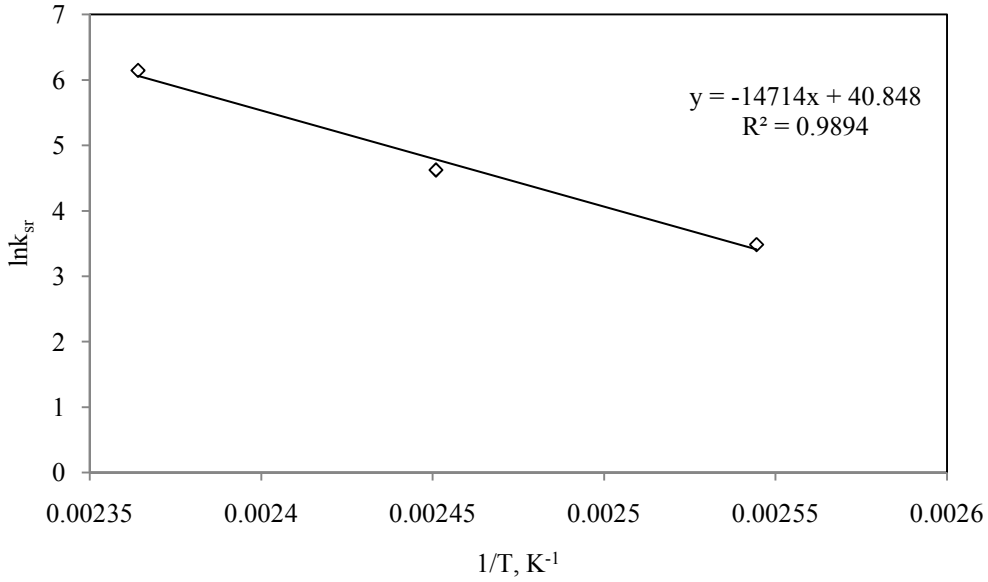

Figure 4.54. lnk_{sr} vs. 1/T plot for CWAO of MA.

Consequently, the reaction rate expression can be written according to MODEL III as follows;

$$-r_{MA} = -\frac{dC_{MA}}{dt}\frac{1}{W} = \frac{5.45x10^{17}\exp\left(-\frac{122.3}{RT}\right)K_{MA}C_{MA}K_{O2}C_{O2}}{\left(1+K_{MA}C_{MA}+K_{O2}C_{O2}\right)^2} \qquad (4.38)$$

The temperature dependency of adsorption equilibrium constants of MA and O_2 are given below;

$$K_{MA} = 3.79x10^{-8}\exp\left(\frac{5510}{T}\right) \qquad (4.39)$$

$$K_{O2} = 6.06x10^{-21}\exp\left(\frac{17725}{T}\right) \qquad (4.40)$$

4.4 Ultrasonic Degradation of Butyric Acid and Maleic Acid

Three different experimental set-ups which were Ultrasonic Reactor, Ultrasonic Bath and Ultrasonic Probe System were used for the degradation of aqueous solutions of butyric acid and maleic acid.

4.4.1 Sonication of butyric acid

4.4.1.1 Sonication of butyric acid in ultrasonic bath

Effect of ultrasonic power or initial concentration

The effect of ultrasonic power or initial concentration were investigated on degradation of butyric acid at room temperature with a solution volume of 1.5 dm^3 in ultrasonic bath. Table 4.13 shows the experimental conditions, the results of degradation degree and the standard deviations (STD) of the obtained degradation degress.

Table 4.13. Effect of Ultrasonic power or initial concentration in sonolysis of butyric acid.

Compound	Initial concentration, g/dm^3	Ultrasonic power, W	Degradation, % (After 1 h)	STD	Parameter
Butyric acid	3^+	70	-	-	Power effect for 3 g/dm^3 butyric acid
Butyric acid	3	84	-	-	
Butyric acid	3	98	-	-	
Butyric acid	0.5^+	70	2.5 (after 3 h)	± 0.02	Power effect for 0.5 g/dm^3 butyric acid
Butyric acid	0.5	84	-	-	
Butyric acid	0.5	98	-	-	
Butyric acid	2	70	-	-	Runs for initial concentration effect for butyric acid plus runs with $^+$ sign
Butyric acid	1.5	70	0.5	± 0.01	
Butyric acid	0.25	70	2.5	± 0.06	

Figures 4.55a and 4.55b show the degradation degree of butyric acid aqueous solutions with initial concentration of 0.5 and 0.25 g/dm^3 at a power intensity of 0.2 W/cm^2, respectively. Experiments were repeated at least 2, at most 5 times. Standard deviations (STD) of the degradation degree were given in the related tables. In literature the most of the sonication experiments were done for a reaction time of 1h (Thoma et al., 1997; Yim et al., 2002; Tezcanli-Güyer and Ince, 2004; Entezari et al., 2006; Liang et al., 2007). In sonication of 3 hours, it became difficult to control the temperature in bath because of the increase in bath temperature from 298 K to about 328 K in 3 hours.

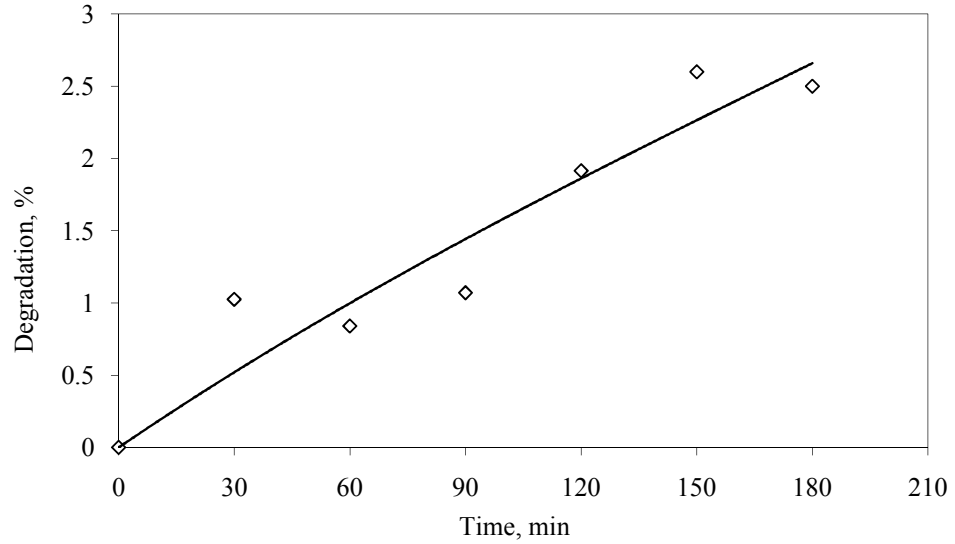

Figure 4.55a. Ultrasonic degradation of 0.5 g/dm^3 butyric acid solution in the ultrasonic bath. (Power=70 W, Frequency=40 kHz, Solution volume=1.5 dm^3)

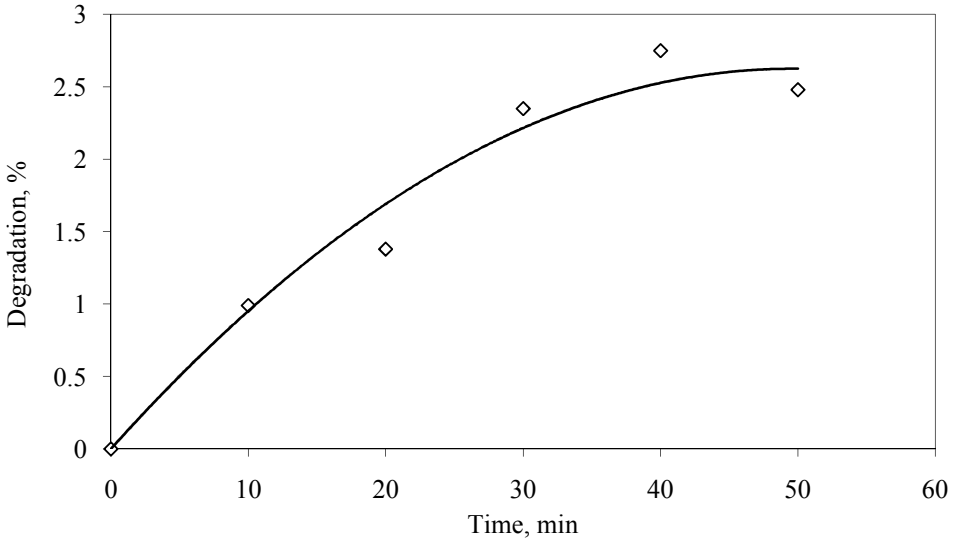

Figure 4.55b. Ultrasonic degradation of 0.25 g/dm^3 butyric acid solution in the ultrasonic bath. (Power=70 W, Frequency=40 kHz, Solution volume=1.5 dm^3)

As seen from Table 4.13, experiments were carried out with 3 g/dm^3 initial concentration of butyric acid at powers of 70, 84 and 98 W at a frequency of 40 kHz. No butyric acid degradation was observed at any power. Because of this, in further experiments lower initial concentrations such as 2, 1.5, 0.5 and 0.25 g/dm^3 were tested in the sonication of butyric acid at a power of 70 W and a power intensity of 0.2 W/cm^2. Figure 4.56 presents the plot of degradation of butyric acid versus power dissipation which was defined as the ratio of power output to solution concentration (W/(g/dm^3)). Degradation increased with increasing power dissipation, that is, with decreasing butyric acid concentration. This was in agreement with the results of other researchers, who showed that at appreciable concentrations, hydrophilic solutes might slightly move away from solution to undergo thermal decomposition (Jiang et al., 2002) It was hard to degrade 2, 1.5 or 0.5 g/dm^3 butyric acid solution in ultrasonic bath (zero, 0.5 % and 0.9% degradation at 2, 1.5 and 0.5 g/dm^3 initial concentration of BA, respectively). The highest degradation degree, 2.5 %, was observed with the lowest initial concentration of butyric acid, namely 0.25 g/dm^3.

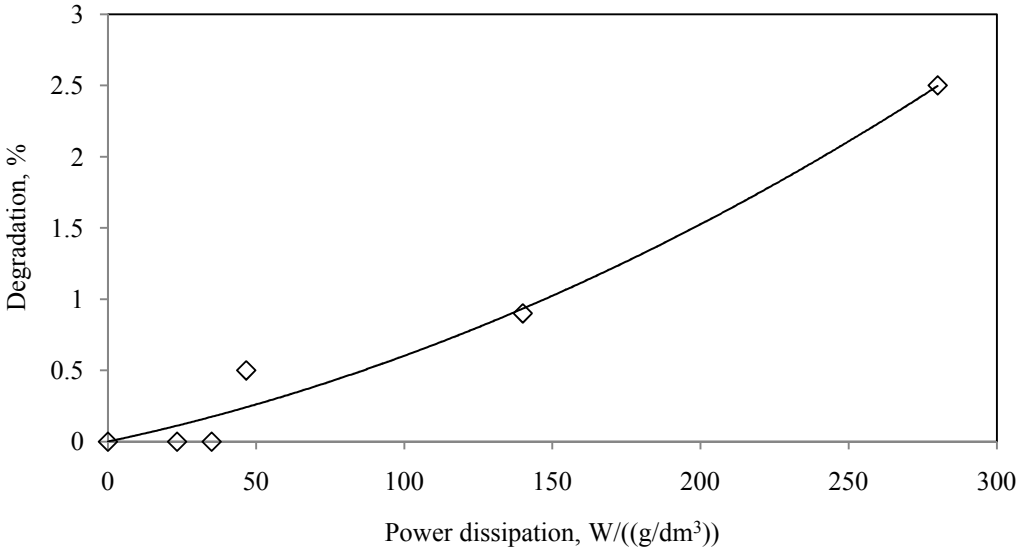

Figure 4.56. Degradation of butyric acid versus power dissipation
(Power=70 W, Frequency=40 kHz, Solution volume=1.5 dm^3)

According to Kim et al. (2001) most reaction takes place at the bubble-liquid interface and decomposition of volatile compound may be limited by available interfacial area. The higher initial concentration of volatile compound and corresponding higher amounts of the intermediates at the interface may inhibit the overall pollutant decomposition (Jiang et al., 2002). On the other hand,

Drijvers et al. (1999), explain the decrease in degradation with increasing initial concentration by the influence of the volatile compounds on the average specific heat ratio, γ, of the gas mixture in the cavitation bubbles, where γ is the ratio of constant pressure and constant volume heat capacities, i.e. C_p/C_v. The proportionally between the concentration of a volatile compound in the bubble and its concentration in the solution will influence the ultrasonic reaction rate as the temperature of bubble collapse is dependent upon the specific heat ratio (γ) of the gas mixture through Equation 4.41:

$$T_{max} = T_0(\gamma - 1)P_{max} / P_{min} \tag{4.41}$$

T_{max} is the final temperature, P_{max} is the liquid pressure at collapse, P_{min} is the minimum pressure in vapour phase and T_0 is the ambient temperature of liquid.

A linear relationship between the specific heat ratio (γ) of the gas mixture and the volatile compound concentration (C_i) in the liquid phase can be assumed as in Equation 4.42;.

$$\gamma = \gamma_0 - KC_i \tag{4.42}$$

K is proportionality constant

As a result, the specific heat ratio of gas mixture decreases with increasing volatile concentration resulting in a lower temperature and pressure within the cavitation bubbles and thus a decrease in rate of sonochemical degradation of volatile compounds is observed.

In literature there are similar results for the effect of initial concentration. Visscher et al. (1997) studied the degradation of ethylbenzene in aqueous solution at 520 kHz. Sonication was performed at initial concentrations of 1 and 0.5 M ethylbenzene. The reaction rate was higher at low initial concentration. In another study, the sonochemical degradation in aqueous solution of methyl violet was studied for different initial concentrations at 393 K and 20 kHz. It was observed that as initial concentration increased degradation rate decreased (Wang et al., 2003). Sivakumar et al. (2002) studied degradation of p-nitrophenol. According to their study rate constant decreased with increasing initial concentration. Gogate et al. (2004) observed that the percentage of phenol degradation was inversely

proportional to the initial concentration at 22.7 kHz and 240 W in the ultrasonic horn. As seen, our results are in good accordance with the data in literature.

In sonication experiments of 0.5 g/dm^3 butyric acid, degradation degree of butyric acid dropped from 0.9 to zero with increasing ultrasonic power from 70 W to 98 W after a sonication time of 1 h. It is known that when power is increased for the same area (here, bath bottom), ultrasound power intensity (power/vibration area) increases and a large number of gas bubbles or cavities exist in the solution. So, a lesser level of energy is focused on organic pollutant solution because of the scattering effect of gas bubbles on the sound waves. As a result, with the increase in the operating intensity, cavitation events may become less violent and lower extent of degradation is obtained. On the other hand, it is possible the coalescence of the cavities in the presence of large number of cavities resulting in the formation of a large cavity which collapses less violently (Entezari et al., 1997; Fındık and Gündüz, 2007). Similar results have been reported by Gogate et al. (2003) in the ultrasonic degradation of formic acid.

Effect of H_2O_2 addition

For the investigation of addition of H_2O_2 into the butyric acid solution, experiments were performed at room temperature with a solution volume of 1.5 dm^3 at a power of 70 W.

Table 4.14 shows the experimental conditions and the results of degradation degree and the values of the standard deviations.

Table 4.14. Effect of H_2O_2 addition in sonolysis of butyric acid.
(Power=70 W, Frequency=40 kHz, Solution Volume=1.5 dm^3)

Compound	Initial concentration, g/dm^3	Addition of H_2O_2, M	Degradation, % (After 1 h)	STD
Butyric acid	0.5	-	0.9	± 0.10
Butyric acid	0.5	0.13	-	-
Butyric acid	0.5	0.26	-	-
Butyric acid	0.5	0.43	0.9	± 0.02
Butyric acid	0.5	0.65	0.8	± 0.04

As seen from Table 4.14, degradation degree of butyric acid drops from 0.9 % to zero with addition of 0.13 M or 0.26 M H_2O_2 into the solution. With the addition of 0.43 or 0.65 M H_2O_2 into 0.5 g/dm^3 butyric acid solution 0.9 and 0.8 % degradation were observed after a sonication time of 1h. The lower or no degradation degree in the presence of H_2O_2 may be attributed to the increased level of OH^* scavenging by H_2O_2 itself via the reaction given by Equation 4.45:

During the sonolysis of aqueous solutions, OH^* and H^* are generated by the thermolysis of water:

$$H_2O \rightarrow OH^* + H^* \quad (4.43)$$

The second pathway is the peroxide production via reaction , Equation 4.44

$$OH^* + OH^* \rightarrow H_2O_2 \quad (4.44)$$

H_2O_2 can scavenge $OH^{\cdot}$ as follows via self scavenging, Equation 4.45

$$OH^* + H_2O_2 \rightarrow H_2O + HO_2^* \quad (4.45)$$

As concentration of H_2O_2 increased, its OH^* scavenging effect may increase causing a decrease in degradation. In literature, there are studies supporting the positive effect of H_2O_2 addition to the solution in the sonolytic degradation of 2 chlorophenol and o-chlorophenol (Visscher et al. 1998; Drijvers et al. 1999) as well as the studies on the scavenging effect of H_2O_2 in sonication as reported by Nam et al. (2003) in the sonolytic degradation of 5,5 dimethyl-1-pyrrline (DMPO).

Effect of zeolite addition

In this part of the study, sonication experiments were done with addition of 1.5 g of zeolite into the butyric acid (0.25 g/dm^3) solution with a solution volume of 1.5 dm^3 at a power of 70 W. No degradation was obtained.

The presence of solid particles affects the cavitational activity in two different and opposing ways, firstly it intensifies the process by providing additional nuclei due to the discontinuities in liquid medium and hence the

number of cavitation events may increase but at the same time due to the scattering of incidient sound waves the net energy dissipation into the system decreases (Gogate et al. 2004). To investigate the solid particle effect, in the present study, natural zeolite was added to butyric acid solutions because it was tested in our previous work for the sonolytic degradation of acetic acid (Dükkancı and Gündüz, 2006). Natural zeolite is rich in clinoptilolite and is obtained from Bigadiç Region of Turkey with an average chemical composition of 78.05 % SiO_2, 2.57 % Na_2O, 1.82 % K_2O, 0.45 % Fe_2O_3, 2.31 % CaO, 6.34 % Al_2O_3, 0.33 % MgO, 8.14 % H_2O, with a particle size of 0.25 mm and with a surface area of 33 m^2/g. It appears that the scattering effect of the incidient sound waves was predominant factor as compared with the enhancement in the number of cavitation event. Similar negative results were reported in sonication literature for phenol degradation in the presence of TiO_2, for degradation of trichloroethylene with CuO (Drijvers et al., 1999).

4.4.1.2 Sonication of butyric acid in ultrasonic probe system

Effect of initial concentration

The effect of initial concentration of butyric acid on degradation degree was studied at a power of 0.4 W, at a frequency of 100 kHz with a solution volume of 0.35 dm^3. Temperature was adjusted to 298 K. Table 4.15 and Figure 4.57 show the results of degradation degree.

Table 4.15. Effect of initial concentration in sonolysis of butyric acid.
(Power=0.4 W, Frequency=100 kHz,Solution volume=0.35 dm^3, Temperature=298 K)

Compound	Initial concentration, g/dm^3	Degradation, % (After 1 h)	STD
Butyric acid	0.25	1.53	± 0.22
Butyric acid	0.5	1.09	± 0.14

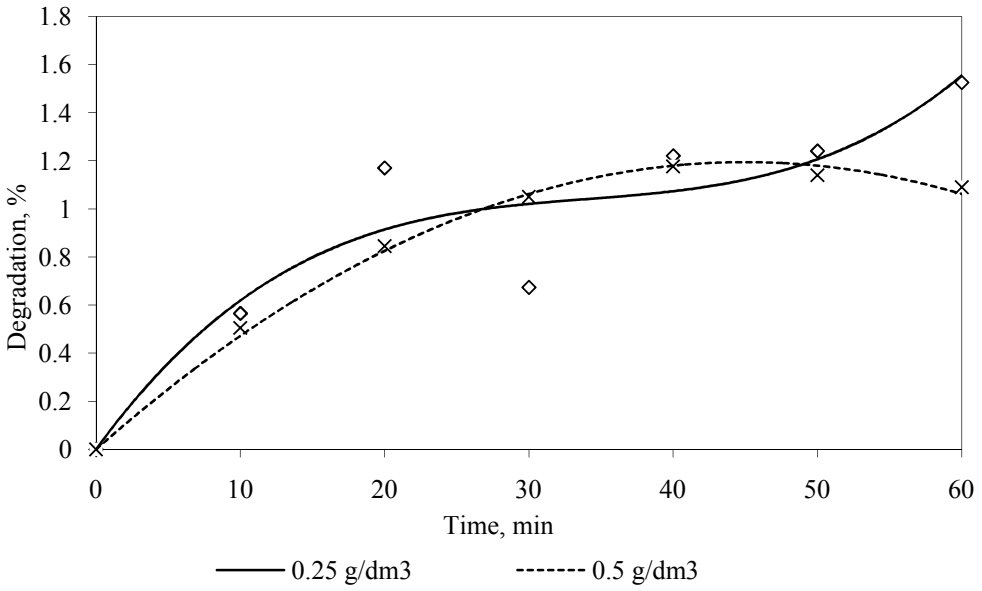

Figure 4.57. Effect of initial concentration of butyric acid in ultrasonic probe system.
(Power=0.4 W, Frequency=100 kHz, Solution volume=0.35 dm^3, Temperature=298 K)

Degradation degree of butyric acid was increased from 1.09 % to 1.53 % by decreasing initial concentration of butyric acid from 0.5 g/dm^3 to 0.25 g/dm^3 according to the explanation given in section 4.4.1.1. Power intensity in ultrasonic probe system was 0.116 W/cm^2 and in the frame of the local electrification of cavitation bubbles theory at such a low intensity of sound, the amplitude of bubble pulsation is so small that a bubble collapse is almost impossible (Margulis and Margulis, 1999; Margulis and Margulis, 2002) which leads to low degradation degrees of butyric acid.

Effect of ultrasonic frequency

Frequency effect on the degradation degree was studied with two different frequencies at a power of 0.4 W, at a temperature of 298 K with solution volume of 0.35 dm^3. Table 4.16 shows the results.

Table 4.16. Effect of ultrasonic frequency in sonolysis of butyric acid.
(Power=0.4 W, Solution volume=0.35 dm^3, Temperature=298 K)

Compound	Initial concentration, g/dm^3	Frequency, kHz	Degradation, % (After 1 h)	STD
Butyric acid	0.5	100	1.09	± 0.14
Butyric acid	0.5	60	0.91	± 0.03

Figure 4.58 shows the effect of frequency on the degradation degree of butyric acid.

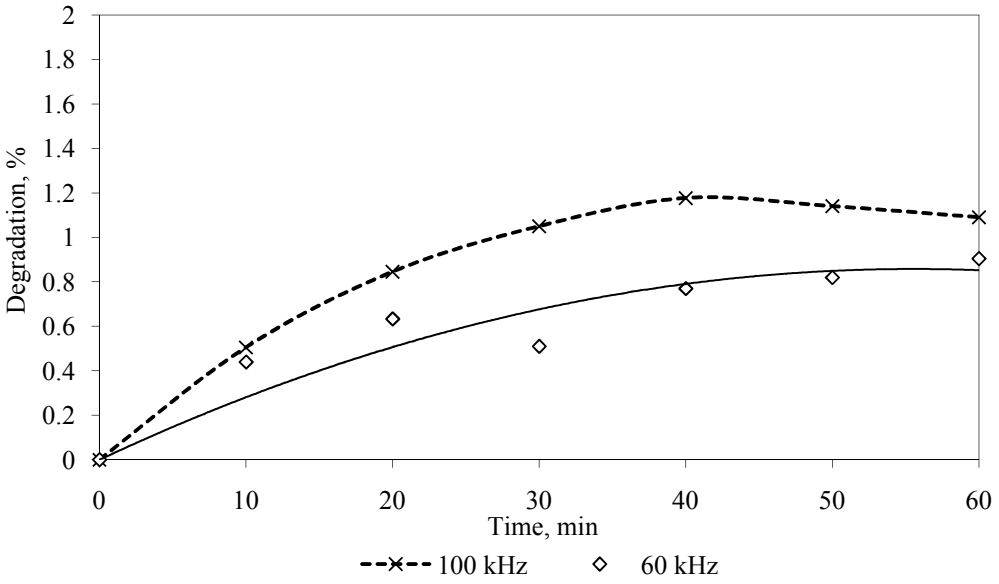

Figure 4.58. Effect of frequency on the degradation degree of butyric acid. (Power=0.4 W, Initial concentration=0.5 g/dm^3, Solution volume=0.35 dm^3, Temperature=298 K)

As seen from Figure 4.58, degradation degree of butyric acid was slightly increased by increasing frequency. As frequency increases life time of a bubble decreases and cavitation phenomenon becomes rapid, that is, the pulsation and collapse of the bubble occur more rapidly causing more radicals to escape from the bubble. In literature, similar results are present in sonolytic degradation of 0.1 g/dm^3 formic acid with a dual frequency flow cell at frequencies of 25, 40 and 25+40 kHz at a power of 120 W (Gogate et al. 2003) , in ultrasonic degradation of 0.06 g/dm^3 carbon tetrachloride in the frequency range of 20-800 kHz at a power of 30 W (Petrier and Francony, 1997) and in sonication of 3-chloroaniline at frequencies of 20 and 482 kHz (David et al., 1998).

Effect of H_2O_2 addition

As known well H_2O_2 is a good oxidant. H_2O_2 decomposes into hydroxyl radicals in ultrasonic environment causing high degradation rates. To investigate the effect of H_2O_2 addition into the butyric acid, experiments were performed at 298 K, at a power of 0.4 W and at a frequency of 100 kHz with a solution volume of 0.35 dm^3. Table 4.17 shows the experimental conditions and the degradation degrees in sonolysis of butyric acid in ultrasonic probe system.

Table 4.17. Effect of addition of H_2O_2 into the butyric acid solution.
(Power=0.4 W, Frequency=100 kHz, Initial concentration=0.5 g/dm^3, Volume=0.35 dm^3)

Compound	Initial concentration, g/dm^3	Addition of H_2O_2, M	Degradation, % (After 1 h)	STD
Butyric acid	0.5	-	1.09	± 0.14
Butyric acid	0.5	0.01	1.15	± 0.28
Butyric acid	0.5	0.03	1.60	± 0.05
Butyric acid	0.5	0.82	1.43	± 0.28
Butyric acid	0.5	1.63	4.03	± 0.48

Addition of 0.01 M H_2O_2 into the solution slightly increased degradation of butyric acid from 1.09 % to 1.15 % whereas addition of 0.03 M H_2O_2 into butyric acid solution increased degradation 1.09 % to 1.60 % . Figures 4.59 and Table 4.17 present this effect clearly. Figure 4.59b shows that when H_2O_2 was present in the solution in great amounts, very high initial degradation rates could be obtained. For instance, the increase in H_2O_2 amount from 0.82 M to 1.63 M for 0.5 g/dm^3 solution of BA, enhances the initial rate from 3.4×10^{-6} to 3.9×10^{-5} mol/dm^3 min. After reaching a maximum at a reaction time of around 20 min (8 % conversion) a decrease in BA degradation (up to 4 % conversion) was observed, after a sonication time of 1 h. It shows that the rate of hydroxyl radicals scavenging by H_2O_2 is higher than the formation of hydroxyl radicals after a reaction time of 20 min.

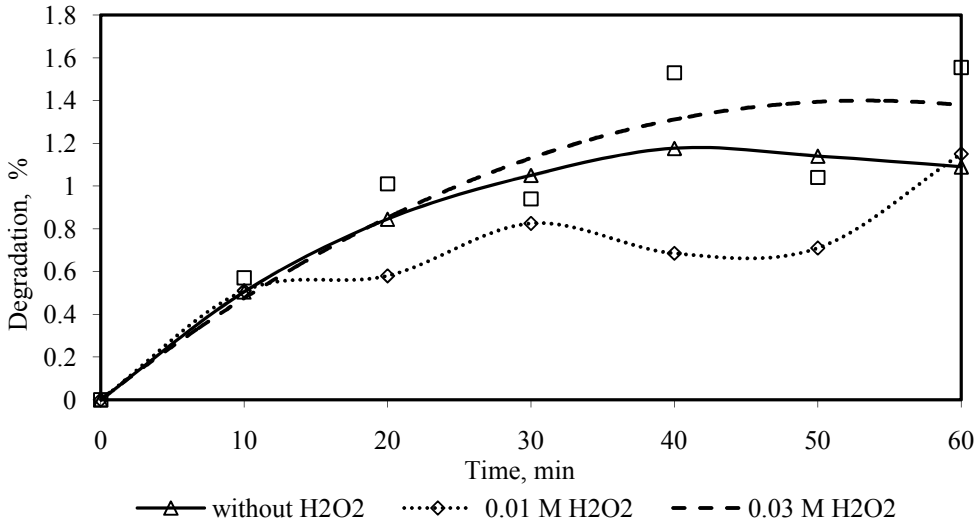

Figure 4.59a. Effect of addition of 0.01 or 0.03 M H_2O_2 into butyric acid solution.
(Power=0.4 W, Frequency=100 kHz, Initial concentration=0.5 g/dm^3, Volume=0.35 dm^3, Temperature=298 K)

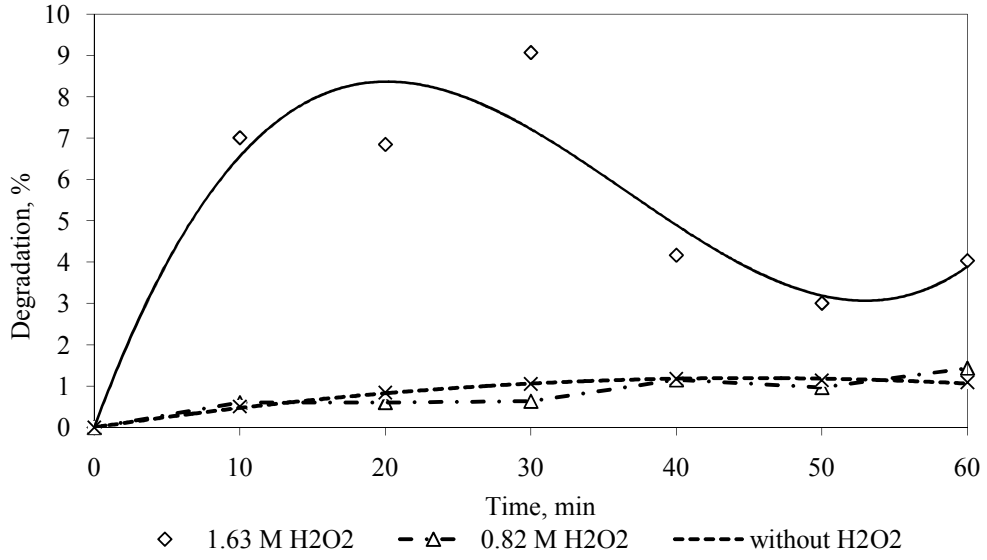

Figure 4.59b. Effect of addition of 0.82 or 1.63 M H_2O_2 into the butyric acid solution. (Power=0.4 W, Frequency=100 kHz, Initial concentration=0.5 g/dm^3, Volume=0.35 dm^3, Temperature=298 K)

Effect of salt (NaCl) addition

Table 4.18 shows the results of the experiments performed with different NaCl concentrations at 298 K, at a power of 0.4 W and a frequency of 100 kHz.

Table 4.18. Effect of NaCl addition into the butyric acid. (Power=0.4 W, Frequency=100 kHz, Volume=0.35 dm^3, Temperature=298 K)

Compound	Initial concentration, g/dm^3	Addition of NaCl, M	Degradation, % (After 1 h)	STD
Butyric acid	0.5	-	1.09	± 0.14
Butyric acid	0.5	0.25	-	-
Butyric acid	0.5	0.5	-	-
Butyric acid	0.5	1.5	-	-

The effect of addition of NaCl (salt) into the butyric acid solution was studied with three different amounts of NaCl (0.25, 0.5 and 1.5 M). Addition of NaCl had negative contribution on degradation of butyric acid. Degradation degree of butyric acid droped from 1.9 % to zero with addition of NaCl at the

concentration studied. As known well, the majority of oxidation reactions occur in the bubble-bulk interface area. Pollutants present in that region undergo degradation due to exposure to free radicals and high temperature and pressure. To enhance concentration in the bubble-bulk interface will change the rate of degradation. NaCl as a salt pushes pollutant molecules from the bulk aqueous phase toward the interface. In addition to this partitioning enhancement, salt decreases the vapor pressure, increases the surface tension and ionic strength of the aqueous phase, which drives the organic compound to the bulk-bubble interface (Goel et al. 2004). All these factors help in collapsing of the bubbles more violently. However, in the present study, this positive effect could not be observed. Salt added to the solution may interfere with the introduction of ultrasound into the liquid. Negative contribution of salt addition was reported in literature for sonolytic degradation of oxalic acid with a power of 98 W and a frequency of 40 kHz for NaCl concentrations over 0.75 M (Seymour and Gupta, 1997; Dükkancı and Gündüz, 2006).

Effect of zeolite or TiO_2 addition

There was no degradation in the experiments performed with 0.35 dm^3 0.25 g/dm^3 butyric acid at a power of 0.4 W, at a frequency of 100 kHz with addition of solid particles (0.0175 g zeolite, 0.0175 g TiO_2) into the solution. It is known that addition of TiO_2 increases cavitation. Because, intrinsic oxygen vacancies in the TiO_2 structure might also play important roles as nucleation sites for cavitation (Nakajima et al., 2007). However in this study, due to the scattering of the incident sound waves, no degradation was observed with the addition of solid particles into the butyric acid solution.

4.4.1.3 Sonication of butyric acid in ultrasonic reactor

Effect of ultrasonic mode

The high frequency generator in ultrasonic reactor can be used in two different modes: continuous (sinusoidal wave) or pulse (square wave) ultrasound. In square wave mode, pulse duty ratio can be adjusted as 5:1, 3:3 and 1:5.

To investigate the effect of ultrasonic mode on sonication of butyric acid, four different modes were tested at room temperature (293±278 K) for 1 h

sonication of 0.35 dm^3 of aqueous acid solutions of 0.25 g/dm^3 at an ultrasonic power of 25 W with a power intensity of 0.65 W/cm^2.

Figure 4.60 shows the effect of sonication mode on butyric acid degradation. As seen from Figure 4.60, the highest degradation degree was obtained in continuous mode and with pulse mode with pulse duration ratio of 5:1 (1.9 % after 1 h) but the highest initial rate ($5x10^{-6}$ mol/dm^3 min) was observed in continuous mode. It was followed by degradation with pulse mode with a pulse duration ratio of 1:5 (1.6 % after 1 h). The lowest degradation degree was obtained for the pulse duration ratio of 3:3 (1.3 % after 1 h) where pulse duration is equal to duration without pulse. In the latter case, the scattering effect of incident sound waves may be higher than the other duration ratios causing a decrease in the net energy dissipation into the system. In the continuous mode, actual sonication time was 1 h and ultrasonic waves may grow and collapse more regularly and violently due to the generation of sound waves continuously. However, in the pulse mode, although the real time was 60 min, the actual sonication time was 50, 30 and 10 min, for the pulse duration ratios of 5:1, 3:3 and 1:5, respectively.

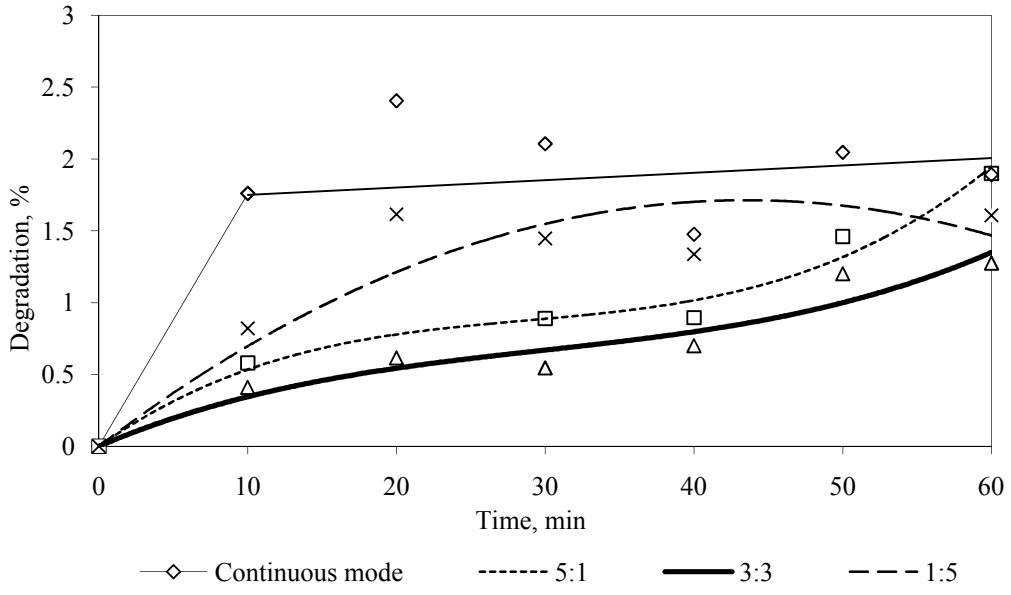

Figure 4.60. Effect of sonication mode on butyric acid degradation.
(Power=25 W, Frequency=850 kHz, Initial concentration=0.25 g/dm^3, Volume=0.35 dm^3)

Effect of ultrasonic power

Experiments of power effect on sonication of butyric acid were performed for a butyric acid concentration of 0.25 g/dm^3 for two different powers such as 25

and 50 W in continuous and pulse modes. The power was the supplied power. Figure 4.61 displays the results of butyric acid sonication for continuous (Figure 4.61a) and pulse mode (Figure 4.61b) with a pulse duration of 5:1. As seen from Figure 4.61, for both sonication modes, degradation degree of butyric acid was increased with decreasing power of irradiation from 50 W to 25 W. As explained in section 4.4.1.1 when power is increased for the same area (here, reactor bottom area), ultrasound power intensity increases (here from 0.65 to 1.3 W/cm^2) and a large number of gas bubbles or cavities are created in the solution and due to the coalescence of these cavities, large cavities are formed and they collapse less violently causing less degradation degree of butyric acid when high power was applied.

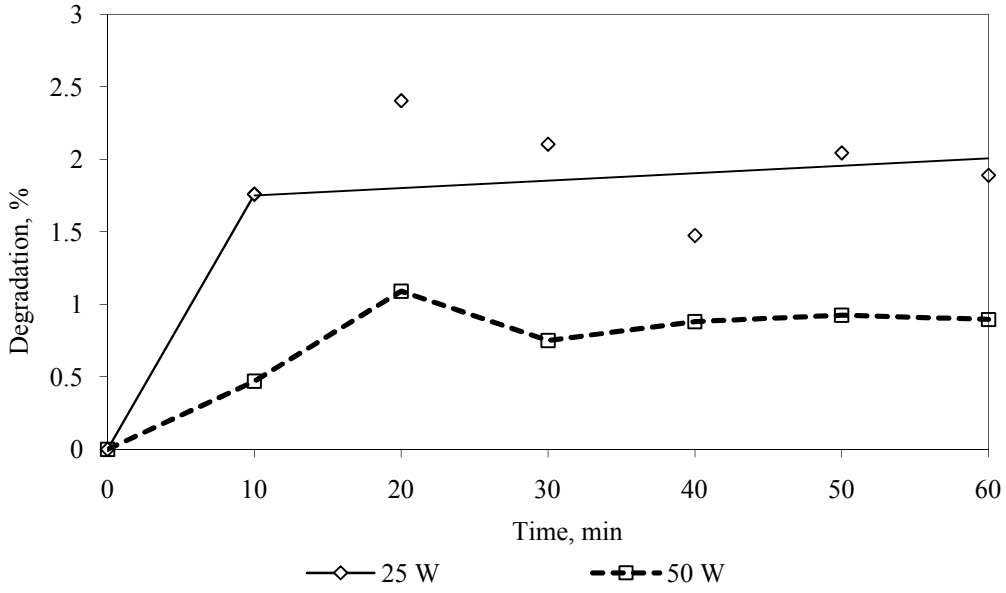

Figure 4.61a. Effect of sonication power on butyric acid degradation in continuous mode. (Frequency=850 kHz, Initial concentration=0.25 g/dm^3, Volume=0.35 dm^3)

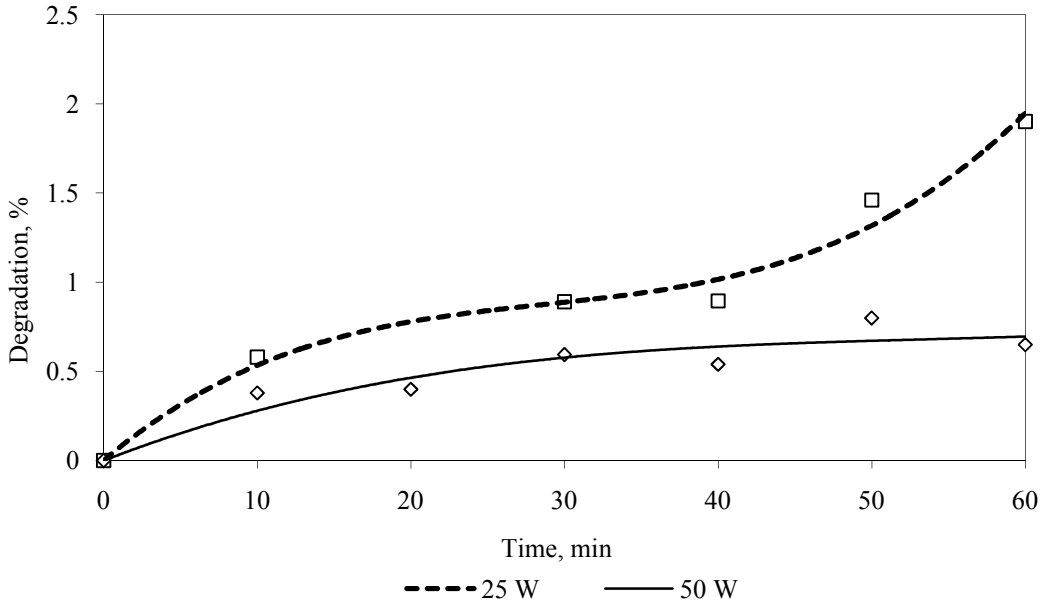

Figure 4.61b. Effect of sonication power on butyric acid degradation in pulse mode with a pulse duration of 5:1.
(Frequency=850 kHz, Initial concentration=0.25 g/dm^3, Volume=0.35 dm^3)

Effect of H_2O_2 addition

In this part of the experiments, to increase the number of hydroxyl radicals which can oxidize the BA, H_2O_2 was used. For the investigation of addition of H_2O_2 to the butyric acid solutions, experiments were performed in continuous sonication mode, at power of 25 W, at room temperature and for initial concentration of butyric acid of 0.25 g/dm^3. Addition of 0.68 M or 0.34 M H_2O_2 into 0.35 dm^3 of butyric acid solution of 0.25 g/dm^3 enhanced the degradation degree of acid from 1.9 % to 12.2 % and 1.9 % to 3.9 %, respectively, Figure 4.62.

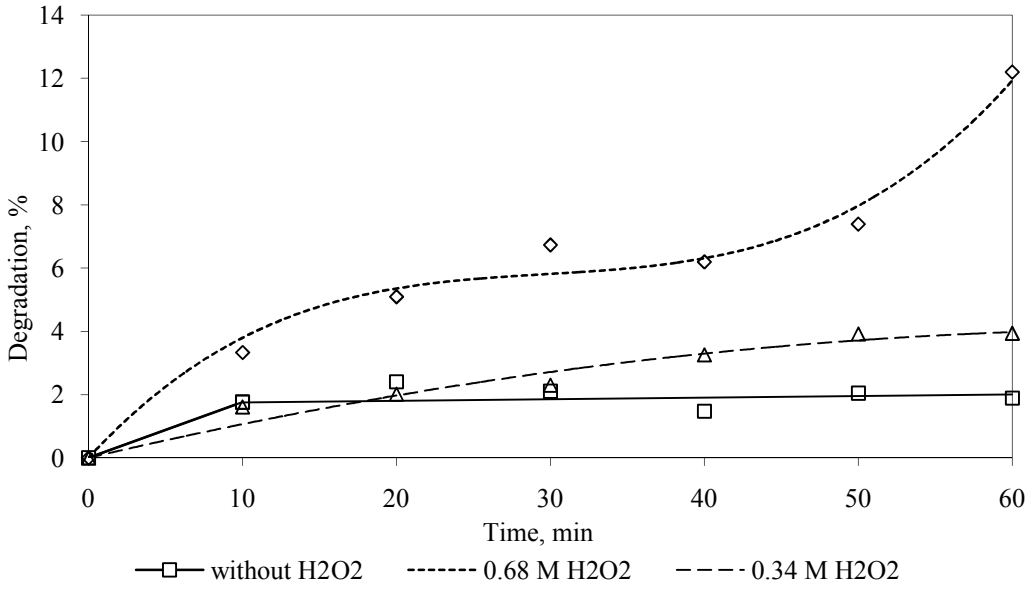

Figure 4.62. Effect of H_2O_2 addition on butyric acid degradation.
(Power=25 W, Frequency=850 kHz, Sonication mode=continuous, Initial concentration=0.25 g/dm^3, Volume=0.35 dm^3)

According to the hot spot theory, the temperature and pressure of localized hot spots formed can excessively reach 5000 K and 1000 atm respectively in the ultrasonic cavitation. Under these extreme conditions H_2O_2 decomposes into hydroxyl radicals causing high degradation rates (Wu et al., 2001).

Effect of initial concentration

For the investigation of initial concentration of butyric acid, experiments were performed at a power of 25 W, at room temperature in continuous ultrasound with different initial concentrations of acids for a solution volume of 0.35 dm^3. Table 4.19 shows the results.

Table 4.19. Effect of initial concentration on degradation degree of butyric acid.
(Power=25 W, Frequency=850 kHz, Sonication mode=continuous, Volume=0.35 dm^3)

Carboxylic acid	Initial concentration, g/dm^3	Degradation, % (after 1 h)	STD
Butyric acid	0.25	1.9	± 0.06
Butyric acid	0.5	-	-
Butyric acid	1	-	-

As seen from Table 4.19, when the initial concentration of butyric acid was increased from 0.25 g/dm^3 to 1 g/dm^3, it was found that there was no degradation. As the initial concentration of pollutant increases, the specific heat ratio of gas mixture at constant pressure and constant volume, $\gamma = C_p/C_v$, decreases resulting in a lower temperature and pressure within the cavitation bubbles and thus a decrease or completely inhibition in sonochemical degradation of volatile compounds is observed, Kim et al. (2001).

Effect of salt (NaCl) or natural zeolite addition

The effect of salt (NaCl, Riedel-de Haen) or natural zeolite was investigated on degradation of butyric acid in continuous mode of ultrasound with a power of 25 W using a solution volume of 0.35 dm^3. Table 4.20 and Figure 4.63 present the experimental conditions and degradation degrees obtained.

Table 4.20. Effect of NaCl or natural zeolite addition in sonolysis of butyric acid.
(Power=25 W, Frequency=850 kHz, Sonication mode=continuous,Volume=0.35 dm^3)

Compound	Initial concentration, g/dm^3	NaCl addition, M	Zeolite addition, g/0.35 dm^3	Degradation, % (after 1 h)	STD
Butyric acid	0.25	-	-	1.9	± 0.06
Butyric acid	0.25	0.5	-	1.5	± 0.15
Butyric acid	0.25	1.5	-	-	-
Butyric acid	0.25	-	0.0175	-	-

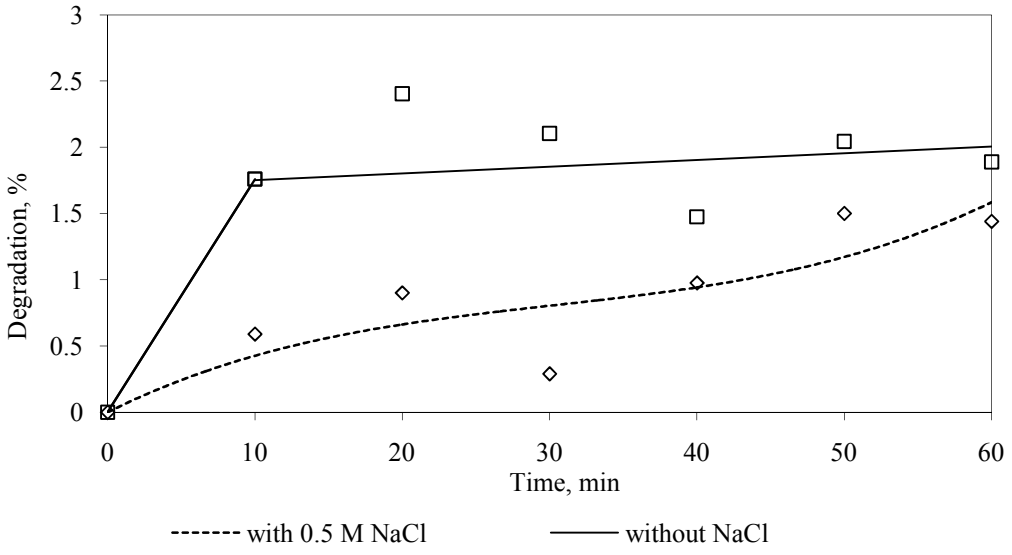

Figure 4.63. Effect of Salt (NaCl) addition on butyric acid degradation.
(Power=25 W, Frequency=850 kHz, Sonication mode=continuous,Volume=0.35 dm^3)

As seen from Table 4.20, degradation degree of butyric acid droped from 1.9 % to zero with addition of natural zeolite or 1.5 M NaCl and it droped from 1.9 % to 1.5 % with addition of 0.5 M NaCl, Figure 4.63.

As seen from all the tables and figures, in the most of the runs the degradation degree of butyric acid was about 2% after a sonication time of 1 h. The highest degradation degree of butyric acid was obtained for a sonication time of 1h, by addition of 0.68 M H_2O_2 into the 0.35 dm^3 BA solution in ultrasonic reactor (12.2 % conversion) and by addition of 1.63 M H_2O_2 addition into the 0.35 dm^3 solution in ultrasonic probe system (4.03 % conversion).

Acetic acid, formic acid and oxalic acid were detected as intermediates in the ultrasonic degradation of butyric acid during one hour sonication. But at such low degradation degrees, the accurate quantification of intermediates became difficult in HPLC analysis due to the weak UV response factors.

In literature, sonication was used in combination with other advanced oxidation processes, such as in the processes of ultrasound/H_2O_2/CuO (Drijvers et al., 1999), UV/Ultrasound (Wu et al., 2001, Tanaka and Harada, 2010), UV/Ultrasound/TiO_2 (Sonophotocatalysis) (Davydov et al., 2001; Mrowetz et al., 2003), UV/O_3/Ultrasound (Naffrechoux et al. 2000; Tezcanli-Güyer and Ince, 2001) ultrasound with Fenton-like reagents (Liang et al., 2007) and ultrasound assisted catalytic wet peroxide oxidation (Nikolopoulos et al., 2006) in order to

increase removal degree of several organic pollutants like phenol, trichloroethylene, salicylic acid, 2-chlorophenol, oxalic acid and 4-chlorophenol from water.

4.4.1.4 Sonication of butyric acid in ultrasonic reactor for 5 hours

As mentioned in section 4.4.1.1, in literature, most sonication experiments were done for a reaction time of 1h. However, in our laboratory sonication of some textile dyes such as, Rhodamine 6G and Orange II were studied in the ultrasonic reactor as a part of a project supported by NASU (National Academy of Science of Ukraine) and TÜBİTAK. In those studies it was observed that decolorization degrees of Rhodamine 6G and Orange II were increased from 1.4 % to 21.6 % and from 8.0% to 17.1 % with increasing sonication time from 2h to 6h at a power of 50 W, respectively. This result was in a good accordance with the study done by Larpparisudthi et al., 2009 on the sonication of several textile dyes. According to these results, in this part of my PhD thesis, sonolytic degradation of BA was investigated in ultrasonic reactor for a reaction time of 5h. The effects of power, initial concentration of BA and addition of H_2O_2 were investigated on the degradation of BA.

Effect of ultrasonic power

Experiments of power effect on sonication of butyric acid were performed for a butyric acid concentration of 0.25 g/dm^3 at three different powers such as 25, 50 and 75 W in continuous mode. It became easy to keep the temperature constant in the sonication runs at 25 and 50 W. However, in the sonication of BA at a power of 75 W temperature increased from about 298 K to about 308 K after an irradiation time of 5h. Figures 4.64a and 4.64b display the results.

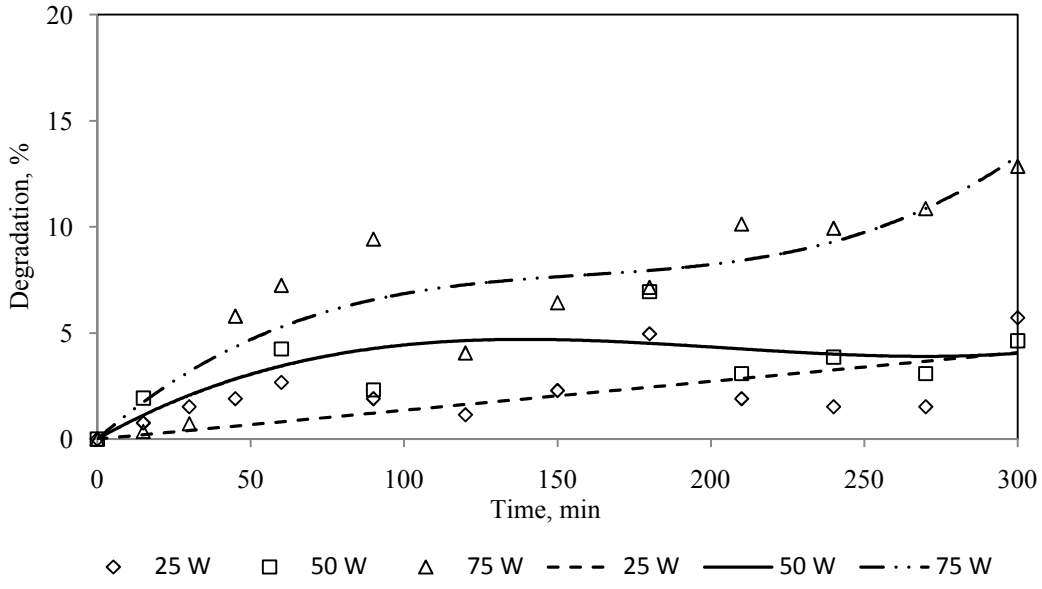

a.

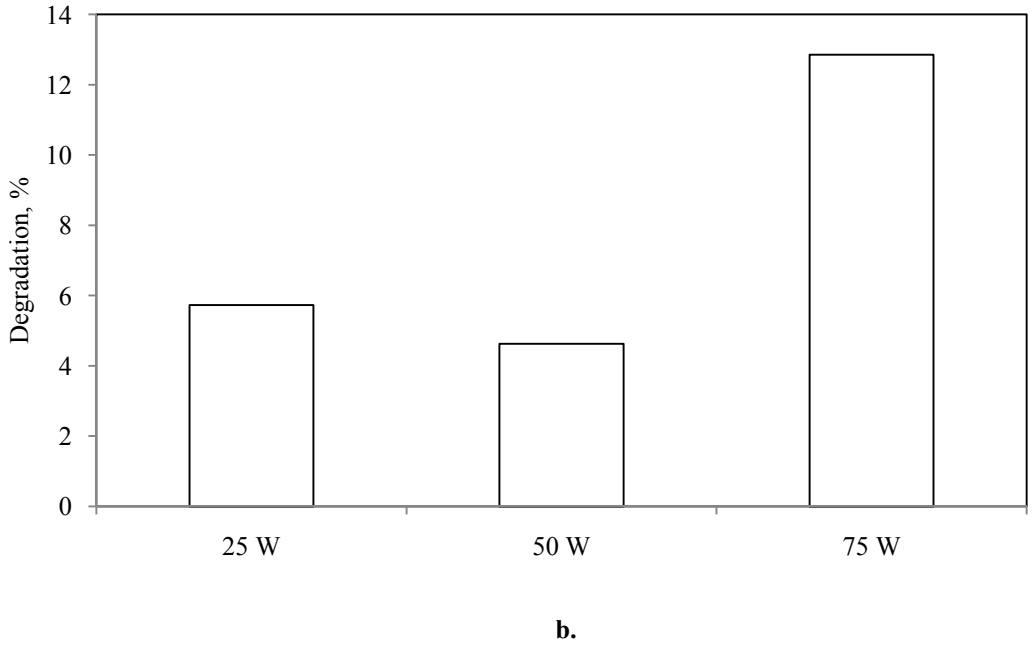

b.

Figure 4.64. Effect of ultrasonic power on degradation of butyric acid.
a., degradation degree vs. time curve, **b.**, degradation degree of BA after an irradiation time of 5h.
(Frequency=850 kHz, Initial concentration=0.25 g/dm^3, Volume=0.35 dm^3)

As seen from Figure 4.64, degradation degree of BA at power of 50 W is a little bit lower than at 25 W (4.6 % and 5.7 % after 5h, respectively). The decrease in degradation observed at 50 W may arise from the formation of large cavities which are created by the coalescence of small ones. But when power was incresed from 50 W to 75 W, degradation degree of BA increased from 4.6 % to 12.9 % because of the increasing of transmittance of ultrasonic energy into the reactor.

Due to this energy, in the reactor the pulsation and collapse of bubble occur more rapidly, number of cavitation bubbles increases and a higher concentration of OH radicals is achieved into the aqueous solution of organic pollutant. These hydroxyl radicals react with the pollutant in the solution. Due to this radical reaction the degradation of butyric acid increased with increasing power. As known well, increasing the ultrasonic power increases the energy of cavitation, lowers the threshold limit of cavitation and enhances the quality of cavitation bubbles (Jiang et al., 2002).

Similar results in degradation by ultrasound have been reported in literature in dibenzothiphene decomposition using an ultrasonic homogenizer at power of 600 W and at a frequency of 20 kHz (Kim et al., 2001).

In the sonolytic degradation of butyric acid in ultrasonic reactor for a reaction time of 5h, acetic acid (AA), oxalic acid (OA) and propionic acid (propA) were detected as intermediates. In litereture in the catalytic wet air oxidation of butyric acid over carbon supported catalysts, acetic and propionic acids were detected as intermediate, too (Gomes et al., 2002a; Gomes et al., 2002b; Gomes et al., 2004; Gomes et al., 2005). Figure 4.65 shows the change in the composition of the reaction medium as a function of time in sonication of 0.25 g/dm^3 BA solution at a power of 75 W. Concentrations of the intermediates show the following ordering: $C_{PropA} > C_{OA} > C_{AA}$. The sum of the organic carbon contributions measured from all the individually detected liquid phase organic intermediates was found to be equal to the total carbon of BA in the initial aqueous solution. This indicates that BA was only converted into intermediates, not to total oxidation product CO_2. In other words, no mineralization occurred during the reaction.

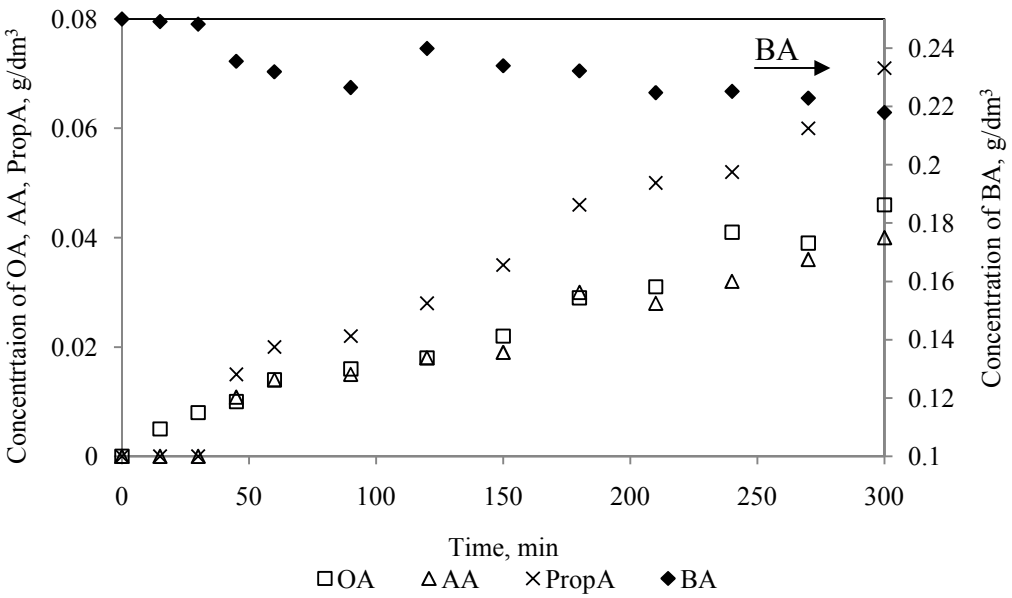

Figure 4.65. Change in the composition of the reaction medium as a function of time in sonication of 0.25 g/dm^3 BA solution.
(Frequency=850 kHz, Power=75 W, initial concentration=0.25 g/dm^3,Volume=0.35 dm^3)

As seen from Figure 4.65, intermediate (oxalic acid, acetic acid and propionic acid) concentration increases with time, which shows that the oxidation of butyric acid by sonolysis might proceed via the formation of propionic acid, oxalic acid and acetic acid in parallel routes in contrast with the pathways (parallel + series) observed in the catalytic wet air oxidation of butyric acid at high pressure, Equations 4.46 – 4.48.

Oxidation of BA to OA

$$C_4H_8O_2 + 9/2\ O_2 \xrightarrow{k_1} C_2H_2O_4 + 2\ CO_2 + 3\ H_2O \qquad (4.46)$$

Oxidation of BA to AA

$$C_4H_8O_2 + 3\ O_2 \xrightarrow{k_2} C_2H_4O_2 + 2CO_2 + 2H_2O \qquad (4.47)$$

Oxidation of BA to PropA

$$C_4H_8O_2 + 3/2\ O_2 \xrightarrow{k_3} C_3H_6O_2 + CO_2 + H_2O \qquad (4.48)$$

According to Equations 4.46 – 4.48, formation rates of OA, AA and PropA can be written as follows:

$$\frac{dC_{OA}}{dt} = k_1 C_{BA}{}^{m} \tag{4.49}$$

$$\frac{dC_{AA}}{dt} = k_2 C_{BA}{}^{n} \tag{4.50}$$

$$\frac{dC_{PropA}}{dt} = k_3 C_{BA}{}^{p} \tag{4.51}$$

By plotting $\ln(\frac{dC_{OA}}{dt})$, $\ln(\frac{dC_{OA}}{dt})$ and $\ln(\frac{dC_{OA}}{dt})$ vs. $\ln(C_{BA})$ graph, the slope of the straight line obtained gives the reaction order with respect to the BA concentration (m, n and p) and the intercept gives the reaction rate constant for each parallel reaction (k_1, k_2, k_3), Equations 4.52-4.54.

$$\ln(\frac{dC_{OA}}{dt}) = \ln k_1 + m \ln(C_{BA}) \tag{4.52}$$

$$\ln(\frac{dC_{AA}}{dt}) = \ln k_2 + n \ln(C_{BA}) \tag{4.53}$$

$$\ln(\frac{dC_{PropA}}{dt}) = \ln k_3 + p \ln(C_{BA}) \tag{4.54}$$

Figure 4.66 gives the related plots.

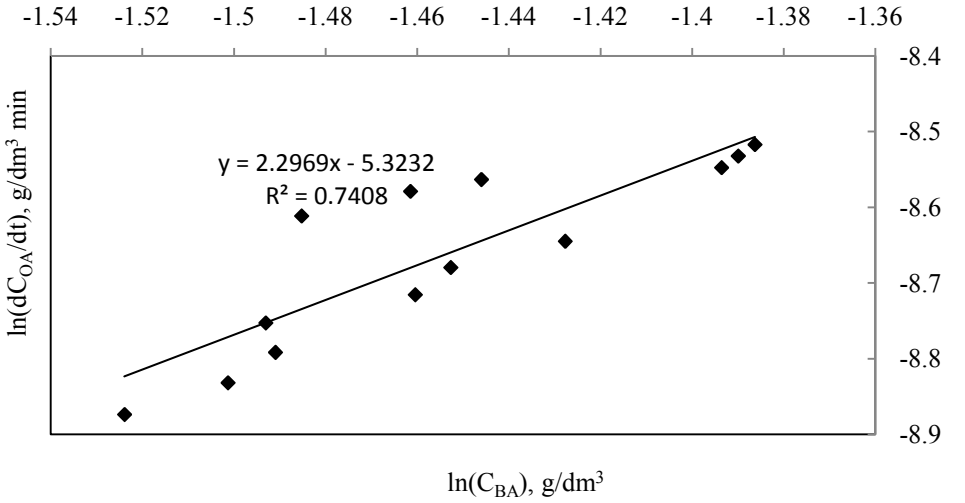

a.

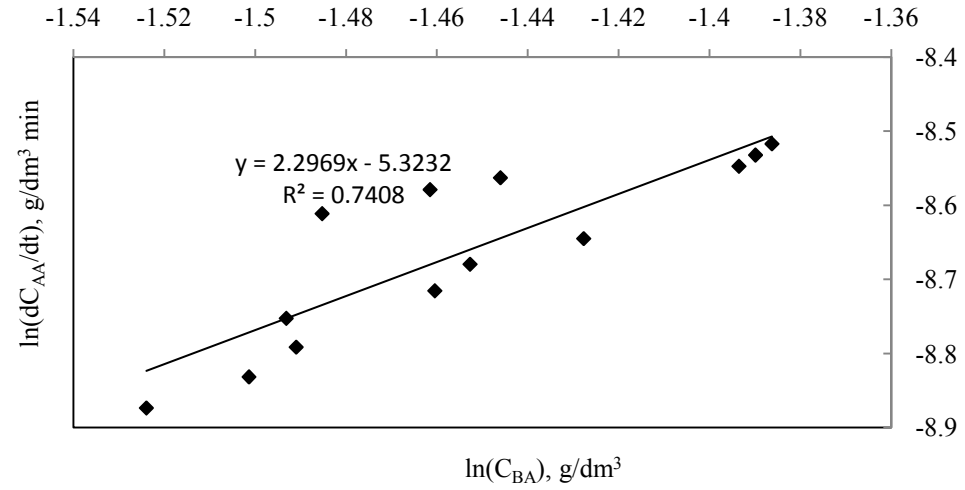

b.

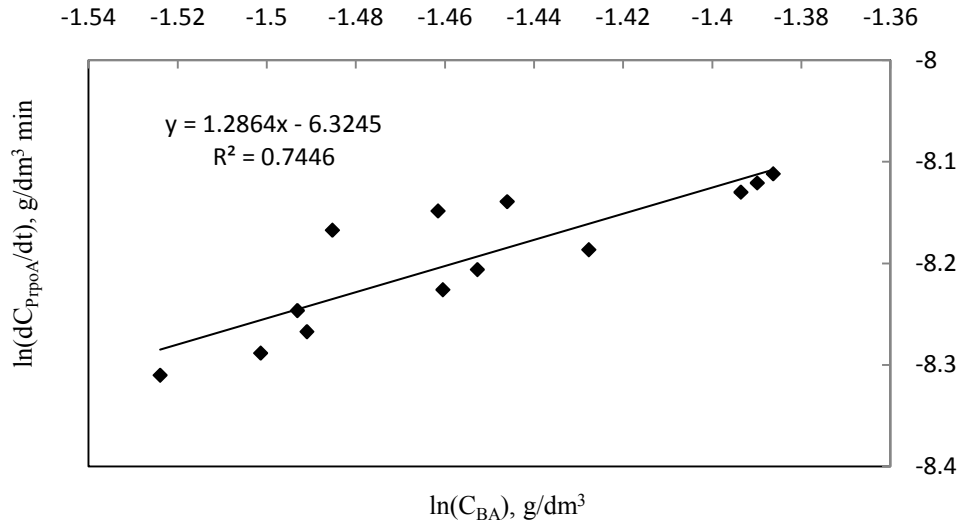

c.

Figure 4.66. Reaction rate vs. concentration of BA a) for OA; b) for AA; c)for PropA (Frequency=850 kHz, Power=75 W, initial concentration=0.25 g/dm^3,Volume=0.35 dm^3)

The order of the oxidation reaction of butyric acid to OA, AA and PropA were obtained to be, 2.29 ~ 2, 2.29 ~ 2 and 1.28 ~1, respectively. The determined k_1 and k_2 values were equal to 0.0049 dm^3 min^{-1} g^{-1} and k_3 was 0.0018 min^{-1}, Figure 4.66 (Fogler, 1999).

Effect of initial concentration

For the investigation of initial concentration of butyric acid, experiments were performed at a power of 75 W in the presence of sound waves continuously with different initial concentrations of acid such as, 0.05, 0.1, 0.25, 0.35 and 0.5 g/dm^3 for a solution volume of 0.35 dm^3. Figures 4.67a and 4.67b present the results.

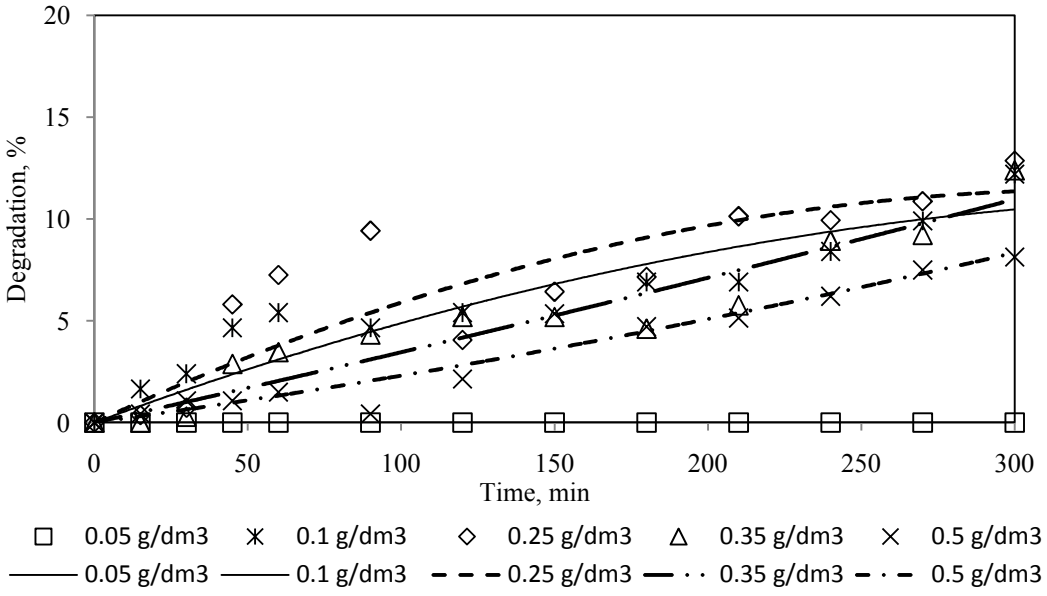

a.

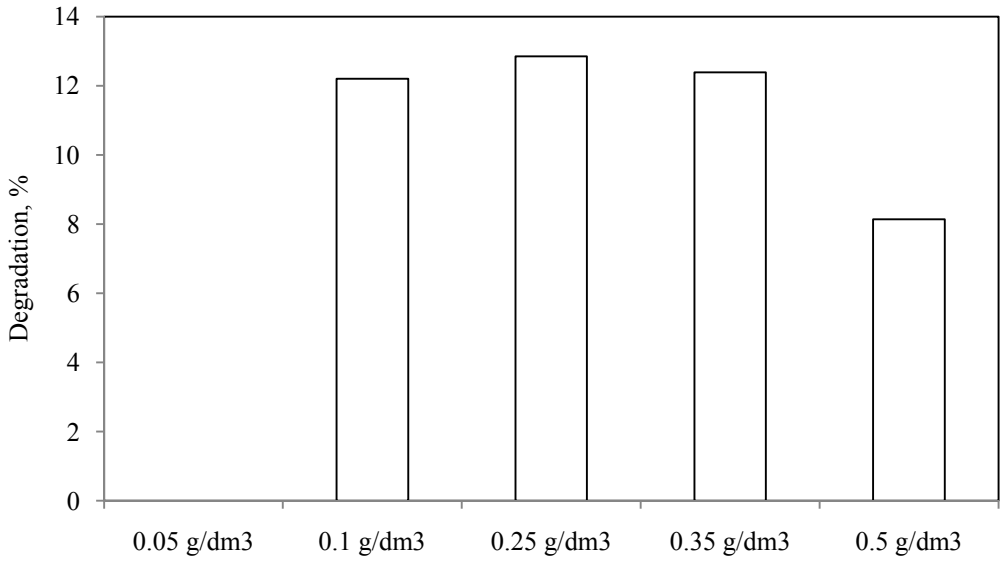

b.

Figure 4.67. Effect of initial concentration on degradation of butyric acid.
a., degradation degree vs. time curve, **b.**, degradation degree of BA after an irradiation time of 5h.
(Frequency=850 kHz, Power=75 W, Volume=0.35 dm^3)

As seen from Figure 4.67, degradation degree of butyric acid increased from zero to 12.9 % after 5h irradiation time with increasing initial concentration from 0.05 to 0.25 g/dm^3, being maximum at initial concentration of 0.25 g/dm^3. After that, degradation degree decreased from 12.9 % to 8.1 % with the increase in concentration from 0.25 to 0.5 g/dm^3. The optimum concentration of BA was 0.25 g/dm^3.

Figure 4.67 shows that, the rate of degradation of BA was high in the initial periods at an initial concentration of 0.25 g/dm^3. As time progressed, the rate of degradation decreased. However, no decrease in the rates of degradation was observed for the case of the higher concentrations (0.35 g/dm^3 and 0.5 g/dm^3). As known well, the consumption of generated free radicals occures in two ways, they attack the pollutant molecules (a beneficial way) resulting in degradation or they recombine with each other, forming hydrogen peroxide (a negative contribution, as free radicals were not available for the desired reaction and the reactivity of hydrogen peroxide was lower as compared to the free radicals). This negative contribution will be more in the case of a lower initial concentration (0.25 g/dm^3) of butyric acid acid and hence the decrease in the extent of degradation rate during the same time was observed as compared to the case of a higher initial concentration (0.35 g/dm^3 or 0.5 g/dm^3). Thus, it can be said that there exists a

limiting or equilibrium concentration, up to which the destruction can be achieved with the use of ultrasound with a significant destruction rate (Gogate et al., 2003).

The reduction in the chemical oxygen demand (COD) of the butyric acid solution was determined by measuring initial COD and final COD (after oxidation for 5 hours) of aqueous BA solution with a Lavibond Checkit Direct COD Vario device (the samples were diluted in 1:2 ratio). The COD reduction was zero, which shows that BA could be oxidized only into lower molecular weight carboxylic acids (oxalic, acetic and propionic acid, Figure 4.65) rather than end product of CO_2. This result also supported the idea obtained total carbon balance that only partial oxidation of BA was achieved, total oxidation to CO_2 (mineralization) could not be realized.

Effect of H_2O_2 addition

For the investigation of the effect of H_2O_2 addition to the butyric acid solution, experiments were performed in continuous sonication mode, at power of 75 W for initial concentration of butyric acid of 0.25 g/dm^3. Three different H_2O_2 concentrations were tested, namely, 0.17, 0.34 and 0.68 M. Figure 4.68 gives the results.

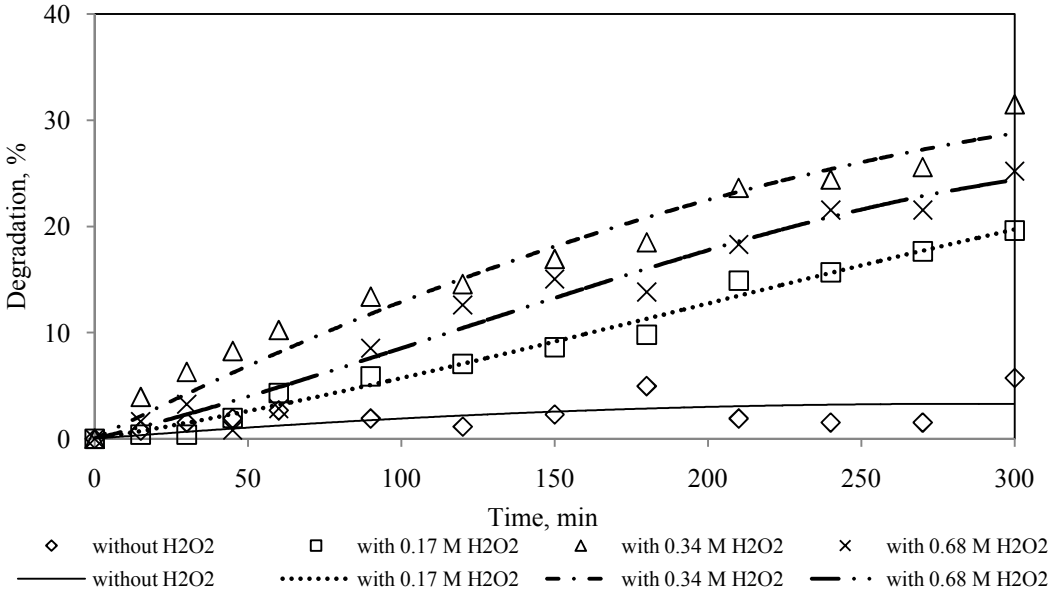

a.

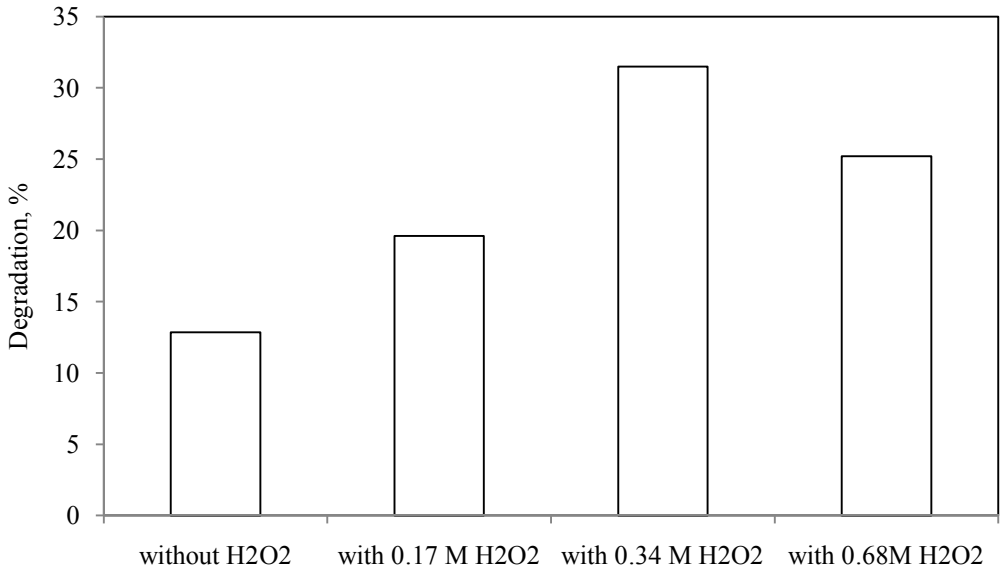

b.

Figure 4.68. Effect of addition of H_2O_2 on degradation of butyric acid.
a., degradation degree vs. time curve, **b.**, degradation degree of BA after an irradiation time of 5h.
(Frequency=850 kHz, Power=75 W, initial concentration=0.25 g/dm^3, Volume=0.35 dm^3)

Addition of 0.17 or 0.34 M of H_2O_2 concentration into butyric acid solution of 0.25 g/dm^3 enhanced the degradation degree of acid from 12.9 % to 19.6 % and 12.9 % to 31.5 %, respectively, due to the increase of formation rate of OH radicals from H_2O_2. Whereas when the H_2O_2 concentration increased from 0.34 to 0.68 M, degradation degree of BA decreased from 31.5 % to 25.2%. It shows that the rate of hydroxyl radicals scavenging by H_2O_2 is higher than the formation of hydroxyl radicals at that concentration value.

The COD reduction was measured to be 7.5 % in the presence of 0.34 M H_2O_2, at a power of 75 W.

4.4.1.5 Sonication assisted CWAO of butyric acid

In this part of the study, combined effect of sonication and CWAO on degradation degree of butyric acid was investigated. For this purpose, CAT1 was used as catalyst which gave the highest catalytic activity in CWAO of butyric acid at atmospheric pressure (section 4.2). Air was used as oxygen source at a flow rate of 0.003 g/dm^3. The temperature was kept constant at 308 K. The power of

ultrasound was adjusted to 75 W because the highest degradation degree of 0.25 g/dm^3 BA was observed at 75 W for sonication time of 5h, Figure 4.64. Figure 4.69 presents the result.

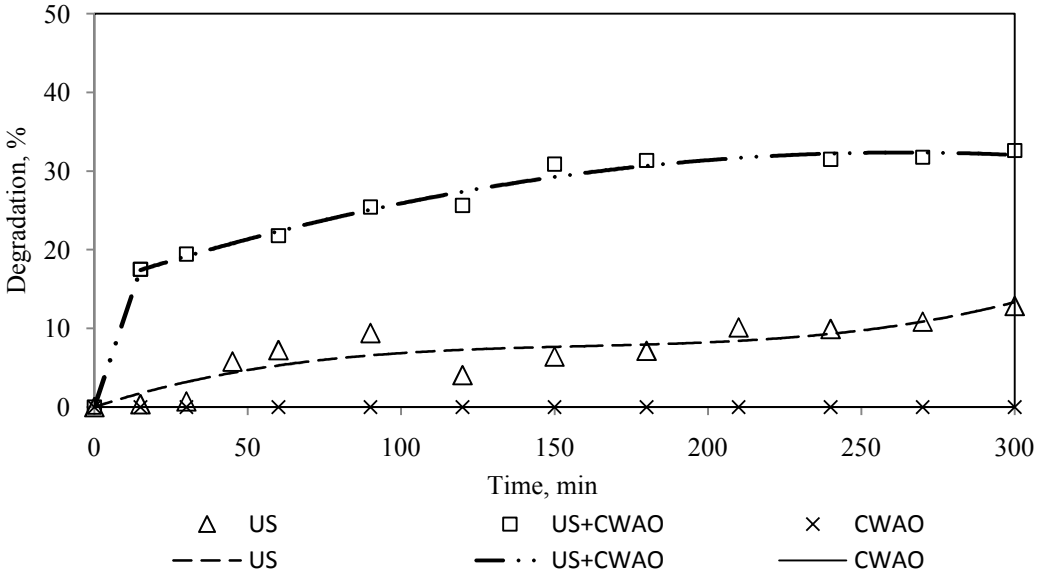

a.

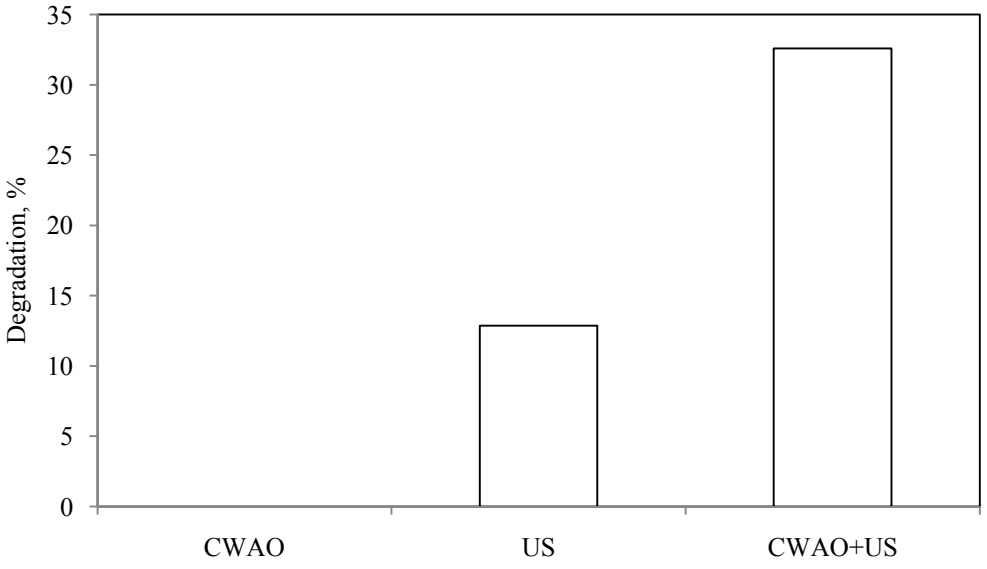

b.

Figure 4.69. Sonication assistant CWAO of BA.
a., degradation degree vs. time curve, **b.**, degradation degree of BA after an irradiation time of 5h.
(Frequency=850 kHz, Power=75 W, initial concentration=0.25 g/dm^3, Volume=0.35 dm^3, Amount of catalyst=2.33 g , Air flow rate=0.003 dm^3/s)

As seen from Figure 4.69, the degradation degree of BA was zero and 12.9 % when CWAO or sonication (US) used alone, respectively. However, in the case of CWAO and US combination, the obtained degradation degree of BA was 32.6 %. This result indicated that in the presence of of external gas, here air, cavitation events increases due to the presence of gas bubbles as additional nuclei. On the other hand, by bubbling air, dissolved oxygen amount in the solution increases. In sonochemical reaction dissolved gas correlates to both the intensity of sonochemical field and to the yield of free radical formation under ultrasonic irradiation. In addition to this, addition of solid particles (here CAT1 catalyst) intensifies the process by providing additional nuclei due to the discontinuities in liquid medium which enhance the number of cavitation events (Wu et al., 2001; Dükkancı and Gündüz, 2006). According to these combined effect (presence of dissolved oxygen and CAT1 catalyst) degradation degree of butyric acid increased from 12.9 % to 32.6. It is important to highlight that US+CWAO simultaneous combination implies synergetic effects rather than the addition of these effects.

Figure 4.70 shows the change in the composition of the reaction medium as a function of time in sonication of 0.25 g/dm^3 BA solution at a power of 75 W in the combined process of US and CWAO.

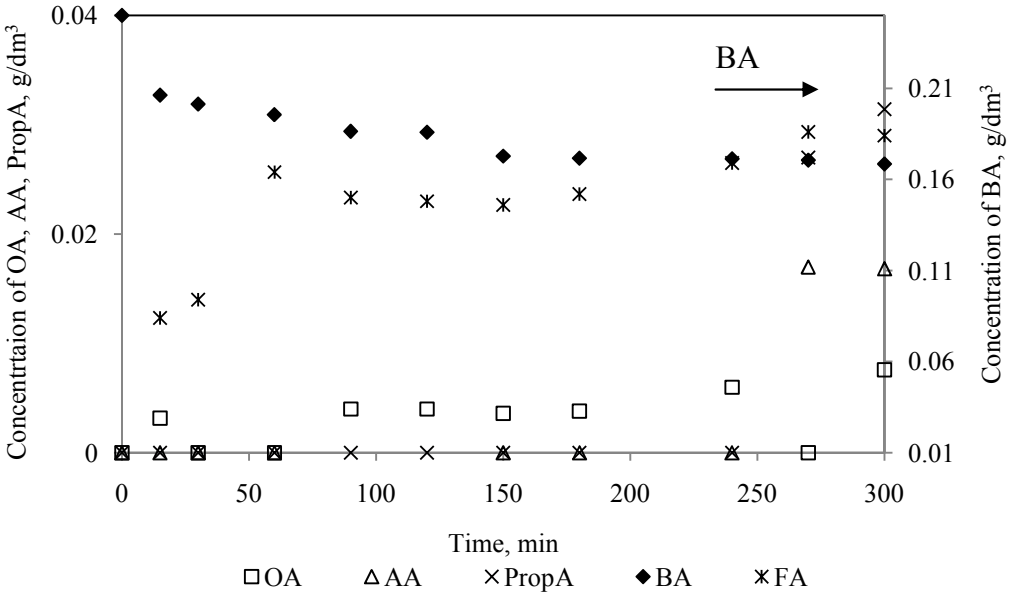

Figure 4.70. Change in the composition of the reaction medium as a function of time in sonication and catalytic wet air oxidation process.
(Frequency = 850 kHz, Power = 75 W, initial concentration = 0.25 g/dm^3, Volume=0.35 dm^3, Amount of catalyst=2.33 g , Air flow rate=0.003 dm^3/s)

As seen from Figure 4.70, formation rate of FA was higher than that of OA, AA and PropA and its concentration increased with time. Propionic acid and acetic acid were also formed as intermediates after an irradiation time of 270 min. Carbon balance done as a function of time showed that BA could be oxidized only into intermediates rather than total oxidation to CO_2 in the combined process of US and CWAO under the experimental conditions used.

4.4.2 Sonication of maleic acid

4.4.2.1 Sonication of maleic acid in ultrasonic bath

Sonication of maleic acid was carried out with 0.1 g/dm^3 initial concentration of maleic acid at two different powers, namely 70 and 84 W. For the investigation of effect of initial concentration of maleic acid, experiments were performed at a power of 70 W with three different initial concentrations such as, 0.1, 0.25 and 0.5 g/dm^3. 0.1 and 0.25 g/dm^3 initial concentrations of maleic acid were selected for the investigation of effect of addition of H_2O_2 in sonication at 70 W. The effect of addition of TiO_2 was tested at 70 W with 0.1 g/dm^3 initial concentration. In all the experiments the solution volume was 1.5 dm^3. Table 4.21 shows the experimental conditions in ultrasonic bath and results of the sonication after a reaction time of 1h.

Table 4.21. Sonication of maleic acid in ultrasonic bath.

Compound	Initial concentration, g/dm^3	Power, W	H_2O_2 amount, M	Zeolite amount, g/1.5 dm^3 MA	Degradation, %
Maleic acid	0.1	70	-	-	-
Maleic acid	0.1	84	-	-	-
Maleic acid	0.25	70	-	-	-
Maleic acid	0.5	70	-	-	-
Maleic acid	0.1	70	0.43	-	-
Maleic acid	0.25	70	0.43	-	-
Maleic acid	0.1	70	-	1.5	-

As seen in Table 4.21, it could not be possible to destruct maleic acid in ultrasonic bath. Maleic acid is a more hydrophilic compound than butyric acid, so it is difficult for maleic acid to transfer into the cavity or cavity-liquid interface, where the most of the degradation occurs (Wu et al., 2001).

4.4.2.2 Sonication of maleic acid in ultrasonic probe system

Sonication of maleic acid was performed at a power of 0.4 W in a reaction time of 1h with 0.35 dm^3 aqueous solution in ultrasonic probe system. The effects of initial concentration of maleic acid, frequency, addition of NaCl or H_2O_2 were investigated on the degradation of maleic acid. Table 4.22 shows the experimental conditions and obtained results.

As seen from Table 4.22, it was also hard to degrade maleic acid in ultrasonic probe system.

Table 4.22. Sonication of maleic acid in ultrasonic probe system.

Compound	Initial concentration, g/dm^3	Frequency, kHz	H_2O_2 amount, M	Addition of NaCl, M	Degradation, %	STD
Maleic acid	0.1	100	-	-	-	-
Maleic acid	0.25	100	-	-	-	-
Maleic acid	0.5	100	-	-	-	-
Maleic acid	0.1	60	-	-	-	-
Maleic acid	0.25	60		-	-	-
Maleic acid	0.1	100	1.63	-	13.9	± 0.40
Maleic acid	0.1	100	-	0.25	-	-

Figure 4.71 shows the effect of addition of 1.63 M H_2O_2 into the 0.1 g/dm^3, 0.35 dm^3 maleic acid solution at a frequency of 100 kHz and at a power of 0.4 W in ultrasonic probe system.

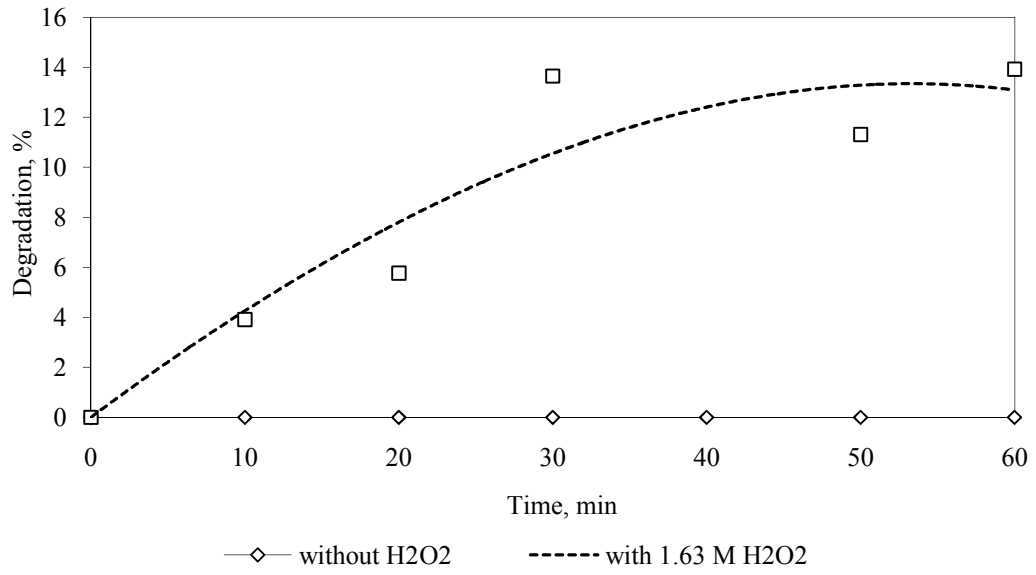

Figure 4.71. Effect of addition of H_2O_2 in sonication of maleic acid.
(Power=0.4 W, Initial concentration = 0.1 g/dm^3 , Frequency= 100 kHz, Volume=0.35 dm^3, Temperature=298 K)

As seen from Table 4.22 and Figure 4.71, there was no destruction of maleic acid at a power of 0.4 W and a frequency of 100 kHz. With the addition of 1.63 M H_2O_2 into the maleic acid solution, degradation increased from zero to 13.9 % after a sonication of 1h due to the increased the formation of OH* radicals which oxidize maleic acid.

4.4.2.3 Sonication of maleic acid in ultrasonic reactor

Sonolytic degradation of maleic acid was investigated in the ultrasonic reactor with a frequency of 850 kHz. The effects of sonication mode (continuous – pulse), initial concentration (0.1, 0.25 g/dm^3), H_2O_2, salt and solid particles (a natural zeolite) were studied on the degradation of maleic acid. In all experiments the volume of the solution and power were kept constant at 0.35 dm^3 and 25 W, respectively. Table 4.23 presents the experimental conditions and obtained results.

Table 4.23. Sonication of maleic acid in ultrasonic reactor.

Compound	Initial concentration, g/dm^3	Sonication mode	H_2O_2 amount, M	Zeolite addition, g/0.35 dm^3	NaCl addition, M	Degradation, %
Maleic acid	0.1	Continuous	-	-	-	-
Maleic acid	0.1	Pulse mode, 5:1	-	-	-	-
Maleic acid	0.1	Pulse mode, 1:5	-	-	-	-
Maleic acid	0.1	Pulse mode, 3:3	-	-	-	-
Maleic acid	0.25	Continuous	-	-	-	-
Maleic acid	0.1	Continuous	0.68	-	-	-
Maleic acid	0.1	Continuous	-	0.0175	-	-
Maleic acid	0.1	Continuous	-	-	0.25	-
Maleic acid	0.1	Continuous	-	-	0.50	-
Maleic acid	0.1	Continuous	-	-	1.5	

Consequently, it was not possible to destruct maleic acid in any ultrasonic equipment under the reaction conditions used in sonolysis of BA. Maleic acid could only be oxidized by sonolysis in ultrasonic probe system by addition of 1.63 M H_2O_2 into the 0.35 dm^3 of maleic acid solution (0.1 g/dm^3) at a power of 0.4 W, at a frequency of 100 kHz. The obtained conversion was measured as 13.9 %.

5. CONCLUSION

In the first part of the study, alumina, silicagel, TiO_2 and activated carbon supported Pt, Ru and Pd catalysts were prepared and catalytic wet air oxidation (CWAO) of maleic (MA) and butyric acid (BA) over prepared catalysts and two commercial catalysts (CAT1 and CAT2) were carried out at atmospheric pressure. The prepared catalysts and commercial catalysts were characterized by nitrogen adsorption, SEM, XRD and IR studies. After the selectivity studies at atmospheric pressure, the effect of initial concentration, catalyst loading, temperature and pressure on CWAO of butyric and maleic acid were discussed over the most selective catalyst in a high pressure reactor. The proper kinetic model was also developed for CWAO of butyric and maleic acid. According to the studies at atmospheric pressure:

- The catalysts of Pt/TiO_2-1, AC and Ru-Pd/AC showed some activity (2.1 %, 21.2 % and 23.9 %, respectively) for MA oxidation and the catalysts of Pt/TiO_2-2, Pt/TiO_2-3, Pd/TiO_2-3, AC and Ru-Pd/AC (2.6 %, 1.8 %, 2.3 %, 24.4 % and 24.6 %, respectively) for BA oxidation.

- Among the prepared catalysts, TiO_2 was determined to be the most suitable support in the oxidation of butyric acid and maleic acid under the experimental conditions used. Although, the achieved degradation degrees were 24.6 % and 23.9 % in the CWAO of butyric and maleic acid over Ru-Pd/AC catalyst at 333 K, the adsorption studies of butyric and maleic acid over AC support at 333 K showed that 22.5 % and 11 % adsoprtion were measured for BA and MA, respectively. This means that, BA and MA could be removed from their aqueous solutions by adsorption + catalytic oxidation under the conditions used.

- CAT1 catalyst showed the highest catalytic activity in the catalytic wet air oxidation of butyric and maleic acid at atmospheric pressure. A degradation of 7.9 % for butyric acid oxidation and a degradation of 11 % for maleic acid oxidation were achieved over this catalyst. Selectivity to CO_2 was 4.4 % for BA oxidation and 5.3 % for MA oxidation.

- In the butyric acid oxidation acetic, oxalic and formic acid were detected as intermediates. Acetic acid covered the surface of the catalyst and caused a retardation in the oxidation rate. The concentrations of acetic acid, formic acid and oxalic acid in the reaction mixture presented the following ordering: FA > AA> OA.

- In the maleic acid oxidation, oxalic acid and formic acid were detected as intermediates and the formic acid concentration was always greater than that of oxalic acid in the reaction medium.

- No measurable Pt leaching was observed with CAT1 catalyst in CWAO of BA and MA under the experimental conditions studied.

The studies on CWAO of BA and MA at pressures higher than atmospheric gave the following results:

- In the oxidation of BA with an initial concentration of 3 g/dm^3 over CAT1 catalyst, initial oxidation rates were increased with increasing oxygen pressure in the range of 2.8 to 9.7 bar and reaction order of 0.56 and 0.87 (~1) were observed with respect to the oxygen pressure and butyric acid concentration, respectively. An activation energy of 24.6 kJ/mol was measured for initial rate. Among the tested heterogeneous kinetic models, in the CWAO of BA on CAT1 catalyst under the experimental conditions studied, the best fitted model was MODEL II with the assumption that reaction occurred at the catalyst surface between the adsorbed butyric acid and molecular adsorbed oxygen. According to this model calculated activation energy was 112.8 kJ/mol.

- The activity of CAT1 catalyst was higher in oxidation of MA than in BA. A degradation degree of 86.5 % was achieved at a temperature of 393 K, at the standard catalyst concentration of 10 g/dm^3 and at an oxygen pressure of 6.9 bar. Almost complete degradation (96.8 %) was achieved at the highest temperature studied (423 K) after an oxidation time of 3h.

- Reaction order was first order with respect to oxygen pressure and the order was 0.34 with respect to MA concentration. Activation energy of initial reaction rate was 16.9 kJ/mol. Among the tested heterogeneous kinetic models, MODEL III fitted the experimental data best with the assumption that reaction occurred at the catalyst surface between the adsorbed maleic acid and molecular adsorbed oxygen with negligible adsorption of FA and OA . According to this model calculated activation energy was 122.3 kJ/mol.

- In MA oxidation selectivity to formic acid increased with increasing oxygen pressure. Fumaric acid and OA were formed in the earliest stage of the reaction. Fumaric acid and oxalic acid concentrations reached a maximum then

they decreased to zero. The formation of FA was increased with time. This result showed that maleic acid and fumaric acid were converted into oxalic acid, then oxalic acid was degraded into formic acid and finally formic acid was oxidized into CO_2 and water. Selectivity to CO_2 changed from 62 % to 73 % in the pressure range of 2.8-6.9 bar at a temperature of 393 K.

- The measured Pt leaching was 2.5 and 3 mg/dm^3 in the oxidation of BA and MA at an oxygen pressure of 6.9 bar after an oxidation time of 3h, respectively. These values were very close to European Union directives (< 2 mg/dm^3).

- Butyric acid and maleic acid are present in the waste water of several industries such as, medicine, detergent, resin, leather, plastic and textile and they are formed in the oxidation of phenol and phenolic compounds as intermediates. In this study the CWAO of these two carboxylic acids over CAT1 catalyst was studied using the laboratory scale experimental set-up to optimize the operating conditions. Optimum conditions obtained can be applied to industrial waste waters containing butyric and maleic acids. The derived reaction rate expression can be used in industrial applications to size the reactor.

In the second part of the study, sonication of butyric and maleic acid were investigated by using different sonication equipment. The following points are highlighted:

- In ultrasonic degradation of butyric and maleic acid, obtained degradation degrees were much lower than in the catalytic wet air oxidation of these acids.

- Sonication equipment used affected the degradation degree. In the ultrasonic degaradation of butyric acid the highest conversion was obtained in ultrasonic reactor with continuous mode as 1.9 %.

- Addition of 0.68 M H_2O_2 into the 0.35 dm^3 butyric acid solution with a concentration of 0.25 g/dm^3 increased the degradation degree from 1.9 % to 12.2 % at a power of 25 W after a sonication time of 1h in ultrasonic reactor.

- The longer the sonication time, the more the degradation of carboxylic acid was obtained. For instance, in the sonication of butyric acid in ultrasonic reactor degradation degrees as high as 31.5 % could be achieved at a power of 75 W, at an initial concentration of butyric acid of 0.25 g/dm^3 with addition of 0.34

M H_2O_2 for a sonication time of 5h. The oxidation of butyric acid by sonolysis proceeded via the formation of intermediates (propionic acid, oxalic acid and acetic acid) in parallel routes.

- The degradation degree of BA was zero and 12.9 % when CWAO or sonication (ultrasonic reactor) used alone for an irradiation time of 5h, respectively. However, in the case of CWAO and US combination, the obtained degradation degree of BA was 32.6 %.

- It was not possible to destruct maleic acid in any ultrasonic equipment under the reaction conditions used in sonolysis of BA. Maleic acid could only be oxidized by sonolysis in ultrasonic probe system by addition of 1.63 M H_2O_2 into the 0.35 dm^3 of maleic acid solution (0.1 g/dm^3) at a power of 0.4 W, at a frequency of 100 kHz. The obtained conversion was measured as 13.9 %.

- Optimization of the reaction parameters is very important when industrial application of sonolytic degradation of above mentioned acids is desired. For this reason, experimental conditions tested should be evaluated from the point of economic analysis of the data. For example for a long irradiation time in sonication higher degradation degree (12.9 % at 75 W) was obtained as compared to shorter reaction time (1.9 % at 25 W) in ultrasonic reactor but here energy consumption should be taken into account. In addition to this the obtained degradation degree of BA was 12.9 % without addition of H_2O_2 into the solution at 75 W whereas 31.5 % and 25.2 % conversions were achieved with addition of 0.34 M or 0.68 M H_2O_2, after a reaction time of 5h. In the industrial applications it is important to use optimum H_2O_2 concentration in order to minimize H_2O_2 cost. In this study, 0.34 M H_2O_2 seems to be the optimum H_2O_2 amount.

6. RECOMMENDATIONS

For future studies, combined effect of ultrasound, UV irradiation and ozonation can be tested in order to increase the removal degree of butyric acid and maleic acid from their aqueous solutions. In addition to this, combination of catalytic wet air oxidation and sonolysis can be studied in detail.

REFERENCES

Andreozzi, R., Caprio, V., Insola, A. and Marotta, R., 1999, Advanced oxidation processes (AOP) for water purification and recovery, *Catalysis Today*, 53:51-59pp.

Barbier, Jr., J., Delanoe, F., Jabouille, F., Duprez, D., Blanchard, G. and Isnard, P., 1998, Total oxidation of acetic acid in aqueous solutions over noble metal catalysts, *Journal of Catalysis*, 177:378-385pp.

Becer, M., 2003, Gas Adsorption in Volumetric System, MSc Thesis, İzmir Institude of Technology, Turkey.

Berberidou, C., Poulios, I., Xekoukoulotakis, N.P. and Mantzavinos, D., 2007, Sonolytic, photocatalytic and sonophotocatalytic degradation of malachite gren in aqueous solutions, *Applied Catalysis B:Environmental*, 74:63-72pp.

Besson, M., Kallel, A., Gallezot, P., Zanella, R. and Louis, C., 2003, Gold catalysts supported in titanium oxide for catalytic wet air oxidation of succinic acid, *Catalysis Communications*, 4:471-476pp.

Beziat, J-C., Besson, M., Gallezot, P. and Durecu, S., 1999, Catalytic wet air oxidation of carboxylic acids on TiO_2-Supported ruthenium catalysts, *Journal of Catalysis*, 182:129-135pp.

Bhirud, U.S., Gogate, P.R., Wilhelm, A.M. and Pandit, A.B., 2004, Ultrasonic bath with longitudinal vibrations: a novel configuration for efficient wastewater treatment, *Ultrasonics Sonochemistry*, 11:143-147pp.

Buzzle.com, 2010 " Waste water Treatment Methods", http://www.buzzle.com/articles/wastewater-treatment-methods.html (Approach year: 2010)

REFERENCES (continued)

Capelo, J.L., Galesio, M.M. and Felisberto, G.M., 2005, Micro-Focused Ultrasonic Solid-Liquid Extraction (μFUSLE) combined with HPLC and Fluorescence Detection for PAHs Determination in Sediments: Optimization and Linking with the Analytical Minimalism Concept., *Talanta*, 66, 1272–1280pp.

Centi, G., Perathoner, S., Torre, T. and Verduna, M.G., 2000, Catalytic wet oxidation with H_2O_2 of carboxylic acids on homogeneous and heterogeneous Fenton-type catalysts, *Catalysis Today*, 55:61-69pp.

Chollier, M.J., Epron, F., Pitara, E.L. and Barbier, J., 1999, Catalytic oxidation of maleic and oxalic acids under potential control of platinum catalysts, *Catalysis Today*, 48:291-300pp.

Cybulski, A. and Trawezynski, J., 2004, Catalytic wet air oxidation of phenol over platinum and ruthenium catalysts, *Applied Catalysis B: Environmental*, 47 :1-13pp.

David, B., Lhote, M., Faure, V. and Boule, P., 1998, Ultrasonic and photochemical degradation of chlorpropham and 3-chloroaniline in aqueos solution, *Water Research*, 32 :2451 :2461pp.

Davydov, L., Reddy, E.P., France, P. and Smirniotis, P.G., 2001, Sonophotocatalytic destruction of organic contaminats in aqueous systems on TiO_2 powders, *Applied Catalysis B :Environmental*, 32 :95-105pp.

Drijvers, D., Langenhove, H.V. and Beckers, M., 1999, Decomposition of phenol and trichloroethylene by the ultrasound/H_2O_2/CuO Process, *Water Research*, 33:1187-1194pp.

Dutta, K., Mukhopadhyay, S., Bhattacharjee, S. and Chaudhuri, B., 2001, Chemical oxidation of Methylene Blue using a Fenton-like reaction, *Journal of Hazardous Materials*, B84:57-71pp.

REFERENCES (continued)

Dükkancı, M., 2004, Ultrasonic degradation of organic pollutants in water, Msc Thesis, Ege University, 54-55pp.

Dükkancı, M. and Gündüz, G., 2006, Ultrasonic degradation of oxalic acid in aqueous solutions, *Ultrasonics Sonochemistry*, 13:517-522pp.

Dükkancı, M., Gündüz, G. and Gündüz, E., 2007, Direct sonication of aqueous oxalic acid solution, 1st International Congres on Green Process Engineering, Toulouse-France, oral presentation, 142p.

Dükkancı, M. and Gündüz, G., 2009, Catalytic wet air oxidation of butyric acid and maleic acid solutions over noble metal catalysts prepared on TiO_2, *Catalysis Communications*, 10:913-919pp.

Eftaxias A., 2002, Catalytic Wet Air Oxidation of Phenol in a Trickle Bed Reactor: Kinetics and Reactor Modelling, PhD Thesis in Chemical Engineering of the Rovira i Virgili University, 3-9pp.

Entezari, M., Kruus, P. and Otson, R., 1997, The effect of frequency on sonochemical reactions III: dissociation of carbon disulfite, *Ultrasonics Sonochemistry*, 4:49-54pp.

Entezari, M.H., Mostafai, M. and Sarafraz-yazdi, A., 2006, A Combination of ultrasound and biocatalyst:removal of 2-chlorophenol from aqueous solution, *Ultrasonics Sonochemistry*, 13:37-41pp.

Epron, F., Chollier-Brym, M.J., Lamy-Pitara, E. and Barbier, J., 1999, Oxidation of maleic acid under control of the catalyst potential in a pressurized electrochemical reactor, *Applied Catalysis A: General*, 176:221-228pp.

Fındık, S., 2005, Ultrasonic oxidation of organic pollutants in aqueous solutions, PhD Thesis, Ege University, 41p.

Fındık, S., Gündüz, G. and Gündüz, E., 2006, Direct sonication of acetic acid in aqueous solutions, *Ultrasonics Sonochemistry*, 13:203-207pp.

REFERENCES (continued)

Fındık, S. and Gündüz, G., 2007, Sonolytic degradation of acetic acid in aqueous solutions, *Ultrasonics Sonochemistry*, 14:152-157pp.

Fogler, H.S., 1999, Elements of Chemical Reaction Engineering, Prentice-Hall International Inc., Third addition, 285-295pp.

Gaalova, J., Barbier, J. and Rossignol, S., 2010, Ruthenium versus platinum on cerium materials in wet air oxidation of acetic acid, *Journal of Hazardous Materials*, (in pres).

Gallezot, P., Laurain, N. and Isnard, P., 1996, Catalytic wet-air oxidation of carboxylic acids on carbon-supported platinum catalysts , *Applied Catalysis B: Environmental*, 9:L11-L17pp.

Gallezot, P., Chaumet, S., Perrard, A. and Isnard, P., 1997, Catalytic wet air oxidation of acetic acid on carbon-supported ruthenium catalysts, *Journal of Catalysis*, 168:104-109pp.

Goel, M., Hongqiang, H., Mujumdar, A.S. and Ray M.B, 2004, Sonochemical decomposition of volatile and non-volatile organic compounds—a comparative study, *Water Research*, 38:4247-4261pp.

Gogate, P.R., Mujumdar, S. and Pandit, A.B., 2003, Sonochemical reactors for waste water treatment: comparison using formic acid degradation as a model reaction, *Advances in Environmental Research*, 7:283-299pp.

Gogate, P.R., Mujumdar, S. and Thampi, J., 2004, Destruction of phenol using sonochemical reactors: scale up aspects and comparison of novel configuration with conventional reactors, *Separation and Purification Technology*, 34:25-34pp.

Gomes, H.T., Figueiredo, J.L. and Faria, J.L., 2000, Catalytic wet air oxidation of low molecular weight carboxylic acids using a carbon supported platinum catalyst, *Applied Catalysis B: Environmental*, 27:L217-L223pp.

REFERENCES (continued)

Gomes, H.T., Figueiredo, J.L. and Faria, J.L., 2002a , Catalytic wet air oxidation of butyric acid solutions using carbon-supported iridium catalysts, *Catalysis Today*, 75:23-28pp.

Gomes, H.T., Figueiredo, J.L., Faria, J.L., Serp, Ph. and Kalck, Ph., 2002b Carbon-supported iridium catalysts in the catalytic wet air oxidation of carboxylic acids: kinetics and mechanistic interpretation, *Journal of Molecular Catalysis A: Chemical*, 182-183: 47-60pp.

Gomes, H.T., Orfao, J.J.M., Figueiredo, J.L. and Faria, J.L., 2004, CWAO of butyric acid solutions: catalyst deactivation analysis, *Industrial Engineering Chemical Res*earch, 43: 1216-1221pp.

Gomes, H.T., Serp, Ph, Kalck, Ph., Figueiredo, J.L. and Faria, J.L., 2005, Carbon supported platinum catalysts for catalytic wet air oxidation of refractory carboxylic acids, *Topics in Catalysis*, 33:59-68pp.

Gonze E., Fourel L., Gonthier, Y., Boldo, P. and Bernis A., 1999, Wastewater pretreatment with ultrasonic irradiation to reduce toxicity, *Chemical Engineering Journal*, 73:93-100pp.

Guedes, A.M.F.M., Madeira, L.M.P., Boaventura, R.A.R. and Costa, C.A.V., 2003, Fenton oxidation of cork cooking wastewater overall kinetic analysis, *Water Research*, 37:3061-3069pp.

Guo, Z., Zheng, Z., Zheng, S., Hu, W. and Feng, R., 2005, Effect of various sono-oxidation parameters on the removal of aqueous 2,4-dinitrophenol, *Ultrasonics Sonochemistry*, 12:461-465pp.

Gündüz, G. and Dükkkancı, M., 2007, Catalytic wet air oxidation of oxalic acid at atmospheric pressure, *International Journal of Chemical Reactor Engineering*, 5, Article A 36: 1-8pp.

REFERENCES (continued)

Harmsen, J.M.A., Jelemensky, L., Andel-Scheffer, P.J.M., Kuster, B.F.M. and Marin, G.B., 1997, Kinetic modeling for wet air oxidation of formic acid on a carbon supported platinum catalyst, *Applied Catalysis A: General*, 165:499-509pp.

Hosokawa, S., Kanai, H., Utani, K., Taniguchi, Y., Saito, Y. and Imamura, S., 2003, State of Ru on CeO_2 and its catalytic activity in the wet oxidation of acetic acid, *Applied Catalysis B:Environmental*, 45:181-187pp.

Ince, N.H., Tezcanli, G., Belen, R.K. and Apikyan, I.G., 2001, Ultrasound as a catalyzer of aqueous reaction systems: the state of the art and environmental applications, *Applied Catalyst B: Environmental*, 29:167-176pp.

Jiang, Y., Petrier, C. and Waite, T.D., 2002, Kinetics and mechanism of ultrasonic degradation of volatile chlorinated aromatics in aqueous solutions, *Ultrasonics Sonochemistry*, 9:317-323pp.

Kidak, R. and Ince, N.H., 2006, Ultrasonic destruction of phenol and substituted phenols: A review of current research, *Ultrasonics Sonochemistry*, 13:195-199pp.

Kim, I.K., Huang, C.P. and Chıu, P.C., 2001, Sonochemical decomposition of dibenzothiophene in aqueous solution, *Water Research,* 35:4370-4378pp.

Klinghoffer, A.A., Cerro, R.L. and Abraham, M.A., 1998, Catalytic wet oxidation of acetic acid using platinum on alumina monolith catalyst, *Catalysis Today*, 40:59-71pp.

Lapparisudthi, O., Mason, T.J. and Paniwnyk, L., 2009, Degaradtion of Chemical Water pollutants using ultrasound, GPE-EPIC, 2nd International Congress on Green Process Engineering, 2nd European Process Intensification Conference, 14-17 June, 2009, Venice, 1-6pp.

Lee, D.K. and Kim, D.S., 2000, Catalytic wet air oxidation of carboxylic acids at atmospheric pressure, *Catalysis Today*, 63:249-255pp.

REFERENCES (continued)

Levec, J. and Pintar, A., 2007, Catalytic wet-air oxidation processes: A review, *Catalysis Today*, 124:172-184pp.

Liang, J., Komarov, S., Hayashi, N. and Kasai, E., 2007, Improvement in sonochemical degradation of 4-chlorophenol by combined use of Fenton-like reagents, *Ultrasonics Sonochemistry*, 14:201-207pp.

Lim, M.H., Kim, S.H., Kim, Y.U. and Khim, J., 2007, Sonolysis of chlorinated cpmpounds in aqueous solution, *Ultrasonics Sonochemistry*, 14:93:98pp.

Luck, F., 1999, Wet air oxidation:past, present and future, *Catalysis Today*, 53:81-91pp.

Margulis, M. A. and Margulis, I. M., 1999, Theory of local electrification of cavitation bubbles: New approaches, *Ultrasonics Sonochemistry,* 6:15-20pp.

Margulis, M. A. and Margulis, I. M., 2002, Contemporary review on nature of sonoluminescence and sonochemical reactions, *Ultrasonics Sonochemistry*, 9:1-10pp.

Mikulova, J., Rossignol, S., Barbier, J., Duprez, D. and Kappenstein, C., 2007a, Characterizations of platinum catalysts supported on Ce, Zr, Pr-oxides and formation of carbonate species in catalytic wet air oxidation of acetic acid, *Catalysis Today*, 124:185-190pp.

Mikulova, J., Barbier, J., Rossignol, S., Mesnard, D., Duprez, D. and Kappenstein, C., 2007b, Wet air oxidation of acetic acid over platinum catalysts supported on cerium-based materails:Influence of metal and oxide crystallite size, *Journal of Catalysis*, 251:172-181pp.

Milone, C., Fazio, M., Pistone, A. and Galvagno, S., 2006, Catalytic wet air oxidation of p-coumaric acid on CeO_2, platinum and gold supported on CeO_2 catalysts, *Applied Catalysis B: Environmental*, 68:28-37pp.

REFERENCES (continued)

Mrowetz, M, Pirola, C. and Selli, E., 2003, Degradation of organic pollutants through sonophotocatalysis in the presence of TiO_2, *Ultrasonics Sonochemitry*, 10:247-254pp.

Naffrechoux, E., Chanoux, S., Petrier, C. and Suptil, J., 2000, Sonochemical and photochemical oxidation of organic matter, *Ultrasonics Sonochemistry*, 7:255-259pp.

Nakajima, A., Hirokazu, S., Kameshima, Y., Okada, K. and Harada, H., 2007**,** Effect of TiO_2 powder addition on sonochemical destruction of 1,4-dioxane in aqueous systems, *Ultrasonics Sonochemitry*, 14:197-200pp.

Nam, S.N., Han, S.K., Kong, J.W. and Choi, H., 2003, Kinetics and mechanisms of the sonolytic destruction of non-volatile organic compounds: investigation of the sonochemical reaction zone using several OH monitoring techniques, *Ultrasonics Sonochemistry*, 10:139-147pp.

Neri, G., Pistone, A., Milone, C. and Galvagno, S., 2002, Wet air oxidation of p-coumaric acid over promoted ceria catalysts, *Applied Catalysis B:Environmental*, 38:321-329pp.

Nikolopoulos, A.N., Markopoulos, O.I. and Papayannakos, N., 2006, Ultrasound assisted catalytic wet peroxide oxidation of phenol: kinetics and intraparticle diffusion effects, *Ultrasonics Sonochemistry*, 13:92-97pp.

Okitsu, K., Nanzai, B., Kawasaki, K., Takenaka, N. and Bandow, H., 2009, Sonochemical decomposition of organic acids in aqueous solution: Understanding of molecular behavior during cavitation by the analysis of a heterogeneous reaction kinetics model, *Ultrasonics Sonochemistry*, 16:155-162pp.

Okuno, H., Yim, B., Mizukoshi, Y., Nagata, Y. and Maeda, Y., 2000, Sonolytic degradation of hazardous organic compounds in aqueous solution, *Ultrasonics Sonochemistry*, 7:261-264pp.

REFERENCES (continued)

Oliviero, L., Barbier Jr., J. and Duprez, L.D., 1999, Role of the metal-support interface in the total oxidation of carboxylic acids over Ru/CeO_2 catalysts, *Catalysis Letters*, 60:15-19pp.

Oliviero, L., Barbier Jr., J., Duprez, D., Guerrero-Ruiz, A., Bachiller-Baeza, B. and Rodriguez-Ramos, I., 2000, Catalytic wet air oxidation of phenol and acrylic acid over Ru/C and $Ru/CeO_2/C$ catalysts, *Applied Catalysis B:Environmental*, 25:267-275pp.

Oliviero, L., Barbier Jr., J., Duprez, D., Wahyu, H., Ponton, J.W., Metcalfe, I.S. and Mantzavinos, D., 2001, Wet air oxidation of aqueous solutions of maleic acid over Ru/CeO_2 catalysts, *Applied Catalysis B: Environmental*, 35, 1-12pp.

Oxford University, 2009. "Safety Data for Butyric acid" and "Safety Data for Maleic acid"
http://msds.chem.ox.ac.uk/BU/butyric_acid.html
http://msds.chem.ox.ac.uk/MA/maleic_acid.html (Aproach year:2010)

Pandit, A.B., Gogate, P.R. and Mujumdar, S., 2001, Ultrasonic degradation of 2:4:6 trichlorophenol in presence of TiO_2 catalyst, *Ultrasonics Sonochemistry*, 8:227-231pp.

Patricio, A., Fernandez, C., Mota, A.M. and Capelo, J.L., 2006, Dynamic *vs* static ultrasonic sample treatment for the solid-liquid pre-concentration of mercury from human urine, *Talanta*, 69:769–775pp.

Perkas, N., Minh, D.P., Gallezot, P., Gedanken, A. and Besson, M., 2005, Platinum and ruthenium catalysts on mesoporous titanium and zirconium oxides for the catalytic wet air oxidation of model compounds, *Applied Catalysis B: Environmental,* 59:121-130pp.

Petrier, C. and Francony, A., 1997, Ultrasonic waste-water treatment: incidence of ultrasonic frequency on the rate of phenol and carbon tetrachloride degradation, *Ultrasonics Sonochemistry*, 4:295-300pp.

REFERENCES (continued)

Pintar, A., Batista, J. and Tisler, T., 2008, Catalytic wet-air oxidation of aqueous solutions of formic acid, acetic acid and phenol in a continuous-flow trickle-bed reactor over Ru/TiO2 catalysts, *Applied Catalysis B: Environmental*, 84: 30-41pp.

Ramirez, J.H., Costa, C.A., Madeira, L.M., Mata, G., Vicente, M.A., Cervantes, M. L. R., Lopez-Peinado, A.J. and Martin-Aranda, R.M., 2007, Fenton-like oxidation of Orange II solutions using heterogeneous catalysts based on saponite clay, *Applied Catalysis B: Environmental*, 71:44-56pp.

Renard, B. , Barbier Jr., J., Duprez, D. and Durecu, S., 2005, Catalytic wet air oxidation of stearic acid on cerium oxide supported noble metal catalysts, *Applied Catalysis B: Environmental*, 55:1-10pp.

Rial-Otero, R., Carreira, R.J. and Cordeiro, F.M., 2007, Sonoreactor-based technology for fast high throughput proteolytic digestion of proteins*, Journal of Proteome Research, 6:*909-912pp.

Rivas, J., Kolaczkowski, S.T., Beltran, F.J. and McLurgy, D.B., 1999, Degradation of maleic acid in a wet air oxidation environment in the presence and absence of a platinum catalyst, *Applied Catalysis B: Environmental*, 22:279-291pp.

Sanchez-Oneto, J., Portela, J.R., Nebot, E. and Martinez-de-la-Ossa, E.J., 2004, Wet air oxidation of long-chain carboxylic acids, *Chemical Engineering Journal*, 100:43-50pp.

Sanchez-Oneto, J., Portela, J.R., Nebot, E. and Martinez-de-la-Ossa, E.J., 2006, Kinetics and mechanism of wet air oxidation of butyric acid, *Industrial Engineering Chemical Research,* 45:4117-4122pp.

REFERENCES (continued)

Sangwichien, C., Aranovich, G.L. and Donohue, M.D., 2002, Density functional theory predictions of adsorption isotherms with hysteresis loops, *Colloids and Surfaces A: Physicochemical and Engineering Aspects*, 206:313–320pp.

Santos, H.M. and Capelo, J.L., 2007, Trends in ultrasonic-based equipment for analytical sample treatment, *Talanta*, 73:795–802pp.

Schultz, T.E., 2005, "Biological waste water treatment " http://www.water.siemens.com/SiteCollectionDocuments/Industries/Hydrocarbon_Processing/Brochures/CE_10-05_biological_trt.pdf, (approach year: 2010)

Seymour, J.D. and Gupta, R.B., 1997, Oxidation of aqueous pollutants using ultrasound: salt-induced Enhancement, *Industrial Engineering Chemical Research*, 36:3453-3457pp.

Shende, R.V. and Mahajani, V.V., 1994, Kinetics of wet air oxidation of glyoxalic acid and oxalic acid, *Industrial Engineering Chemical Research*, 33:3125-3130pp.

Shende, R.V. and Mahajani, V.V., 1997, Kinetics of wet oxidation of formic acid and acetic acid, *Industrial Engineering Chemical Research*, 36:4809-4814pp.

Shende, R.V. and Levec, J., 1999a, Wet oxidation kinetics of refractory low molecular mass carboxylic acids, *Industrial Engineering Chemical Research,* 38:3830-3837pp.

Shende, R.V. and Levec, J., 1999b, Kinetics of Wet Oxidation of propionic and 3-hydroxypropionic acids, *Industrial Engineering Chemical Research,* 38:2557-2563pp.

Sivakumar, M., Tatake, P.A. and Pandit, A.B., 2002, Kinetics of p-nitrophenol degradation: effect of reaction conditions and cavitational parameters for a multiple frequency system, *Chemical Engineering Journal*, 85:327-338pp.

REFERENCES (continued)

Smith, J. M., 1981, Rate Equations for Fluid-Solid Catalytic Reactions, Chemical Engineering Kinetics, McGraw-Hill Book Company, United States of America, 3. Edition, 359-388pp.

Stasinakis, A.S., 2008, Use of selected advanced oxıdatıon processes (AOPs) for wastewater treatment – a mını revıew, *Global NEST Journal*, 10:376-385pp.

Suslick, K.S., 1994, "The Chemistry of Ultrsound " http://www.scs.uiuc.edu/suslick/britannica.html (Approach year: 2010)

Tanaka, H. and Harada, H., 2010**,** Sonolysis of an oxalic acid solution under xenon lamp irradiation, *Ultrasonics Sonochemistry*, 17:770-772pp.

Tezcanli-Güyer, G. and Ince, N.H., 2001, Individual and combined effects of ultrasound, ozone and UV irradiation:a case study with textile dyes, *Ultrasonics*, 42:603:609pp.

Tezcanli-Güyer, G. and Ince, N.H., 2004, Individual and combined effects of ultrasound, ozone and UV irradiation: acase study with textile dyes, *Ultrasonics*, 42:603-609pp.

Thoma, G., Swofford, J., Popov, V. and Som, M., 1997, Sonochemical destruction of dichloromethane and o-dichlorobenzene in aqueous solution using a nearfield acoustic processor, *Advanced in Environmental Research*, 2:178-193pp.

Torrades, F., Garcia-Montano, J., Garcia-Hortal, J.A., Nunez, L., Domenech, X. and Peral, J., 2004, Decolorization and mineralization of homo- and hetero-bireactive dyes under Fenton and photo-Fenton conditions, *Color Technology,* 120:188-194pp.

Tromans, D., 1998, Temperature and pressure dependent solubility of oxygen in water: a thermodynamic analysis, *Hydrometallurgy*, 48:327-342pp.

Tufan (Gündüz), G. and Akgerman, A., 1982, Kinetics and modeling of benzene oxidation, *Chemical Engineering Communication*, 13:361-367pp.

REFERENCES (continued)

Visscher, A. De, Langenhove, H.Van and Eenoo, P.Van, 1997, Sonochemical degradation of ethylbenzene in aqueous solution: a product study, *Ultrasonics Sonochemistry*, 4: 145-151pp.

Visscher, A. De and Langenhove, H.Van, 1998, Sonochemistry of organic compounds in homogeneous aqueous oxidising systems, *Ultrasonics Sonochemistry*, 5: 87-92pp.

Vospernik, M., Pintar, A. and Levec, J., 2006, Application of a catalytic membrane reactor to catalytic wet air oxidation of formic acid, *Chemical Engineering and Processing*, 45:404-414pp.

Wang, X.K., Chen, G.H. and Guo, W.L., 2003, Sonochemical degradation of kinetics of methyl violet in aqueous solution, *Molecules*, 8:40-44pp.

Wang, J., Pan, Z., Zhang, Z., Zhang, X., Wen, F., Ma, T., Jiang, Y., Wang, L., Xu, L. and Kang, P., 2006, Sonolytic degradation of methyl parathion in the presence of nanometer and ordinary anatase titanium dioxide catalysts and comparison of their sonocatalytic abilities, *Ultrasonics Sonochemistry*, 13: 493-500pp.

Wang, J., Zhu, W., He, X. and Yang, S., 2008, Catalytic wet air oxidation of acetic acid over different ruthenium catalysts, *Catalysis Communications*, 9:2163:2167pp.

Wibetoe, G., Takuwa, D.T., Lund, W.D. and Sawula, G., 1999, Fresenius, *Journal of Analytical Chemistry, 363*, 46–54pp.

Wikipedia, 2010, " Butyric acid" and "Maleic acid "
,http://en.wikipedia.org/wiki/Butyric_acid;
http://en.wikipedia.org/wiki/Maleic_acid (Approach year:2010)

Wu, C., Wei, D., Fan, J. and Wang, L., 2001, Photosonochemical degradation of trichloroacetic acid in aqueous solution, *Chemosphere*, 44: 1293-1297pp.

REFERENCES (continued)

Xu, J., Sun, K. , Zhang, L., Ren, Y. and Xu, X., 2005, A highly efficient and selective catalyst for liquid phase hydrogenation of maleic anhydride to butyric acid, *Catalysis Communications*, 6:462-465pp.

Yang, S., Zhu, W., Jiang, Z., Chen, Z. and Wang, J., 2006, The surface properties and the activities in catalytic wet air oxidation over CeO_2–TiO_2 catalysts, *Applied Surface Science*, 252:8499-8505pp.

Yim, B., Okunu, H., Nagata, Y., Nishimura, R. and Maeda, Y., 2002, Sonolysis of surfactants in aqueous solutions:an accumulation of solute in the interfacial region of the cavitation bubbles, *Ultrasonics Sonochemistry*, 9:209-213pp.

Yoo, Y.E., Takenake, N., Bandow, H., Nagata, Y. and Maeda, Y., 1997, Characteristics of volatile fatty acids degradation in aqueous solution by the action of ultrasound, *Water Research*, 31:1532:1535pp.